3-D PRINTED RECOMBINANT COLLAGEN TYPE 2 AND CALCIUM PHOSPHATE CEMENT CARTILAGE TISSUE SCAFFOLDS FOR JOINT CARTILAGE DEFECTS

A THESIS SUBMITTED TO
THE GRADUATE SCHOOL OF NATURAL AND APPLIED SCIENCES
OF
ANKARA UNIVERSITY

by

Hümeyra Hande YAVUZ

DEPARTMENT OF BIOMEDICAL ENGINEERING

ANKARA
2023

All rights reserved

ABSTRACT

Master's Thesis

3-D PRINTED RECOMBINANT COLLAGEN TYPE 2 AND CALCIUM PHOSPHATE CEMENT CARTILAGE TISSUE SCAFFOLDS FOR JOINT CARTILAGE DEFECTS

Hümeyra Hande YAVUZ

Ankara University
Graduate School of Natural and Applied Sciences
Department of Biomedical Engineering

Supervisor: Assoc. Prof. Açelya YILMAZER AKTUNA

Osteochondral defects present a significant clinical challenge due to their complex nature involving both articular cartilage and underlying bone damage. To address this challenge, biphasic scaffolds have been developed to mimic the structures of both tissues, offering a potential solution for osteochondral reconstruction. However, the avascular and low-cell-density characteristics of articular cartilage hinder its natural healing, necessitating alternative methods for nutrient supply and waste removal. This limitation, coupled with the lack of chondrocytes in its extracellular matrix, underscores the need for innovative approaches. In this research, biphasic scaffolds were designed to mimic bone and cartilage tissues separately. The upper layer of the cartilage scaffold was composed of recombinant collagen, a precise and controllable material with a reduced risk of immunogenicity compared to animal-derived collagens, in conjunction with alginate. For bone engineering, the lower layer consisted of calcium phosphate cement (CPC), a biocompatible, osteoconductive, and bioactive material known for its ability to support both bone and cartilage tissue growth. For the cartilage component, sodium alginate and recombinant collagen scaffolds were designed and 3D printed. These calcium phosphate cement scaffolds and recombinant collagen/alginate scaffolds were then separately tested for their osteochondrogenic and chondrogenic differentiation potential in vitro using adipose-derived mesenchymal stem cells (ADMSCs). Various aspects, including mechanical properties, cell viability, proliferation, morphology, and differentiation characteristics, were thoroughly investigated. The study findings suggest that the combination of biphasic calcium phosphate bone cement and recombinant collagen/alginate scaffolds holds great promise for repairing osteochondral defects. This approach provides mechanical support resembling subchondral bone while offering a chondrogenic scaffold for cartilage repair. This study contributes valuable insights into advanced regenerative strategies for addressing osteochondral defects, ultimately improving patient outcomes in clinical settings.

October 2023, 188 Pages

Key Words: Osteochondral cartilage repair, cartilage regeneration scaffolds, cartilage tissue engineering, recombinant collagen, calcium phosphate cement, cartilage tissue scaffold

ÖZET

Yüksek Lisans Tezi

EKLEM KIKIRDAK DEFEKTLERI IÇIN 3-BOYUTLU BASKILANAN REKOMBINANT KOLAJEN VE KALSIYUM FOSFAT ÇIMENTOSU KIKIRDAK DOKU İSKELELERI

Hümeyra Hande YAVUZ

Ankara Üniversitesi
Fen Bilimleri Enstitüsü
Biyomedikal Mühendisliği Anabilim Dalı

Danışman: Doç. Dr. Açelya YILMAZER AKTUNA

Osteokondral defektler hem eklem kıkırdağı hem de altta yatan kemik hasarını içeren karmaşık yapıları nedeniyle önemli bir klinik zorluk teşkil etmektedir. Bu zorluğun üstesinden gelmek için, her iki dokunun yapısını taklit eden ve osteokondral rekonstrüksiyon için potansiyel bir çözüm sunan çift fazlı iskeleler geliştirilmiştir. Bununla birlikte, eklem kıkırdağının avasküler ve düşük hücre yoğunluğu özellikleri doğal iyileşmesini engellemekte, besin temini ve atıkların uzaklaştırılması için alternatif yöntemler gerektirmektedir. Bu sınırlama, hücre dışı matriksindeki kondrosit eksikliği ile birleştiğinde, yenilikçi yaklaşımlara duyulan ihtiyacın altını çizmektedir. Bu araştırmada, kemik ve kıkırdak dokularını ayrı ayrı taklit etmek için bifazik iskeleler tasarlanmıştır. Kıkırdak iskelesinin üst katmanı, aljinat ile birlikte, hayvan kaynaklı kolajenlere kıyasla daha az immünojenite riski taşıyan, hassas ve kontrol edilebilir bir malzeme olan rekombinant kolajenden oluşmuştur. Kemik mühendisliği için alt katman hem kemik hem de kıkırdak doku büyümesini destekleme kabiliyetiyle bilinen biyouyumlu, osteokondüktif ve biyoaktif bir malzeme olan kalsiyum fosfat çimentosundan (CPC) oluşmaktadır. Osteogenezi ve doku büyümesini teşvik etmek için yaklaşık 300 μm makro gözeneklere sahip CPC iskeleleri araştırıldı, bu nedenle birbirine bağlı makro gözeneklere sahip CPC iskeleleri oluşturmak için dolaylı 3D baskı yöntemi kullanıldı. Kıkırdak katmanı için sodyum aljinat ve rekombinant kolajen iskeleler tasarlanmış ve 3D olarak basılmıştır. Bu kalsiyum fosfat çimento iskeleleri ve rekombinant kolajen/aljinat iskeleler daha sonra adipoz kaynaklı mezenkimal kök hücreler (ADMSC'ler) kullanılarak in vitro osteokondrojenik ve kondrojenik farklılaşma potansiyelleri açısından ayrı ayrı test edilmiştir. Mekanik özellikler, hücre canlılığı, proliferasyon, morfoloji ve farklılaşma özellikleri dahil olmak üzere çeşitli yönleri kapsamlı bir şekilde araştırılmıştır. Çalışma bulguları, bifazik kalsiyum fosfat kemik çimentosu ve rekombinant kolajen/aljinat iskelelerin kombinasyonunun osteokondral defektlerin onarımı için umut vaat ettiğini göstermektedir. Bu yaklaşım, subkondral kemiğe benzer mekanik destek sağlarken, kıkırdak onarımı için kondrojenik bir iskele sunarak, osteokondral defektler için gelişmiş rejeneratif stratejilere değerli bilgiler katmakta ve klinik ortamlarda hastaları iyileştirmesi umut edilmektedir.

Ekim 2023,188 Sayfa

Anahtar kelimeler: Osteokondral defekt, kıkırdak rejenerasyonu, kıkırdak doku iyileştirilmesi, Kıkırdak doku mühendisliği, rekombinant kolajen, kalsiyum fosfat çimentosu, kıkırdak doku biyoiskelesi

ACKNOWLEDGEMENTS

I feel incredibly fortunate to have completed my master's studies in such an enriching and supportive environment. Firstly, I want to express my sincere gratitude to my supervisor, Associate Professor Dr. Açelya Yılmazer Aktuna, for her unwavering guidance and support throughout my thesis work. I greatly admire her for her outstanding contributions to scientific research, unwavering commitment to advancing science, exceptional work ethic, and constant kindness.

I wish to extend my heartfelt thanks to Professor Dr. Pınar Yılgör Huri. Her dedication to sharing knowledge with students, her impressive expertise, and her valuable contributions and ideas have greatly enriched my research. Her unwavering interest and support during my thesis process are deeply appreciated.

During the course of my thesis, I must express my deep appreciation for my friend, Utku Serhat Derici, who not only provided motivation but also shared invaluable ideas that greatly influenced the early stages and execution of my thesis. He was not just a colleague but a dear friend and research partner, imparting knowledge and offering continuous support on both academic and personal fronts.

I want to express my gratitude to my lab friends; Esen Kirit, Cemile Gökçe, Cansu Gürcan, Berfin İlayda Öztürk, and Buse Altun who have been with me throughout my master's thesis journey. They provided invaluable assistance and support during my experiments, shared in my moments of joy and sadness, and generously shared their knowledge and experience with me.

I want to share my gratitude to Emre Yılmaz and grateful to Permed Sağlık Ürünleri for generously funding my study and for their support. Their contributions to my thesis are highly appreciated.

I would like to thank Şeyda Gökyer and Barış Burak Altunay; I am grateful for their contributions to my thesis process and help in my experiments.

Finally, I want to express my deep gratitude to my parents, Şevket Yavuz and Ayşe Yavuz, who have always been a source of happiness and support in my life. Their unwavering determination and constant encouragement have played a pivotal role in shaping my journey to this point today. Regardless of the outcomes, they have consistently stood by my side, offering support and their unconditional love has been a constant source of strength in my life. I'm proud to have parents who have done their absolute best for me, and I thank them from the bottom of my heart as well as my sisters, Zeynep Betül Yavuz and Münteha Nur Yavuz, for their endless encouragement, love, care, and support throughout my education and life.

For all the people who contributed in many other ways, I am forever grateful.

Hümeyra Hande YAVUZ
Ankara, October 2023

TABLE OF CONTENTS

THESIS APPROVAL
ETHICS ..... **i**
ABSTRACT ..... **ii**
ÖZET ..... **iii**
ACKNOWLEDGEMENTS ..... **iv**
TABLE OF CONTENTS ..... **v**
LIST OF SYMBOLS ..... **ix**
LIST OF FIGURES ..... **xi**
LIST OF TABLES ..... **xiv**
1. INTRODUCTION **1**
2. LITERATURE SURVEY **4**
2.1 Osteochondral Tissue **4**
2.1.1 Articular cartilage **6**
2.1.2 Calcified cartilage **7**
2.1.3 Subchondral bone **8**
2.2 Osteochondral Defects **10**
2.2.1 Osteoarthritis (OA) **12**
2.3 Treatment for OC Defects Repair **14**
2.4 Tissue Engineering **17**
2.4.1 Osteochondral tissue engineering **19**
2.4.1.1 Cells in osteochondral tissue engineering **21**
2.4.1.1.1 Mesenchymal stem cells for osteochondral tissue engineering **26**
2.4.1.1.2 Bone marrow derived mesenchymal stem cells (BMSCs) **29**
2.4.1.1.3 Adipose-derived MSCs **30**
2.4.1.1.4 Induced pluripotent stem cells (iPSCs) **33**
2.4.1.2 Growth factors **34**
2.4.1.3 Biomaterials for Osteochondral Tissue Engineering **35**
2.4.1.3.1 Natural polymers **36**
2.4.1.3.1.1 Collagen for osteochondral tissue engineering **38**
2.4.1.3.1.2 Recombinant collagen technology **41**
2.4.1.3.1.3 Alginate hydrogel for osteochondral tissue engineering **45**
2.4.1.3.2 Synthetic polymers **47**
2.4.1.3.3 Metallic materials **48**

2.4.1.3.4 Bioceramics **49**
2.4.1.3.4.1 Calcium phosphates **51**
2.4.1.3.4.2 Calcium phosphate cement **52**
2.4.1.3.4.2.1 3D printing of CPC **58**
2.4.1.4 Scaffold architecture **59**
2.4.1.4.1 Monophasic scaffolds **63**
2.4.1.4.2 Biphasic scaffolds **63**
2.4.1.4.3 Triphasic and multiphasic scaffold **66**
2.4.1.4.4 Gradient scaffolds **67**
2.4.1.5 Cell-free strategies for osteochondral regeneration **68**
2.4.1.5 Commercial products of osteochondral defects **69**
2.4.1.6 Scaffold fabrication methods **72**
2.4.1.6.1 Lyophilization **73**
2.4.1.6.2 Solvent casting and particulate leaching **74**
2.4.1.6.3 Electrospinning **74**
2.4.1.6.4 3D bioprinting **75**
2.4.1.6.4.1 Difficulties of fabrication scaffold with 3d printing process **78**
2.4.1.6.5 Indirect 3D printing **80**
2.5 Scope and Novelty of the Study **81**
3. MATERIAL AND METHODS **83**
3.1 Materials **83**
3.1.1 Cell line **83**
3.1.2 Culture and growth AD-MSC cell line **83**
3.1.3 Chondrogenic differentiation media **83**
3.1.4 Osteogenic Differentiation Media **83**
3.1.5 Preparation of CPC Scaffold **84**
3.1.6 Preparation of Alginate/Collagen Scaffold **84**
3.1.7 For optimization trials of CPC for 3D printing **84**
3.1.8 Cell viability Assay **85**
3.1.9 Differentiation Staining **85**
3.2 Methods **85**
3.2.1 Designing the biphasic scaffold **85**
3.2.2 Preparation of the subchondral part of the biphasic scaffold **87**
3.2.2.1 3D Printing process of sacrificial PCL scaffold **89**
3.2.3 Cell toxicity analysis of CPC scaffolds **94**
3.2.4 AD-MSC cell culture **98**

3.2.5 Cell seeding on CPC scaffolds 98
3.2.6 Cell Viability (Alamar BlueTM) Test of CPC Scaffolds 100
3.2.7 Cell activity and differentiation 100
3.2.7.1 Alizarin Red Staining 100
3.2.8 Characterization of CPC scaffolds 101
3.2.8.1 Mechanical measurements 101
3.2.8.2 FTIR analysis of CPC scaffolds 102
3.2.9 Scanning Electron Microscopy analysis of CPC scaffolds 104
3.3 Preparation Of Chondral Part Of Biphasic Scaffold 104
3.3.1 3D Printing process of alginate/recombinant collagen scaffold 106
3.3.2 Mechanical measurements of alginate/recombinant collagen scaffolds 108
3.3.2.1 Compression test 108
3.3.3 Cell toxicity analysis of alginate/recombinant collagen scaffold 109
3.3.4 AD-MSC cell culture 110
3.3.5 Cell seeding on alginate/recombinant collagen scaffolds 110
3.3.6 Cell viability (Alamar Blue™) test of alginate/recombinant collagen scaffolds 111
3.3.7 Chondrogenic differentiation of AD-MSC on the alginate/recombinant collagen scaffolds 112
3.3.7.1 Alcian Blue Staining 112
3.3.8 SEM analysis of the cell-seeded alginate/recombinant collagen scaffold 113
3. 4 Statistical analysis 113
4. RESULTS AND DISCUSSION 114
4.1 Bone part of biphasic scaffold 114
4.1.1 Cell toxicity analysis of CPC scaffolds 114
4.1.2 Mechanical Testing of CPC Scaffolds 118
4.1.3 FTIR Analysis of CPC Scaffolds 121
4.1.4 Cell viability (Alamar Blue™) test of CPC scaffolds 124
4.1.5 SEM analysis of CPC scaffolds 128
4.1.6 Alizarin Red Staining 133
4. 2 3D printing trials of CPC 136
4.3 Chondral Part of Biphasic Scaffold 143
4.3.1 Cell toxicity analysis of alginate/recombinant collagen scaffold 143
4.3.2 Cell Viability (Alamar Blue™) Test of Alginate/Recombinant Collagen Scaffolds . 145
4.3.3 Mechanical testing of alginate/recombinant collagen scaffolds 148
4.3.4 SEM analysis of alginate/recombinant collagen scaffolds 150
4.3.5 Alcian Blue Staining 156

5. CONCLUSION 159
REFERENCES 161
APPENDICES 187
APPENDIX 1 187
ÖZGEÇMİŞ 188

LIST OF SYMBOLS

mm	Millimeter
nm	Nanometer
µg	Microgram
µl	Microliter
µm	Micrometer

Abbreviations

ALG	Alginate
AD-MSC	Adipose derived Mesenchymal Stem Cell
BMSC	Bone Marrow derived Mesenchymal Stem Cell
OC	Osteochondral
OA	Osteoarthrisis
OAT	Osteochondral Autograft Transfer
OCA	Osteochondral Allograft Transplant
CPC	Calcium Phosphate Cement
DMEM	Dulbecco's Modified Eagle Medium
PLA	Polylactic Acid
PCL	Polycaprolactone
PLGA	Poly (L-lactic-co-Glycolic Acid)
PEG	Polyethylene Glycol
PVA	Polyvinyl Alcohol
ECM	Extracellular Matrix
HA	Hydroxyapatite
TCP	Tricalcium Phosphate
TE	Tissue Engineering
TTCP	Tetra calcium Phosphate
ME	Material Extrusion
MEW	Melt Electro-Writing

ES	Electro-Spinning
SLA	Stereolithography
DLP	Digital Light Processing
MSC	Mesenchymal Stem/Stromal Cell
GAG	Glycosaminoglycans
IGF	Insulin-like Growth Factor
BMP	Bone Morphogenetic Proteins
FGF	Fibroblast Growth Factor
TGF	Transforming Growth Factor
SEM	Scanning Electron Microscope

LIST OF FIGURES

Figure 2.1 Osteochondral Unit 4
Figure 2.2 Comparison of healthy knee joint and osteoarthritis 13
Figure 2.3 Progress in the treatment of osteochondral lesions 16
Figure 2.4 Illustration of tissue engineering 19
Figure 2.5 Decision-making procedure during the creation of osteochondral tissue scaffold 20
Figure 2.6 Schematic of using cells in tissue engineering 22
Figure 2.7 Utilization of Stem cells in osteochondral defects 23
Figure 2.8 The schematic representation of sources of mesenchymal stem cells 27
Figure 2.9 The differentiation of AD-MSCs into chondrogenic and osteogenic cells and their use in osteochondral tissue engineering 32
Figure 2.10 Synthetic and Natural Biomaterials in Osteochondral Tissue Engineering 36
Figure 2.11 Schematic of crosslinking collagen 40
Figure 2.12 Structural units of the alginate block types 45
Figure 2.13 Calcium phosphate cement paste preparation 54
Figure 2.14 Injectable calcium phosphate cement (CPC) 55
Figure 2.15 Scaffold designs in Osteochondral Tissue Engineering 62
Figure 2.16 Osteochondral Tissue Engineering Scaffold Fabrication Methods 73
Figure 2.17 Examples of various bioprinting techniques 76
Figure 3.1 Schematic of CPC/Recombinant collagen biphasic scaffold and in vitro analysis for osteochondral defects using AD-MSCs 86
Figure 3.2 Process followed to use 3D Printed Sacrificial PCL Scaffold to obtain porosity CPC scaffold 88
Figure 3.3 3D Printing process of PCL Scaffold 90
Figure 3.4 3D Printed Sacrificial PCL Scaffold 91
Figure 3.5 Unset CPC paste in Sacrificial PCL Scaffolds 92
Figure 3.6 CPC/PCL Scaffolds after drying 1 day 92
Figure 3.7 CPC/PCL Scaffolds in DCM Solvent 93
Figure 3.8 Porous CPC Scaffold after solved in DCM Solvent 93
Figure 3.9 Final porous CPC Scaffold 94
Figure 3.10 Extract medium of CPC bulk and CPC scaffold and filtration process of extract media of CPC scaffold 96

Figure 3.11 24 Well for cell Toxicity analysis of 4 groups 97
Figure 3.12 96 well plates of Alamar Blue Analysis of CPC Scaffold, CPC Bulk, negative and positive groups 97
Figure 3.13 AD-MSC p:1 with a light microscope (Scale bar: 100 μm) 98
Figure 3.14 Process of cell seeding on CPC Scaffolds and adding control/osteogenic Medium 99
Figure 3.15 Universal Testing Machine of Shimadzu 101
Figure 3.16 CPC Scaffolds during the compression 102
Figure 3.17 Fourier Transform Infrared-Attenuated Total Reflectance (FTIR-ATR) spectroscopy (The JASCO FTIR-4600) 103
Figure 3.18 FTIR Analysis of CPC Scaffold 103
Figure 3.19 Zeiss EVO-40 Scanning Electron Microscope 104
Figure 3.20 (A-B) Preparation process of alginate solution and recombinant collagen solution (C) obtained mixed Homogenous Alginate/ Recombinant Collagen Solution…..... 106
Figure 3.21 3D Printing set-up of Alginate/recombinant collagen scaffold 107
Figure 3.22 3D Printed Alginate/Recombinant Collagen Scaffold..... 108
Figure 3.23 3D Printed Alginate/recombinant collagen scaffold crosslinking process in CaCl2 bath..... 108
Figure 3.24 The images of the Alginate/Recombinant Collagen scaffold during the compression test..... 109
Figure 3.25 Schematic of Alamar Blue Assay 112
Figure 4.1 Variation of cell layer spreading at 24, 48, and 72 hours according to experimental groups after the addition of extraction fluid. (10x) 114
Figure 4.2 Changes in cell morphology at 24, 48, and 72 hours after the addition of extraction fluid according to experimental groups (40x) 115
Figure 4.3 Changes in the number of viable cells according to experimental groups 72 hours after the addition of extraction fluid; results are normalized to the negative control group..... 116
Figure 4.4 % cell growth inhibition; results are relative to the positive control group 117
Figure 4.5 Compressive strength graphs of CPC Scaffold Samples..... 119
Figure 4.6 FTIR Spectrum of CPC Scaffold..... 121
Figure 4.7 FTIR spectra of calcium phosphates in the domains of internal vibrations of phosphate ions FTIR spectra of calcium phosphates in the domains of internal vibrations of phosphate ions..... 123
Figure 4.8 Cell proliferation of AD-MSCs cultured on CPC scaffolds of biphasic scaffolds with different mediums..... 125

Figure 4.9 SEM Images of CPC Scaffold's surface with cultured in control media at day 21(100 μm) 128
Figure 4.10 Sem Images of CPC scaffold without cells 129
Figure 4.11 SEM images of AD-MSCs cultured on the CPC scaffold surfaces for 7,14 and 21 days in the control medium 130
Figure 4.12 SEM images of AD-MSCs cultured on the CPC scaffold surfaces for 7,14 and 21 days in the osteogenic medium 132
Figure 4.13 Photographs of AD-MSC cells in culture medium, (A) without and (B) with osteogenic differentiation agents, after staining with Alizarin Red S for identification of the calcium deposit in cells on days 7, 14, and 21 134
Figure 4.14 Variation of cell layer spreading at 24, 48, and 72 hours according to experimental groups after the addition of extraction fluid. (10x) 144
Figure 4.15 Variation of cell layer spreading at 24, 48, and 72 hours according to experimental groups after the addition of extraction fluid. (40x) 145
Figure 4.16 The effect of chondrogenic differentiation medium and control medium on cell viability of Alginate/Recombinant Collagen Scaffolds. Cell numbers were determined by measurement of Alamar blue assay... 146
Figure 4.17 Compressive Strength of Alginate/Recombinant Collagen Scaffolds 148
Figure 4.18 Sem Image of Alginate/Recombinant Collagen Scaffolds surface (100 μm) 151
Figure 4.19 Sem Image of AD-MSC cell attached to the scaffolds macropores (10 μm) 152
Figure 4.20 Sem Images of AD-MSC cell seeded Alginate/Recombinant Collagen Scaffolds from day 7 to day 21 cultured in control medium. (Red arrows show AD-MSC cells Blue shows cytoplasm extension) 153
Figure 4.21 Sem Images of AD-MSC cell seeded Alginate/Recombinant Collagen Scaffolds from day 7 to day 21 cultured in chondrogenic medium 154
Figure 4.22 Microscopy Images of Alcian blue staining Alginate/Recombinant Collagen Scaffolds 156

LIST OF TABLES

Table 2.1 Grading system for OC tissue defects 11
Table 2.2 Risk factors of OA 12
Table 2.3 Summarizes the different traditional treatments for osteochondral defects 15
Table 2.4 Stem cells in Osteochondral Tissue Engineering 24
Table 2.5 Signaling molecules that MSCs release to promote chondrogenesis 29
Table 2.6 Comparison table of adipose-derived mesenchymal stem cells (AD-MSCs) and bone marrow mesenchymal stem cells (BM-MSCs) 31
Table 2.7 Crosslinking Methods 39
Table 2.8 Comparison of animal-derived collagen and recombinant collagen 43
Table 2.9 Bioceramic Materials Using in Osteochondral Tissue Engineering 50
Table 2.10 Several calcium phosphates, their properties, and applications 52
Table 2.11 Important properties of CPC 53
Table 2.12 Summary of advantages of prefabricated CPC scaffolds 57
Table 2.13 Scaffold Design factors and their explanations 60
Table 2.14 The mechanical function requirements for osteochondral scaffolds 61
Table 2.15 Commercial Products of Osteochondral Defects 70
Table 2.16 Summarizes the challenges of 3D bioprinting 79
Table 3.1 Benefits of using Indirect 3D Printing for Fabricating CPC scaffold 88
Table 3.2 Cytotoxicity evaluation criteria 94
Table 3.3 Cytotoxic response index and cytotoxicity assessment 95
Table 4.1 Results of biocompatibility test evaluation criteria 117
Table 4.2 Biocompatibility evaluation results for CPC Bulk and CPC Scaffold 118
Table 4.3 Compressive Strength of CPC Scaffold Samples 119
Table 4.4 Several Experiments to Make CPC 3D Printable in this thesis 139
Table 4.5 Compressive Strength of Alginate/Recombinant Collagen Scaffolds Samples 149

1. INTRODUCTION

Tissue engineering research is promising for the treatment of cartilage problems, as injured hyaline cartilage has a limited ability for self-healing due to its avascular nature and low cell density, hence restricting therapy choices. Osteochondral defects arise from acute trauma and extend to the subchondral bone and bone marrow, creating a challenging clinical scenario for joint preservation. The avascular nature of cartilage makes it less responsive to repairing normal tissue damage, unlike cartilage lesions that lead to spontaneous cellular repair through subchondral proliferation. Consequently, unlike cartilage lesions, spontaneous healing of osteochondral defects degenerates over time and eventually progresses to osteoarthritis (OA) (Ochi, Uchio, Tobita, & Kuriwaka, 2001).

A degenerative disease characterized by pain and swelling in its early stages, OA usually follows the destruction of cartilage lesions and always extends deep into the subchondral bone, eventually becoming an osteochondral defect. Attempts to repair or reverse the effects of cartilage destruction present significant challenges due to the limited capacity of cartilage regeneration. Treatment strategies for osteochondral defects should address both the subchondral bone and the overlying cartilage surface. Current techniques include autologous cartilage grafting, osteochondral grafting, and a combination of autologous cartilage grafting as well as closed-to-lesion grafting. Newer treatments include tissue engineering using monophasic, biphasic, and multiphasic scaffolds for effective osteochondral repair (J.-N. Fu et al., 2022).

In all tissue engineering strategies, osteochondral scaffold structures must support cell proliferation, nutrient transport, and metabolic waste removal through interconnected 3D porous networks like other tissue engineering applications. Calcium phosphate cements (CPC) have received much attention for their osteoconductive and bone replacement properties, making them very promising for various clinical applications, especially when mimicking natural bone tissue in 3D scaffold designs (Xu et al., 2017).

Collagen is a ubiquitous polymer in bone tissue and provides an ideal scaffold or matrix for tissue engineering because it supports a variety of connective tissues such as skin,

tendons, bone, cartilage, blood vessels, and ligaments. Incorporating collagen into composites provides more cell recognition sites and accelerates biomaterial degradation, allowing rapid replacement with new bone. However, the use of collagen is limited due to cost and potential problems with antigen and pathogen transmission. Recent advances in the development of recombinant human collagen derived from animal-free sources have provided a reliable, predictable, and chemically defined source of purified human collagen. This use of recombinant human collagen improves safety, performance, biocompatibility, and durability in materials engineering compared to existing alternatives. Furthermore, the application of recombinant technology to complex molecules such as collagen provides a model that may play a role in the design of other innovative materials for specific tissue engineering applications (L. Liu et al., 2007).

Evonik has developed VECOLLAN®, an advanced recombinant collagen platform produced through a fermentation-based process that contains no animal or human-derived ingredients. VECOLLAN® offers a highly soluble and pure form of collagen designed to mimic many of the properties of natural collagen, reliable interaction with cells and tissues, easy absorption, regeneration by the body, and facilitating adaptation to shapes, and forms and it provides different processing methods. In addition, VECOLLAN® has the potential to be used in a wide range of applications in the medical, pharmaceutical, cell culture, and tissue engineering markets.

In respect of these developments, the study aims to develop biphasic scaffolds meticulously designed to mimic bone and cartilage tissues separately; ultimately providing a comprehensive solution for repairing osteochondral defects. The upper layer of the cartilage scaffold incorporates recombinant collagen, known for its precision and controllability, as well as reduced immunogenicity compared to animal-derived collagens. This collagen layer is combined with alginate to enhance its functionality.

As for the bone engineering aspect, the lower layer of the scaffold is constructed using calcium phosphate cement (CPC), known for its biocompatibility, osteoconductive properties, and bioactivity, making it suitable for both bone and cartilage tissue growth. These CPC scaffolds feature deliberate design with around 300 μm macropores to

facilitate osteogenesis and tissue ingrowth. The creation of these macroporous CPC scaffolds involves an indirect 3D printing method, incorporating sacrificial scaffolds made of polycaprolactone (PCL) to infuse CPC pastes.

Additionally, the study explores the cartilage component, involving the design and 3D printing of scaffolds consisting of sodium alginate and recombinant collagen, and the bone component, involving the design and indirect 3D printing of scaffolds consisting of calcium phosphate cement. Both the calcium phosphate cement scaffolds and recombinant collagen/alginate scaffolds undergo separate in vitro tests, specifically assessing their potential to induce osteochondrogenic and chondrogenic differentiation using adipose-derived mesenchymal stem cells (ADMSCs).

2. LITERATURE SURVEY

2.1 Osteochondral Tissue

The osteochondral unit is an intricate composite structure within the musculoskeletal system, consisting of two primary components: the articular cartilage and the subchondral bone. The subchondral bone can be subdivided into four distinct zones, progressing from the surface to the depth: the superficial zone, the middle region, the deep zone, and the calcified zone (Fig 2.1). These components are closely interrelated in terms of the mechanical, biochemical, and physiological aspects. This indicates they function as a cohesive system to withstand and distribute the mechanical stresses and loads that occur during joint movement and weight-bearing activities. These forces and loads may be thought of as a combination of tension and compression (Lyons, McClure, Stoddart, & McClure, 2006).

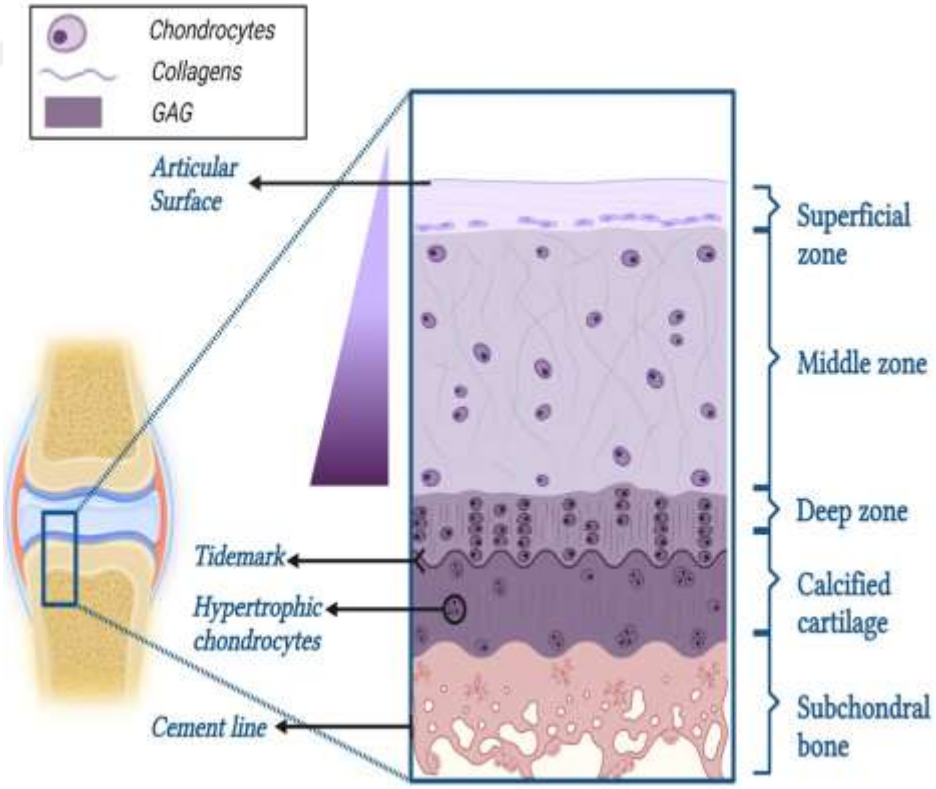

Figure 2.1 Osteochondral Unit

In addition, the osteochondral unit's biochemical and physiological linkages include signaling pathways, nutrition exchange, and metabolic activities, all of which contribute to the joint's general health and functionality. These interactions are necessary for preserving the osteochondral unit's integrity and homeostasis, which in turn ensures optimal joint function and supports an individual's capacity to successfully bear weight.

Each component of the osteochondral unit consists of a unique structure, composition, and function, described in the sections below (Goldring & Goldring, 2016; Piluso et al., 2019)

Articular cartilage, which covers the joint surfaces, performs the function of an interface that is both smooth and low-friction, enabling smooth joint mobility. Calcified cartilage is a transitory layer that acts as a buffer between the articular cartilage and the subchondral bone. It is located between the articular cartilage and the subchondral bone. The subchondral cortical and trabecular bone, which may be found underneath the calcified cartilage, are responsible for providing the joint with structural support and stability (Lyons et al., 2006).

These elements of the osteochondral unit collaborate to ensure that the joint is loaded correctly and can support the weight. They prevent an excessive stress concentration from occurring on any one component by evenly distributing loads and pressures throughout the joint. Because of the mechanical connectivity, the articular cartilage can efficiently transfer forces to the calcified cartilage, which then transfers those forces to the subchondral bone. Hyaline cartilage is a prevalent type of cartilage found extensively in the human body, with a significant presence in articular cartilage. This type of cartilage is known for its clear appearance and smooth texture, which contribute to joint stability and reduce friction. A comprehensive understanding of hyaline cartilage is crucial for studying joint health and developing treatments for joint-related conditions (Sophia Fox, Bedi, & Rodeo, 2009)

2.1.1 Articular cartilage

Articular cartilage, composed mostly of hyaline cartilage, stands as the predominant form of cartilage in the human body. Its key role is to provide structural support to synovial joints, facilitate their smooth articulation, and provide basic protection to the bone involved in these joint movements. In addition, it effectively dissipates and absorbs mechanical stress and forces associated with joint movement. This function is of profound importance and cannot be overstated (Sophia Fox et al., 2009).

Compared to bone, articular cartilage has distinct characteristics and composition. Articular cartilage is primarily composed of water, constituting around 65-80% of its total mass, which facilitates shock absorption and lubrication of joint movements. Collagen, mainly type II collagen, comprises 10-20% of its weight, providing structural support. The presence of proteoglycans, particularly aggrecans, enhances cartilage resilience and elasticity by retaining the water (Buckwalter & Mankin, 1997). While additional forms of collagen and proteoglycans exist in lower concentrations, comprehending this composition is vital for investigating cartilage properties, function, and responses to injuries or diseases (Bayliss & Roughley, 1985).

The distinctive feature of articular cartilage is the lack of blood vessels and nerves. Unlike bone, articular cartilage relies on other mechanisms for nutrient delivery and detritus elimination. The lack of blood vessels makes it difficult for cartilage to self-repair and makes it more susceptible to injury and slower to heal. This indicates that it is incapable of sensing discomfort or transmitting sensory signals. While the absence of nerves contributes to the fluid and painless movement of joints, it can also be a disadvantage because injuries or damage to cartilage may go undetected until severe symptoms appear (Sophia Fox et al., 2009).

2.1.2 Calcified cartilage

The calcified cartilage is a layer characterized by significant mineralization, indicating a substantial presence of minerals. Its main function is to act as a connector or anchor between the soft hyaline cartilage and the underlying subchondral bone. This layer is densely mineralized that serves as an intermediary region between soft cartilage and rigid bone. It facilitates the transition of stiffness and aids in transmitting various forces from the cartilage to the bone (St-Pierre et al., 2012).

An essential characteristic of the calcified cartilage layer is its ability to facilitate a gradual change in stiffness from the soft cartilage to the more rigid bone. The function of this entity is to serve as a buffer or intermediary region that facilitates the distribution and transmission of various forms of forces. The forces encompassed in this context consist of compressive forces, which involve the application of pressure inwards, shear forces, which act parallel to the surface, and tensile forces, which entail the pulling or stretching of the material (J. Farr & Gomoll, 2014).

To understand the differences in stiffness between cartilage, calcified cartilage, and bone, it is necessary to examine their respective elastic moduli. Young's modulus highlights these differences: articular cartilage has lower stiffness (1-15 MPa), calcified cartilage exhibits higher stiffness (0.3 GPa), and bone surpasses both (2 GPa). (J. Farr & Gomoll, 2014).

The extracellular matrix (ECM) of calcified cartilage is composed of type X collagen, hydroxyapatite, type II collagen, and glycosaminoglycans. Type II collagen is an additional variant of the collagen protein that plays an important role in the overall structure and elasticity of cartilage. Glycosaminoglycans (GAGs) are polysaccharides composed of extended chains of sugar molecules. These biomolecules play an important role in maintaining proper levels of water and giving cartilage its cushioning properties (J. Farr & Gomoll, 2014).

In addition, alkaline phosphatases are found in the extracellular matrix (ECM) of calcified cartilage. Alkaline phosphatases are enzymatic proteins that are involved in the process of hydroxyapatite deposition (Orimo, 2010). These substances facilitate the mineralization process by promoting the transformation of certain molecules into hydroxyapatite, thereby playing an important role in the development of the mineralized matrix within the calcified cartilage and contributing to the cartilage's strength (Ohira & Ishikawa, 1986).

Between the deep zone of cartilage and the calcified cartilage is a layer which is called the tidemark layer, which may be very important for maintaining the stability and individuality of the two tissues (Sophia Fox et al., 2009). The structure is a discrete band composed of calcified cartilage, with an approximate thickness of 5 μm and the structure can be visualized with histological staining with hematoxylin. Tidemark layer may possess a certain level of permeability, enabling a certain degree of diffusion. The observed diffusion of molecules implies that the tidemark layer plays a role in facilitating intracellular communication between the cartilage and the underlying bone (Choe, Devoy, Jabari, Packer, & Fisher, 2021). When examining the biomechanics, it becomes evident that the wavelike or undulating structure of the tidemark plays a crucial role in safeguarding the joint against shearing pressures. This unique geometric design acts as a protective barrier, resisting intra-articular shearing stresses and preventing the shearing (Fawns & Landells, 1953; Ohira & Ishikawa, 1986).

2.1.3 Subchondral bone

Osteochondral subchondral bone is essential for shock absorption, mechanical load transfer, and nutrient delivery to the overlying cartilage and is separated from calcified cartilage by cement lines. This line acts as a boundary between two structures. The subchondral bone phase that lies beneath the calcified cartilage protects the integrity of all chondrocytes and provides mechanical support to the notochord tissue. Protein structures such as collagen type I, proteoglycans, glycosaminoglycans, and sialoproteins are important components of the organic part of the subchondral bone structure (van der Harst et al., 2004).

Unlike cartilage, the subchondral bone is composed primarily of highly mineralized ECM-containing type I collagen. The organic component makes up about 30% and consists mainly of type I collagen, which provides the structural framework and strength of the bone. The mineral component makes up about 60% and is mainly composed of calcium hydroxyapatite. These mineral components give the bone hardness and the ability to absorb shock and help its ability to resist compressive forces (B. Zhang, J. Huang, & R. Narayan, 2020).

The biomechanics of the bone-cartilage interface are influenced by factors like porosity, pore size, and mechanical properties in the subchondral bone. These factors help distribute loads evenly between cartilage and bone, contributing to joint function and damage prevention. Subchondral bone exhibits varying porosity (ranging from 5% to 90%) and pore size (ranging from 0.1 to 2000 μm), with higher values in the trabecular bone layer compared to cortical bone (G. Li et al., 2013).

Cell composition in bone differs significantly from cartilage, with various cell types like osteoblasts, osteoclasts, chondrocytes, endothelial cells, and mesenchymal stem cells. Osteoblasts, responsible for hydroxyapatite production, constitute 4-6% of total bone tissue cells and are typically found on the bone's surface (Vashishth, Gibson, Kimura, Schaffler, & Fyhrie, 2002). The hydroxyapatite minerals in the structure are the key component of the inorganic portion that hardens the bone (Stewart & Kawcak, 2018). The proportion of hydroxyapatite minerals in the osteochondral intermediate surface is greater than in the calcified tissue (Y. Zhang et al., 2012).

The mechanical properties of subchondral bone show depth-dependent complexity, which contributes to its multifaceted role in the joint biomechanics (Walker, Kawcak, & Hill, 2013). The changes in compressive and tensile modulus across the layer emphasize the dynamic response to mechanical demands, which include deep region stiffness for compressive resistance and surface flexibility for absorbing tensile stress. This regulation of mechanical properties enhances bone's ability to maintain joint integrity, promote optimal load distribution, and contribute to the overall joint function (Madry, van Dijk, & Mueller-Gerbl, 2010).

Nerves and blood vessels are located in the subchondral bone, which is located under the cartilage. These properties help blood flow and supply the cartilage with nutrients including glucose, oxygen, and water. The blood supply of these canals and ampoules provides the cartilage with approximately 50% of its nutritional needs. The flow of synovial fluid, the lubricating fluid in the joint, into the cartilage provides the remaining nutrients (Madry et al., 2010; Pan et al., 2009).

In cartilage and subchondral bone, alterations in chondrocyte populations and extracellular matrix components are detected. The number of chondrocytes and type II collagen levels decrease, while proteoglycans, type I collagen, and hydroxyapatite compounds increase. Subchondral bone is composed of subcartilaginous plates and trabeculae and plays a vital role in promoting joint function, reducing mechanical stress, and providing nutrients to adjacent cartilage. Consequently, preserving the health of the subchondral bone appears to be a decisive factor in the successful healing of cartilage defects (Neogi et al., 2010; Orava et al., 2022).

2.2 Osteochondral Defects

The avascular nature of articular cartilage, coupled with its sparse cellular density, severely limits its regenerative potential, making its healing capacity significantly lower than that of other body tissues. Unlike well-vascularized tissues such as skin or muscle, articular cartilage faces limitations in access to oxygen, nutrients, and immune cells. In addition, the lack of chondrocytes, the cells of cartilage, in its extracellular matrix contributes to its limited ability to self-renew. These chondrocytes are sparsely distributed in the tissue, which prevents their migration to the site of injury and prevents the initiation of a strong healing response (Temenoff & Mikos, 2000). Therefore, when articular cartilage is damaged or develops defects, its avascularity and low cell density inhibit the healing process. The limited availability of essential resources and the constrained cellular response impede the formation of fresh cartilage tissue, ultimately obstructing the restoration of both structural and functional integrity.

Osteochondral defect (OCD) is a small focal area of damage to the subchondral bone and articular cartilage. The osteochondral complex is made up of two main parts: which are articular cartilage and subchondral bone. These two components are inextricably linked and constitute an interconnected and integrated framework. Damage often causes these defects to occur simultaneously. Any damage to the articular cartilage and underlying bone is referred to as an osteochondral defect. Early diagnosis and treatment of OCD are essential to improve the outlook for motor function and prevent the progression of osteoarthritis (Ochi et al., 2001).

Osteochondral defects are a frequent issue that can result from trauma, age, or genetic factors. Treating these defects is a major challenge in clinical practice, and if they are neglected, they may lead to the development of degenerative disorders such as osteoarthritis, which can have a serious effect on a person's well-being (Baumann, Hinckel, Bozynski, & Farr, 2019). Successful management of OCD in orthopedic surgery is complicated by the inherent inability of cartilage tissue to heal naturally. Innovative approaches are essential for effective treatment. Early identification and intervention are vital to improve motor function and prevent osteoarthritis, as OCD often occurs alongside injuries (Redman, Oldfield, & Archer, 2005). The grading system for osteochondral (OC) tissue defects serves the objective of assessing the severity of the injury and guiding the selection of suitable treatment options (Acebes, Roman-Blas, Delgado-Baeza, Palacios, & Herrero-Beaumont, 2009).

Table 2.1 Grading system for OC tissue defects

Grade	Description
0	Normal chondral tissue is smooth and has a uniform appearance. There are no defects or irregularities.
1	Swelling and softening of chondral tissue is characterized by a loss of firmness and elasticity. The cartilage may also appear discoloured.
2	Partial thickness chondral defects involve damage to the superficial layer of cartilage. The defect does not extend to the subchondral bone.
3	Full-thickness chondral defects involve damage to the entire thickness of cartilage. The defect extends to the subchondral bone.
4	OCD causes destruction to the whole cartilage thickness including the subchondral bone. The deficiency may potentially affect the soft tissues beneath.

2.2.1 Osteoarthritis (OA)

Osteoarthritis is the most prevalent and debilitating form of arthritis, affecting a considerable portion of the global population. The global prevalence of this condition is estimated to impact more than 7% of the world's population, encompassing approximately 500 million individuals. In the United States alone, around 32.5 million people are affected by it (Zhao et al., 2019). Consequently to the World Health Organization (WHO), around 25% of persons with osteoarthritis have difficulties doing daily chores, and 80% have restricted mobility (Hunter, March, & Chew, 2020). This number is expected to increase as the population ages and the number of obesity increases (Lementowski & Zelicof, 2008; A. R. Sun et al., 2021).

Table 2.2 Risk factors of OA

Risk Factor	Description
Age	More common in people over the age of 50
Crystals	In joint fluid or cartilage
Bone mineral density	Individuals with high bone mineral density are more likely to develop osteoarthritis in their hips
Immobilization	Individuals who have been immobilized for a long time are more likely to develop osteoarthritis
Joint injury	An injury to a joint can damage the cartilage and make it more susceptible to osteoarthritis.
Joint hypermobility	Individuals with joint hypermobility or instability have joints that are more flexible than normal.
Obesity	Major risk factor for osteoarthritis, especially in weight-bearing joints.
Peripheral neuropathy	Difficult to control the joints, thereby increasing the strain on cartilage.
Occupational or sports stress	Individuals who engage in activities that exert significant strain on their joints are at an increased risk of developing osteoarthritis.

Those who participate in activities that place a substantial amount of stress on their joints are more likely to develop osteoarthritis, limiting their daily activities. This not only affects the quality of life of individuals but also imposes a financial burden on society due to health costs and reduced productivity (Loeser, 2010). Several factors can influence the development of OA, such as type of work, participation in sports activities, previous musculoskeletal injuries, overweight or obesity, and gender-related factors. These factors affect the likelihood that people will develop OA (Hunter & Bierma-Zeinstra, 2019). The presence of one or more of these risk factors does not assure the onset of osteoarthritis. However, they may heighten the chances of experiencing symptoms. Additionally, the influence and presence of these risk factors can differ among individuals and the specific joints involved.

OA results from a disruption of the normal balance between catabolic and anabolic processes in joint tissues, with increased innervation of subchondral bone contributing significantly to pain; In a healthy joint, a balance is typically maintained between the breakdown (catabolism) and synthesis (anabolism) of joint components such as cartilage, bone, and synovial fluid, but this balance is disrupted in OA (Arden & Nevitt, 2006).

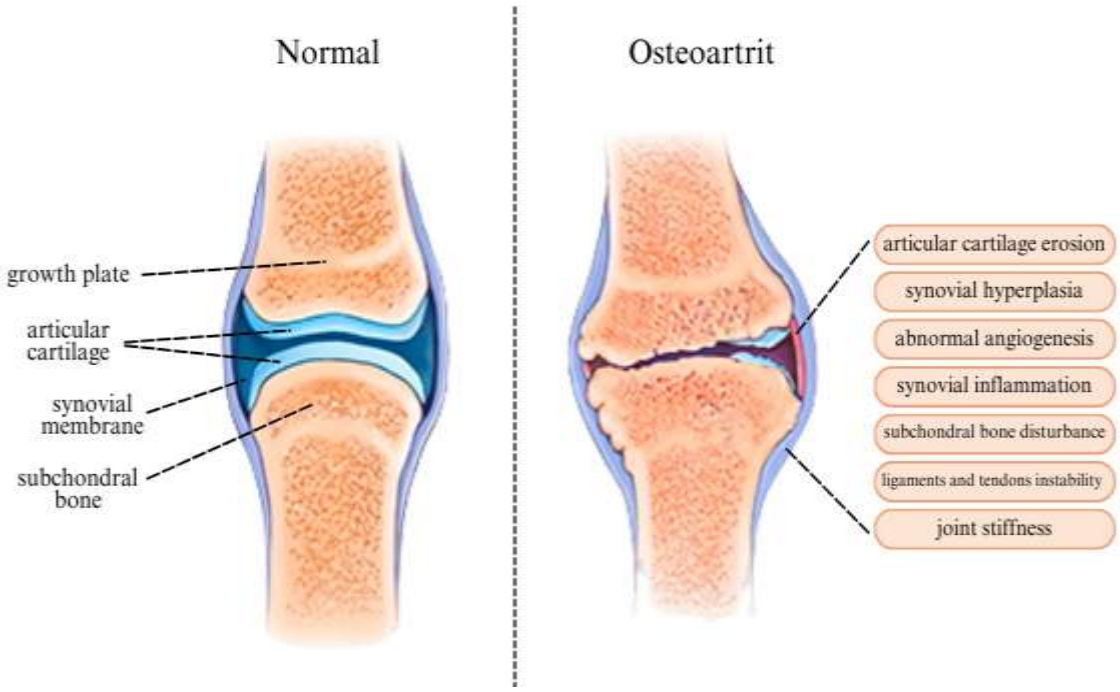

Figure 2.2 Comparison of healthy knee joint and osteoarthritis

In osteoarthritis, the hyaline cartilage eventually deteriorates, a process often linked to the depletion of its proteoglycan and collagen components that provide structure and resilience. As the cartilage diminishes, the underlying bone may be exposed, resulting in direct bone-to-bone contact within the joint, resulting in pain, inflammation, and limited function. Various factors, including joint mechanical stress, genetic susceptibility, inflammation, and metabolic imbalances, contribute to this cartilage breakdown, upsetting its equilibrium and leading to a greater breakdown relative to repair and synthesis. It is noteworthy that the most common joint type in the human body is the cartilage joint, which includes joints such as the knee, hip, and shoulder (Scott, Smith, Lohmander, & Chard, 2003).

OA, the involvement of the subchondral bone is regarded as one of the primary causes of pain. Changes in the subchondral bone, such as microcracks, increased vascularity, and nerve growth, can activate and sensitize pain-sensing nerves as OA progresses. This may cause pain and discomfort within and around the affected joint (Wei & Dai, 2021).

The progression of osteoarthritis is characterized by the destruction of the osteochondral junctions that connect cartilage and bone, with changes such as microcracks, the duplication of the tidemark boundary, and blood vessel/nerve growth. Importantly, osteoarthritis affects not only cartilage, but also synovium, subchondral bone, ligaments, and meniscus, which can worsen symptoms and progress the disease.

2.3 Treatment for OC Defects Repair

Given hyaline cartilage's limited regenerative capacity, addressing osteochondral defects requires diverse therapeutic approaches. Successful management involves a comprehensive strategy targeting both cartilage and bone components of the osteochondral unit. The healing disparity between non-vascular cartilage and well-vascularized bone introduces recovery variations. The intricate osteochondral architecture poses challenges in regenerative medicine research design (Camarero-Espinosa et al., 2016; Kwon et al., 2019).

Surgical techniques are necessary to alleviate pain, repair damaged tissue, and restore joint motion. The selection of surgical intervention is influenced by the degree of symptomatology, the size of the lesion, and its severity, which can be evaluated using the ICRS or Outerbridge classification systems. Additionally, the patient's general health condition is taken into consideration (Jack Farr & Gomoll, 2018). Currently, the most common methods utilized in clinical settings include autologous chondrocyte implantation (ACI), matrix-induced autologous chondrocyte implantation (MACI), microfracture, as well as the application of autografts and allografts (Revell & Athanasiou, 2009). ACI and MACI are surgical strategies involving the extraction of a patient's own healthy chondrocytes, which are then cultured, isolated, and expanded on a supporting matrix for several weeks before being transplanted into the damaged area (Bartlett et al., 2005).

Table 2.3 summarizes the different traditional treatments for osteochondral defects

Traditional Treatment Methods	Description
Autologous chondrocyte implantation (ACI)	Healthy cartilage cells are extracted from another location of the patient's own body and implanted in the affected part.
Matrix-induced autologous chondrocyte implantation (MACI)	Before implantation, cartilage cells are generated on a biodegradable scaffold.
Microfracture	Small holes are drilled into the bone below the damaged cartilage.
Autografts	Pieces of cartilage taken from another part of the patient's body are transplanted to the damaged area.
Allografts	Pieces of cartilage taken from a cadaver are transplanted to the damaged area.

However, a noteworthy drawback is the tendency for these techniques to foster the development of fibrocartilage primarily composed of type I collagen, leading to limited long-term durability. Additionally, these methods are unable to effectively address osteochondral lesions extending into the subchondral bone (Niemeyer et al., 2008).

Microfracture is a surgical technique for osteochondral defects smaller than 1 cm2, involving the creation of small perforations in cartilage and subchondral bone to stimulate mesenchymal stem cell migration for tissue formation. However, recent comparative studies suggest its efficacy in delaying cartilage degeneration is limited to the short term, despite continued recommendations by the FDA and medical professionals. Effectiveness tends to decrease beyond five years post-surgery, regardless of lesion size (Goyal, Keyhani, Lee, & Hui, 2013; Gudas et al., 2013). This method results in the development of fibrocartilage and provides therapeutic benefits for approximately one year (Gilbert, 1998; A. M. Yousefi, Hoque, Prasad, & Uth, 2015).

Mosaicplasty is an alternative method that involves the transfer of autologous osteochondral tissue plugs from healthy non-weight-bearing areas to the damaged area. However, mosaicplasty has limitations due to the availability of donor sites and the risk of complications at the donor site (Getgood, Brooks, Fortier, & Rushton, 2009).

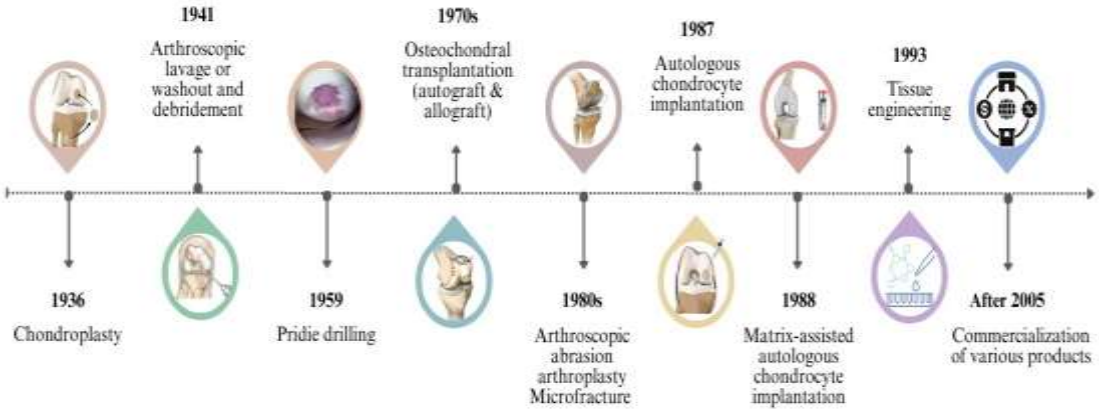

Figure 2.3 Progress in the treatment of osteochondral lesions

Allografts offer a versatile option for addressing significant defects, typically ranging from 1 to 4 cm^2 in size. However, they can potentially address larger osteochondral defects, they come with certain disadvantages, including the risk of immune rejection, restricted fusion with the recipient's tissue, and the risk of disease transmission and compromised cell viability (Sandra Camarero-Espinosa, Barbara Rothen-Rutishauser, E. Johan Foster, & Christoph Weder, 2016; H. T. Kim, Teng, & Dang, 2008). Total joint

replacement, an invasive treatment used predominantly for cases of severe osteoarthritis, is not permanent due to implant wear and the possibility of revision surgery. Autografting is hampered by the limited availability of donor tissue, donor site complications, and graft fixation difficulties, as well as the risk of long-term instability and suboptimal integration with native cartilage. Existing surgical techniques for osteochondral defects have limitations, necessitating additional research into innovative and long-lasting treatment options (Alford & Cole, 2005).

Evidently, the existing surgical treatments do not offer enduring resolutions for cartilage regeneration. Tissue engineering has developed as a supplementary option to standard medical treatments for speeding osteochondral injury healing. Given the constraints of existing treatment options, tissue engineering strategies have garnered significant research attention (J. Yang, Zhang, Yue, & Khademhosseini, 2017).

2.4 Tissue Engineering

The global demand for organ and tissue transplantation has arisen due to prevalent organ and tissue loss. This procedure involves autogenic transplantation using the patient's own tissue and allogenic transplantation using donor tissue. However, the persistent challenge of growing patient waitlists for transplantation is influenced by three key factors. Firstly, the limited availability of autologous tissue poses constraints. Secondly, finding suitable allogeneic donors is complex due to the scarcity of willing contributors. Lastly, concerns regarding immune responses in allogeneic transfers persist, as the recipient's immune system might react against the transplanted allogeneic tissue. Therefore, trying to completely restore the entire organization and its functions is a big challenge (Furth & Atala, 2014).

The field of tissue engineering (TE) is currently making significant progress, driven by the need to overcome limitations associated with conventional therapies. This interdisciplinary field integrates engineering and life science principles with the aim of creating biological substitutes to regenerate, perpetuate, or enhance tissue functionality. Tissue engineering involves the integration of cells and scaffolds together, with the aim

of creating structures that efficiently restore and maintain the internal structure and operational capabilities of damaged tissues and organs (Knight & Evans, 2004). (Knight & Evans, 2004). This scientific discipline is primarily concerned with the development of functional and sustainable tissues or organs that can be utilized for transplantation or regeneration purposes. The fundamental constituents of TE are cells, biomaterials, and signaling molecules, commonly referred to as growth factors (Furth & Atala, 2014; Dietmar W. Hutmacher, 2000; Langer & Vacanti, 1993).

The target tissue is taken into consideration when choosing the right kind of cells for tissue engineering. These cells may come from a number of places, including the patient's own tissues (autologous cells) or from donors (allogeneic cells). Particularly stem cells have attracted a lot of interest in tissue engineering because of their extraordinary capacity to specialize into multiple cell types, making them useful and adaptable for rebuilding different tissues (Larson et al., 2019; J. Y. Park et al., 2014). The success of tissue engineering also depends on biomaterial selection. The unique morphological, chemical, and mechanical properties of diverse biomaterials require careful alignment with the intended tissue characteristics (Ghassemi et al., 2018).

Also, growth factors, which are pivotal signaling molecules governing an array of biological functions including cellular division, migration, and proliferation, are strategically integrated into cells or biomaterials to evoke targeted responses. This capacity empowers tissue engineers to orchestrate cellular behavior and tissue maturation by judiciously selecting appropriate growth factors. For instance, growth hormones hold the potential to guide stem cells toward specific differentiative pathways crucial for tissue regeneration (Ren, Zhao, Lash, Martino, & Julier, 2020).

In addition, multidisciplinary research teams with expertise in biology, engineering, medicine, and regulatory affairs are essential for successfully navigating the complex path from the laboratory to the clinic. By overcoming these obstacles, tissue engineering can realize its maximum potential to revolutionize healthcare and provide innovative treatments for patients with tissue and organ deficiencies (Ashkan Shafiee & Atala, 2017).

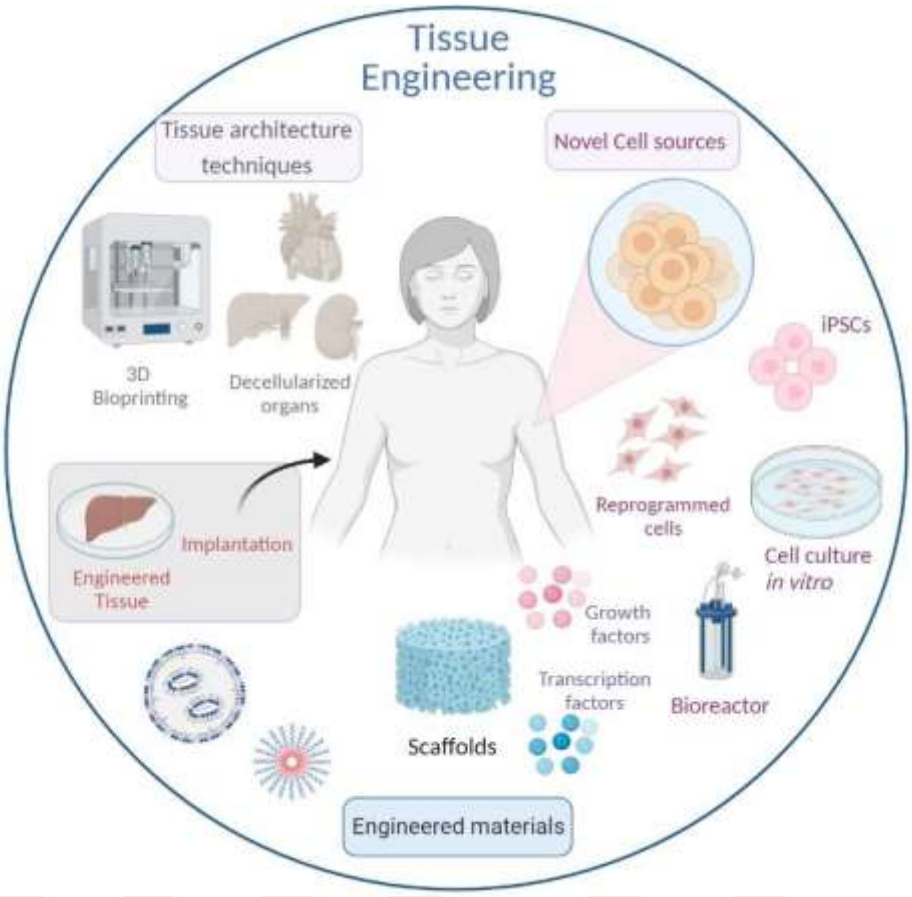

Figure 2.4 Illustration of tissue engineering

2.4.1 Osteochondral tissue engineering

One of the strategies of tissue engineering is osteochondral tissue engineering. Osteochondral tissue engineering is a regenerative medicine discipline that focuses on developing artificial or engineered tissues to repair or replace injured osteochondral units, which are made up of both cartilage and bone components. This method is especially useful for treating joint conditions like osteoarthritis that damage both the underlying bone and the cartilage (H. T. Kim et al., 2008). Since its emergence in the 1990s, OC tissue engineering has made impressive progress and constantly evolving subject in which novel technologies, improved biomaterials, and unique structures have evolved in recent years also because of the rising numbers of osteoarthritis (OA) patients, this field has drawn great interest from researchers over the last decade.

Such advancements have addressed some of the limits of previous techniques, but new issues have also emerged. The exciting advancement in this subject has resulted in the development of superior scaffolds that better resemble the original tissue environment, resulting in greater tissue regeneration capabilities. Moreover, the incorporation of advanced biomaterials has enhanced the mechanical resilience and biological functionality of the scaffolds, promoting enhanced cell proliferation, adhesion, and differentiation (Turnbull et al., 2018).

In osteochondral tissue engineering, the utilization of multiple scaffold phases has been found to enhance the likelihood of successful osteochondral unit formation. The process of regenerating osteochondral tissue is intricate, as it encompasses multiple tissue elements, including cartilage, subchondral bone, and the transitional region between them. Cartilage and bone exhibit unique mechanical, structural, and chemical characteristics, adding complexity to the task. To achieve favorable outcomes, it is imperative to construct a scaffold with precision and select cells that align with the targeted tissue properties (Qiu Li Loh & Cleo Choong, 2013).

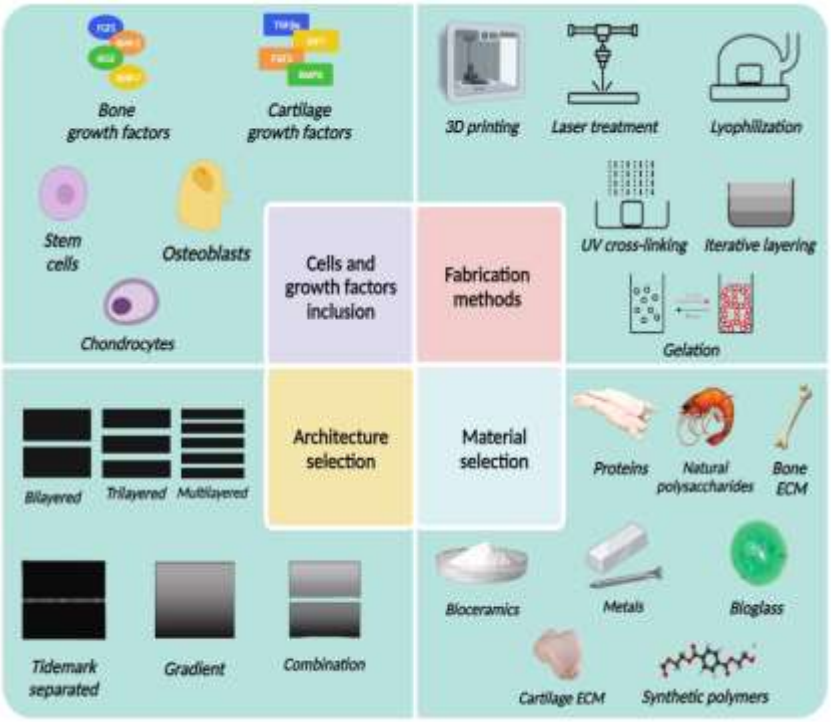

Figure 2.5 Decision-making procedure during the creation of osteochondral tissue scaffold

Despite the great potential of tissue engineering for healing osteochondral tissues, its complexity, which involves multilayer scaffolds and diverse cell types, offers obstacles. Significant progress has been achieved, but new hurdles exist, notably in scaffold design. Current regenerative approaches are limited in providing long-lasting, complete regeneration due to factors like aging, obesity, genetics, and injuries. Nevertheless, various tissue engineering methods, encompassing biomaterials, cells, scaffold architecture, and fabrication techniques, have emerged in recent decades. These advancements offer practical pathways to create implantable structures that hold promise for superior clinical outcomes.

2.4.1.1 Cells in osteochondral tissue engineering

The careful selection of appropriate cells for integration into osteochondral repair scaffolds is a critical step in tissue engineering. This decision significantly influences the success and functionality of the engineered tissue. Factors like the intended application, research stage (in vitro or in vivo), ethical considerations, cell availability, and regulatory approval play a role in determining the suitable cell type. Additionally, considering the cell's ability to adhere to the scaffold, survive, proliferate, and integrate with the host tissue is crucial during the selection process (Graceffa et al., 2019).

Osteochondral repair commonly relies on two types of cells: progenitor cells and tissue-specific cells. Conventionally, tissue-specific primary cells, such as chondrocytes for instance, encourage the creation of more functioning cartilage tissue, and osteoblasts are used in cartilage and bone tissue engineering since they are native to these tissues and promote tissue-specific regeneration. However, there are limitations to using chondrocytes. They are present in limited numbers in the body, making their translational application challenging, as they constitute less than 5% of cartilage volume. Moreover, isolating chondrocytes is a difficult task due to the need for thorough collagenase digestion, which can have adverse effects on the cells (Graceffa et al., 2019). Furthermore, the use of chondrocytes is further discouraged by their susceptibility to losing their phenotype during the culture and expansion process (Huckle et al., 2003). Also, the isolation and cultivation of primary cells present certain challenges, including

time consumption, cost, and the potential for cell dedifferentiation (Darling & Athanasiou, 2005).

Stem cells provide a vital and advantageous cell source for osteochondral tissue engineering, showing promising regenerative potential in addressing osteochondral defects. One of the most notable benefits is their ability to be extracted from the patient's own body therefore this feature is particularly valuable, as it mitigates the risk of immune rejection. Consequently, stem cells offer an extremely promising path for the advancement of osteochondral tissue engineering. Offering a range of benefits that make them an attractive option for researchers and clinicians alike (Barry & Murphy, 2004). Stem cells can be employed in two distinct ways: either directly injected into the bloodstream or tissues, or combined with supporting scaffolds.

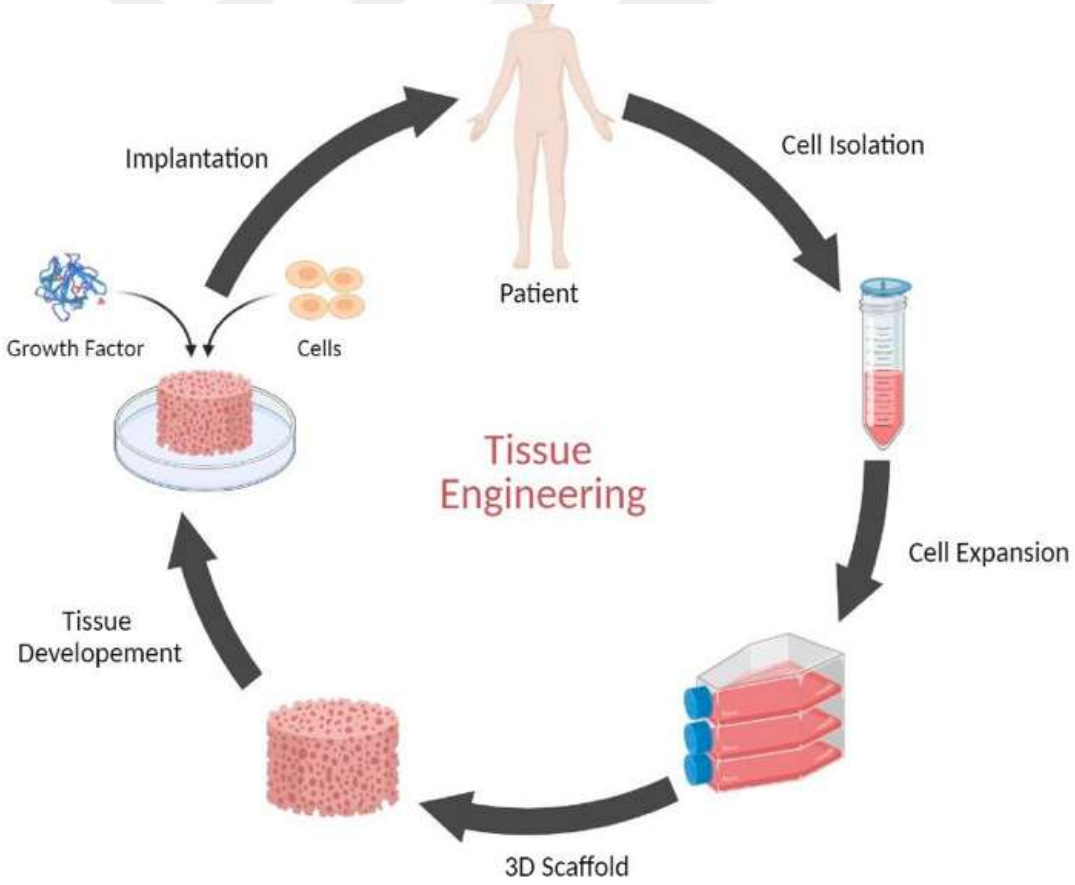

Figure 2.6 Schematic of using cells in tissue engineering

These stem cell-based approaches are considered highly promising in overcoming the limitations of ACI therapies. In contrast to primary differentiated cells, stem cells may multiply and differentiate into particular cells, depending on their potential and source. This remarkable versatility renders stem cells a potentially potent tool for promoting tissue regeneration in osteochondral repair (Y. Liu, Shu, & Prestwich, 2006).

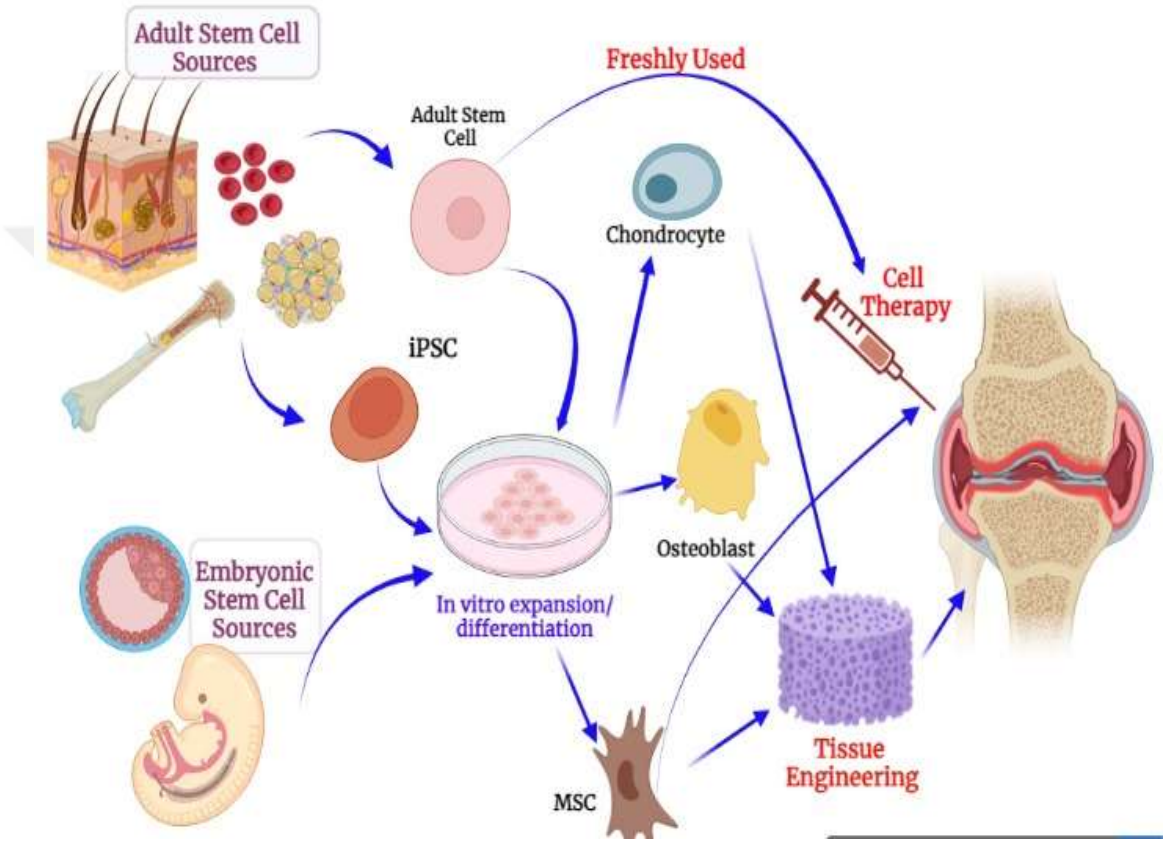

Figure 2.7 Utilization of Stem cells in osteochondral defects

Table 2.4 Stem Cells in Osteochondral Tissue Engineering

Cell resource	Cell type	Characteristics	References
Stem cells	Umbilical cord MSCs	Enhance the integration between tissue and scaffold. Multipotency characteristic	(Baksh, Yao, & Tuan, 2007; M.-Y. Chen, Lie, Li, & Wei, 2009)
		Rapid rates of proliferation, enhanced expansion potential, and extensive multipotency	
		Simple isolation and culture, non-invasive and easy obtainment, low-cost and high efficiency	
	Amniotic fluid–derived stem cells	When encapsulated in a 2% alginate solution, has the capacity to develop into osteoblasts and chondrocytes.	(Bajek et al., 2014; Kolambkar, Peister, Soker, Atala, & Guldberg, 2007)
		The differentiation process is controlled by growth factors such as TGF-, IGF-1, and EGF, and follows the normal pattern reported for mesodermal-derived cells.	
		Do not require a specialized medium for osteochondral differentiation and generate a protein-rich extracellular matrix (ECM).	
	Synovium-derived MSCs	Possess the remarkable capability to differentiate into both osteoblasts and chondrocytes.	(Sasaki et al., 2018; Zheng et al., 2015)
		Bone marrow-derived mesenchymal stem cells (MSCs) are marginally more effective in forming bone formation, but they make up for this with their exceptional ability to seamlessly integrate with the chondrogenic differentiation performance	
		Ability to integrate into the neighbouring cartilage, contributing to its overall structure and function	

Table 2.4 Stem Cells in Osteochondral Tissue Engineering (continue)

Cell resource	Cell type	Characteristics	References
Stem cells	Adipose tissue-derived MSCs	They demonstrate an enhanced ability for osteogenic differentiation achieved via allylamine modification, which notably prompts a strong inclination of these cells to develop into osteoblasts, essential for bone formation.	(Chaves, Alshomer, Palgrave, & Kalaskar, 2016; Griffin et al., 2017; Murata, Fujimoto, & Nakayama, 2020)
		The presence of chemical groups like NH2 and COOH significantly affects the behavior of these cells, distinctly influencing their specialization into either cartilage-forming (chondrogenic) or bone-forming (osteogenic) lineages.	
	Bone marrow-derived MSCs	Possess the capacity to differentiate into either cartilage or bone lineages, avoiding the creation of fibrous tissue	(Y. Sun et al., 2018; Y. Xiao, Mareddy, & Crawford, 2010)
		Commonly employed, the process of obtaining them involves significant invasiveness	
		They seamlessly integrate with surrounding tissues and elicit a minimal immune response from the host.	
Tissue-specific cells	Chondrocytes	Make up cartilage and are responsible for its mechanical stability.	(Tallheden et al., 2005; Tallheden et al., 2004)
		Can dedifferentiate, which means they can revert back to a more primitive state and be expanded in culture.	
		Can integrate well into the surrounding tissue.	
		Excel in forming functional cartilaginous tissue	
		Exhibit both clinical and histological stability.	
	Osteoblasts	Show heightened SPP1 mRNA expression.	(Graceffa et al., 2019; K. Hu & Olsen, 2016; Komori, 2016, 2019)
		VEGF produced by osteoblasts supports bone healing and balance.	
		The increase in RUNX2 is followed by a decrease upon maturation.	

In recent times, there has been a significant body of both laboratory and live studies aimed at examining the potential of specific stem cells to undergo chondrogenic and osteogenic differentiation. The primary objective of these research endeavors has been to unravel the mechanisms that govern the conversion of stem cells into chondrocytes and osteoblasts and to identify the elements that influence this differentiation and maturation process. These stem cells include BMSCs, ADSCs, UCMSCs, and AFSCs, among others these, mesenchymal stem cells (MSCs) are particularly favored (Berg et al., 2009; Y. Liu et al., 2006; Natesan, Baer, Walters, Babu, & Christy, 2010).

Although some positive results have been seen in preliminary clinical trials and preclinical studies, it is essential to note that stem cell treatments for osteochondral abnormalities are not yet well-established or widely accepted as a standard of therapy. This approach is currently being researched.

2.4.1.1.1 Mesenchymal stem cells for osteochondral tissue engineering

Mesenchymal stem cells (MSCs) have a pivotal function in tissue repair and regeneration through their interactions with the immune system, moving to injury sites, reducing inflammation, supporting tissue healing, and exhibiting extraordinary differentiation and replication capacity. Because of their distinctive characteristics, MSCs possess significant promise for a wide array of regenerative medicine therapies and tissue engineering (Song, Baksh, & Tuan, 2004).

The ability of MSCs to be develop into cartilage, tendon, synovium, bone marrow cells has led to encouraging findings in a variety of tissues. This extensive availability of cell sources facilitates their accessibility and viability for clinical applications. MSCs are cells with elongated shapes, malleable adhering qualities, and a variety of capacities, including anti-inflammatory, anti-apoptotic, antifibrotic, and immunomodulatory abilities (Dominici et al., 2006).

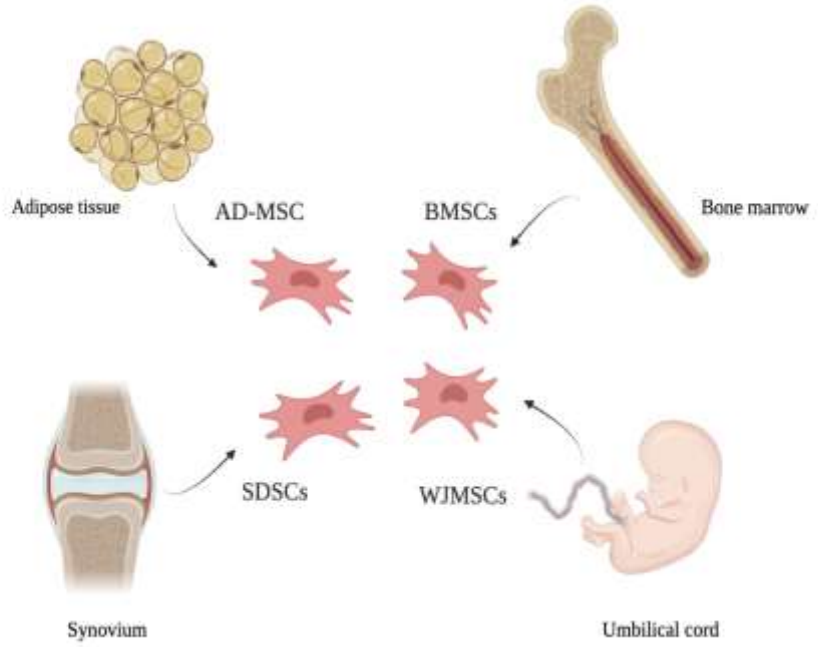

Figure 2.8 The schematic representation of sources of mesenchymal stem cells

Despite their comparable morphology, MSCs exhibit distinct biological functions that account for their heterogeneous capacities for cartilage repair. They possess an exceptional potential for transforming into chondrocytes, the key cells responsible for creating and sustaining cartilage, making them uniquely capable of generating fresh cartilage tissue within specific environments and under the influence of growth-inducing factors. When introduced into an osteochondral defect, MSCs can differentiate into chondrocytes, producing vital components like collagen II and aggrecan crucial for cartilage repair, while also concurrently undergoing osteoblastic differentiation to accelerate the regeneration of injured bone tissue (Steck et al., 2005). The dual capacity of MSCs to promote the restoration of both bone and cartilage renders them highly promising in the field of regenerative medicine, especially in addressing issues with osteochondral structures (Boeuf & Richter, 2010).

The paracrine function of MSCs is of paramount importance in chondrogenesis, as they release signaling molecules that exert a diverse range of effects on neighboring cells. These effects include the reduction of cell death and inflammation, the enhancement of cell growth and mobility, and the promotion of cartilage formation. These findings hold

significant value for researchers and medical practitioners engaged in the development of regenerative therapies for conditions characterized by cartilage deterioration or loss (Ahmed & Hincke, 2010). In addition, MSCs have a robust capacity for self-renewal and proliferation, which is essential for generating the sufficient cell population required for the repair of chondral wounds. This is because a large number of cells are often needed for successful cartilage restoration. The interaction between chondrocytes and other MSCs, as well as the regulation of vital cellular processes like cell survival, differentiation, and migration, are all controlled by this freshly formed ECM (Gazit, Pelled, Sheyn, Kimelman, & Gazit, 2011). Additionally, the ECM has a role in tissue remodeling, which is the process of modifying or adapting tissues, as well as tissue morphogenesis, which is the process of creating new tissues.

The knowledge of how MSCs promote chondrogenesis is helping to pave the way for new treatments for cartilage loss and degeneration. Their paracrine activity guides chondrogenesis by significantly reducing cell apoptosis and inflammation, while simultaneously promoting cell proliferation and mobilization (da Silva Meirelles, Fontes, Covas, & Caplan, 2009). Notably, among these molecules, TGF-β and BMP-2 stand out, as they both promote the differentiation of MSCs into chondrocytes, which are responsible for producing cartilage, also stimulate the production of the cartilage matrix (Ahmed & Hincke, 2010). IGF-1 is another important signalling molecule released by MSCs; it supports essential processes like cell proliferation and mobility, crucial for cartilage repair and regeneration (Gugjoo et al., 2017).

Additionally, HGF serves as a protective factor for chondrocytes by preventing apoptosis, or programmed cell death, thereby contributing to the overall health and maintenance of cartilage tissue (Toh, Foldager, Pei, & Hui, 2014) (TABLE). This understanding holds significance for researchers and medical practitioners working on regenerative solutions for conditions marked by cartilage loss or degeneration.

Table 2.5 Signalling molecules that MSCs release to promote chondrogenesis

Signalling molecules	Functions
TGF-β	Promotes the differentiation of MSCs into chondrocytes and the production of cartilage matrix. Also, can modulate the immune response, induce fibrosis.
BMP-2	Promotes the differentiation of MSCs, enhance the production of cartilage matrix, stimulates cell proliferation and mobility, protects chondrocytes from apoptosis, and modulates the immune response.
IGF-1	Promotes cell proliferation and mobility, which are essential for cartilage regeneration. Stimulates the growth of cartilage and bone by promoting the differentiation, proliferation, and of chondrocytes and osteoblasts.
HGF	Helps to protect chondrocytes from apoptosis, or programmed cell death.

The optimization of MSCs' differentiation into chondrocytes requires specific culture conditions, including serum-free environments and scaffold materials. During differentiation, MSCs help form in the development of a cartilaginous matrix, which regulates interactions, cellular processes, tissue remodeling, and morphogenesis.

2.4.1.1.2 Bone marrow derived mesenchymal stem cells (BMSCs)

Bone marrow-derived mesenchymal stem cells (BMSCs) represent a prominently researched cell type in the field of cartilage tissue engineering. Even though bone marrow aspiration is a relatively invasive and painful procedure, it is important to recognize that BMSCs, a type of MSCs derived from bone marrow, have been identified as a highly promising cell source for the regeneration of cartilage tissue. Numerous studies have demonstrated the potential of BMSCs when implanted onto a compatible scaffold with chondrogenic inducers. Multiple researchers have demonstrated that these cells undergo chondrogenesis and generate ECMs predominantly constituted of aggrecan, collagen type II, and collagen type VI (A. He et al., 2017; Toh et al., 2014).

BMSCs possess the same immunomodulatory properties as other MSCs, enabling them to efficiently regulate the immune response and diminish inflammation. This attribute positions BMSCs as promising candidates for transplantation and engraftment procedures. Their ability to secrete numerous immunomodulatory factors, such as cytokines and growth factors, is responsible for BMSCs' ability to modulate the immune system. These factors can inhibit immune cell activation and proliferation, reducing inflammation and fostering tissue repair. Therefore, BMSCs have tremendous therapeutic potential for a variety of immune-related disorders (Y. Sun et al., 2018). The findings highlight the necessity for further study into the usage of BMSCs for cartilage tissue regeneration. To improve the area of regenerative medicine, it is essential to continue researching the potential of BMSCs in this field.

2.4.1.1.3 Adipose-derived MSCs

MSCs from a variety of sources, including bone marrow, adipose tissue, placenta, umbilical cord, and Wharton's jelly, have been subject to in-depth assessment and investigation. Adipose tissue has emerged as a remarkably reliable and conveniently accessible source of MSCs within the human body. This recognition is primarily attributed to its significant yield, ease of acquisition through minimally invasive techniques such as liposuction, and the absence of ethical concerns associated with its extraction. Notably, adipose-derived MSCs, obtained with minimal disruption to the donor site, result in negligible patient discomfort (Dragoo & Chang, 2017).

Adipose-derived stem cells (AD-MSCs) have garnered significant attention due to their potential therapeutic benefits (Puetzer, Petitte, & Loboa, 2010). Based on scientific studies, it has been shown that adipose-derived mesenchymal stem cells exhibit certain benefits in comparison to BMSCs. Adipose-derived stem cells are found in abundance, accounting for approximately 5% of nucleated cells, while BMSCs make up only 0.0001-0.01% of cells. This substantial disparity in quantity renders the extraction of adipose-derived MSCs more easily accessible and straightforward for both research purposes and therapeutic use (Zhu et al., 2008).

AD-MSCs exhibit remarkable immunomodulatory qualities when compared to BMSCs, which can be ascribed to their increased production of factors such as interleukin-6 (IL-6) and transforming growth factor-beta 1 (TGF-β1) (C.-y. Li et al., 2015). Furthermore, AD-MSC which the reduced immunogenicity of renders them a secure option for allogeneic transplantation, thereby mitigating the likelihood of unfavorable reactions such as inflammation and rejection (Nakao et al., 2010).

It has been shown that when AD-MSC cells age, their ability for differentiating diminishes therefore, indicating a possibility for sustained regenerative capacities. Additionally, these cells have been found to possess enhanced immunosuppressive properties, suggesting their potential use in therapeutic interventions aimed at modulating immune responses. Furthermore, it is evident from growth curves, cell cycle analysis, and telomerase activity assessments that they have a higher capacity for proliferation (Tsuji, Rubin, & Marra, 2014).

Table 2.6 Comparison table of AD-MSCs and BM-MSCs Characteristics

Characteristic	**AD-MSCs**	**BM-MSCs**
Origin	Adipose tissue	Bone marrow
Availability	More abundant	Less abundant
Isolation	Less invasive	More invasive
Expansion	Easier	More difficult
Differentiation potential	Multipotent	Multipotent
Immunogenicity	Less immunogenic	More immunogenic
Safety	Considered safe for use in humans	Considered safe for use in humans
Clinical applications	Cartilage repair, bone regeneration, wound healing, heart disease, neurological disorders	Cartilage repair, bone regeneration, wound healing, heart disease, neurological disorders

Previous research has also demonstrated the capacity of AD-MSCs to differentiate into osteogenic or chondrogenic lineages under suitable culture environment. Additional

investigation is required to have a comprehensive understanding of the possible applications of adipose-derived mesenchymal stem cells within therapeutic environments (H. J. Kim & Im, 2009; Mei et al., 2017) (Fig 2.19).

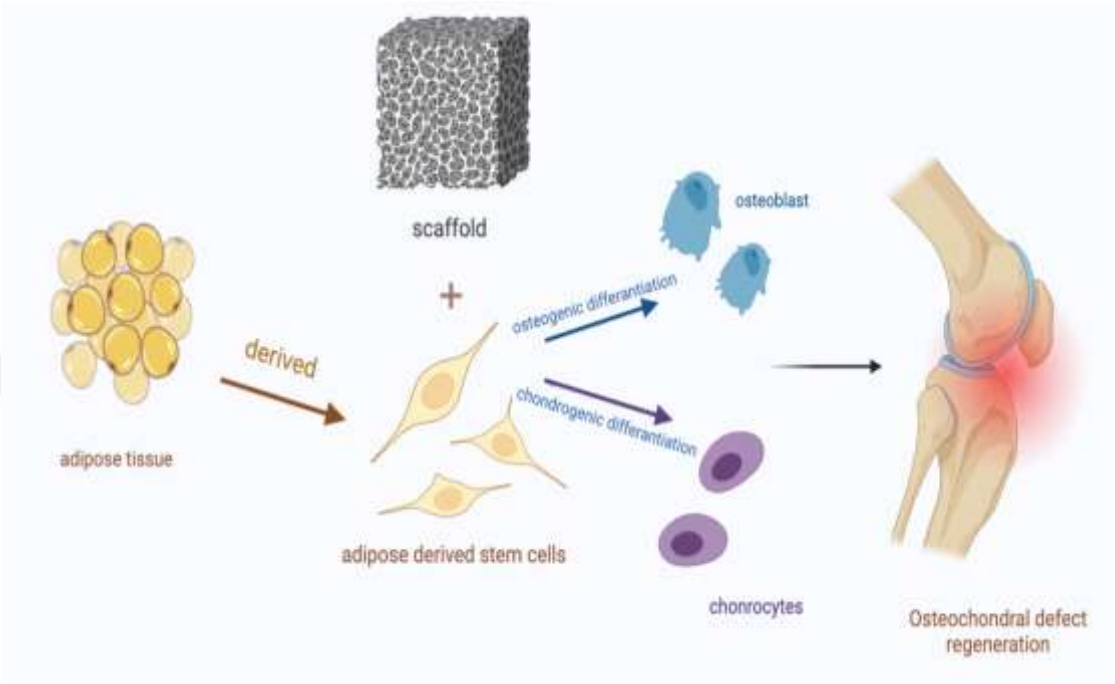

Figure 2.9 The differentiation of AD-MSCs into chondrogenic and osteogenic cells and their use in osteochondral tissue engineering

The differentiation of adipose-derived stem cells into chondrocytes is significantly impacted by the culture conditions, similar to osteogenesis. Usually, in standard procedures, researchers utilize growth factors obtained from the transforming growth factor-beta (TGF-β) to promote the chondrogenesis process (Worster, Nixon, Brower-Toland, & Williams, 2000; X. Yang et al., 2001).

Immunohistological staining of type II collagen or the expression of glycosaminoglycan in the regenerated tissue, which closely resembled hyaline cartilage, confirmed the successful differentiation of the tissue (de Vries–van Melle et al., 2014; Hass, Kasper, Böhm, & Jacobs, 2011; Vinardell, Thorpe, Buckley, & Kelly, 2009). With the exception of a single study, (Frisbie, Kisiday, Kawcak, Werpy, & McIlwraith, 2009) all research indicates that the introduction of adipose-derived MSCs has a positive regenerative impact on articular cartilage in animal models (D. H. Lee et al., 2020).

AD-MSCs have the serious potential to significantly advance cartilaginous tissue engineering studies. Due to their higher bioavailability and simpler harvesting process in comparison to other types of MSCs such as BMSC. Nonetheless, the method of directing these stem cells to undergo differentiation into chondrocytes, the specialized cells responsible for cartilage formation, continues to be a developing field of research.

2.4.1.1.4 Induced pluripotent stem cells (iPSCs)

For cartilage tissue engineering, induced pluripotent stem cells (iPSCs) have emerged as a promising cell source. These adult somatic cells have been reprogrammed to a pluripotent state with the help of specific transcription factors, including OCT4, SOX2, KLF4, and c-MYC. This reprogramming allows them to regain embryonic stem cell-like properties, allowing them to differentiate into numerous cell types (F. Li, Bronson, & Niyibizi, 2010), such as osteochondrocytes for cartilage regeneration.

In the realm of cartilage tissue engineering, induced pluripotent stem cells (iPSC) show great potential and highly promising cellular resources. Induced pluripotent stem cells (iPSCs) possess significant advantages, such as patient-specificity and ethical acceptability, as they circumvent issues of immune rejection and ethical concerns associated with embryonic stem cells. However, the process of directing iPSCs towards specific cell types poses challenges, resulting in variations in cell maturity that may compromise therapeutic safety and efficacy. The variability in iPSC differentiation raises concerns regarding potential tumorigenic risks. Hence, it is crucial to improve the consistency of iPSC differentiation, thereby ensuring dependable and efficient therapeutic results (Zhong, Liu, Pan, & Zhu, 2022).

One notable distinction between MSC cells and iPSCs is that the former can solely differentiate into mesenchymal germ layer cells. This characteristic of iPSCs poses a considerable risk of teratoma formation, as residual cells may exist in newly formed tissue or organs (Gutierrez-Aranda et al., 2010). Yamashita et al. (2018) demonstrated the feasibility of converting any nucleated cell into induced pluripotent stem cells (iPSCs),

which can be cultured and expanded without compromising their differentiation potential. As a result, iPSCs are highly desirable for cartilage regeneration, as they offer a plentiful supply of cells from minimally or non-invasive sources. Nevertheless, the process of differentiation of iPSCs is marked by a notable level of immaturity. Despite a substantial body of literature on this topic, a universally accepted method for achieving this differentiation has yet to be established (Castro Viñuelas et al., 2018; Tsumaki, Okada, & Yamashita, 2015).

2.4.1.2 Growth factors

In osteochondral tissue engineering, growth factors play a pivotal role by fostering cell proliferation, differentiation, and the synthesis of essential extracellular matrix components like collagen and proteoglycans, promoting a suitable environment for tissue formation by means of chondrogenesis. This process involves the differentiation of mesenchymal stem cells into chondrocytes, responsible for cartilage production. Enhanced chondrogenesis via growth factors leads to improved quality and quantity of cartilage, offering promising outcomes in tissue engineering. Consequently, the integration of growth factors holds significant potential for the development of effective therapies in cartilage repair and regeneration, showing promise for superior treatments in addressing joint injuries and degenerative conditions (Sohier et al., 2006)

Fibroblast growth factors (FGFs) and other transforming growth factor-beta (TGF-β) families can stimulate the production of the ECM under specific culture conditions. Conversely, bone morphogenetic proteins (BMPs) trigger the initiation of bone tissue formation (osteogenesis) in cells. The utilization of these growth factors induces distinct effects that foster the development of both bone and cartilage tissues.

Mohan and colleagues created scaffolds with a continuous gradient of bone morphogenetic protein-2 (BMP-2) and TGF-1 and performed in vivo experiments to assess their effects. The findings indicated that the scaffolds effectively promoted full integration with the bone, and the cartilage component displayed positive characteristics, including a significant glycosaminoglycan (GAG) content, suitable thickness, and

seamless integration with surrounding tissues. This research suggests that integrating growth factors into scaffolds holds promise for osteochondral tissue engineering (Mohan et al., 2011).

Several studies have shown that growth factors play a critical role in determining stem cell regeneration potential (Davidson et al., 2005). These findings show that manipulating growth factors could be a useful strategy for improving stem cell therapeutic potential in regenerative medicine. The importance of growth factors in tissue engineering and stem cells emphasizes the need for more research into the mechanisms behind their interactions, as well as the creation of techniques to maximize their effects.

2.4.1.3 Biomaterials for Osteochondral Tissue Engineering

In the field of regenerative medicine, biomaterials are likely to be an important factor, particularly in mimicking the chemical and physical properties of the extracellular matrix (ECM). Creating a conducive environment for controlled stem cell proliferation using specialized growth factors and scaffold biomaterials is a pivotal element in the effective reconstruction of bone and cartilage tissue.

Osteochondral regeneration research has, in fact, centered on the use of a wide variety of biomaterials to resolve the difficulties of repairing or regenerating damaged osteochondral tissue (Fig. 2.10) To ensure the successful restoration of damaged tissue, the biodegradation rate of scaffold material used in in vivo treatments must align with the growth rate of the tissue. Successfully integrating osteochondral tissue poses a challenge due to the need to encourage cartilage growth, and vascularization, and address the mechanical requirements of the joint environment (Ghassemi et al., 2018; H.-p. Lee, Gu, Mooney, Levenston, & Chaudhuri, 2017).

The scaffold material must be biocompatible to avoid rejection reactions and is crucial for successful bone and cartilage repair in tissue engineering. Various categories of materials are employed for osteochondral (OC) tissue engineering, guided by these

criteria. They can be divided into four main categories; Natural and synthetic polymers, metal-based materials, inorganic materials which are ceramics, and bioglasses and composites. All of these materials are intended to produce functional osteochondral tissue that closely resembles the characteristics and structure of the native tissue (Fig 2.10).

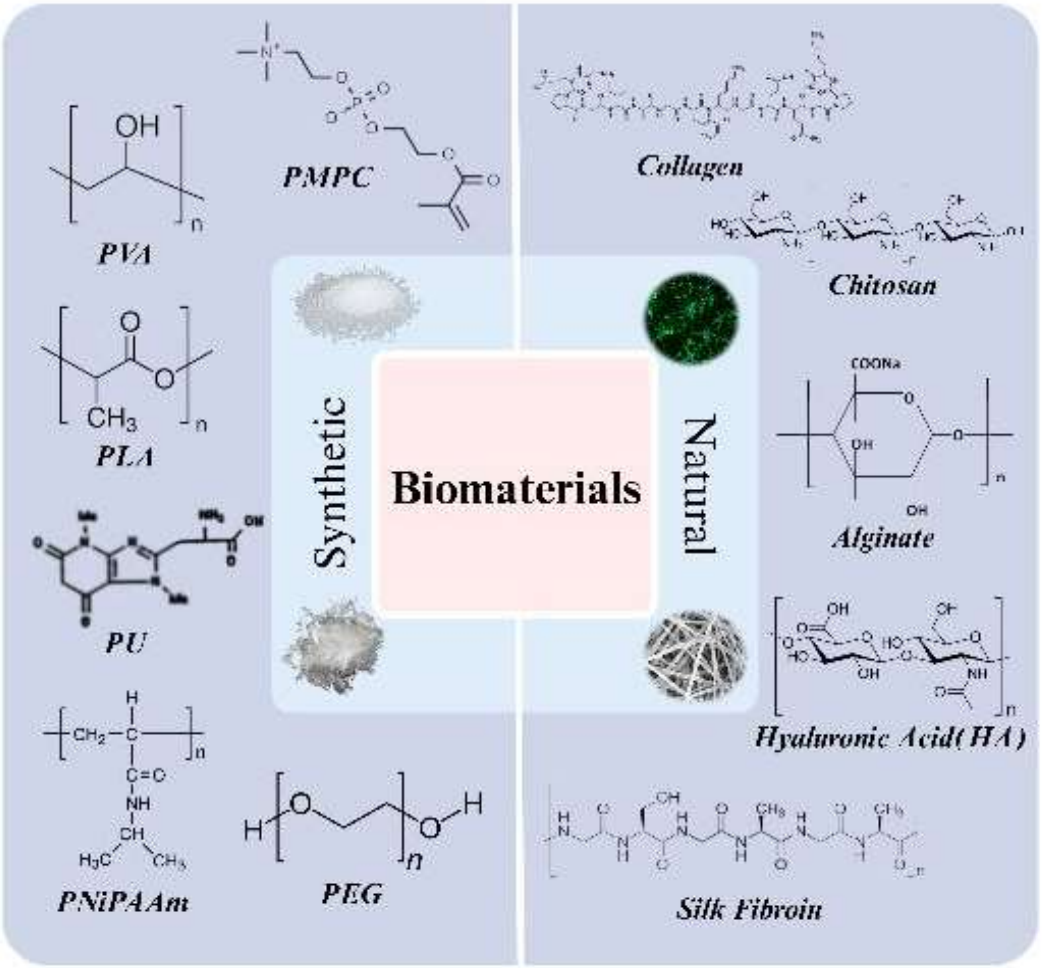

Figure 2.10 Synthetic and Natural Biomaterials in Osteochondral Tissue Engineering

2.4.1.3.1 Natural polymers

Due to their inherent biocompatibility, biochemical resemblance to the extracellular matrix (ECM), and provision of binding motifs to facilitate cellular adhesion, natural polymers like collagen, alginate, gelatine, fibrin, hyaluronic acid, and chitosan are

considered suitable materials for osteochondral tissue engineering owing to their innate biocompatibility, similarity to the extracellular matrix (ECM), and ability to provide binding sites that aid in cellular adhesion. Natural polymers usually have better bioactivity and cell compatibility than synthetic polymers, but their mechanical qualities are weaker, and it is difficult to manage how quickly they degrade (P. J. Yang & Temenoff, 2009).

Natural polymers, when compared to ceramics, natural polymers such as collagen, chitosan, starch, hyaluronic acid, glycosaminoglycan, alginate, and bacterial-derived poly (hydroxy alkanoates) are generally characterized by lower strength which is a disadvantage of osteochondral tissue engineering and their softer properties. However, they possess unique advantages due to their inherent flexibility and the ability to adapt their shape using various molding and casting techniques, because they are highly flexible and can be cast and molded into different shapes and forms. This property makes them suitable for a wide range of applications (Fuchs, Shariati, & Ma, 2020).

Natural polymers possess a significant attribute in their ability to engage with the immune system. This interaction leads to an advantageous immunomodulatory response, playing a crucial role in reducing instances of inflammation and ensuring seamless integration of the scaffold material within the body's biological framework (Tzianabos, 2000). The immunomodulatory ability of the scaffold is of significant importance as it significantly helps in reducing inflammatory processes, therefore confirming the scaffold's natural biocompatibility.

The other advantage is, that many natural polymers come from renewable sources like plants and marine life, which makes them sustainable options instead of synthetic materials created from fossil fuels (Tzianabos, 2000). Additionally, natural polymers possess unique molecular domains that aid and direct cells during their growth, leading to an improved biological interaction between the scaffold and host tissue. Collagen, fibronectin, and laminin, which are natural polymers, consist of specific peptide sequences that encourage cell adhesion and migration. These sequences serve as binding

sites for cell receptors, allowing cells to attach to the scaffold and navigate through the material (Mano & Reis, 2007).

Glycosaminoglycans and proteoglycans have the capacity to interact with bioactive signals, affecting cellular behavior, tissue regeneration, and stem cell differentiation capacity. interactions are essential for maintaining tissue health and expediting natural recovery processes. A noteworthy research focus involves examining how polymers influence MSCs differentiation capacity into specific cell types. The extensive application of polymers in the guise of hydrogels has been prominent in the field of cartilage tissue engineering. Hydrogels, being highly hydrated 3D polymeric networks, create a conducive cellular environment similar to the natural extracellular matrix (ECM) (Sánchez-Téllez, Téllez-Jurado, & Rodríguez-Lorenzo, 2017).

The challenges associated with using natural polymer-based scaffolds on a larger scale and their translation to therapy should not be underestimated. These challenges, including concerns about immune responses, purification methods, limited access to specific polymers, and inconsistent outcomes due to batch variations, must be addressed to effectively integrate natural polymer-based scaffolds into various medical and regenerative applications. The search for and development of resolutions to these issues is crucial in fully utilizing the inherent capabilities of natural polymers to facilitate progress in various therapeutic domains (S. Camarero-Espinosa, B. Rothen-Rutishauser, E. J. Foster, & C. Weder, 2016).

2.4.1.3.1.1 Collagen for osteochondral tissue engineering

Collagen is a natural biomaterial present in various connective tissues, including cartilage and bone. This protein, characterized by its high molecular weight, features three intertwined polypeptide chains forming a triple helix structure, measuring around 300 nanometres in length and weighing 300 kilodaltons. Collagen is notably widespread and constitutes the most plentiful protein in the human body, constituting roughly 25% of total protein content by weight. While distributed widely, its concentration is particularly notable in vital areas in the body. Its pivotal role in preserving the structural integrity of

these tissues cannot be understated, as they predominantly reside within the ECM, offering indispensable structural support to diverse tissues and organs (Gelse, Pöschl, & Aigner, 2003).

Table 2.7 Crosslinking Methods

Crosslinking Method	Advantages	Disadvantages	Examples
Chemical crosslinking	Most common method	Toxic to cells,nor recommended	Glutaraldehyde, EDTA, Nhydroxysuccinimide (NHS)
	Effective	Costly	
	Easy to control	Require thorough washing to remove cross-linkers.	
Physical crosslinking	Less toxic than chemical crosslinking	Not as easy to control	Heat-induced crosslinking, radiation-induced crosslinking, Ultraviolet irradiation (UV)
	Safe	Elevated temperatures have a tendency to induce denaturation of collagen.	
Enzyme-mediated crosslinking	Least toxic method	Not as effective as chemical crosslinking	Transglutaminase-mediated crosslinking,Genipin
	Does not damage cells	Blue reaction after cross-linking	
	Good biocompatibility	Dependency on enzymes, Limited range of applications	

The material exhibits biocompatibility, biodegradability, hydrophilicity, minimal immunogenicity, inherent flexibility, and the ability to facilitate cell attachment, making it highly relevant for emulating the characteristics of the natural tissue environment. The molecular structure of collagen facilitates the presence of binding sites that enable cells to adhere and proliferate. The mechanism described facilitates the attachment and growth of cells on the scaffold (J. Y. Park et al., 2014).

The most prevalent types of collagens are I, II, and III, which form recognizable fibril bundles in tissues. These bundles are the result of collagen molecules assembling into triple helices, with adjacent molecules staggered and covalent cross-links stabilizing the

fibrils. The self-assembly of collagens is dependent on the triple helical structure, which is characterized by repeating amino acids (Gly-X-Y) n, often featuring proline and hydroxyproline (Shoulders & Raines, 2009).

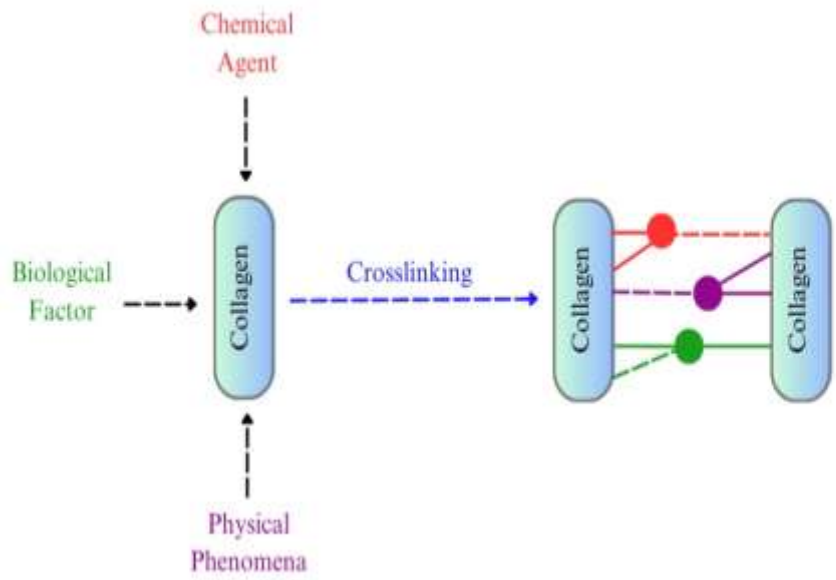

Figure 2.11 Schematic of crosslinking collagen

Nevertheless, the application of this material is impeded by inherent limitations pertaining to mechanical attributes and accelerated degradation. In response to these inherent constraints, the utilization of a method termed cross-linking has emerged. Cross-linking involves the establishment of chemical bonds between distinct functional groups within collagen molecules and other chemical entities (Tanzer, 1973).

This strategic intervention serves to augment the mechanical robustness and longevity of collagen, both in its unadulterated form and when conjoined with diverse organic or inorganic moieties, thereby elevating its comprehensive performance profile. The landscape of collagen cross-linking encompasses a repertoire of diverse methodologies (Adamiak & Sionkowska, 2020).

The multifunctionality of collagen as a scaffold material enables researchers to develop constructions that promote the regeneration of osteochondral tissue. By the manipulation of many aspects of collagen-based scaffolds, including their composition, design, and mechanical properties, scientists can develop platforms that successfully direct the growth and differentiation of osteogenic and chondrogenic cells. Furthermore, these scaffolds are frequently subject to modification by the inclusion of growth factors, signaling molecules, and cells, augmenting their regeneration capacity. However, researchers face significant challenges when attempting to develop collagen scaffolds for osteochondral tissue regeneration (Yan et al., 2010). The aims of the study involve the development of scaffolds that possess mechanical qualities similar to those of the original tissue, as well as assuring compatibility with the immune system to mitigate any potential adverse effects. Furthermore, there is a desire to enhance the techniques employed for the accurate incorporation of growth factors and signaling molecules into collagen scaffolds, while simultaneously tackling obstacles associated with cell viability and differentiation on those scaffolds (L. Chen et al., 2020; Friess, 1998; A. Y. Wang et al., 2008)

Collagen-based biomaterials and collagen scaffolds have emerged as a promising solution and exhibit promise in osteochondral tissue engineering. Because of their biocompatibility, biodegradability, and they can facilitate cell adhesion and also, they are key components of the ECM. Researchers have been exploring the integration of biologically reactive substances, such as growth factors, signaling molecules, and cells, into collagen-based biomaterials. This approach holds great potential for advancing the field of osteochondral tissue engineering (Patel et al., 2020).

However, immunogenic, scalability, and purification issues associated with the clinical use of natural polymers present significant obstacles (Bassas-Galia, Follonier, Pusnik, & Zinn, 2017).

2.4.1.3.1.2 Recombinant collagen technology

The presence of a significant amount of collagen is crucial in a diverse range of applications. Nevertheless, a significant issue is associated with the usage of collagens

obtained from bovines, which happens to be the predominant source of collagen employed in medical, aesthetic, and tissue engineering contexts. There exists a potential hazard of disease transmission arising from collagen obtained from bovines, given that animals have the capacity to harbor pathogens. In light of this inherent risk, there exists a distinct and urgent necessity for an alternative source of collagen that ensures enhanced safety (Lynn, Yannas, & Bonfield, 2004).

Biomedical products derived from animal collagen and collagen-based biomedical materials are generally considered safe for humans. Porcine collagen membranes were tested for bone regeneration, showing biocompatibility and low allergenicity (Salamanca et al., 2016). However, concerns remain about the presence of non-collagenous compounds associated with these animal-derived collagens. In addition, there is controversy regarding the potential to induce autoimmunity in humans using products containing collagen II (Bayrak, Prüger, Stock, & Seifert, 2013). Yet, concerns persist about disease transmission from pigs to humans and religious restrictions on their use. Therefore, research and analysis are needed to address potential concerns and improve our understanding of their effects.

The utilization of recombinant collagen variations exhibits substantial promise within the field of tissue engineering. Recombinant human collagens offer a safer, more predictable, and chemically well-defined source of collagen for biomedical uses. This approach offers a viable alternative to relying on collagen materials sourced from animals. Moreover, the development of recombinant collagen technologies could facilitate access to collagen types that are less abundant and difficult to isolate from natural tissues, thereby addressing scarcity issues. This shift towards recombinant human collagens not only enhances safety but also provides a more versatile and sustainable resource (L. Liu et al., 2007).

Table 2.8 Comparison of animal-derived collagen and recombinant collagen

Parameter	Animal-derived collagen	Recombinant collagen
Source	Various animal tissues, including skin, bones, tendons, and cartilage, which are then subjected to extraction, processing, and purification methods to obtain collagen proteins for different applications.	The utilization of specified and genetically similar expression methods in the production of recombinant collagen guarantees the attainment of consistent, predictable, and adjustable results across a range of applications.
Safety	Allergenicity, disease transmission risk, contaminants, ethical/environmental issues, variability, and cultural considerations	More safety than animal derived collagen. No risk of prion/animal virus contamination. Providing comprehensive safety data
Predictability	Mixture of type I and type III collagen chains can exhibit high batch-to-batch variability due to differences in their properties, complex interactions, processing challenges, tissue source variations, and difficulties in predicting behaviour, requiring careful control and quality assurance measures during production to maintain consistent product performance.	The potential for achieving consistent and replicable results. Requires meticulous optimization of genetic engineering, cultivation, and purification processes and exhaustive testing and characterization to ensure reliable and anticipated results.
Structure	Triple helical structure composed of three polypeptide chains, each predominantly consisting of repeating Gly-X-Y amino acid sequences	Its triple helical structure, formed of three polypeptide chains with repeating Gly-X-Y amino acid sequences, resembles genetically engineered microorganism-produced type I collagen.
Product Recovery	Complex steps including: enzymatic treatment to release collagen fibers, solubilization through pH adjustments, purification to eliminate impurities, concentration, drying, and potential additional processing steps.	Through mild cell/tissue breakdown in pharmaceutical-style bioprocessing, reproducible intracellular products, such as recombinant collagen, can be recovered while maintaining stability and usefulness.
Intellectual Property	Limited	The possibility of obtaining patents for distinctive compositions and procedures, as well as trademarks for branding is a viable option, provided that all legal prerequisites are met and legal counsel is sought.

Table 2.8 Comparison of animal-derived collagen and recombinant collagen(continue)

Parameter	Animal-derived collagen	Recombinant collagen
Customizability	Limited	Presents a notable degree of flexibility through the application of genetic engineering, enabling the customization of structural and functional properties to suit specific purposes, spanning from medical to industrial domains.

Notwithstanding the inherent promise of these variations, their extensive implementation in tissue engineering applications may necessitate additional investigation, advancement, and verification to tackle the obstacles encountered by the discipline and guarantee their efficient incorporation into clinical practice. In 2020, Evonik, a leading German chemical company, presented an innovative biotechnological process for the manufacture of human-like recombinant collagen. This technology has various applications in pharmacy, medicine, cell culture, and tissue engineering. Evonik's VECOLLAN® is a pioneering recombinant collagen platform produced by animal- and human-free fermentation processes.

It provides a highly soluble, pure, and safe collagen product with excellent scalability. VECOLLAN® closely mimics natural collagen with its triple helix structure and tuneable properties that ensure reliable interactions with cells and tissues, it is adaptable to different forms and shapes, and works well with different processing and crosslinking techniques. This means significant progress in medicine, pharmacy, cell culture, and tissue engineering ("Evonik achieves a major biotech breakthrough with a new animal-free and fermentation-based collagen platform. Evonik Industries. (2021, March 16). ,")

Recombinant collagens are anticipated to become a crucial research tool, enabling the study of collagenous protein families and contributing to a comprehensive understanding of the extracellular matrix as a cohesive entity. Despite market dynamics, recombinant

collagens are poised to play a significant role in advancing scientific knowledge beyond their immediate commercial applications.

2.4.1.3.1.3 Alginate hydrogel for osteochondral tissue engineering

Alginate is a biomaterial which is polysaccharide and contains of α-L-guluronate (G blocks) and (1,4)-linked β-D-mannuronate (M blocks) and it is well known for its biocompatibility, which is essential for applications involving tissue engineering and it has the capacity to retain substantial quantities of water, rendering it an appropriate contender for use in soft tissue engineering contexts (Leone, Torricelli, Chiumiento, Facchini, & Barbucci, 2008; You, Chen, Cooper, Chang, & Eames, 2018) (Fig 2.12).

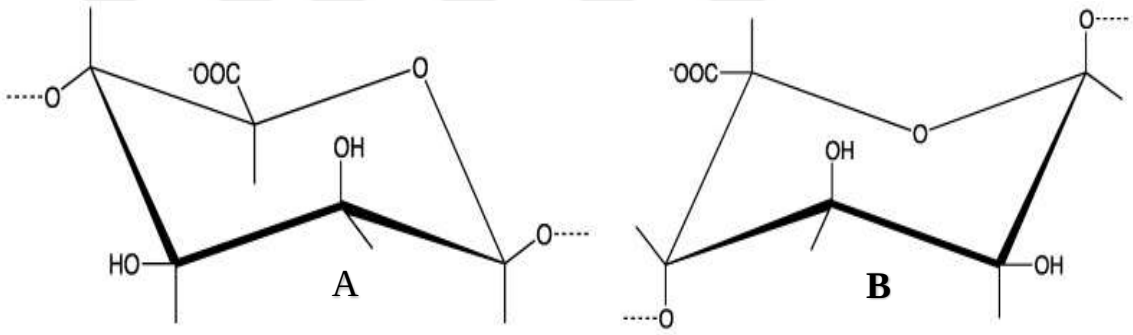

Figure 2.12 The structural components of alginate block varieties (A) β-(1–4)-d-Mannuronic acid; (B) α-(1–4)-l-Guluronic acid

Alginate is a biomaterial that exhibits remarkable versatility and numerous advantages in biomedical applications. Its compatibility with living tissues, minimal immune response provocation, and degradability render it a highly desirable material. Alginate is also highly adaptable for processing and is particularly well-suited for 3D printing, making it a valuable tool in tissue engineering and cell encapsulation. Its non-immunogenic properties significantly reduce the risk of adverse reactions, while its gradual degradation supports tissue replacement during the healing process (Axpe & Oyen, 2016).

When exposed to divalent cations like calcium ions (Ca^{2+}), it can form a hydrogel structure through ionic cross-linking, a process that is moderate and compatible with physiological conditions. This property allows alginate to maintain cell survival within printed scaffolds, highlighting its process flexibility and excellent printability. This adaptability in processing facilitates the creation of various structures, including hydrogels, microbeads, and larger scaffolds (Shim, Lee, Kim, & Cho, 2012). Researchers can customize cell encapsulation processes to meet specific cell type needs, creating a controlled environment within a supportive hydrogel matrix that shields cells from the immune system and allows precise delivery of therapeutic agents. For example, alginate scaffolds can maintain the shape of enclosed chondrocytes. However, their rapid gelling with calcium ions can lead to size reduction and inadequate stiffness for osteochondral tissue applications (Akkineni et al., 2016).

In several research investigations, alginate, a naturally occurring polymer sourced from algae, is subjected to mixing or combination with other polymers. This process aims to enhance the structural integrity and durability of the alginate-based material, particularly in relation to its mechanical strength and flexibility (Y. Yang et al., 2020). Examples of polymers combined with alginate are; collagen (T. Hu & Lo, 2021), methylcellulose (Gonzalez-Fernandez et al., 2019), Hap (You et al., 2018), agarose (Oliver-Ferrándiz et al., 2021), chitosan (Banihashemian, Zamanlui Benisi, Hosseinzadeh, Shojaei, & Abbaszadeh, 2023), gelatine (Y. Yang et al., 2020), fibrinogen (K. Ma, Titan, Stafford, Zheng, & Levenston, 2012), gellan gum (Y. Chen et al., 2020). In each of the aforementioned instances, the amalgamation of alginate with other polymers affords researchers the opportunity to customize the material's characteristics to suit particular applications, thereby attaining enhanced functionality and biocompatibility.

Alginate facilitates the maintenance of chondrocyte morphology and phenotype, demonstrating that it possesses significant potential for in vitro cartilage tissue engineering (Hauselmann et al., 1996; Miralles et al., 2001; Y. Park, Sugimoto, Watrin, Chiquet, & Hunziker, 2005). Furthermore, alginate is dimensionally stable and devoid of adhesive domains that may impede chondrogenesis, making it an ideal and best candidate for promoting chondrogenic differentiation. These characteristics make alginate a

promising biomaterial for applications in cartilage tissue engineering fields (Kun Ma, Titan, Stafford, hua Zheng, & Levenston, 2012).

Chondrogenic differentiation of BMSCs and AD-MSCs in alginate hydrogels has been confirmed several times (Michail, Hicham, & Athanasios, 2019). Furthermore, Diduch et al. discovered that incorporating MSC into an alginate gel can stimulate the development of cartilage tissue. The finding demonstrates that using alginate gel as a scaffold for MSC transplantation could be a promising technique for cartilage repair (Diduch, Jordan, Mierisch, & Balian, 2000).

2.4.1.3.2 Synthetic polymers

Synthetic polymers possess consistent chemical and physical properties and can be customized to meet specific requirements, including degradation rates, mechanical properties, and biological functions. They offer numerous benefits when compared to natural polymers. They tend to be more cost-effective, allowing for large-scale production and extended shelf life which is essential to meet anticipated clinical demands and also offer precise control over molecular weight distribution, diverse chemical compositions, and various processing techniques. However, because of their hydrophobic surface, synthetic polymers generally have limited bioactivity (Reddy, Ponnamma, Choudhary, & Sadasivuni, 2021).

Biodegradable synthetic polymers, including PLGA, poly (propylene fumarate), PCL, poly(dioxanone), PLA, PGA, polyorthoesters, polycarbonates, polyanhydride, and polyphosphazene, are used in various applications, including tissue engineering. Laboratory studies conducted in controlled environments demonstrated that PVA/PCL scaffolds effectively promoted the proliferation of mesenchymal stem cells (MSCs) and encouraged their differentiation into chondrocytes (Abbas Shafiee et al., 2011). Likewise, He and colleagues employed electrospun nanofibers containing collagen-PLCL and chondrocytes to produce cartilage-like tissue in animal experiments, demonstrating the compatibility of these membranes with the native extracellular matrix. These

investigations underscore the adaptability of synthetic polymers in osteochondral tissue engineering endeavors (X. He et al., 2013).

Synthetic polymers lack inherent bioactivity for integration with surrounding host tissue, but they can be modified by incorporating bioactive molecules. This modification enhances synthetic polymer scaffolds by enabling cellular interactions, promoting cell attachment, and stimulating matrix production. Consequently, this approach holds significant potential for modulating osteochondral tissue engineering (Di Luca et al., 2016; Rozila et al., 2021).

2.4.1.3.3 Metallic materials

The utilization of metals in orthopedic implants has been widespread owing to their advantageous mechanical properties, and biocompatibility, being versatile and reliable. Among the metals and alloys commonly employed in orthopedic implants are: titanium, titanium alloys, stainless steels, and Cobalt-base alloys (Shunyu Liu & Shin, 2019).

In the field of osteochondral tissue engineering, metallic biomaterials have been employed as the subchondral bone component in biphasic scaffolds. These scaffolds serve to provide the requisite mechanical support and load-bearing capacity for the subchondral bone region. The objective of these biphasic scaffolds is to emulate the natural structure of osteochondral tissue, which comprises both the cartilage layer and the underlying subchondral bone (X. Wei et al., 2019; T. Yang et al., 2021).

In a study led by Bal and colleagues, they developed a biphasic osteochondral construct by combining porous tantalum metal with a PEG hydrogel loaded with MSCs. When implanted in rabbit knee defects for 12 weeks, the porous tantalum material promoted subchondral bone growth and effectively integrated with the surrounding host bone. Moreover, the study observed the regeneration of hyaline cartilage-like tissue and the expression of collagen type II in the articular cartilage (Bal et al., 2010).

The application of metallic materials faces restrictions due to their non-degradable properties and the risk of releasing particles or products from wear and corrosion which can trigger inflammation and adverse tissue reactions in implanted devices. To overcome these challenges, researchers are investigating surface modifications as a potential solutions (Omarov, Nauryz, Talamona, & Perveen, 2023). While metallic materials offer advantages in orthopaedic applications, it is imperative to address these limitations to optimize tissue engineering. Recent progress in material science and the comprehension of material-biological interactions are driving the development of more effective and biocompatible implant solutions for conditions such as osteochondral defects (Sing et al., 2017).

2.4.1.3.4 Bioceramics

In osteochondral defects involving damage to the subchondral bone, repair of the underlying bone is essential for complete tissue regeneration. Bioceramics, known for their biocompatibility and mechanical strength, are often used in combination with natural or synthetic polymers to promote subchondral bone tissue regeneration, complementing osteochondral tissue repair efforts in these defects (Hench & Polak, 2002).

Although polymers have been extensively researched and used to mimic the natural environment of hyaline cartilage tissue for the purpose of regenerating cartilage tissue, Successful engineering of the underlying bone is also critical for the complete restoration of osteochondral tissue. They are an ideal choice for osteochondral tissue engineering owing to their biocompatibility, which ensures their acceptance by the body without eliciting an immune response and, they possess osteoconductive, which provides a framework for bone cells to adhere to and proliferate. Their excellent osteoinductive properties enable them to release growth factors that promote bone formation, which provides a framework for bone cells to adhere to and proliferate. Their excellent osteoinductive properties enable them to release growth factors that promote bone formation (Rahaman et al., 2011). Bioceramics possess the advantage of biodegradability, which allows them to gradually break down and be replaced by newly generated bone tissue over time. Upon implantation in the body, bioceramics have the ability to stimulate

the development of a bone-like apatite layer on their surface through osseointegration or bioactive bonding. This bioactive reaction results from the bioceramic material's interaction with its biological surroundings which is a critical factor in ensuring the stability and efficacy of the implant throughout the long-term (Roseti et al., 2017).

Bioceramics, when integrated with natural or synthetic polymers, significantly promote subchondral bone regeneration. This combination enhances the mechanical strength and biocompatibility of the resulting material. Bioceramic-polymer composites act as scaffolds, offering structural support and encouraging cell adhesion, growth, and differentiation (Rao, Harini, Shadamarshan, Kalimuthu, & Selvamurugan, 2017). From a wider viewpoint, a number of bioceramics can be identified, such as hydroxyapatite, tetra calcium phosphate, tricalcium phosphate, calcium silicate, and amorphous bioactive glass (BG). These materials have been extensively studied for their potential use in tissue engineering applications due to their biocompatibility, and bioactivity.

Table 2.9 Bioceramic Materials Using in Osteochondral Tissue Engineering

Application	Bioceramic materials	Function	References
Cartilage	PLGA / nano HAp	Investigate OC repair potential	(Xue et al., 2010)
Cartilage	PLDLA / nano HAp enriched with sodium alginate	Articular cartilage treatment	(Żylińska et al., 2017)
Cartilage	ß - TCP scaffolds seeded with autologous chondrocytes	Repair of OC defects	(X. Guo et al., 2004)
Cartilage	B - TCP / collagen type I	Improve articular cartilage restoration and reconstruction	(Bian et al., 2012)
Deep OC defects	Biphasic implant of ß - TCP and fibrous collagen type I and type III	Bone reconstruction and cartilage regeneration	(Gotterbarm et al., 2006)
OC defect regeneration	Biphasic scaffolds of silk fibroin and silk - nano Cap	OC defect regeneration	(J. J. Li et al., 2015)
OC tissue engineering	Biphasic chitosan / HAp - based scaffolds	OC tissue engineering	(Malafaya & Reis, 2009)

The study by Lv and Yu assessed a composite lamellar scaffold's effectiveness in repairing articular osteochondral defects in canine knee joints. This scaffold contained nanoscale tricalcium phosphate and collagen types I and II. The research showed that the scaffold could regenerate both bone and cartilage simultaneously in these defects. As the scaffold gradually degraded, it coincided with the formation of new cartilage tissue. This study highlights the potential of biomimetic scaffold design for tissue regeneration and provides promising insights into osteochondral defect repair (Lv & Yu, 2015).

Xue et al. (2019) investigated a composite scaffold for cartilage tissue engineering. The PLGA/nano HAp hybrid scaffold effectively repaired cartilage. The scaffold improved cartilage regeneration, MSC viability, and proliferation. These results imply that PLGA and nano HAp in the scaffold enhanced cartilage regeneration and MSC development (Xue et al., 2010).

Various bioceramic-based materials and scaffolds have gained regulatory approval as substitutes for bone grafts. Some of these include CERAMENT™G, Bonalive (from Vivoxid Ltd), NovoMax® (BioAlpha Inc.), Chronos (DePuySynthes), Straumann® BoneCeramic™, and Geistlich Bio-Oss®.

Bioceramics represent significant materials in tissue engineering nonetheless, they are accompanied by drawbacks like brittleness and inadequate mechanical characteristics. Addressing these limitations necessitates doing a comprehensive study to understand their interactions with biological tissues better and develop structures that can maintain long-term functionality. Enhancing the mechanical properties of biomedical materials, particularly their ability to withstand cyclic loads, is of the utmost significance to improve their efficacy and longevity in intricate biomedical applications. (Roseti et al., 2017)

2.4.1.3.4.1 Calcium phosphates

In the field of orthopedic and dental applications, calcium phosphate (CaP) is a natural substance in the body that resembles the mineral composition of various mineral tissues.

These bioceramics have excellent biocompatibility, bone conductivity, and biores orption and are effectively integrated into living tissue through a process similar to bone regeneration. This incorporation occurs when some CaP dissolves in the surrounding medium and releases ions that cause protein adsorption and the generation of biological apatite crystals on the surface of the biological material. CaP is cost-effective and easily qualified for medical use (Bohner, 2000; Sergey V. Dorozhkin, 2007).

The various CaPs exhibit unique chemical compositions, solubility, and properties. Based on their in-situ degradation rates, CaPs can be classified as follows: MCPM displays the highest rate of degradation, succeeded by TTCP and α-TCP, DCPD, OCP, β-TCP, and HAp exhibits the slowest rate of degradation (LeGeros & Legeros, 2003) (Table 2.10).

Table 2.10 Several calcium phosphates, their properties and applications

Calcium Phosphates	Properties	Applications
Hydroxyapatite (HA)	Biocompatible, osteoconductive, and biomimetic	Bone repair, bone regeneration, dental implants
Tricalcium phosphate (TCP)	Biocompatible, osteoconductive, and biodegradable	Bone repair, bone regeneration, drug delivery
Tetracalcium phosphate (TTCP)	Biocompatible, osteoconductive, and biodegradable	Bone repair, bone regeneration, drug delivery
Biphasic calcium phosphate (BCP)	Combination of HA and TCP	Bone repair, bone regeneration, dental implants
Calcium phosphate cement (CPC)	Mixture of HA and TCP or TTCP with a binder	Bone repair, bone regeneration, dental implants
Calcium phosphate nanocarriers	Nanoparticles of calcium phosphate	Drug delivery, gene delivery, tissue engineering

2.4.1.3.4.2 Calcium phosphate cement

LeGeros, Brown, and Chow introduced calcium phosphate cement (CPC) as a revolutionary alternative to the cumbersome bone graft bioceramics in the early 1980s. Their primary objective was to develop materials that can consolidate in their intended

location and effectively treat bone or dental defects. LeGeros and colleagues introduced a biocompatible and osteoconductive CPC in 1981, while Brown and Chow's 1983 publication described the development of a resorbable variant (WE, 1983).

The culmination of these efforts was the FDA approval of the first commercial CPC, Norian SRS, in 1990 for use in the United States. This milestone marked the beginning of a dynamic landscape for CPCs, leading to the subsequent development and approval of several other CPCs for diverse clinical applications. Consequently, CPCs made their clinical début in the 1990s, when they were utilized to treat maxillofacial defects and fractures (L. C. Chow & Takagi, 2001). As time progressed, CPCs found their way into a growing number of applications, including spinal fusion, dental implants, foot and ankle surgery, orthopedic procedures, craniofacial interventions, oral and maxillofacial therapies, and veterinary surgery. CPC is favored as a bone substitute due to its remarkable qualities, including biocompatibility, osteoconductivity, and resorbability. These attributes enable CPC to be well-tolerated by the body, promote new bone growth, and gradually break down to facilitate the formation of fresh bone tissue. Importantly, CPC exhibits robust bone-conduction capabilities and mechanical strength comparable to cancellous bone. (L. C. Chow & Takagi, 2001).

Table 2.11 Important properties of CPC

Property	Description
Biocompatibility	CPC is non-toxic and does not cause an inflammatory response in the body.
Osteoconductivity	CPC is able to bond to bone and promote the growth of new bone cells.
Biodegradability	CPC is slowly broken down by the body over time, which allows for the gradual replacement of the scaffold with new bone tissue.
Injectability	CPC can be injected into the body using a minimally invasive procedure.
Moldability	CPC can be molded into any desired shape, which makes it suitable for a variety of applications.
Compressive strength	CPC has a compressive strength that is similar to that of bone, which makes it suitable for weight-bearing applications.
Porosity	CPC is a porous material, which allows for the flow of nutrients and waste products and promotes cell infiltration.
Solubility	CPC is slowly soluble in body fluids, which allows for its gradual degradation and replacement with new bone tissue.

CPCs are composed of a CaP-based powder and a liquid component that, when mixed, undergo a chemical reaction, forming a crystalline solid at body temperature (Bohner, 2000). This process involves the dissolution of some CPC particles on the surface and the initiation of a setting reaction, resulting in a hardened micro or nanoporous structure. Importantly, this setting reaction is non-toxic and not exothermic. The specific chemical reaction during the CPC setting can vary, depending on the CaP compounds in the powder phase. It may involve hydrolysis or an acid-base interaction, determined by the CaP precursor compounds, which typically include TTCP or β-TCP as basic components and dicalcium phosphate anhydrous (DCPA) or monocalcium phosphate monohydrate (MCPM) as acidic reactants.



Figure 2.13 Calcium phosphate cement paste preparation

Following the curing process, CPC undergoes a transformation into hydroxyapatite (HA), a compound that closely resembles the primary inorganic constituent of natural bone. This similarity to hydroxyapatite positions CPC as a leading contender for potential bone graft substitutes (Brown, 1986).

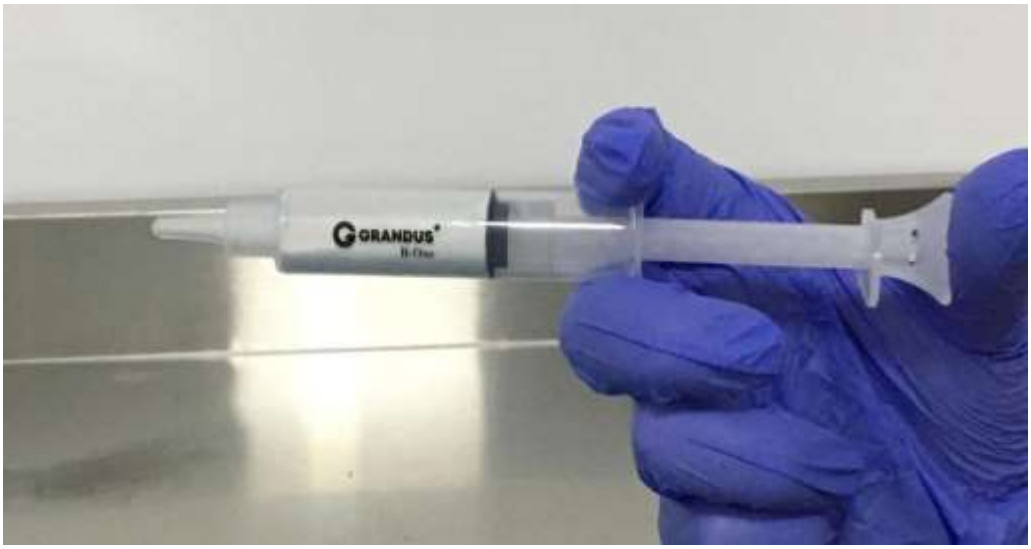

Figure 2.14 Injectable calcium phosphate cement (CPC)

CPC can be divided into two main types based on the final product: apatite cement (AP) and DCPD or brushite cement. This classification is determined based on the pH level of the cement paste after undergoing the hardening process. When the paste's pH surpasses 4.2, apatite cement (AP) is produced. These cements are mainly composed of apatite crystals and are often desired for their excellent biocompatibility and similarity to the mineral composition of natural bone. On the other hand, when the pH value of the paste is less than 4.2, anhydrous dicalcium phosphate cement (DCPD or brushite) is preferred. However, it is important to note that brushite formation can occur even at pH levels below 6.5 under certain kinetic conditions. Brushite cement is known for its unique properties and is used in a variety of biomedical applications (A. Yousefi, 2019).

CPCs offer important advantages because they harden in vivo by a low-temperature reaction. These materials can be molded when mixed and are very suitable for use in repairing osteochondral defects. Non-invasive injection is possible, which is a big advantage compared to traditional calcium phosphate ceramics. In addition, CPCs show another important property, which is that they do not cause exothermic reactions during the curing process. This unique property allows CPCs to efficiently incorporate various drugs and other important biomolecules. This feature holds promise for osteochondral tissue engineering, as it enables the controlled delivery of therapeutic agents to target sites

(Ginebra, Traykova, & Planell, 2006). This increases the potential of CPCs in the development of innovative and versatile therapies for osteochondral diseases.

Unlike bioceramics, which necessitate high-temperature sintering CPCs are created using a dissolution-precipitation process that occurs at ambient or body temperature. This process leads to the formation of a crystalline matrix that gradually becomes denser over time, ultimately achieving its maximum mechanical properties (J. Zhang, Liu, Schnitzler, Tancret, & Bouler, 2014).

Typically, the microporosity level in CPC falls within the range of 30% to 55%, and it depends on the liquid-to-powder (L/P) ratio; higher L/P ratios result in greater microporosity. While excessive porosity can be problematic in load-bearing applications, it is intentionally introduced to enhance the material's ability to be absorbed by the body and its capacity for biological interactions. This increased porosity also provides a larger surface area for reactions. Additionally, having some level of porosity makes CPCs suitable for use as carriers in controlled drug delivery systems. If necessary, techniques can be employed to introduce larger macropores into the CPC (Vezenkova & Locs, 2022).

Numerous studies have explored and confirmed the potential of CPC. However, the optimal porosity level for CPC scaffolds tailored to specific applications remains undefined. Diverse research efforts have concentrated on increasing the biological features of CPCs, such as their biocompatibility, biodegradability, osteoconductivity, osteoinductivity, and cell reactions (Xu et al., 2017).

The situation with injectable CPCs is complex for injectable formulations, the key factor is completing the setting reaction. Proper solidification is crucial to prevent cytotoxic effects, and incomplete solidification or premature dissolution can have serious consequences. Insufficient solidification may lead to strong inflammatory responses, blood clot formation, and the potential development of cement emboli, solid fragments that can travel through the circulatory system, potentially causing blockages or other complications. (Krebs et al., 2007; Ueyama et al., 2001).

Nevertheless, the utilization of prefabricated CPC scaffolds presents certain advantages. Prefabricated CPC scaffolds can be produced in a controlled environment, ensuring that the setting reaction is complete prior to in vivo use. This is of paramount importance, as an incomplete setting may trigger inflammatory reactions in the body (Ishikawa, 2014)

Furthermore, prefabricated CPC scaffolds can be designed with interconnected macropores, which is crucial for tissue engineering, as it facilitates the ingrowth of blood vessels and cells, essential for tissue regeneration. Conversely, self-setting CPCs tend to possess smaller micropores and limited pore interconnections, rendering them less suitable for tissue engineering applications. (Laurence C Chow, 2009). In summary, prefabricated CPC scaffolds offer several advantages over injectable CPCs. They are more likely to be fully set, can be designed with interconnected macropores, and are more convenient for use in minimally invasive procedures.

Table 2.12 Summary of advantages of prefabricated CPC scaffolds

Advantages of prefabricated CPC scaffolds	
Complete setting reaction	The setting reaction of CPC scaffolds can be carefully managed and monitored in a laboratory setting. This controlled environment allows researchers or manufacturers to ensure that the scaffold's setting reaction is complete and thorough before it is introduced to the body. This is important because incomplete setting can lead to inflammatory reactions in the body.
Interconnected macropores	Essential for tissue engineering and regenerative medicine. These macropores enable the ingrowth of blood vessels and cells, facilitate nutrient and oxygen transport, and aid in waste product removal. This design aspect enhances the scaffold's potential to support tissue regeneration and integration into the body.
Ease of use	The uncomplicated insertion process employed by this method obviates the necessity for intricate mixing and injection protocols often associated with injectable calcium phosphate cement (CPCs). The implementation of this technology has the potential to optimize medical procedures, mitigate risks, and enhance the reliability of outcomes across a range of clinical applications.

Prefabricated CPCs have gained recognition for their positive biocompatibility in both short-term and long-term studies. Numerous research efforts involving diverse animal models like rats (Takechi et al., 1998), rabbits (H. Guo, Su, Wei, Kong, & Liu, 2009),

dogs (Félix Lanao et al., 2014), sheep (Apelt et al., 2004), and goats (Del Real, Ooms, Wolke, Vallet-Regi, & Jansen, 2003), along with in vitro tests utilizing various cultured cell types, collectively confirm the suitability of pre-set CPCs for interaction with living tissues and cells (H. Guo et al., 2009).

2.4.1.3.4.2.1 3D printing of CPC

CPCs are used in both prefabricated scaffolds and injectable pastes. The advent of 3D printing technology has opened up exciting opportunities for precisely crafting CPC scaffolds, enabling the construction of complex biomimetic structures previously inaccessible through conventional methods. This innovation has the potential to usher in an era of advanced and intelligent CPCs, offering precise, customizable, and intricate structures that can support tissue regeneration and other applications in regenerative medicine.

3D printing in reconstructive surgery offers advantages in creating custom implants with intricate features, such as interconnected pores and precise measurements, overcoming limitations of conventional methods. Personalized CPC scaffolds have the potential to improve recovery, streamline surgeries, and provide aesthetically pleasing results. The setting time of CPC is a crucial factor that influences the printing process and needs to be considered during customization. One of the significant challenges that is the allocated time for completing the 3D printing optimization for CPCs is insufficient. There are several studies on this in the literature.

A study found that a CPC formulation with a 1:1 molar ratio of powder constituents (TTCP and DCPA) and a polyvinyl alcohol-based liquid adhesive had a short 10-minute printing time, which is challenging for most printing applications (C. Li, Gao, Chen, & Liu, 2015). To improve this, mesoporous calcium silicate was added to the CPC paste, extending the printable time to about 120 minutes (C. Li et al., 2015). Another strategy involved incorporating gelatin, which delayed the onset of the CPC setting reaction, providing more time for printing before solidification. These adjustments aim to optimize the formulation of the direct printing ink (Maazouz et al., 2014).

A specific printable CPC paste composition consists of Targon 1128 as a dispersant, hydroxypropyl methylcellulose (HPMC) as a thickening agent, polyethyleneimine (PEI) as a gelling agent and an oil-based CPC paste that solidifies upon contact with water. Importantly, this formulation does not have a printing time limit, making it highly suitable for specific applications where extended printing duration is essential (Marques et al., 2017).

Optimizing settings for the 3D printing of CPC scaffolds requires more study. Additionally, for clinical applications, obstacles such as optimizing composition, developing reproducible manufacturing techniques, and testing on animal models must be overcome. These challenges are essential to ensure biocompatibility, bone regeneration, durability, safety, and efficacy. Once addressed, CPC scaffolds enriched with various components could potentially transform the treatment of bone defects and osteochondral tissue defects, offering new avenues for medical advancements.

2.4.1.4 Scaffold architecture

The design of scaffold structures is of paramount importance in cartilage and osteochondral tissue engineering. To produce successful tissue based on the scaffold's structural design, which must mimic the distinct features of different tissue layers, such as cartilage and bone, to preserve their inherent heterogeneity. Therefore, the scaffold's structural composition significantly impacts the effectiveness of cartilage or osteochondral tissue regeneration. Careful consideration in its design is essential to achieve the best outcomes. The architectural characteristics of the scaffold encompass its physical makeup, arrangement, and configuration, all crucial for supporting cell growth, tissue integration, nutrient diffusion, waste removal, and mechanical functionality (Appelman, Mizrahi, & Seliktar, 2011; D. W. Hutmacher, 2000; Xigeng, 2008).

Table 2.13 Scaffold Design factors and their explanations

Scaffold Design Factors	Explanations
Biocompatibility	Make reference to the characteristics of the scaffolding materials that allow them to be physiologically compatible with the live cell tissue and to elicit the appropriate reaction in the recipient tissues.
Pore size and porosity	In order to facilitate the attachment and proliferation of cell tissues, the scaffold need to have a pore size that is relatively large in addition to a porosity that is connected. The scaffold needed pores with a minimum size of 100 micrometers, while the generally regarded average percentage of porosity should be between %60 and %70.
Surface characteristic	Since the scaffold's surface plays key roles in the interaction of biomaterials, including the management of cell tissue growth following successful attachment to the surface, the surface should have features that are acceptable and suitable.
Mechanical properties	To prevent stress shielding, which inhibits cell proliferation, the scaffold must have mechanical strength attributes that are commensurate with those of the surrounding tissue.
Biodegradability	The scaffold must be able to degrade rapidly in vivo or in vitro in order to provide an environment for cell tissue growth. Creating biodegradable scaffolds promotes tissue development, imitates natural processes, and improves the efficacy of tissue regeneration.

Tissue engineering scaffolds are intricate 3D constructs engineered to emulate the ECM and create a conducive environment for cellular growth. They play an important role in influencing various cell activities like adhesion, migration, proliferation, and differentiation as cells interact with them. This interaction guides cell behavior and ultimately leads to the development of functional tissue. Scaffolds also act as stimuli for cells, aiding tissue growth and regeneration through both physical and chemical mechanisms. Over time, cells generate their ECM, gradually replacing the scaffold material. The scaffold's properties, including mechanical strength, porosity, and bioactivity, significantly impact cellular responses during these interactions. The pore size and porosity of scaffolds play an essential role in driving osteochondral tissue regeneration. Research has demonstrated that the enhancement of cell migration, growth, and nutrient exchange is associated with larger pore sizes and increased porosity in scaffolds. In addition, the capacity of a scaffold to promote osteogenesis or chondrogenesis is significantly influenced by the size and porosity of its pores (Seo, Mahapatra, Singh, Knowles, & Kim, 2014).

In practice, several studies have provided practical guidance regarding the influence of pore size in scaffold design. To promote direct osteogenesis and enhance vascularization, it's recommended to use scaffolds with a porosity of over 50% and pores larger than 300 μm (Karageorgiou & Kaplan, 2005). Conversely, for favorable chondrogenesis, smaller pores around 90–120 μm have been suggested. These smaller pores encourage the proliferation of MSCs and the development of cartilage tissue on the scaffold (K. Kim, Yeatts, Dean, & Fisher, 2010). These findings underscore the significance of tailoring pore size according to specific tissue engineering objectives.

Native cartilage, calcified cartilage, and subchondral bone exhibit varying pore characteristics. Native cartilage has an average pore size of about 6 nm, while calcified cartilage has a porosity of approximately 22%. Subchondral bone shows a wider porosity range from 64% to 94%. To promote effective tissue repair or replacement, scaffold pore size and porosity should be customized according to the specific tissue being targeted (Nuernberger et al., 2011; O'brien, 2011).

Table 2.14 The mechanical function requirements for osteochondral scaffolds

Requirement	Description
Porosity	The scaffold should be porous enough to allow for cell infiltration and tissue growth, but not so porous that it loses its structural integrity.
Permeability	The scaffold should be permeable to nutrients and waste products, allowing for efficient diffusion throughout the tissue.
Compressive strength	The scaffold should be able to withstand the compressive forces experienced in a joint during normal activity.
Shear strength	The scaffold should be able to withstand the shear forces experienced in a joint during movement.
Young's modulus	The scaffold should have a Young's modulus that is similar to that of the surrounding bone and cartilage, to minimize stress shielding.
Toughness	The scaffold should be tough enough to resist cracking and breaking under impact or fatigue.
Fatigue resistance	The scaffold should be able to withstand the repeated loading and unloading that occurs in a joint during normal activity.
Wear resistance	The scaffold should be wear-resistant to minimize the formation of debris and the need for revision surgery.
Corrosion resistance	The scaffold should be corrosion-resistant to prevent the release of metal ions and other harmful substances into the body.

For the development of the optimal scaffold for osteochondral tissue engineering, it's essential to find the right balance between pore size, porosity, and mechanical strength. This balance ensures that cells behave optimally, and the scaffold remains durable. Effective pore interconnectivity facilitates cell movement and substance exchange. Moreover, scaffold materials should degrade at a rate that matches tissue formation to avoid issues like rapid degradation compromising tissue support or overly slow degradation hindering natural tissue remodeling. Achieving this balance requires careful selection of biomaterials, cell types, scaffold designs, and fabrication methods. Future efforts should focus on improving scaffold porosity and establishing standardized approaches in this field (W. Wei & Dai, 2021a; B. Zhang, J. Huang, & R. J. Narayan, 2020). Over the past few decades, there has been a significant evolution in the development of osteochondral scaffolds, monophasic, biphasic, triphasic, multiphasic, and gradient scaffolds (Fig 2.14)

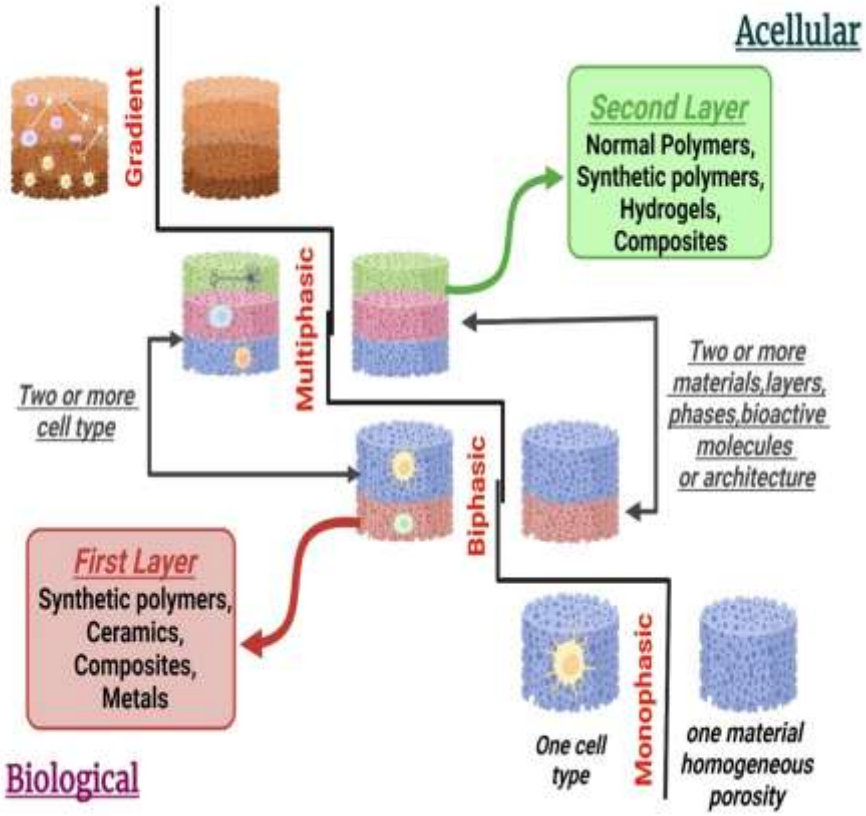

Figure 2.15 Scaffold designs in osteochondral tissue engineering

2.4.1.4.1 Monophasic scaffolds

Monophasic scaffolds, characterized by a uniform composition and structure throughout, are commonly used to treat OC damage. While they enhance the recruitment and proliferation of essential cell types like chondrocytes and osteoblasts for OC tissue regeneration, they lack the structural complexity of native osteochondral tissue. These scaffolds maintain consistent material distribution and porosity across their entire framework, promoting cell activity through a combination of different cell types and mechanical stimulation (Deng et al., 2019).

Monophasic scaffolds, despite their structural uniformity, primarily support the growth of evenly organized regenerating tissue in osteochondral defects. However, it is crucial to acknowledge that monophasic scaffolds, despite the aforementioned alterations, are incapable of adequately facilitating both chondrogenesis and osteogenesis concurrently. Typically, these scaffolds exhibit a preference for one tissue type over the other and may not offer an optimal environment for the regeneration of osteochondral tissue. Consequently, their ability to faithfully mimic the intricate biological environment required for successful OC tissue replacement is significantly limited (W. Wei & Dai, 2021b).

2.4.1.4.2 Biphasic scaffolds

Developing monophasic scaffolds that can create ideal microenvironments for both chondrogenesis (cartilage formation) and osteogenesis (bone formation) is a formidable task. The reason behind this challenge lies in the significant differences in the requirements for promoting bone and cartilage growth. These two tissue types exhibit distinct compositions, mechanical properties, and cellular behaviors. Devising a single scaffold capable of effectively catering to the specific demands of both bone and cartilage tissue regeneration represents a complex undertaking in the field of tissue engineering.

Biphasic scaffolds consist of two distinct layers, each specifically designed to address the requirements of bone and cartilage regeneration. Inspired by the natural structure of subchondral bone and cartilage, researchers have developed biphasic scaffolds featuring a cartilage layer and a subchondral bone layer (Duan et al., 2019). In the context of osteochondral tissue engineering, the creation of bilayer tissue scaffolds, including biphasic structures, involves exploring various combinations of materials, morphologies, and characteristics for both layers. These materials possess unique properties tailored to the specific tissue type, resulting in biphasic scaffolds comprising a distinct chondral component and an osteal component (Mahapatra et al., 2019).

Various materials have been explored in the synthesis of bioinspired biphasic scaffolds with diverse characteristics (Lin et al., 2020). Historically, most biphasic scaffolds have been constructed from natural or synthetic polymers, high-stiffness materials, or their combinations. While many of these materials have yielded promising results, some studies have reported imprecise outcomes (Zhou et al., 2020). The frequently used approach in the development of biphasic scaffolds possessing chondrogenic and osteogenic properties involves the utilization of polymers, and hydrogels for the cartilage layer which mimics the viscoelastic and hydrated extracellular matrix (ECM) of cartilage and polymer-embedded bioceramics for the bone layer (Erickson et al., 2019; Gao et al., 2018; Han et al., 2021; Natarajan, Sivadas, & Nair, 2021).

Biphasic scaffolds, comprising a flexible polymer layer and a rigid bioceramic layer, offer promising potential for concurrently restoring cartilaginous and osseous tissues. The polymer layer's flexibility, customizable mechanical properties, and moisture-retaining capacity create an environment conducive to chondrocyte growth and chondrogenesis, closely mimicking cartilage tissue conditions. In contrast, the bioceramic layer promotes osteoblast-mediated osteogenesis. This approach, supported by preclinical studies, holds promise for addressing deficiencies in both cartilage and bone tissues within tissue engineering applications. Common polymers used in the cartilage layer include hyaluronic acid, polyethylene glycol, chitosan, and collagen, which support chondrogenesis and cartilage cell growth. Meanwhile, the subchondral layer employs stiffer materials such as Tricalcium phosphate (TCP), Tetra calcium Phosphate (TTCP),

and bioceramics, offering mechanical support and stimulating osteoblast-mediated bone formation. The integration of these layers in biphasic scaffolds presents a potential solution for regenerating both cartilage and subchondral bone tissues in osteochondral defects.

A recent computational study has investigated the interfaces of biphasic polymeric scaffolds. The findings indicate that certain combinations, particularly polycaprolactone (PCL)/gelatine methacrylate and PCL/polyethylene glycol diacrylate (PEGDA), demonstrate enhanced tensile, compressive, and shear properties when compared to other polymer scaffolds fabricated using 3D printing methods (Choe et al., 2022). This insightful finding offers guidance for future research endeavors in the design of polymeric biphasic scaffolds, facilitating the selection of appropriate biomaterials for the construction of such scaffolds.

The bonding strength between layers in biphasic scaffolds is crucial for surgical handling and stability. Strong interlayer bonds ensure that the scaffold remains intact during and after implantation, which is essential for surgical success. Delamination, the separation of layers, can compromise the scaffold's structural integrity over time and hinder tissue growth. Preventing delamination is vital to maintaining scaffold integrity and ensuring effective treatments during various procedures (Xuezhou Li, Ding, Wang, Zhuang, & Chen, 2015). To address potential instability and integration problems at the interface of biphasic scaffolds, researchers propose the addition of a middle layer, often referred to as the calcified cartilage layer. This addition aims to transform the scaffold into a trilayered configuration, enhancing its performance and integration for the regeneration of osteochondral defects.

For example, Lin et al. have presented a novel strategy that highlights the utilization of controlled crosslinking to form a long-lasting bond. This serves as an additional example of the practical application of controlled crosslinking. The methodology involves the fabrication of permeable scaffolds using a substance called poly (glycerol sebacate) (PGS). The most significant characteristic of this technology is the utilization of a solvent-free urethane crosslinking procedure (Lin et al., 2020).

Various methods have been explored to enhance the mechanical properties and integration of biphasic scaffolds for bone and cartilage regeneration (Kesireddy & Kasper, 2016). Crosslinking (X. Li et al., 2015), laser drilling, and the use of bio-glue have shown promise in improving interfacial mechanical responses However, limited permeability at the interface can hinder cell migration and differentiation, affect the integration of newly regenerated bone and cartilage layers (Dormer, Berkland, & Detamore, 2010). Another approach involves creating biphasic scaffolds from a single polymeric material with distinct pore size distributions to reduce mechanical weakness at the interface. While these scaffolds exhibit mechanical characteristics similar to natural tissues, in vivo tissue healing remains restricted (Duan et al., 2019). The simplification of materials may lead to unexpected changes in stiffness between the two layers (Chan et al., 2012).

2.4.1.4.3 Triphasic and multiphasic scaffold

In osteochondral tissue engineering, addressing the challenge of securely connecting materials with varying mechanical properties, such as hydrogel and bioceramic, has been a longstanding issue. Traditional methods like gluing or stitching often result in post-implantation instability. To enhance integration and bonding strength, researchers propose the inclusion of a calcified cartilage layer between the bone and cartilage components (Simkin, 2012). This additional layer acts as a protective barrier and significantly improves implant stability. Consequently, the development of a three-layered scaffold (osteal, calcified cartilage, and chondral) holds promise for more effective osteochondral tissue regeneration (Mancini et al., 2020).

Tampieri and collaborators developed a scaffold using a biomimetic mineralization process that incorporated hydroxyapatite nanocrystals onto collagen fibers. This resulted in a triphasic structure comprising an upper layer of hyaluronan-charged collagen, a lower subchondral bone layer rich in biomineralized collagen with a high mineral content (70% HAp by weight), and an intermediary region containing biomineralized collagen with a lower mineral content (40% HAp by weight), mimicking the properties of the calcified zone in natural tissue (Tampieri et al., 2008).

This nano-composite triphasic scaffold showed favourable mechanical and biological properties in treating chondral and osteochondral lesions in equine and ovine models, and is now commercially available as MaioRegen® for clinical applications (Kon et al., 2011; Elizaveta Kon, Marco Delcogliano, et al., 2010; Elizaveta Kon, Giuseppe Filardo, et al., 2010).

Triphasic scaffold designs offer improved biological performance compared to biphasic scaffolds, but they present challenges due to their increased complexity. These scaffolds consist of an additional layer, which can make achieving precise layer thicknesses, alignment, and overall structural integrity challenging. Integrating three distinct layers, each with different properties and functions, can be difficult in ensuring smooth transitions and strong bonding at every interface. To ensure the scaffold's effectiveness, optimizing compatibility across all layers is crucial. Triphasic scaffolds often incorporate materials with varying mechanical properties, and managing these mechanical differences requires a delicate balance between providing support for bone structures and flexibility for cartilage balance between providing support for bone structures and flexibility for cartilage (Kosik-Kozioł, Heljak, & Święszkowski, 2019).

2.4.1.4.4 Gradient scaffolds

Multilayered scaffolds have been developed to mimic the zonal organization of native osteochondral tissue, integrating phases with unique characteristics However, the issue of inadequate integration at interfaces might be addressed by employing gradient scaffolds (L. Fu et al., 2020). In addition, it should be emphasized that gradient scaffolds are highly effective in regenerating subchondral bone, cartilage, and the bone-cartilage interface (Radhakrishnan, Manigandan, Chinnaswamy, Subramanian, & Sethuraman, 2018).

Gradient scaffolds offer a unique approach to addressing the challenge of integrating different tissues. They are intentionally designed to have a gradual change in properties, including mechanical and biological attributes, from one end to another, resembling the natural variations found in osteochondral tissue. Gradient scaffolds have shown greater success in promoting integration between different tissue layers or zones, improving the overall stability and functionality of implants. These scaffolds have also been effective in reconstructing not only cartilage and bone but also the complex transition region between them. Another advantage is their ability to transition smoothly between properties, reducing tension between adjacent zones and ensuring implant stability and integrity (L. Fu et al., 2020).

Creating gradient scaffolds involves overcoming several challenges, including establishing a mechanical gradient capable of withstanding compressive stress, modifying properties to mimic natural tissue variations, and creating a pore network resembling native osteochondral tissue. Additionally, promoting cellular differentiation along osteogenic and chondrogenic pathways is crucial for successful tissue regeneration therefore careful design is necessary to replicate the inherent mechanical variations in native tissues and effectively manage specific stresses.

2.4.1.5 Cell-free strategies for osteochondral regeneration

These methodologies, which utilize cell-free scaffolds, have been developed to mitigate certain constraints associated with existing techniques, particularly their limited suitability for treating minor injuries. These procedures are dependent on the implementation of scaffolds and the induction of microfractures to attract pre-existing cells within the articular region (Maia, Carvalho, Oliveira, & Reis, 2018).

Cell-free approaches for treating osteochondral defects are gaining attention as cost-effective alternatives, but their clinical application remains controversial due to limited evidence comparing them to cell-laden treatments. Preclinical studies show promise, often using animal models with freshly drilled holes that allow bone marrow to support chondrogenic differentiation. Successful outcomes hinge on subchondral bone repair,

emphasizing scaffold osteoconductivity and osteoinductivity. Additionally, these procedures are emerging as innovative treatments for knee and ankle lesions, capitalizing on their distinct joint characteristics, reduced costs, and greater accessibility compared to cell-based methods.

Crucial factors to take into account encompass verifying the scaffold's compatibility with the human body and its inherent capacity for biodegradation. The material ought to promote cellular adhesion, proliferation, and specialization while undergoing degradation when fresh tissue formation occurs (Seo et al., 2014).

2.4.1.5 Commercial products of osteochondral defects

To date, few artificial scaffolds specifically developed for osteochondral lesions have successfully entered the commercial market, and a subset of these have obtained authorization from the European Union. Prominent examples encompass MaioRegen™, TruFit™, Agili-C™ ChondroMimetic®, and BioMatrix CRD (S. Chubinskaya et al., 2019).

Table 2.15 Commercial Products of Osteochondral Defects

Product	Company	Classification	Materials	Features	Figures
TruFit™	Smith and Nephew	Biphasic	PLGA-PGA (75:25), calcium sulfate	Biphasic scaffold, designed to promote the regeneration of both cartilage and bone	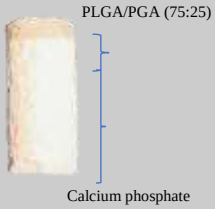
MaioRegen™	Finceramica	Triphasic	Type I collagen, magnesium-enriched hydroxyapatite	Commercial product, designed to enhance the regeneration of damaged joint surfaces and promote the integration of new tissue	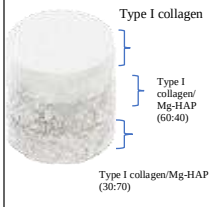
ChondroMimetic™	TiGenix	Biphasic	Type II collagen, type I collagen, chondroitin sulfate calcium phosphate	Biomimetic osteochondral scaffold, designed to replicate the natural structure and function of cartilage and bone	-
Agili-C™	CartiHeal Ltd	Biphasic	Hyaluronic acid, crystalline aragonite	Resorbable scaffold, designed to provide mechanical support while promoting tissue regeneration	
BioMatrix CRD	Kensey Nash	Biphasic	Bovine collagen, ß-TCP, PLA	Collagen-based scaffold, designed to provide a supportive environment for cartilage regeneration in osteochondral defects	

Numerous advanced scaffolds, mostly biphasic, have been tested in animal models for osteochondral defects in preclinical studies. A comprehensive assessment of the clinical use of the TruFitTM Plug, a commercial bilayer scaffold, has identified a lack of readily available data that can establish its superiority or equivalency when compared to conventional treatments such as mosaicplasty or microfracture. As a result, there is an inadequacy of scientific evidence to substantiate the superior efficacy of the TruFitTM Plug in relation to alternative treatment choices (Verhaegen et al., 2015).

MaioRegenVR has shown a higher rate of clinical implantation compared to TruFitTM Plug, likely due to its earlier approval over several years. MaioRegenVR is a bilayer scaffold composed of deantigenated type I equine collagen and hydroxyapatite loaded with magnesium. Both TruFitTM Plug and MaioRegenVR hold significant potential as treatments for osteochondral abnormalities. However, further research is essential to determine their effectiveness and safety conclusively (D'Ambrosi, Valli, De Luca, Ursino, & Usuelli, 2019).

Agili-C™ is an aragonite-based cell-free scaffold designed for treating chondral and osteochondral defects in joints, including those affected by arthritis. Its primary purpose is to restore the osteochondral unit by promoting the regrowth of articular cartilage and underlying subchondral bone, aiming to restore the original structure and function of damaged tissues. Agili-C™ achieves regeneration through two key processes: the differentiation of bone marrow-derived stem cells into chondrocytes and the migration, proliferation, and extracellular matrix deposition of cartilage cells from surrounding native tissue. Its biocompatibility and cell-attracting properties make it a promising option, potentially outperforming or matching other biomimetic scaffolds (Dhollander et al., 2012). For instance, Trufit™ exhibited varying outcomes in terms of facilitating functional cartilage and bone regeneration, whereas MaioRegen™ demonstrated regenerative potential in a sheep model, although the long-term effects remain uncertain (E. Kon et al., 2010).

Numerous studies have not conclusively proven that implanted cells directly participate in new tissue formation when treating osteochondral defects. Instead, they likely exert their effects through paracrine mechanisms. As a result, cell-free scaffold-based treatments are emerging as a promising therapeutic approach for knee and ankle chondral and osteochondral lesions, leveraging the unique biochemical and metabolic characteristics of cartilage in these joints. These strategies offer benefits such as reduced costs and increased accessibility compared to cell-based methods (Susan Chubinskaya et al., 2019). Although biphasic or multiphasic scaffolds have achieved notable accomplishments, they have faced obstacles in the context of clinical trials. The problems encompass various concerns, including the occurrence of scaffold delamination, inadequate fusion with the surrounding tissue, inferior quality of the regenerated tissue, discomfort in the knee region, and the probable requirement for subsequent surgical interventions.

2.4.1.6 Scaffold fabrication methods

Scaffolds play a crucial role in tissue engineering, particularly when addressing intricate osteochondral tissue repair. Achieving successful tissue regeneration necessitates scaffolds possessing specific attributes, including porosity, surfaces conducive to cell attachment and growth, mechanical properties akin to adjacent tissues, biocompatibility, and controlled degradation. Recent advancements include custom scaffolds designed using computer-aided technologies and various fabrication methods, aiming to improve scalability, sustainability, and spatial control of scaffold materials in osteochondral tissue engineering.

The selection of a fabrication technique is of paramount importance as it significantly impacts the mechanical, physicochemical, and biological properties of the scaffold. In the creation of osteochondral tissue scaffolds, two primary methods are commonly utilized: conventional techniques and 3D printing. For manufacturing scaffolds, conventional techniques, which have been used for decades in diverse disciplines including tissue engineering, involve manual processes and material manipulation.

Common methods for osteochondral tissue scaffold fabrication include freeze drying, gas foaming, solvent casting electrospinning, and particulate leaching. Both approaches have advantages and disadvantages, and the choice between them depends on variables such as the intended scaffold properties, design complexity, and available resources.

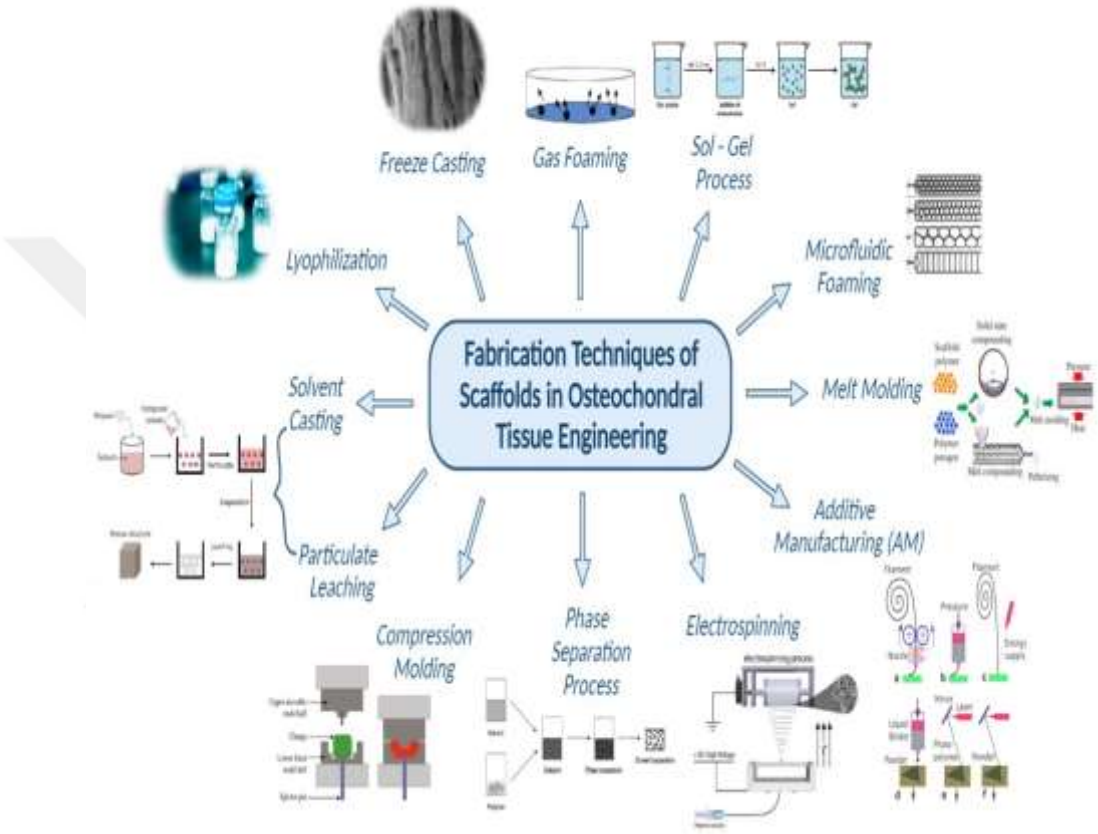

Figure 2.16 Osteochondral Tissue Engineering Scaffold Fabrication Methods

2.4.1.6.1 Lyophilization

The use of freeze casting as a technique for producing bioactive scaffolds has attracted considerable attention in recent years (H. Liu, Nakagawa, Kato, Chaudhary, & Tadé, 2011). The freeze-drying method, also known as lyophilization, involves sublimating frozen water directly into vapor under controlled low-temperature and negative pressure conditions. This technique is used to create three-dimensional scaffolds that mimic the arrangement and dimensions of ice. The process includes freezing the scaffold material

and then removing the ice through sublimation, resulting in a porous structure (C. Liu, Xia, & Czernuszka, 2007).

Abarrategi A. and colleagues evaluated the survival of cells and the formation of bone within scaffolds composed of rhBMP-2 (a growth factor), multiwall carbon nanotubes (MWCNT), and chitosan (CHI) using the freeze-casting method in a previous study (Abarrategi et al., 2008). The technique is notable for its substantial practical value and potential for advancement, as it enables the creation of structures that closely resemble the organization of biological tissues (Shao, Hanaor, Shen, & Gurlo, 2020).

It is important to note that the choice of solvents for freeze-drying can have cytotoxic effects on cells. This necessitates a meticulous cleaning procedure in order to effectively remove these solvents and mitigate their potential negative effects on cellular health. In addition, it is essential to realize that scaffolds produced by the freeze-drying method tend to have less compositional consistency than those produced by solvent.

2.4.1.6.2 Solvent casting and particulate leaching

Solvent casting is a scaffold fabrication technique that involves dissolving scaffold material in a solvent to create a uniform solution. This solution is poured into a mold, forming a solid structure. After removing the solvent, a porous scaffold is created, crucial for tasks like cell growth and nutrient exchange (Sin et al., 2010). Combining this method with particulate leaching efficiently controls scaffold properties like pore size and porosity (Murphy, Dennis, Kileny, & Mooney, 2002). However, leaching can lead to poor interconnection in scaffold fabrication, affecting cell distribution in vitro.

2.4.1.6.3 Electrospinning

Electrospinning is widely used in crafting scaffolds for tissue engineering. It is a technique that creates nanofibers using an electrically charged polymer solution or melt flow, driven by electrostatic force. This method produces nanofibers with large surface

areas and adaptable mechanical properties, making them versatile for various applications Crucially, it's possible to arrange these fibers in a manner that emulates the hierarchical organization of the native ECM. In the context of osteochondral scaffolds, this technique holds the promise of constructing a cartilage layer possessing a pliable and elastic structure closely mirroring the ECM characteristics of hyaline cartilage (Casanova, Reis, Martins, & Neves, 2018). Researchers have also developed innovative scaffold designs using techniques like dynamic liquid electrospinning, such as the nanofiber yarn-collagen type I/hyaluronate hybrid (Yarn-CH)/TCP scaffold, which has shown promise in promoting the regeneration of both cartilage and bone tissues (S. Liu et al., 2015).

2.4.1.6.4 3D bioprinting

3D bioprinting is gaining significant attention in regenerative medicine and tissue engineering. This technique leverages digital tools to create intricate tissues that closely mimic natural tissue organization and structure. It enables precise customization of size parameters and the layer-by-layer printing of complex biomaterial structures using computer-aided design (CAD) models (D. X. Chen & Chen, 2019; Ouyang et al., 2020).

The process involves two main components: the biological printer (printing equipment) and the biological ink (material being printed) (Moroni et al., 2018). Researchers use 3D bioprinting to build scaffolds that replicate the natural architecture of healthy tissues, providing frameworks for cell growth and organization. Computer models and design tools help mimic complex geometries and patterns found in biological tissues, allowing the replication of intricate tissue structures (Jesse K. Placone & Adam J. Engler, 2018).

3D printing emerges as a promising avenue for crafting implants that align closely with anatomical structures (Jesse K Placone & Adam J Engler, 2018). This technique enables a more accurate replication of articular cartilage properties, including rigidity, diffusivity, and tissue density (Gruber, Ghosh, Mueller, Whitlock, & Lin, 2019; Kosik-Kozioł, Heljak, & Święszkowski, 2020; Kai Li et al., 2021).

Bioprinting methods can be categorized into main types based on ASTM standards: extrusion-based (Ozbolat & Hospodiuk, 2016), jetting-based (or droplet-based) (X. Li et al., 2020), vat photopolymerization-based (or light-based bioprinting) (Ng et al., 2020) and laser-assisted bioprinting (Ventura, 2021).

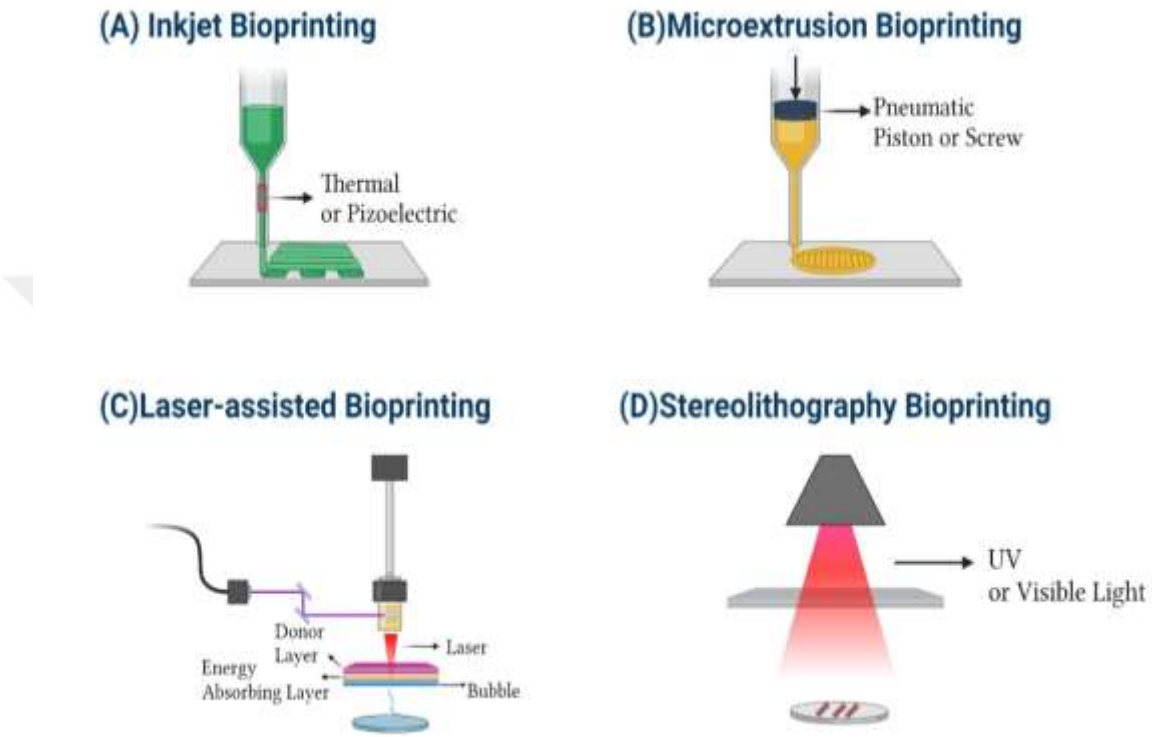

Figure 2.17 Examples of various bioprinting techniques

A) Inkjet bioprinters, which use piezoelectric actuator to create a pressure difference that forces small droplets of hydrogel and cells onto a substrate. B) Microextrusion bioprinters, which neumatic or manual force to deposit a cell-laden liquid solution onto a substrate. This technique is relatively simple and can be used to create structures with complex geometries. C) Laser-assisted bioprinting, utilizes heat to propel bioink onto a substrate, enabling precise and complex pattern and structure creation. D) Stereolithography bioprinters, employing UV or visible light selectively cross-link bioinks layer by layer to build intricate 3D structures with high resolution.

The potential of 3D-printed biomaterials for cartilage and osteochondral repair is significant. Various 3D printing techniques are used for creating scaffolds in articular osteochondral tissue engineering. However, several factors must be carefully considered when fabricating 3D-printed scaffolds. Biomaterial properties related to printing and solidification need optimization to achieve structurally sound constructs that match the intended design. Additionally, protecting embedded cells within the hydrogel from

mechanical damage during printing is crucial. Parameters such as printing pressure, temperature, bio-ink viscosity, and nozzle dimensions require precise adjustment to improve printing accuracy, mechanical properties, and cell viability (K. Li et al., 2021).

The ability to achieve precise control over material deposition is essential when fabricating three-dimensional structures. Factors such as material properties, printing techniques, and printer settings play a significant role in determining the spatial and temporal control of the printed structure, as well as the incorporation of biological components (Chimene, Lennox, Kaunas, & Gaharwar, 2016).

Optimizing printing parameters is essential for achieving high-resolution structures. In osteochondral research using 3D printing, biomaterials like alginate, methylcellulose, GelMa, PEGDA-based hydrogels, PCL, PLA, and PLGA have gained attention. These biomaterials are often combined with other components to enhance their physical and biological properties (Chaala et al., 2023; Luo et al., 2023; Mu et al., 2023). These common biomaterials are often combined with additional substances to amplify their physical and biological attributes.

Notably, hydrogels are frequently utilized to print the hyaline cartilage layer. On the other hand, metallic materials hyaluronic acid, and bioceramics are found to be more appropriate for printing the subchondral bone. The persistent effort to create novel materials that exhibit enhanced biocompatibility, flexibility, and adjustability represents a pivotal factor in driving the future progress of the discipline (Ozbolat & Hospodiuk, 2016). In conclusion, 3D bioprinting has received a lot of attention due to its ability to produce artificial tissues that are highly similar to their native counterparts in terms of organization and structure. The potential for this technology to improve biomedical analysis and lead to novel therapeutics is enormous.

2.4.1.6.4.1 Difficulties of fabrication scaffold with 3d printing process

Despite significant advancements in 3D bioprinting technology, several challenges remain that require resolution. One of the main obstacles encountered in the field of 3D bioprinting involves the identification of an optimal bio-ink that possesses both biocompatibility in challenging printing environments and the desired mechanical and biofunctional characteristics post-printing.

Rigid materials require solidification during or after printing for structural integrity but need additional steps like cell seeding or biomolecule treatment for biocompatibility. In contrast, soft materials like hydrogels, can be printed. However, post-printing structural stability relies on gelation techniques like chemical reactions, photo-crosslinking, shear thinning, and thermal properties to ensure the integrity of the printed object therefore optimization is crucial for strong, stable scaffolds while maintaining accurate details (Galarraga, Kwon, & Burdick, 2019).

Scaffold materials can be divided into two groups: one that can integrate cells during printing and another that cannot due to certain features and processing conditions. High temperatures or hazardous solvents may hinder cell integration. Understanding the thermomechanical behavior of biocomposite materials during melting and solidification is vital for shaping the printing process and assessing the feasibility of incorporating live cells. The printing process must be gentle to avoid cell damage, as they are critical for tissue growth and health (Y. Chen et al., 2020).

The successful transition of a 3D-printed tissue scaffold from the laboratory to clinical practice involves the consideration of various factors. When contemplating the use of a scaffold in surgical procedures, multiple considerations arise. Surgical requirements, including innovative techniques or multiple surgeries, can pose challenges and impact regulatory approval. Complex surgeries may lead to higher costs. While less invasive procedures are preferred, they may not always be feasibleThe utilization of a scaffold in clinical applications involves a thorough evaluation of its therapeutic benefits versus the associated costs and potential risks. Beyond regulatory and surgical expenses, material

costs, market potential, patient demographics, and intellectual property considerations also impact the decision to advance a scaffold from the research stage to the clinical use (Pashuck & Stevens, 2012).

Sterilization is a vital step to ensure that scaffolds are free from harmful microorganisms, ensuring optimal cell viability, and, more importantly, preventing potential infections or diseases when these structures are implanted in patients. The choice of sterilization method is crucial in handling scaffold materials for tissue engineering. Various techniques, including thermal, radiative, and chemical methods, can impact the scaffold's properties (Dai, Ronholm, Tian, Sethi, & Cao, 2016). Factors like high temperatures or specific chemicals can modify the scaffold's structure, mechanical strength, or bioactivity. Therefore, selecting an appropriate sterilization method is essential to maintain the scaffold's structural integrity and ensure its safety for the implantation (Shyam & Palaniappan, 2023).

Table 2.16 Summarizes the challenges of 3D bioprinting

Challenge	Description
Bioink development	Finding an ideal bioink that is biocompatible, printable, and has the desired mechanical and biofunctional properties.
Sterilization	Sterilizing 3D bioprinted scaffolds without damaging the cells or biomolecules.
Scale-up	The 3D bioprinting process is often labor-intensive and slow. This makes it difficult to scale up the production of 3D bioprinted scaffolds.
Regulatory approval	3D bioprinted scaffolds are categorized as medical devices and require approval from regulatory agencies before clinical use, which can be a lengthy and costly procedure.
Cost	The high cost of 3D bioprinting materials, equipment, and labor.

2.4.1.6.5 Indirect 3D printing

Scaffolds can be created through various methods, including particle leaching, freeze-drying, phase separation, gas foaming, and electrospinning, allowing for the production of porous structures with adjustable pore sizes. However, achieving consistent and controlled structures, especially interconnected porosity, can be challenging. 3D printing provides benefits such as the ability to design patient-specific scaffolds, control porosity, and choose from various materials (Wen et al., 2017).

The application of 3D printing techniques, including sacrificial molds and sacrificial mold-assisted processes, offers practical solutions for producing uniform and precisely controlled structures across various fields. These applications encompass microfluidic channels, polymeric scaffolds, inorganic 3D matrix materials, and microneedles, among others (Goh & Hashimoto, 2018). Additionally, by co-printing the scaffold with sacrificial materials, it becomes possible to control the direction and shape of customized channels.

Indirect 3D printing is a promising technology for the fabrication of osteochondral scaffolds because it allows for the creation of scaffolds with complex geometries and controlled porosity. This approach involves using RP techniques to create a negative mold. This mold is then filled with castable materials, such as ceramic slurry, and later removed from the dried body. Importantly, the mold preparation is separate from the casting process, allowing for flexibility in adapting the technique to various scaffold materials. An inherent benefit of indirect 3D printing lies in its capacity to offer a versatile selection of mold materials. This technique can be tailored to accommodate an extensive range of materials, encompassing resins, plastics, and even metals, contingent upon the precise application at hand.

Sacrificial biomaterials are gaining traction in tissue engineering for their ability to create vascular and porous structures that promote cell growth (Compaan, Christensen, & Huang, 2017). These biomaterials, whether integrated with hydrogel-based scaffolds or used as molds, allow for the formation of desired pores, channels, and hollow structures

while maintaining biocompatibility. In various fields, including metals, ceramics, and polymers, 3D porous scaffolds find widespread use (Chiesa et al., 2020). Biodegradable synthetic polymers like PGA, PLLA, PLGA, and PCL are popular choices due to their availability, cost-effectiveness, and adaptability for customized 3D structures and pore distributions, making them suitable for diverse application (S. Li, Liu, Liu, & Hu, 2016; Shi et al., 2008).

Poly(ε-caprolactone) (PCL) is a versatile synthetic polymer widely used in tissue engineering due to its exceptional biodegradability and biocompatibility. It offers excellent mechanical properties, including high flexibility and elongation-at-break, making it suitable for various applications. PCL's extended degradation time of up to 24 months is advantageous for long-term use (Ogueri, Jafari, Escobar Ivirico, & Laurencin, 2019). It can also serve as a sacrificial mold material, allowing for the creation of complex, porous structures (Yao et al., 2006).

PCL's solubility in organic solvents makes it compatible with different fabrication techniques and tissue types. Its favorable thermal properties, including a low glass transition temperature of -60 °C and a melting temperature of 55–60 °C make it ideal for extrusion-based 3D printing, enabling precise and intricate structure fabrication (Teoh, Goh, & Lim, 2019). With FDA clearance and the ability to control its degradation rate, PCL is a versatile material in tissue engineering and 3D printing (Y. Guo, Liang, & Ji, 2019)

2.5 Scope and Novelty of the Study

In this research, biphasic scaffolds were designed to mimic bone and cartilage tissues separately. The upper layer of the cartilage scaffold was composed of recombinant collagen, a precise and controllable material with a reduced risk of immunogenicity compared to animal-derived collagens, in conjunction with alginate. For bone engineering, the lower layer consisted of calcium phosphate cement (CPC), a biocompatible, osteoconductive, and bioactive material known for its ability to support both bone and cartilage tissue growth. CPC scaffolds with approximately 300 μm

macropores were explored to promote osteogenesis and tissue ingrowth therefore, an indirect 3D printing method was employed to create CPC scaffolds with interconnected macropores. Polycaprolactone (PCL) sacrificial models were initially 3D printed, and CPC pastes were perfused into these models, followed by self-setting. Subsequent removal of the PCL models resulted in macroporous CPC scaffolds with uniform shapes, a 3D interconnected structure, and the required compressive strength for subchondral bone repair.

For the cartilage component, sodium alginate and recombinant collagen scaffolds were designed and 3D printed. These calcium phosphate cement scaffolds and recombinant collagen/alginate scaffolds were then separately tested for their osteochondrogenic and chondrogenic differentiation potential in vitro using adipose-derived mesenchymal stem cells (ADMSCs). Various aspects, including mechanical properties, cell viability, proliferation, morphology, and differentiation characteristics, were thoroughly investigated. The study findings suggest that the combination of biphasic calcium phosphate bone cement and recombinant collagen/alginate scaffolds holds great promise for repairing osteochondral defects. This approach provides mechanical support resembling subchondral bone while offering a chondrogenic scaffold for cartilage repair.

The study involves the use of a specially formulated TTCP-based CPC which is produced by Permed (Turkey) has not been previously documented in the literature. This study examines the osteogenic capacity of this TTCP-based CPC for the first time by using an AD-MSC cell line and also the study introduces a novel scaffold design using TTCP based CPC intended for osteochondral defect treatment, which has not been previously tested.

Recombinant collagen from Evonik is used for the first time as a scaffold material in this research. The research investigates the chondrogenic differentiation capacities of AD-MSCs using recombinant collagen, representing a novel application of these materials and cells. The study is pioneering in multiple aspects, including the novel material (Permed, Turkey), unique scaffold design, and innovative use of recombinant collagen and AD-MSCs, all of which have not been previously explored in this context.

3. MATERIAL AND METHODS

3.1 Materials

3.1.1 Cell line

Adipose-derived Mesenchymal Stem Cells (Lonza)

3.1.2 Culture and growth AD-MSC cell line

Dulbecco's Modified Eagle Medium, with Glutamax^{TM,} 1g/L Glucose (DMEM; high glucose) (GIBCO, USA)
Fetal Bovine Serum (FBS) (GIBCO-Invitrogen, USA)
Penicillin/Streptomycin Solution (GIBCO-Invitrogen, USA)
DPBS (without Ca2+ and Mg2+) 10X (PAN Biotech, Germany)
Trypsin-EDTA Solution, 1X (Sigma, USA)
Fibroblast growth factor-2 (FGF-2) (Sigma-Aldrich)

3.1.3 Chondrogenic differentiation media

StemPro™ Chondrogenesis Differentiation Kit (Gibco)

3.1.4 Osteogenic Differentiation Media

Fetal Bovine Serum (FBS) (GIBCO-Invitrogen, USA)
Penicillin/Streptomycin Solution (GIBCO-Invitrogen, USA)
β-glycerophosphate (Serva)
Dexamethasone (AppliChem, Germany)
L-ascorbic acid-2-phosphate (AppliChem, Germany)
Dulbecco's Modified Eagle Medium, 1g/L Glucose (DMEM; low glucose)

Other chemicals used in cell culture are as follows, Trypsin (Biological Industries), Dimethyl Sulfoxide (DMSO) (Sigma-Aldrich), Triton X100 (Merck) DPBS (without Ca^{2+} and Mg^{2+}) 10X (PAN Biotech, Germany)

3.1.5 Preparation of CPC Scaffold

Polycaprolactone (PCL) (Perstorp AB)
Dichloromethane (DCM), HPLC grade (Sigma Aldrich)
Envision TEC 3D-Bioplotter
Calcium phosphate cement (Permed, Turkey)

3.1.6 Preparation of Alginate/Collagen Scaffold

Alginic acid sodium salt (Sigma, USA)
Recombinant collagen (Evonik)
Calcium chloride dihydrate (Sigma, USA)
PBS
Envision TEC 3D-Bioplotter

3.1.7 For optimization trials of CPC for 3D printing

Gelatin (Serva)
Carboxymethyl cellulose (Sigma)
Methylcelluse (Sigma)
PEG 400
PVA (Sigma)
Pluronic F-127 (Sigma)
CPC (Permed, Turkey)
Glycerol (Kimyalab)
Sodium Alginate (Sigma,USA)

3.1.8 Cell viability Assay

Cell viability assay was determined by the Alamar Blue test (Thermo Fisher)

3.1.9 Differentiation Staining

Alcian Blue (Sigma) was used to determine the chondrogenic differentiation of the cells, and Alizarin red (Sigma) was used to determine the osteogenic differentiation. Paraformaldehyde (PFA) (Merck) was used to fix the fluorescent staining samples.

3.2 Methods

3.2.1 Designing the biphasic scaffold

In the realm of tissue engineering, osteochondral scaffolds are designed to replicate the 3D architecture of natural cartilage and bone tissues, promoting cell attachment, proliferation, and tissue regeneration. The ultimate aim is to create innovative scaffolds tailored to meet the specific needs of distinct tissues, including cartilage and bone. To successfully repair osteochondral defects by designing a biphasic scaffold, it's crucial that, each layer of the scaffold possesses mechanical properties that closely match those of the surrounding tissues. Additionally, these mechanical properties should be sufficient to withstand the cyclic physiological loads typically experienced by the joint.

In this study, the bone section of the scaffold was meticulously designed to feature larger pores, each measuring 300 μm, and possess suitable mechanical properties to withstand applied loads. The bone part utilized a TTCP-based self-hardening injectable CPC sourced from Permed Health Products in Turkey, closely replicating the subchondral component. In the context of bone regeneration, porous bone scaffolds are of paramount importance as they function as conduits for nutrient transport, facilitate cell attachment, migration, proliferation, and support vascularization. This material exhibits biomechanical properties akin to lamellar bone and was initially developed for the

purpose of filling bone defects. In conclusion, it is intended to enhance osteogenic differentiation of the substrate in the biphasic scaffold when combined with adipose-derived stem cells (AD-MSCs) during in vitro experiments.

The chondral part of the scaffold was meticulously engineered to incorporate smaller pores, measuring approximately 150 μm, and was composed of a recombinant collagen/alginate hydrogel blend. Hydrogels have gained significant attention in the field of cartilage regeneration due to their ability to closely emulate the characteristics of the natural extracellular matrix. They play a pivotal role in facilitating chondrogenesis and promoting the regeneration of cartilage. In this context, the chondrogenic differentiation of the upper layer in the biphasic scaffold was aimed to be enhanced by combining it with AD-MSCs during in vitro experiments.

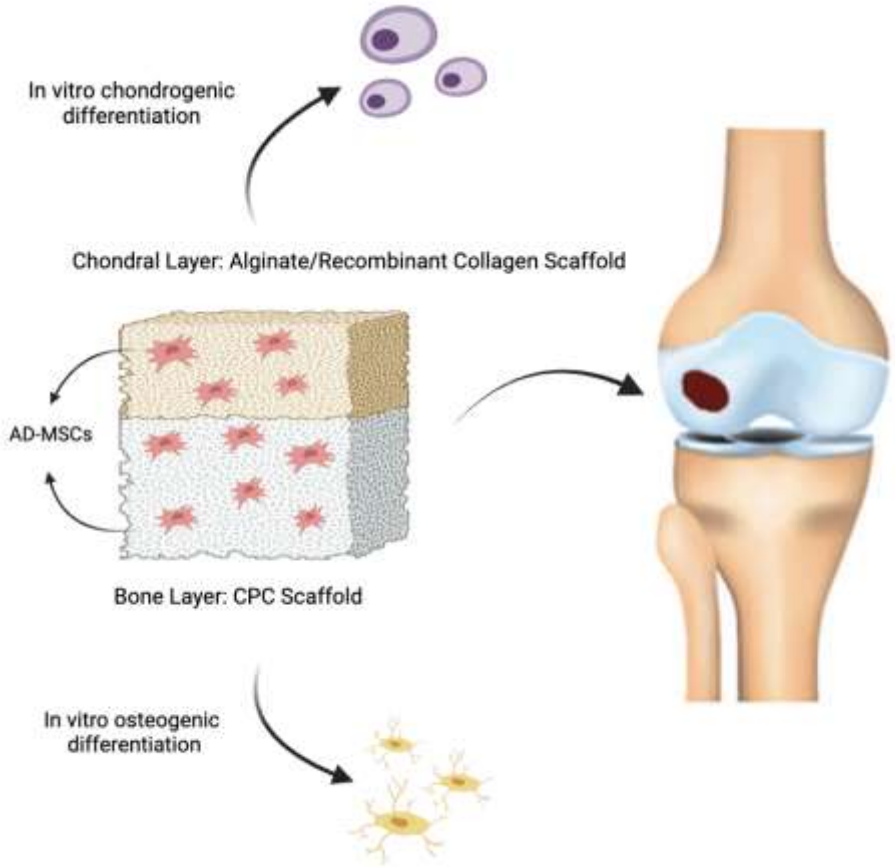

Figure 3.1 Schematic of CPC/Recombinant collagen biphasic scaffold and in vitro analysis for osteochondral defects using AD-MSCs

3.2.2 Preparation of the subchondral part of the biphasic scaffold

Macropores are important for facilitating the ingrowth of new bone and blood vessels, which are critical for tissue regeneration while micropores play a role in promoting the adsorption of proteins that can enhance cell behavior and tissue development within the biomaterial. The combination of both macropores and micropores in biomaterials can optimize the tissue engineering process, ultimately leading to more successful outcomes in regenerative medicine applications (Wu et al., 2013).

Scaffolds with well-interconnected macropores in the 300–500 μm range are recommended in tissue engineering, particularly for bone regeneration. This scaffold geometry facilitates nutrient and waste transport, supports vascular ingrowth, promotes direct osteogenesis, provides mechanical support, ensures uniform cell distribution, and facilitates tissue integration—making it conducive to the successful regeneration of functional tissues (D. Xiao et al., 2020). The interconnected macropores create a more uniform distribution of cells throughout the scaffold, ensuring that cells are not confined to the surface but are able to infiltrate deep into the scaffold. This is essential for even tissue growth and regeneration. The creation of interconnected macropores within CPC effectively solves the problem of slow degradation. These macropores have dual advantages: they increase the specific surface area of the CPC, accelerate its dissolution by allowing better fluid infiltration, and promote the ingrowth of bone tissues and blood vessels, thus increasing the biodegradation of the CPC. Various methods have been proposed to achieve interconnected macropores in the CPC (S. Hesaraki, F. Moztarzadeh, & D. Sharifi, 2007; Qian, Wu, & Ye, 2023)

One promising technique is indirect 3D printing, which combines direct 3D printing with traditional scaffold preparation methods. This process involves three main steps: preparation of sacrificial scaffolds, perfusion of these scaffolds, and removal of sacrificial scaffolds. Indirect 3D printing offers significant advantages over traditional 3D printing. It provides precise control over the pore structure, size, and porosity of the scaffold while maintaining repeatability. Importantly, when indirect 3D printing is used to create CPC scaffolds, it does not interfere with the CPC hydration response.

Table 3.1 Benefits of using Indirect 3D Printing for Fabricating CPC Scaffold

Benefit	Description
Does not negatively impact the CPC's hydration reaction	Indirect 3D printing does not expose the CPC to harsh chemicals or temperatures during the printing process, which allows the hydration reaction to proceed normally. The hydration reaction is essential for CPC's transformation into hydroxyapatite, a critical mineral for bone regeneration.
Offers the advantage of creating complex scaffold geometries with controlled porosity	This can influence mechanical properties, cell infiltration, and tissue regeneration in bone regeneration applications.

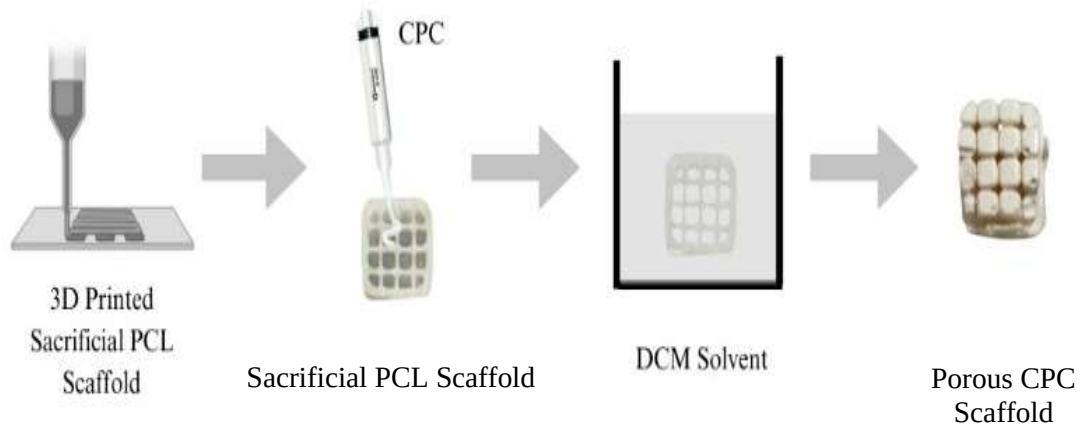

Figure 3.2 Process followed to use 3D Printed Sacrificial PCL Scaffold to obtain porosity CPC scaffold

In this thesis, The thesis utilized a Tetra Calcium Phosphate (TTCP)-based Calcium Phosphate Cement (CPC) manufactured by Permed, known as Grandus® B-One. This medical device has a setting time of 8–10 minutes, making it suitable for applications where rapid adhesion is crucial. Grandus® B-One is injectable, self-setting, and exhibits high adhesion strength upon application. Noteworthy is the use of TTCP, a tetra calcium phosphate, as a key component. TTCP has a higher Ca/P molar ratio than hydroxyapatite, a primary constituent of bone. Combined with other raw materials in the product, Grandus® B-One possesses the ability to synthesize hydroxyapatite autonomously. This feature renders it osteoconductive, bioactive, and biodegradable.

The material facilitates accelerated bone healing by transporting osteoblasts to the targeted area, contributing to faster modeling. Importantly, Grandus® B-One is absorbed and reduced during treatment, maintaining its strength throughout the process as it concurrently forms new bone. This makes it a promising option for applications requiring both rapid adhesion and sustained strength during the healing period.

Grandus® B-One undergoes a dissolution-precipitation reaction, similar to other calcium phosphate cements, to form hydroxyapatite. This process is isothermic, presenting a significant advantage over acrylic cements, as it does not release heat. Hydroxyapatite, a crucial building block of bone and a phase of osteogenesis, is formed through this reaction. The primary raw material in Grandus® B-One is Tetra Calcium Phosphate (TTCP). Notably, TTCP is the only calcium phosphate compound with a Ca/P ratio higher than hydroxyapatite, boasting a Ca/P ratio of 2.0 compared to HA's 1.67. This unique property allows TTCP in Grandus® B-One to autonomously generate hydroxyapatite, contributing to its effectiveness in bone-related applications.

3.2.2.1 3D Printing process of sacrificial PCL scaffold

Scaffolds were printed according to the architecture of the model using poly(εcaprolactone) (PCL) by melting and extrusion of PCL. Polycaprolactone (PCL) is an FDA-approved synthetic polymer widely used in tissue engineering for bone regeneration (Dwivedi et al., 2020). It is biocompatible and biodegradable, with a slow degradation rate of 2-4 years. PCL possesses excellent mechanical properties, including stiffness and strength, making it suitable for maintaining mechanical strength in tissue-engineered bone substitutes. It is often used in combination with natural polymers and bioceramics to create customized materials for bone regeneration applications, serving as a long-lasting scaffold for supporting bone tissue growth and regeneration (Cooper, Bhattarai, & Zhang, 2011; Woodruff & Hutmacher, 2010).

In the process of preparing PCL (Polycaprolactone) models, the printing platform temperature was intentionally set at a low temperature of 4°C. This low temperature was chosen because it helps in the solidification of the PCL material once it is extruded during the 3D printing process. Solidification is essential for maintaining the desired shape and structure of the printed object.

PCL scaffolds were printed through the melt extrusion technique using a commercial bioprinting system m (3D-Bioplotter Manufacturer Series, EnvisionTEC). First, the PCL struts were melted at 130 °C in a heating barrel and incubated for 20 min prior to printing to be equilibrated. PCL material was extruded through a heated 23G nozzle.

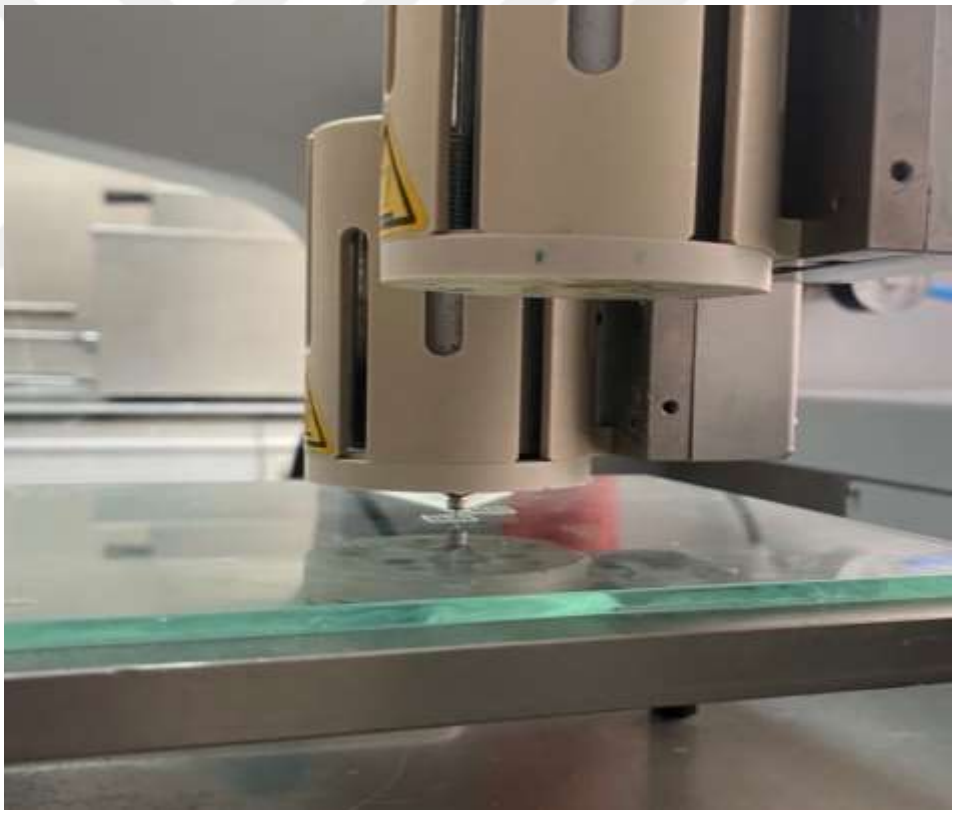

Figure 3.3 3D Printing process of PCL Scaffold

Eight-layer scaffolds with a diameter of 8.35 mm x 8.35 mm x 0.4 mm were designed. The scaffolds were designed in a lay-down pattern of 0/90°, forming square pores. All scaffolds were fabricated using the same parameters: a 23G nozzle, a layer thickness of 3

mm, a distance of 2 mm between the two strands, a temperature of 130, and a speed of 2.5 mm/s. Following this condition, the PCL scaffolds were built in a layer-by-layer manner to make a 3D structure with uniform height and porosity. After fabricating the multi-layered structure, the fabricated scaffold was sterilized in 70% EtOH.

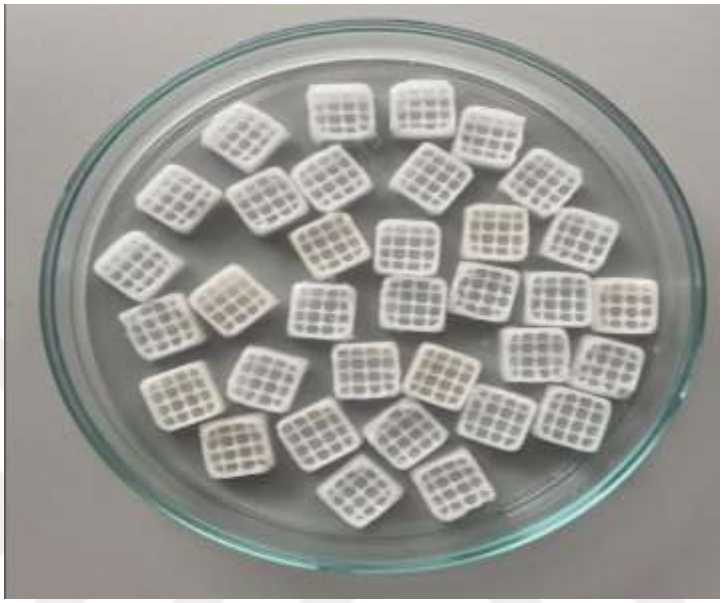

Figure 3.4 3D Printed Sacrificial PCL Scaffold

After the sacrificial PCL Scaffold is printed, self-setting CPC (Permed, Turkey) is prepared. CPC powder consisted of TTCP and dicalcium phosphate anhydrous (DCPA). The procedure can be summarized as follows: (1) CPC pastes were obtained via mixing CPC solid and liquid stages in accordance with the liquid-to-solid ratio of 1:3 mL/g; (2) The pastes, were aspersed into the PCL models which were placed in glass Petri-dishes, and incubated at 37 °C under 97 % humidity with the duration of 3 days. Since self-setting CPC sets in 8-8.5 minutes, this time was taken into consideration when plastering into sacrificial PCL scaffolds.

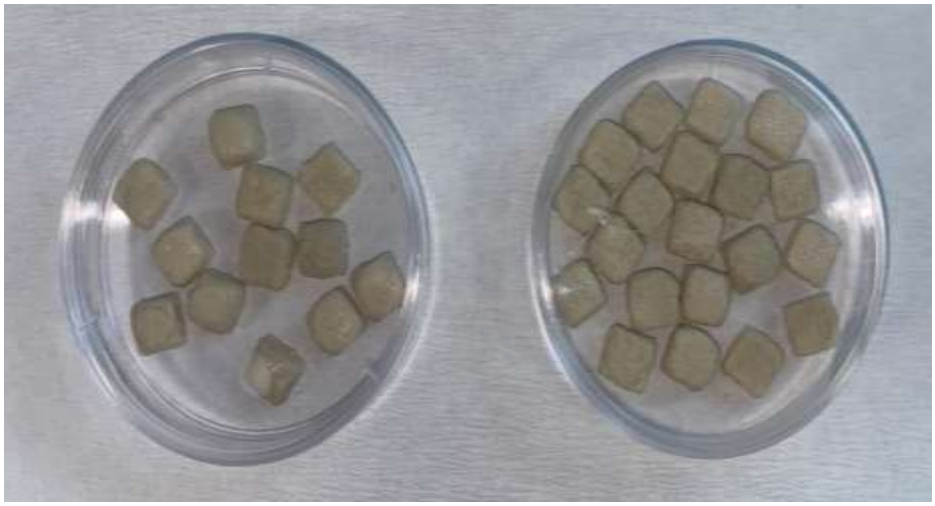

Figure 3.5 Unset CPC paste in Sacrificial PCL Scaffolds

The samples were left to dry at 37 °C for 24 hours in glass petri dishes.



Figure 3.6 CPC/PCL Scaffolds after drying 1 day

After the samples have dried thoroughly, the samples were immersed in dichloromethane (Sigma Aldrich) as a solvent until the PCL templates were completely removed.

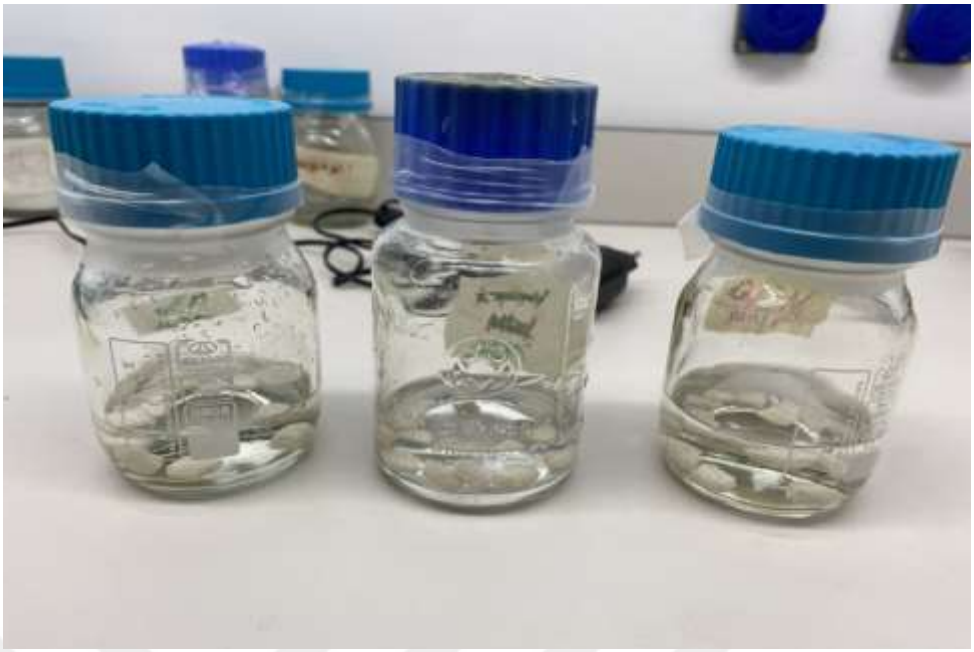

Figure 3.7 CPC/PCL Scaffolds in DCM Solvent

The samples were kept in dichloromethane for about 30 minutes to dissolve the PCL. In the end, macroporous CPC scaffolds were acquired after drying naturally for 2 h in a fuming cupboard; and then at 60 °C in an oven for 12 h successively.

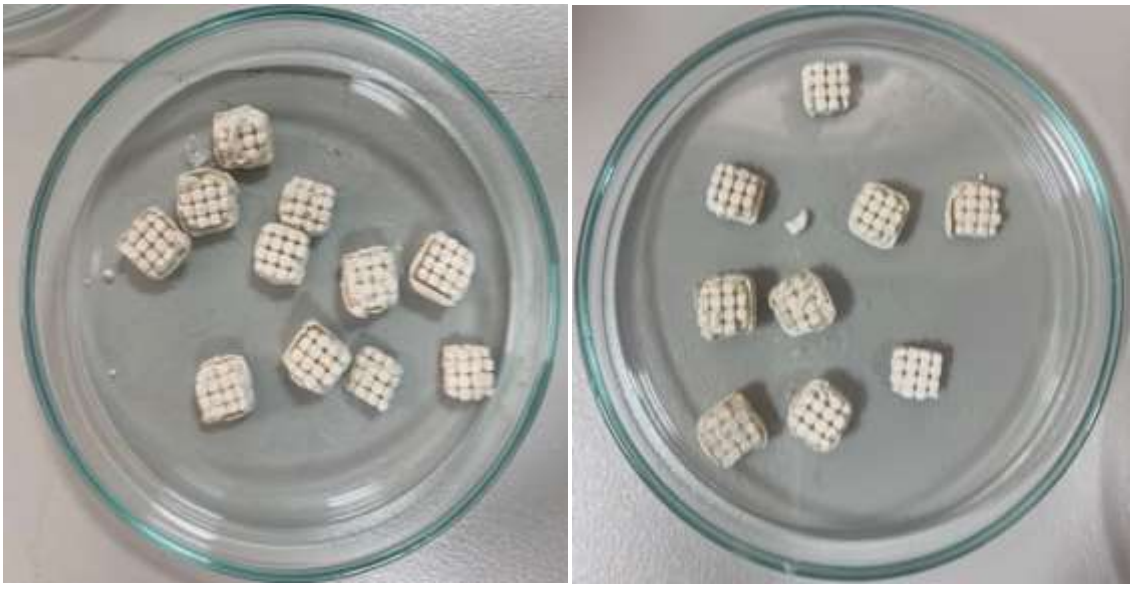

Figure 3.8 Porous CPC Scaffolds after solved in DCM Solvent



Figure 3.9 Final macroporous CPC Scaffold

3.2.3 Cell toxicity analysis of CPC scaffolds

To determine the toxicity of the CPC scaffolds that is, whether they release extracts that may be biologically harmful, an indirect cytotoxicity test was applied as the first step. The biocompatibility of the materials was evaluated according to the MEM-extraction test specified in ISO 10993/EN 30993.

Table 3.2 Cytotoxicity evaluation criteria

	Evaluation criteria	Scor
Cell layer spreading	%100	0
	%90-100	1
	%60-90	2
	%30-60	3
	%0-30	4
Amount of dead cells	Never seen	0
	Little change, few cells affected	1
	%5-10	2
	%10-20	3
	≥ %20	4
Change in cell morphology	No change observed	0
	Little change, few cells affected	1
	Moderate change, change in morphology of some cells observed	2
	Moderate change, changes in the morphology of many cells were observed	3
	There is a high level of change, a change in the morphology of the whole cell was observed	4

Table 3.2 Cytotoxicity evaluation criteria (continue)

	Evaluation criteria	Scor
Cell growth inhibition	%0-10	0
	%10-30	1
	%30-50	2
	%50-70	3
	%70-100	4

The data obtained from microscopic examination and cell counting were corrected for the negative control group and graded according to the evaluation criteria given in Table 3.2. The grades obtained for the first three criteria (spread of the cell layer, number of dead cells and change in cell morphology) were averaged. This average grade was summed with the grade obtained from the last criterion (cell growth inhibition) and used to obtain the final cytotoxic response index value ranging from 0-8 (Table 3.3). This value was used to evaluate whether the material produced was cytotoxic or not.

Table 3.3 Cytotoxic response index and cytotoxicity assessment

Cytotoxic Response Index	Reactivity	''Material is cytotoxic"
0-1	None	No
1-3	Slight	No
3-5	Mild	Should be re-evaluated
5-7	Modarate	Yes
7-8	Severe	Yes

The 4 groups used in the experiment were determined as bulk CPC, CPC Scaffold, positive control, and negative control (latex), respectively. The samples were shaped in 8 mm x 8 mm x 4 mm dimensions and placed in sterile falcon tubes. Sterilization was carried out by treatment with 70% (v/v) ethyl alcohol for 20 minutes, followed by UV irradiation for 30 minutes. The samples were then washed with PBS. A standard cell

culture medium was used as the extraction liquid. The composition of the medium used was as follows: 10% FBS (FBS, Gibco, USA), 1% penicillin/streptomycin (Gibco, USA) in high glucose DMEM (Gibco, USA).

The samples were each taken into 10 mL of extraction liquid and kept under constant agitation at 60 rpm for 24 hours at 37ºC. After 24 hours, the extraction liquid was passed through a 0.2 μm membrane filter and collected into sterile 15 mL falcon tubes.

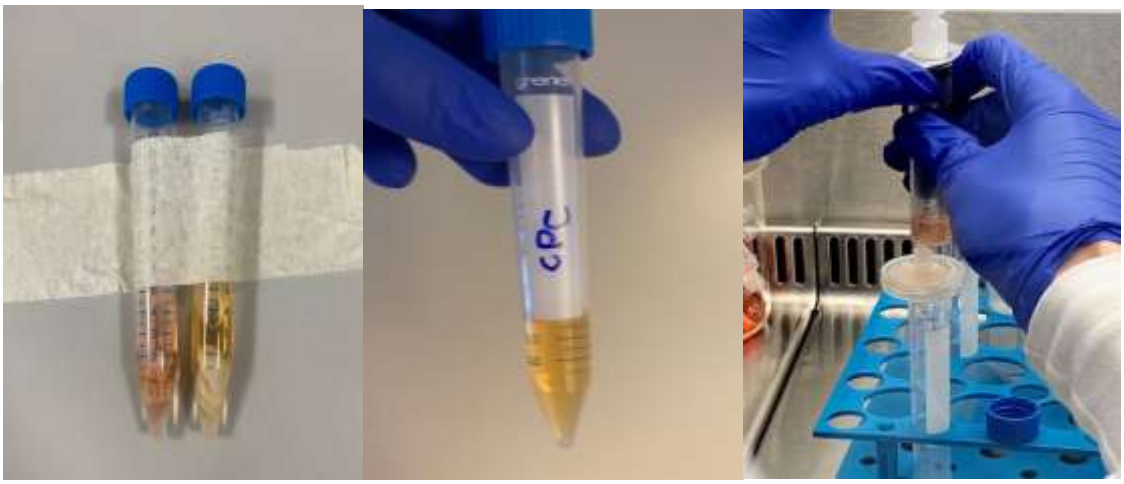

Figure 3.10 Extract medium of CPC bulk and CPC scaffold and filtration process of extract media of CPC scaffold

Passage 26 L929 cells were thawed and transferred to T75 flasks in a standard cell culture medium. Cells cultured in an incubator at standard culture conditions (37ºC, 5% CO2 and humidity) for 1 day were then taken out from the flask by trypsin (Cat. No. 25200056, Gibco, USA) application and seeded into 24-well cell culture dishes at a concentration of 10,000 cells/cm2 (20,000 cells for a 24-well dish) and 3 replicates for each group.

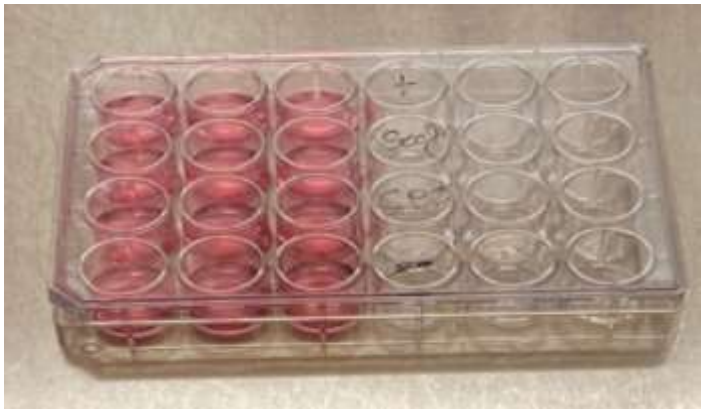

Figure 3.11 24 Well for cell toxicity analysis of 4 groups

When the cells, which were cultured under standard culture conditions for 24 hours, became approximately 70% confluent, morphological evaluations were made with a microscope, and then the extraction liquids were added to the cell layers at 500 µL/well. 24, 48, and 72 hours after the addition of the extraction fluids, the extent of the cell layer (confluency), the number of dead cells, and the changes in cell morphology were evaluated by microscopic examination. At the end of 72 hours, the quantity of viable cells in the wells was determined via the Cell-Titer Blue® method.



Figure 3.12 96 well plates of Alamar Blue Analysis of CPC Scaffold, CPC Bulk, negative and positive groups

3.2.4 AD-MSC cell culture

AD-MSCs (Lonza) cell lines were used for all the experiments. As a procedure, they were grown in high glucose DMEM (1 g/L) containing 10% (v/v) FBS, 100 unit/mL penicillin/streptomycin %1 Fibroblast growth factor-2 (FGF-2), and incubated at 37^0C, in 5% CO2 and 90% humidity in a CO2 incubator (Thermo Scientific, Steri-Cycle CO_2 Incubator, USA). Every other day, the medium was regularly changed. After culturing in a growth medium to 80–90% confluency, cells were detached and passaged. AD-MSC Passage 1 cells were used in all experiments.

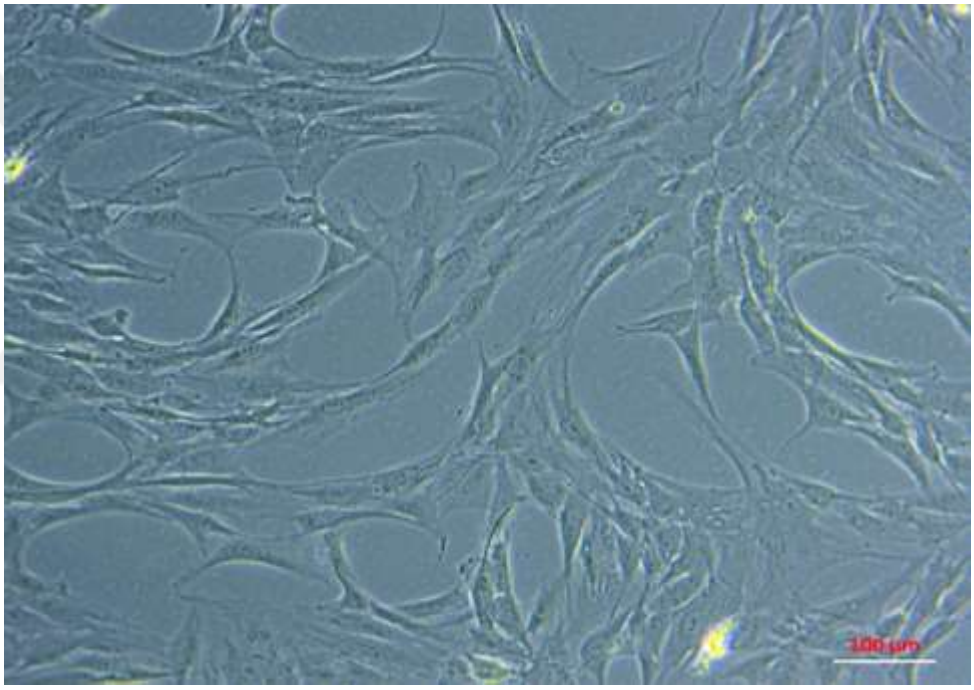

Figure 3.13 AD-MSC p:1 with a light microscope (Scale bar: 100 μm)

3.2.5 Cell seeding on CPC scaffolds

For the differentiation analysis, AD- MSC passage 1 that reached >80% confluency was harvested enzymatically in Trypsin-EDTA (0.25%) (Gibco). CPC Scaffolds were sterilized by UV irradiation and immersion in 70% ethanol for 30 minutes, washed thrice with PBS, and incubated in culture media overnight. Scaffolds were then transferred into 24 well plates and each scaffold was seeded with 50μL media containing 15×10^4

cells/scaffold AD-MSCs cell line. Cells were incubated for 1 hour at 37°C and 5% CO_2, before the addition of 1 ml media into each well.

After incubation, 12 samples of scaffolds were cultured with 1000 µL osteogenic medium (high glucose DMEM addition with b-glycerophosphate 10^{-2} M, dexamethasone 10^{-4} M, and ascorbic acid 50 mg mL^{-1}) and the control group 12 samples of CPC scaffold were cultured with 1000 µL control medium (high glucose DMEM (1 g/L) containing 10% (v/v) FBS, 100 unit/mL penicillin/streptomycin %1 Fibroblast growth factor-2 (FGF-2)).

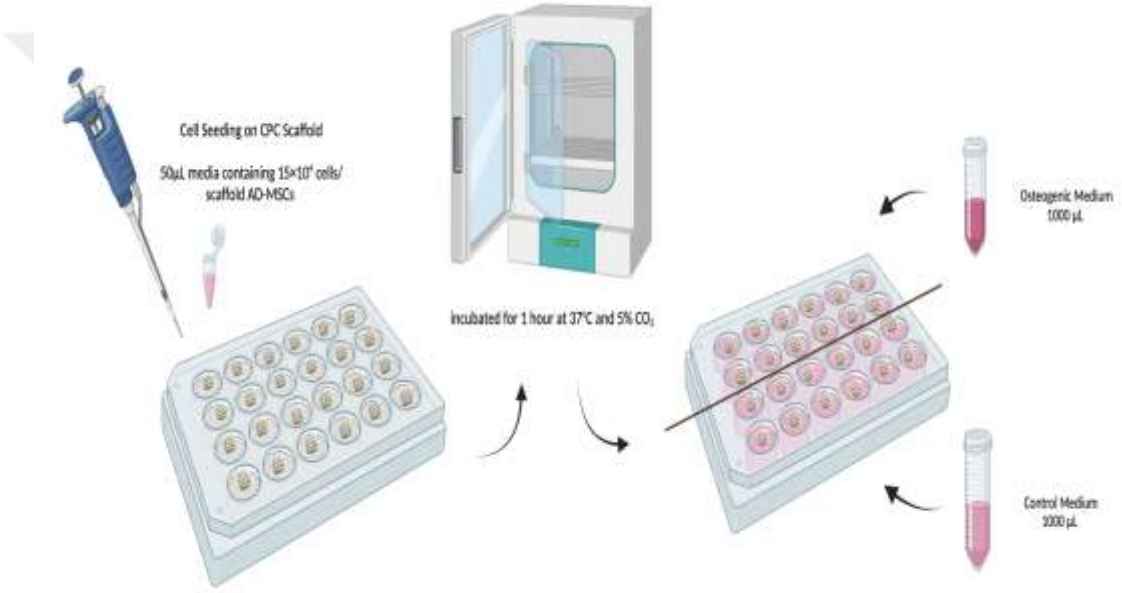

Figure 3.14 Process of cell seeding on CPC Scaffolds and adding control/osteogenic medium

Cells were allowed to adhere to the scaffolds for 1 h in standard condition, and then fresh medium was added to wells. Seeded scaffolds were maintained in culture for 7, 14, and 21 days at 37°C and 5% CO_2 with media changes every two days.

3.2.6 Cell Viability (Alamar BlueTM) Test of CPC Scaffolds

At the end of experimental times, cell proliferation and viability were measured by Alamar Blue assay. Initially, the culture medium was removed from the cell-containing well plates and followed by a PBS rinse. Subsequently, a 5% Alamar Blue solution, prepared in colorless Dulbecco's Modified Eagle Medium (DMEM), was added to the scaffolds. The scaffolds were then placed in a dark incubation chamber at 37°C with 5% CO2 for 1 hour. After the incubation period, the solution containing the dye was collected from the well plates and transferred to 96 well plates. Using a microplate reader, absorbance readings were taken at wavelengths of 570 nm and 595 nm. After the Alamar Blue solution remaining on the cells was removed, the scaffolds were washed with PBS and the culture was continued by adding fresh medium. This process was repeated on days 1, 7, 14, and 21 during the culture period. The decrease in absorbance values was quantified, and a calibration curve was utilized to determine the number of viable cells present at each time point.

3.2.7 Cell activity and differentiation

3.2.7.1 Alizarin Red Staining

In this experiment, both control and experimental groups were assessed for calcium production at three different time points (7, 14, and 21 days) during a treatment period. The assessment involved staining the samples with alizarin red solution (Sigma-Aldrich), which binds to calcium salts. The stained samples were washed several times and then treated with cetylpyridinium chloride to elute the stain. The results were reported as the molar equivalent of calcium, taking into account the binding ratio of alizarin red to calcium. This method is commonly used in studies related to bone tissue engineering and osteogenesis to evaluate calcium mineralization in cells and scaffolds.

3.2.8 Characterization of CPC scaffolds

3.2.8.1 Mechanical measurements

CPC scaffolds, after their incubation at 50°C for 72h, compressive strength, and compressive modulus were measured with a crosshead displacement rate of 1 mm/min by using the Universal Testing Machine of Shimadzu (Autograph AGS-X Series), in the Laboratory of Biomechanics and Strength of Materials, Department of Biomedical Engineering, Ankara University.

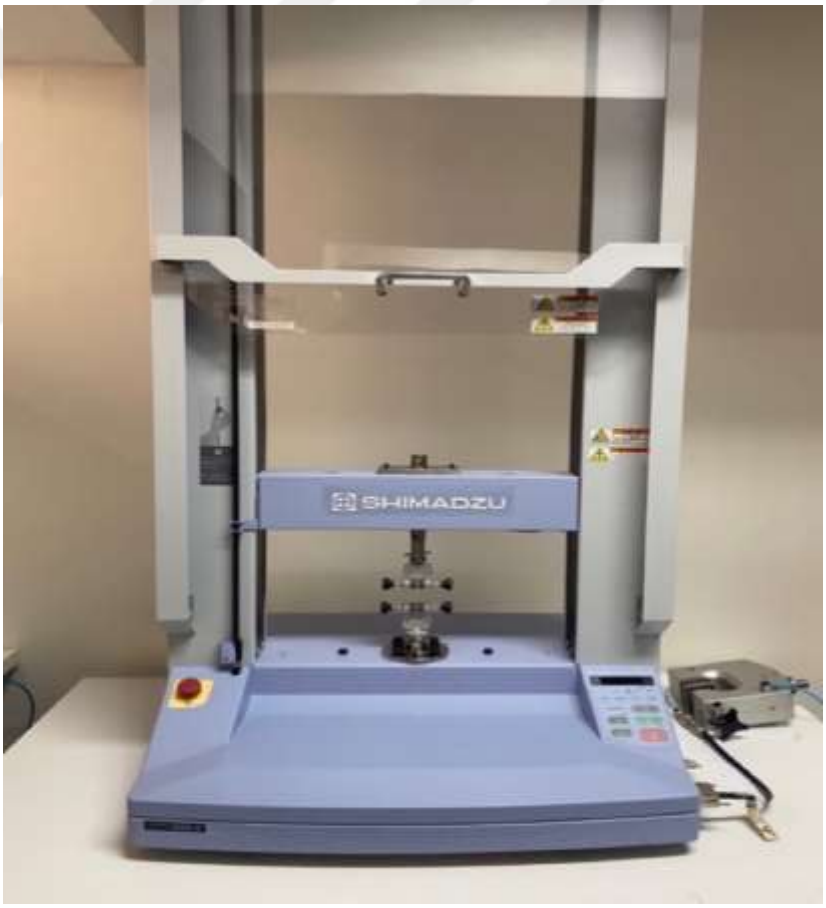

Figure 3.15 Universal Testing Machine of Shimadzu

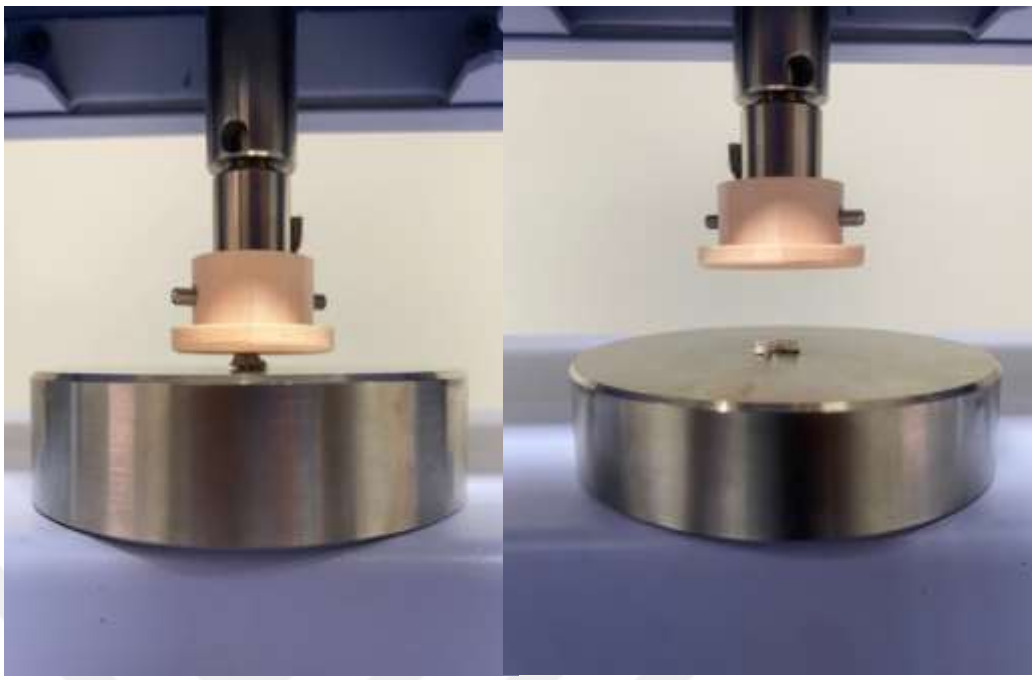

Figure 3.16 CPC Scaffolds during the compression test

The Young's modulus and ultimate compressive strength of the CPC scaffolds were measured using a mechanical testing machine (Shimadzu, Japan) with a 5 kN load cell, and a cross-head speed of 1.0 mm min^{-1}.

The samples under study (n=3) with a diameter of 8.5 mm and a height of 9 mm were compressed in the Z direction until they fractured. The resulting data obtained was used to calculate the mean compressive strength and Young's modulus. Data processing was completed using MATLAB and Microsoft Excel.

3.2.8.2 FTIR analysis of CPC scaffolds

Fourier Transform Infrared-Attenuated Total Reflectance (FTIR-ATR) spectroscopy analysis (The JASCO FTIR-4600) was utilized to ascertain probable modifications of the chemical constitution of the polymers during processing as well as to determine the remaining solvent within the CPC scaffold in the Department of Biomedical Engineering,

Ankara University. Samples were analyzed in 4000–600 cm^{-1} wavenumber range and transmittance mode.

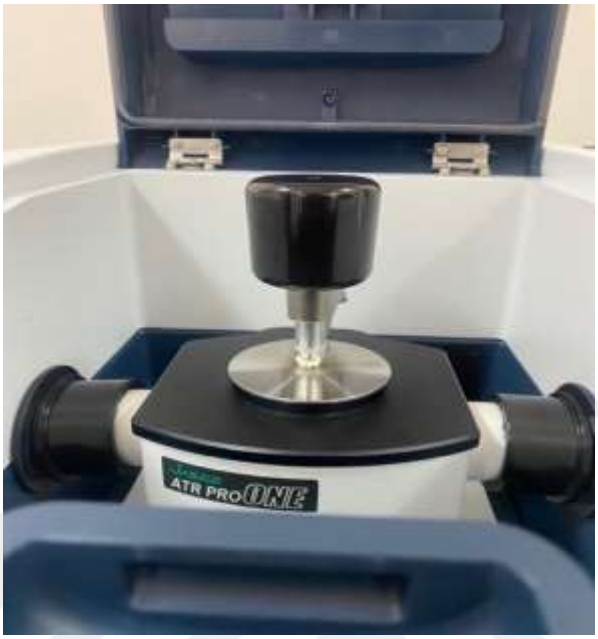

Figure 3.17 The JASCO FTIR-4600 device

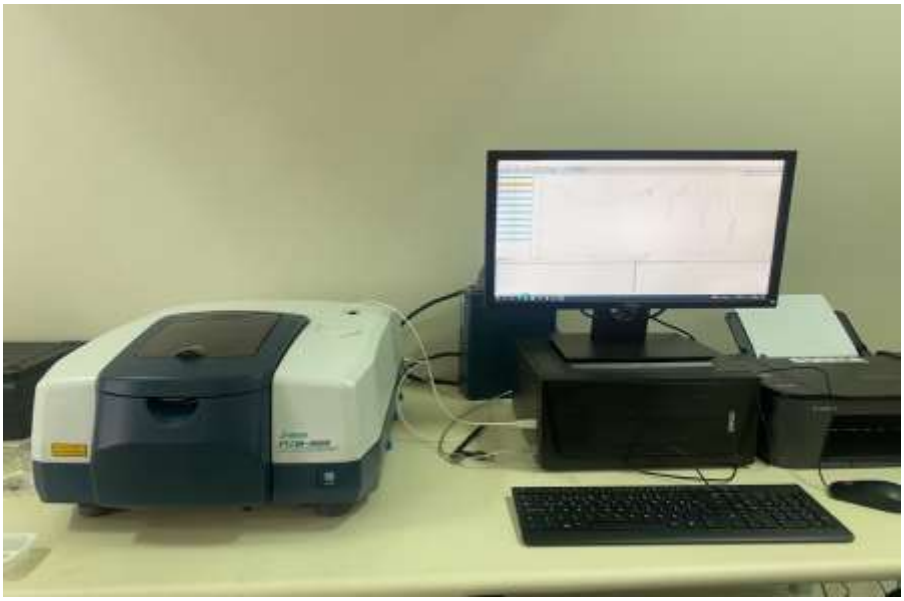

Figure 3.18 FTIR Analysis of CPC Scaffold

3.2.9 Scanning Electron Microscopy analysis of CPC scaffolds

AD-MSCs cultured with both control medium and osteogenic medium on CPC scaffolds for 7,14 and 21 days were rinsed with saline buffer, fixed with 3.7% paraformaldehyde for 4 hours, subjected to graded alcohol dehydrations, and rinsed with PBS. In order to prepare the samples for SEM observation, they were first stored at -20 and then air-dried for 24 hours. Then samples were mounted on metal discs and sputter-coated with gold, SEM investigation was carried out using the Carl Zeiss EVO 40 Scanning Electron Microscope (Germany) device by the expert personnel of the Institute of Nuclear Sciences operating at 15kV on the samples.



Figure 3.19 Zeiss EVO-40 Scanning Electron Microscope

3.3 Preparation Chondral Part of Biphasic Scaffold

Alginate, which cations could readily crosslink, has shear-thinning properties that are popular for extrusion-based bioprinting. However, it could be chemically modified with other biomaterials to improve alginate's mechanical and biological properties. The

biocompatibility and cellular tolerance of alginate are critical factors for the efficacy of tissue engineering applications. Alginate has been demonstrated to facilitate chondrogenic differentiation, a process that involves the conversion of undifferentiated cells into chondrocytes, or cartilage cells. This transformation is marked by the production of type II collagen and proteoglycans, which are fundamental constituents of cartilage tissue. These findings underscore the importance of alginate as a biomaterial for tissue engineering, particularly in the development of cartilage tissue.

However, alginate lacks the important sites and signals that cells need to attach, grow, and interact within their environment. On the contrary, collagen is a significant component of the extracellular matrix in various tissues, providing crucial binding sites for cells via its integrin-binding regions. This substance is very compatible with living tissue and facilitates cell attachment, movement, and growth. By blending alginate and collagen, it's possible to form a hybrid hydrogel scaffold that capitalizes on the advantages of both materials. Alginate supplies the needed structural support and encapsulation properties, while collagen delivers the essential active molecules that enable cells to connect and thrive within the scaffold. This combination is designed to enhance cell attachment, growth, and the overall regeneration of tissues. Due to these features and the hydrophilic nature of alginate, it can be used as an extracellular material suitable for providing cell growth. Thus in the present study alginate was selected as the chondral part of the scaffold.

Therefore, the goal of this study was to mimic the cartilaginous component of the osteochondral scaffold by combining sodium alginate and recombinant collagen in predefined ratios. Sodium alginic acid (Sigma) at a concentration of 0.1 g/mL (1.6 grams of alginate dissolved in 15 mL of Dulbecco’s Phosphate Buffer Solution) was prepared by dissolving it in Dulbecco’s Phosphate Buffer Solution and agitating it overnight at 37°C with a rotation speed of 400 rpm.

Simultaneously, a 15 mg/mL solution (75 mg of recombinant collagen powder dissolved in 5 mL of DPBS) of recombinant collagen was generated by dissolving the recombinant collagen powder in Dulbecco’s Phosphate Buffer Solution at 4°C over the course of a

night. Following the dissolution of recombinant collagen, the resulting solution was filtered through a sterile 0.2-micron membrane and kept at 4°C. Subsequently, the alginate solution and recombinant collagen solution were mixed in a sterile glass container, and with gentle agitation, the two solutions were blended until complete dispersion was achieved, resulting in a viscous homogenous solution.

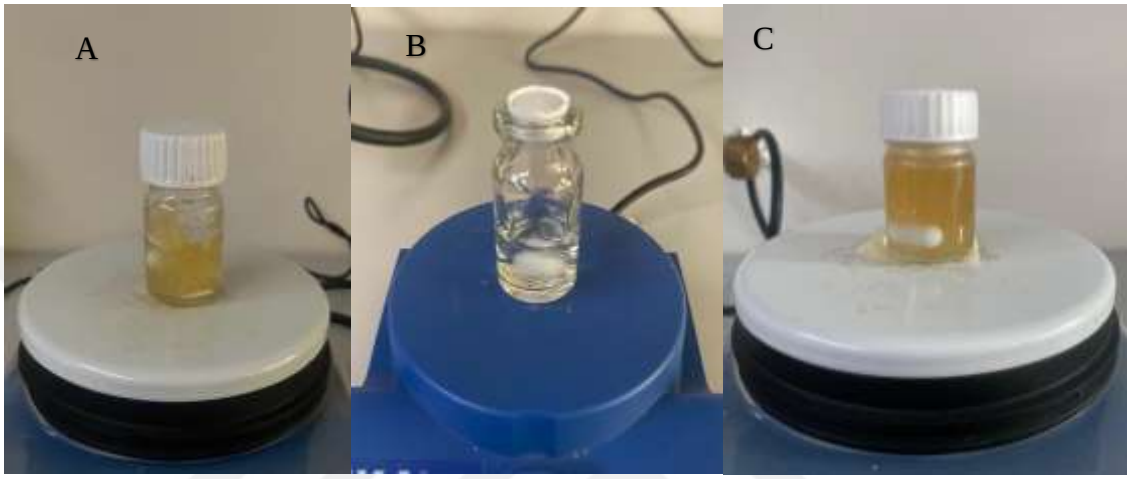

Figure 3.20 (A-B) Preparation process of alginate solution and recombinant collagen solution (C) obtained mixed Homogenous Alginate/Recombinant Collagen Solution

3.3.1 3D Printing process of alginate/recombinant collagen scaffold

For the fabrication of chondral part scaffolds of 8.30 × 8.30 x 2 mm dimensions and 150 µm of pore size were printed by means of a 3D bioplotter device (Envisiontec GmbH, Germany) equipped with three syringes and one FDM extruder, consisting of hardware and Designer software. Prepared alginate/recombinant collagen solution was loaded into the 5 ml syringe, and 3D printing was performed with a 3D bioplotter device (Envisiontec GmbH, Germany).

The dimensions of square-shaped scaffolds consist of 7 layers resulting in the macroporous scaffold. Printing parameters, including factors like pressure and speed, underwent extensive testing to ensure successful printing. Through systematic optimization studies, the appropriate concentration of hydrogels to be utilized in the

printing process was identified. The dimensions of square-shaped scaffolds consisting of 7 layers (total height ca. 2 mm) were fabricated in a glass bed using a 5 mL syringe, 25 G conical nozzle inner diameter. Printing parameters were as follows; 1.5 mm strand distance, 7.5 mm/s of nozzle speed, pressure 1.2 bar, temperature 30°C.



Figure 3.21 3D Printing set-up of Alginate/recombinant collagen scaffold

After the printing process, crosslinking of 3D printed Alginate/Recombinant Collagen scaffold was achieved by treatment with 6,8 M $CaCl_2$.



Figure 3.22 3D Printed Alginate/Recombinant Collagen scaffold

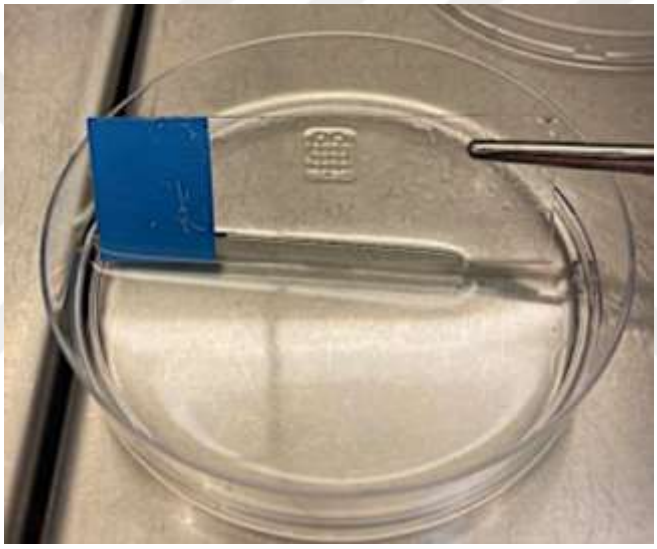

Figure 3.23 3D Printed Alginate/recombinant collagen scaffold crosslinking process in $CaCl_2$ bath

3.3.2 Mechanical measurements of alginate/recombinant collagen scaffolds

3.3.2.1 Compression test

3D-printed hydrogel scaffolds were affixed to the apparatus using a metal pin, securing them to the tensioner system of the testing machine. Biomechanical loading was assessed once the relevant parameters were configured. The crosshead's maximum displacement was set to 1 mm, with a speed of 0.1 mm/min. The equilibrium modulus (measured in

kPa) was determined by dividing the equilibrium force-to-cross-sectional area ratio by the applied strain. The uniaxial tension test was conducted using the Universal Testing Machine of Shimadzu (Autograph AGS-X Series), in the Laboratory of Biomechanics and Strength of Materials, Department of Biomedical Engineering, Ankara University.

The constructs were stretched at a rate of 2 mm/min until sample failure occurred, all at room temperature. The modulus was derived from the initial linear regions of the stress-strain curves. The experimental group underwent testing with three samples. Images depicting one of the samples during the compression test are provided for reference.

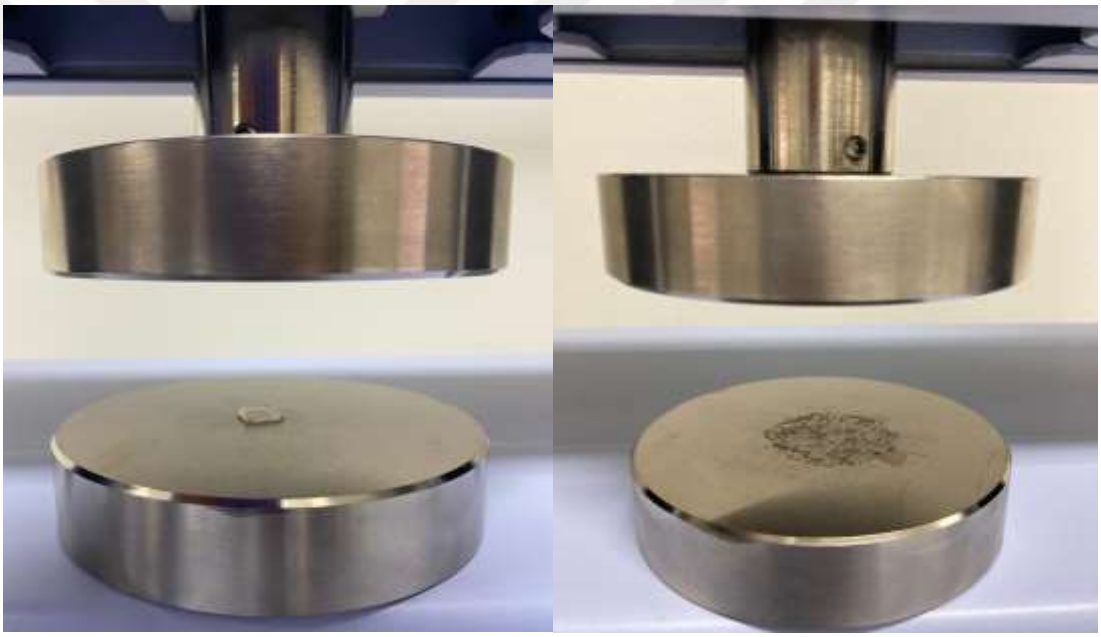

Figure 3.24 The images of the Alginate/Recombinant Collagen scaffold during the compression test

3.3.3 Cell toxicity analysis of alginate/recombinant collagen scaffold

The biocompatibility of the materials was evaluated according to the MEM-extraction test specified in ISO 10993/EN 30993. L929 mouse fibroblast cell line was used in the cytotoxicity test. Passage 26 L929 cells were thawed and transferred to T75 flasks in a standard cell culture medium. Cells cultured in an incubator at standard culture conditions (37°C, 5% CO2 and humidity) for 24 hours were then removed from the flask by trypsin

(Cat. No. 25200056, Gibco, USA) application and seeded into 24-well cell culture dishes at a concentration of 10,000 cells/cm2 (20,000 cells for a 24-well dish) and 3 replicates for each group. When the cells, which were cultured under standard culture conditions for 24 hours, became approximately 70% confluent, morphological evaluations were made with a microscope, and then the extraction liquids were added to the cell layers at 500 µL/well.

24, 48, and 72 hours after the addition of the extraction fluids, the extent of the cell layer (confluency), the number of dead cells, and the changes in cell morphology were evaluated by microscopic examination. At the end of 72 hours, the number of viable cells in the wells was determined by the Cell Titer Blue® method.

3.3.4 AD-MSC cell culture

AD-MSCs were used for all the experiments. They were grown in high glucose DMEM (1 g/L) containing 10% (v/v) FBS, 100 unit/mL penicillin/streptomycin %1 Fibroblast growth factor-2 (FGF-2) and incubated at 37 0C, in 5% CO2 and 90% humidity in CO2 incubator (Thermo Scientific, Steri-Cycle CO2 Incubator, USA). The medium was replenished every other day. After culturing in a growth medium to 80–90% confluency, cells were detached and passaged. AD-MSCs passage 1 cells were used in the experiments.

3.3.5 Cell seeding on alginate/recombinant collagen scaffolds

Before cell seeding, the 3D-printed alginate/recombinant collagen scaffolds were sterilized by ultraviolet irradiation. All scaffolds were washed twice with PBS, and subsequently immersed in a complete culture medium overnight. The scaffolds were then transferred into 24 well plates, rinsed with plenty of PBS, and each scaffold was seeded with 10 µL media containing 15×10^4 cells/scaffold AD-MSCs cell line on the top surfaces, and cultured in a 24-well plate. Cells were allowed to adhere to the scaffolds for 1 h at 37°C and 5% CO_2, before the addition of 500 µL fresh media into each well.

12 samples of scaffolds were cultured with chondrogenic medium (StemPro® Osteocyte/Chondrocyte Differentiation Basal Medium/StemPro® Chondrogenesis Supplement) and the other 12 samples of scaffold were cultured with control medium (high glucose DMEM (1g/L) containing 10% (v/v) FBS, 100 unit/mL penicillin/streptomycin %1 Fibroblast growth factor-2 (FGF-2)). Seeded scaffolds were maintained in culture for 7, 14, and 21 days at $37^{O}C$ and 5% CO_2 with media changes every two days.

3.3.6 Cell viability (Alamar Blue^{TM}) test of alginate/recombinant collagen scaffolds

The Alamar Blue cell viability test was employed to determine the number of viable cells. This test is advantageous as it enables the measurement of metabolic activity without affecting cell viability or metabolism. It finds widespread use in assessing chemical cytotoxicity, evaluating cell proliferation, and quantifying overall cell health. Importantly, it provides a means to gauge metabolic activity while preserving cell viability and metabolism.

Cell viability was assessed through the Alamar Blue assay. Initially, the cultured medium was taken out from the well plate containing the cells, followed by a PBS wash. A 5% Alamar Blue solution prepared in colorless DMEM was supplemented, and the cells were incubated for 1 h. at 37°C and 5% CO^2 in the dark. After incubation, the dye solution was collected from the well plate, and absorbance was gauged at 570 and 595 nm wavelengths utilizing a microplate reader. This process was repeated on days 1, 7, 14, and 21 of the culture, with the reduction in absorbance values quantified to determine the number of live cells, guided by a calibration curve.

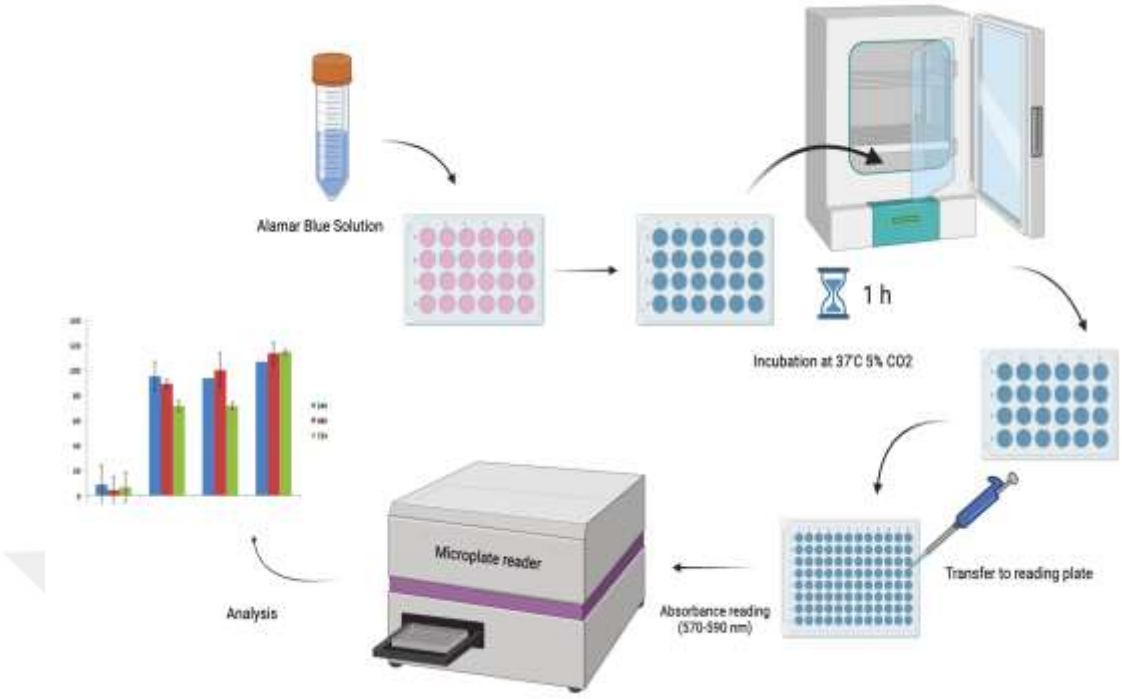

Figure 3.25 Schematic of Alamar Blue Assay

3.3.7 Chondrogenic differentiation of AD-MSC on the alginate/recombinant collagen scaffolds

3.3.7.1 Alcian Blue Staining

The chondrogenic differentiation of the cells was evaluated using Alcian Blue staining under acidic conditions. Alcian Blue was employed to detect the presence of glucosaminoglycans and proteoglycans like aggrecan, which are typically present in the extracellular matrix (ECM) of articular cartilage tissue. Components of cartilage tissue, including carboxylate and sulfate groups found in hyaluronic acid, heparan sulfate, dermatan sulfate, and chondroitin sulfate, become ionized at a pH of 2.5, resulting in a negative charge.

To specifically visualize proteoglycans and hyaluronic acid components in cartilage tissue, Alcian Blue staining was performed at a pH of 2.4–2.5, leading to a blue coloration after staining. Following fixation, the cells were treated with a 1% (w/v) Alcian Blue

solution (Sigma-Aldrich) in 3% acetic acid at pH 2.4 for a duration of 30 minutes. Subsequently, the samples were washed with distilled water several times and examined under a light microscope (Primovert, Axiocam ERC55, Zeiss, Germany).

3.3.8 SEM analysis of the cell-seeded alginate/recombinant collagen scaffold

Cell morphology on the Alginate/Recombinant Collagen Scaffold was studied by SEM (Carl Zeiss EVO 40 Scanning Electron Microscope) analysis on days 7, 14, and 21 at the Ankara University, Institute of Nuclear Sciences. Samples were fixed with paraformaldehyde (3.7% in PBS, pH 7.4) for 4 h under gentle agitation. They were then washed with pipes buffer several times, lyophilized, and sputter-coated with gold prior to SEM examination. The fixed samples were placed on carbon tapes adhered to SEM sample holders (stub). After the sputter coating with gold, the samples were viewed with the Carl Zeiss EVO 40 Scanning Electron Microscope (Germany) device by the expert personnel of the Institute of Nuclear Sciences operating at 15kV on the samples.

3. 4 Statistical analysis

Statistical analyses were performed using GraphPad Prism (version 10) software. Statistical differences were determined by analysis of variance (ANOVA) followed by Tukey's multiple comparison test or Student's *t*-test where appropriate. Numerical and graphical results are displayed as mean ± standard deviation. Significance was accepted at a level of $p < 0.05$. Sample size (n) is indicated within the corresponding figure legends.

4. RESULTS AND DISCUSSION

4.1 Bone part of biphasic scaffold

4.1.1 Cell toxicity analysis of CPC scaffolds

The cytotoxicity properties of CPC Bulk and CPC Scaffold samples were examined by indirect toxicity test as described in Section 3.2.3. At 24, 48, and 72 hours after the addition of extraction fluid, cell layer spreading and the number of dead cells were examined by light microscopy at 10x magnification according to the experimental groups. The cell layer spread observed at 24, 48, and 72 hours is given in Figure 4.1. Changes in cell morphology throughout the culture were examined at 40x magnification and the results are presented in Figure 4.2.

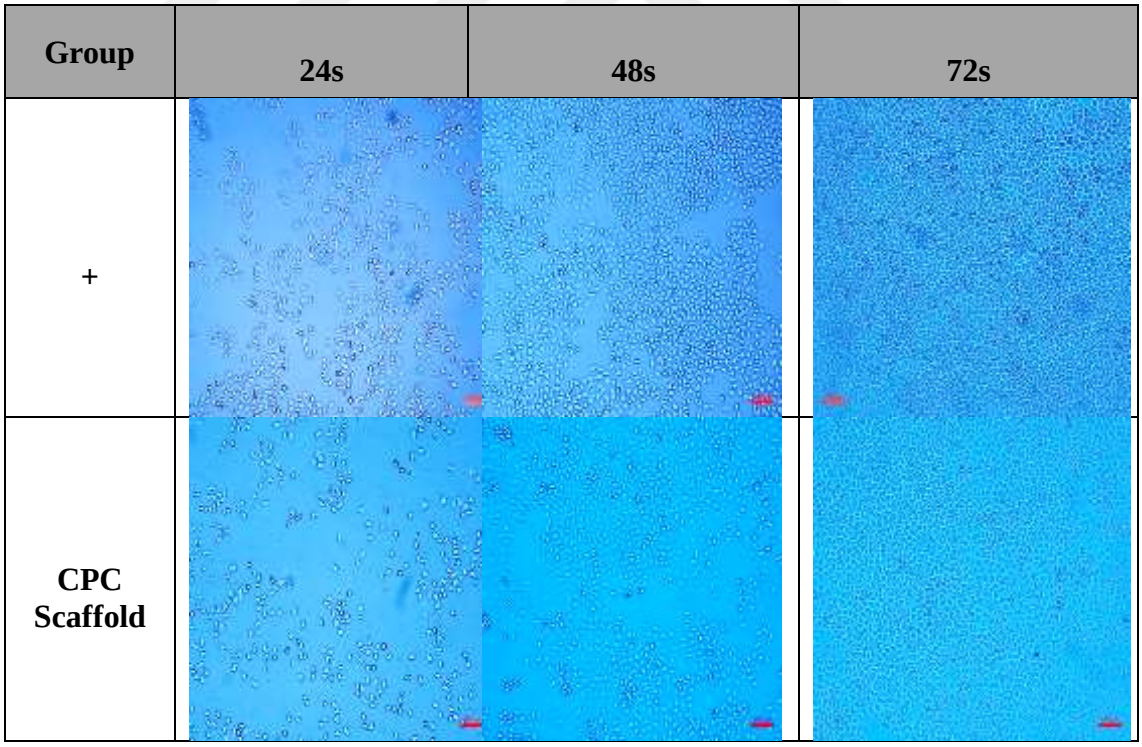

Figure 4.1 Variation of cell layer spreading at 24, 48 and 72 hours according to experimental groups after the addition of extraction fluid. (10x)

Group	24s	48s	72s
CPC Bulk		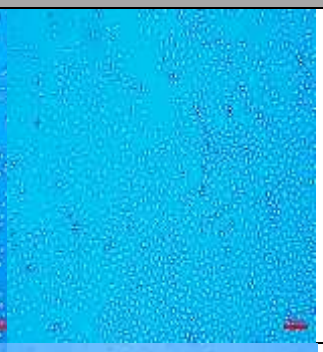	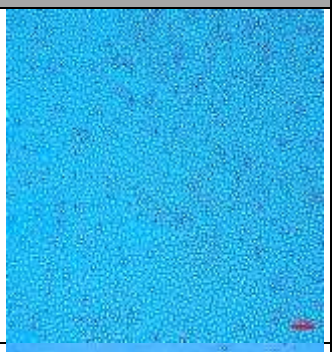
-	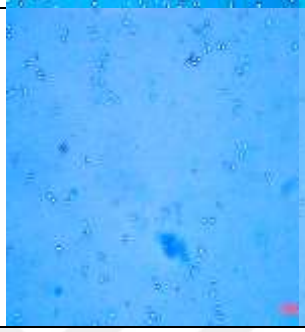	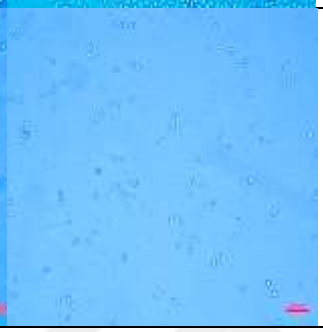	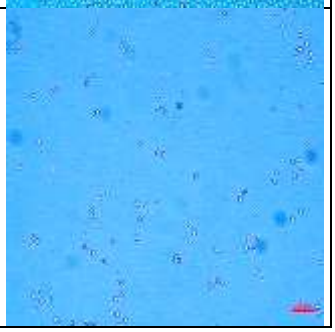

Figure 4.1 Variation of cell layer spreading at 24, 48 and 72 hours according to experimental groups after the addition of extraction fluid. (10x) (continue)

Group	24s	48s	72s
+	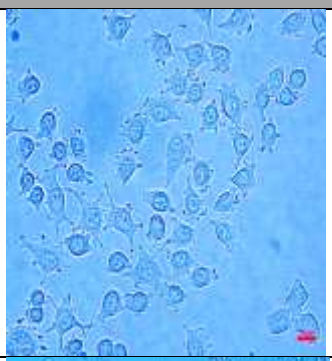	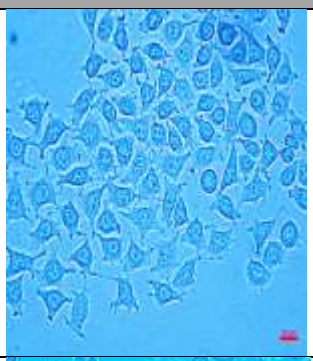	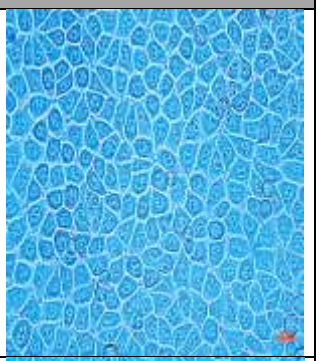
CPC Scaffold		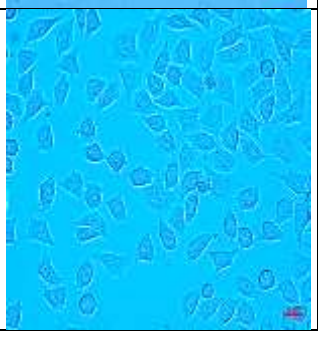	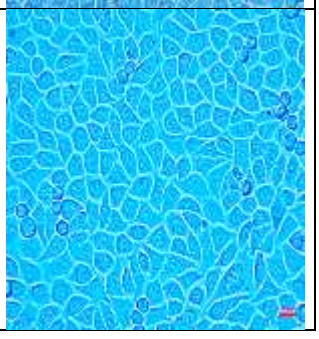

Figure 4.2 Changes in cell morphology at 24, 48, and 72 hours after the addition of extraction fluid according to experimental groups (40x)

Group	24s	48s	72s
CPC Bulk	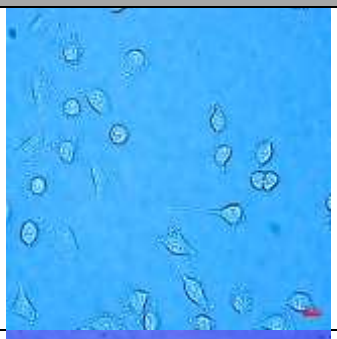		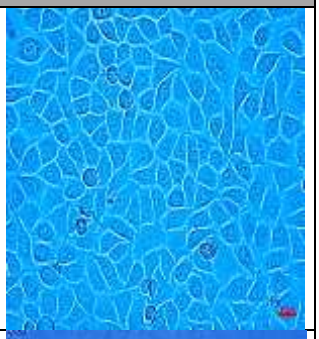
-	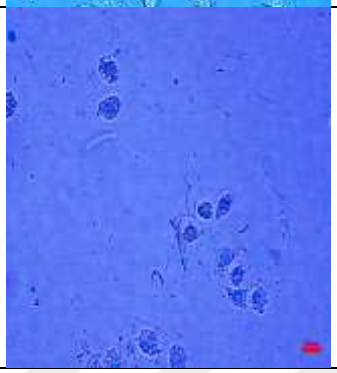	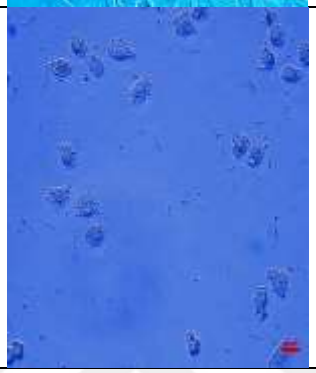	

Figure 4.2 Changes in cell morphology at 24, 48, and 72 hours after the addition of extraction fluid according to experimental groups (40x) (continue)

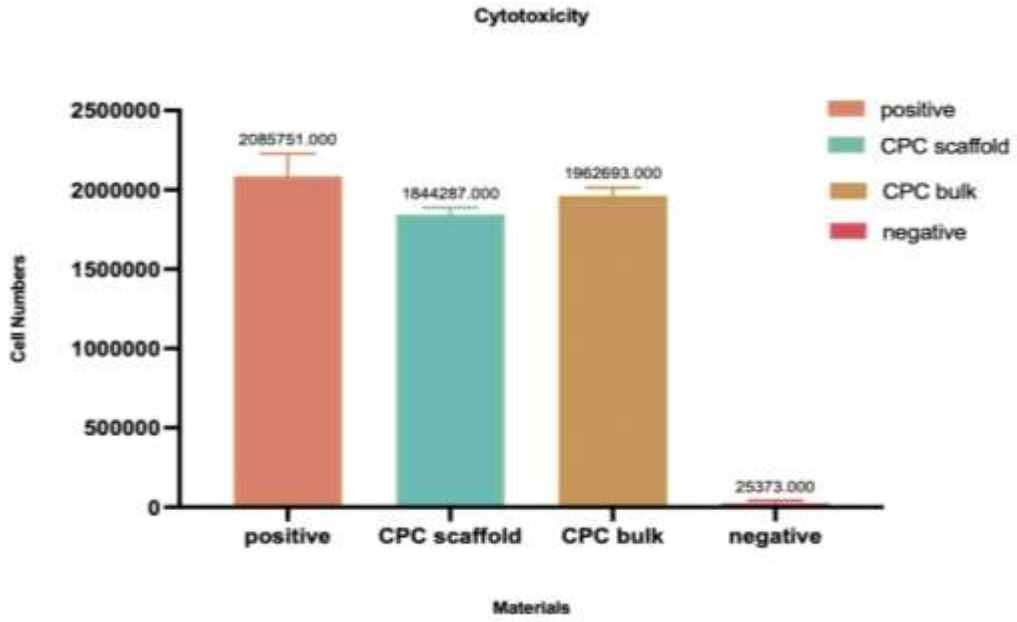

Figure 4.3 Change in the number of viable cells according to experimental groups 72 hours after the addition of extraction fluid; results are normalized to the negative control group

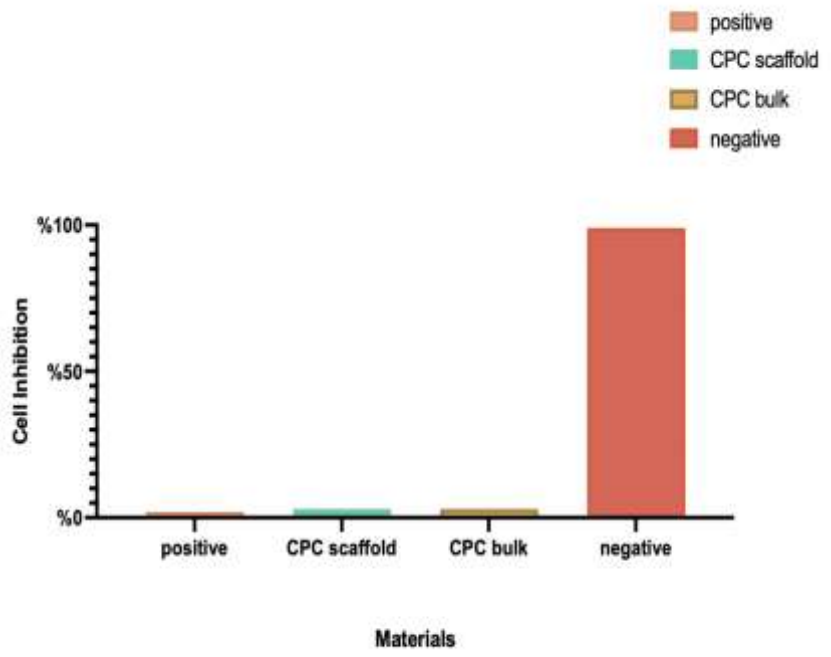

Figure 4.4 % cell growth inhibition; results are relative to the positive control group.

According to the results of microscopic examination and cell counting, the results of the experimental groups according to the " cytotoxicity test evaluation criteria" scoring scale are presented in Table 4.1

Table 4.1 Results of cytotoxicity test evaluation criteria

	Group	Score		Group	Score
Cell layer spreading (Confluency)	CPC Scaffold	1	Change in cell morphology	CPC Scaffold	1
	CPC Bulk	1		CPC Bulk	1
Number of dead cells (floating cells)	CPC Scaffold	1	Cell growth inhibition	CPC Scaffold	0
	CPC Bulk	1		CPC Bulk	0

According to these results, the cytotoxic response index evaluation results for the produced materials are presented in Table 4.2 According to these data, CPC Bulk and CPC Scaffold are non-toxic.

Table 4.2 Cytotoxic evaluation results for CPC Bulk and CPC Scaffold

Group	Cytotoxic Response Index	"Material is Cytotoxic"
CPC Bulk	1	No
CPC Scaffold	1	No

4.1.2 Mechanical Testing of CPC Scaffolds

The mechanical function requirements for osteochondral scaffolds are critical to ensure their effectiveness in supporting tissue regeneration and providing the necessary structural support to the repaired joint. The scaffold should be able to withstand compressive forces without collapsing or deforming. The mechanical requirements of osteochondral scaffolds are highly dependent on the specific application and the location within the joint. This is especially important for the bone layer, which bears a significant portion of the mechanical load.

Three samples with a dimension of 8.35 mm × 8.35 mm × 4.5 mm were tested for each scaffold. To conduct the compressive test, each CPC scaffold was positioned on a stainless-steel flat plate, and a stress-strain curve was generated by applying a load at a crosshead speed of 0.5 mm/min. The compressive strength of each cement sample was assessed using an indentation method at two central positions, with a minimum separation of 2 mm within the CPC scaffold. An indenter with a cylindrical shape, measuring 3 mm in diameter, was placed in the center of the test specimen.

Before initiating the test, the upper crosshead plate was lowered to establish initial contact with the specimen, accomplished by applying a preload of 1 N. The reaction force-deflection curve was recorded as the test proceeded at a crosshead speed of 0.5 mm/min until the scaffold fractured. The deflection at the point of breakage was defined as the deflection occurring when the highest reaction force was observed on the curve. The compression moduli of the scaffolds were determined by analyzing the stress-strain curves and calculating Young's modulus based on the results obtained from the compression tests.

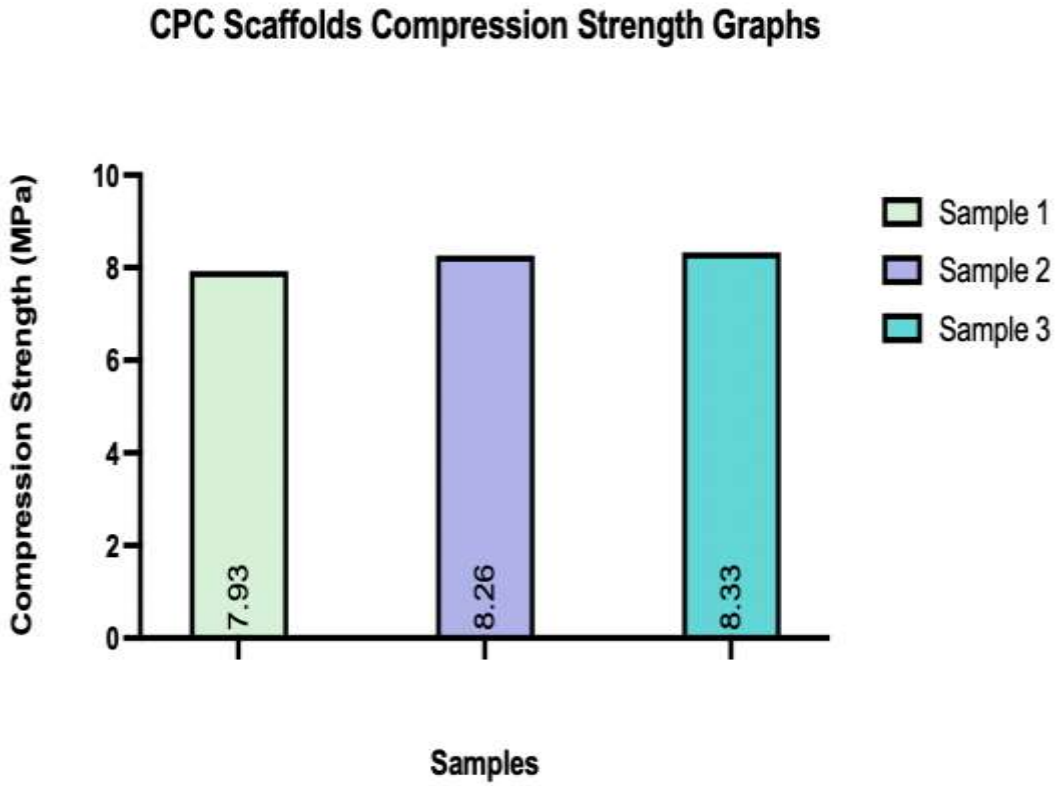

Figure 4.5 Compressive strength graphs of CPC Scaffold Samples

Table 4.3 Compressive Strength of CPC Scaffold Samples

Samples	Length(cm)	Area	Compression Strength (MPa)
Sample 1	0,45	8	7,93
Sample 2	0,45	8	8,26
Sample 3	0,45	8	8,33

The mechanical strengths of CPC scaffold samples were measured as 7.93 MPa, 8.26 MPa, and 8.33 MPa respectively (Figure 4.5). The compressive strength requirements for osteochondral scaffolds are contingent upon their designated application and their placement within the joint structure. Weight-bearing joints, such as the knee or hip, necessitate scaffolds with elevated compressive strength capabilities to endure the substantial mechanical loads experienced during typical daily activities. Conversely, non-weight-bearing joints, like the shoulder or elbow, may have less stringent compressive strength prerequisites. Furthermore, the specific location within the osteochondral unit significantly influences the compressive strength criterion. The subchondral bone layer, situated beneath the articular cartilage, typically imposes more demanding compressive strength criteria. This is attributed to the subchondral bone's pivotal role in providing structural support to the joint and its responsibility for mitigating compressive forces.

In essence, the compressive strength imperative for an osteochondral scaffold mandates careful consideration of the particular joint, its weight-bearing characteristics, and the intended stratum within the osteochondral unit. This tailored approach ensures the scaffold's capacity to perform optimally and endure the mechanical demands imposed upon it. The mechanical strength of all CPC scaffold samples meets the requirement of repairing osteochondral defects. A compressive strength of 8.33 MPa falls within the range of reported compressive strengths for osteochondral scaffolds in existing literature. For instance, Chen et al. introduced a 3D-printed osteochondral scaffold consisting of polycaprolactone (PCL) and hydroxyapatite (HA) with a compressive strength of 8.3 MPa (Suo, Chen, Liu, Wang, & Xu, 2021). Similarly, Kim et al. (2018) developed a composite osteochondral scaffold composed of PCL, HA, and collagen, which exhibited a compressive strength of 8.5 MPa. These findings suggest that the CPC scaffold's compressive strength aligns with values reported in previous research, demonstrating its suitability for osteochondral applications.

Furthermore, the in vivo compressive strength of the material, exceeded expectations compared to the highest in vitro measurement. This notable difference is attributed to bone ingrowth into cement pores that were not filled during in vitro testing. This

discovery challenges the reliability of in vitro assessments of bone cements, especially calcium phosphate cements, suggesting that their in vivo strength is significantly greater due to successful osseointegration. The study prompts a reconsideration of the conventional evaluation of these cements' mechanical properties solely based on in vitro data (Van Lieshout, Van Kralingen, El-Massoudi, Weinans, & Patka, 2011).

4.1.3 FTIR Analysis of CPC Scaffolds

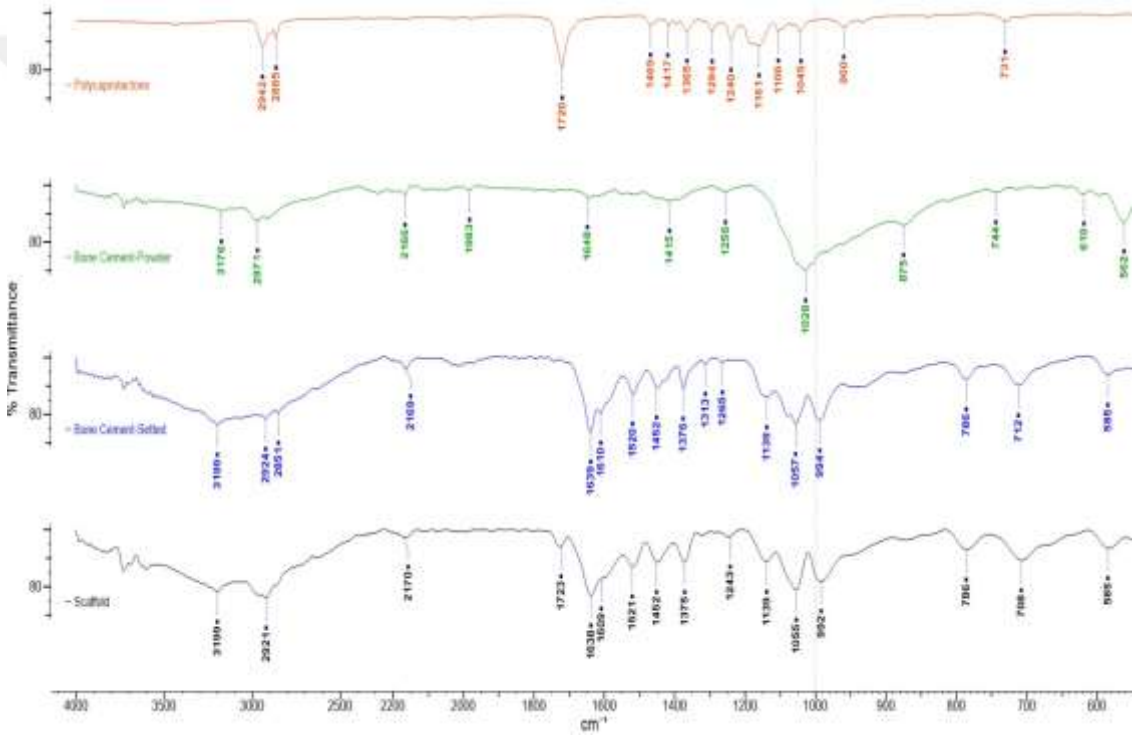

Figure 4.6 FTIR Spectrum of CPC Scaffold

FTIR is a powerful analytical technique used in chemistry and materials science to study the chemical composition and molecular structure of materials. It measures the absorption of infrared radiation by molecules, providing information about the functional groups and chemical bonds present in a sample. In the context of CPC scaffolds, various components are mixed together to form the final material. These components may include calcium phosphate powders, a liquid phase (often water or another aqueous solution), and possibly

other additives or materials. During the mixing and setting process, interactions between these components can occur, potentially affecting the properties of the final scaffold. FTIR analysis is employed to examine the chemical bonds and functional groups within the CPC scaffold components (Fig 4.6).

The first objective is to demonstrate the presence of PCL in the Scaffold. PCL, a type of polyester, can be identified through its FTIR spectrum, which exhibits the following distinctive bands:

- 2942 cm^{-1}: Asymmetric CH_2 stretching
- 2865 cm^{-1}: Symmetric CH_2 stretching
- 1720 cm^{-1}: C=O stretching

Upon analyzing the FTIR spectrum of the scaffold, a prominent band at 1723 cm^{-1} is observed, which aligns with the characteristic C=O stretching of PCL. This observation indicates the presence of little PCL residue within the scaffold. In the process of preparing CPC scaffolds, residual PCL may be present on the scaffold's surface and within its pores due to the use of dichloromethane during fabrication. Despite efforts to remove it entirely, some dichloromethane-containing PCL residue may persist, particularly within the CPC matrix. However, it's important to note that PCL is biocompatible and biodegradable, and any remaining PCL is not expected to negatively impact the CPC scaffold's biological performance. Indeed, in bone tissue engineering, PCL scaffolds are commonly used as a three-dimensional framework that supports the growth and regeneration of bone tissue. The slow biodegradation of PCL aligns with the gradual development of new bone, making it a suitable material for long-term bone regeneration applications. Its combination of biocompatibility, biodegradability, and mechanical properties makes it an attractive choice for creating scaffolds and implants that support and promote the healing and regeneration of bone tissue.

The second objective is to validate the presence of hydroxyapatite in setted CPC scaffold while excluding TTCP powder from the analysis. Hydroxyapatite, a critical component under investigation, exhibits distinct FTIR bands that serve as indicative markers:

- 1637 cm-1: Signifying H-O-H bending
- 1055 and 992 cm-1: Corresponding to P-O stretching

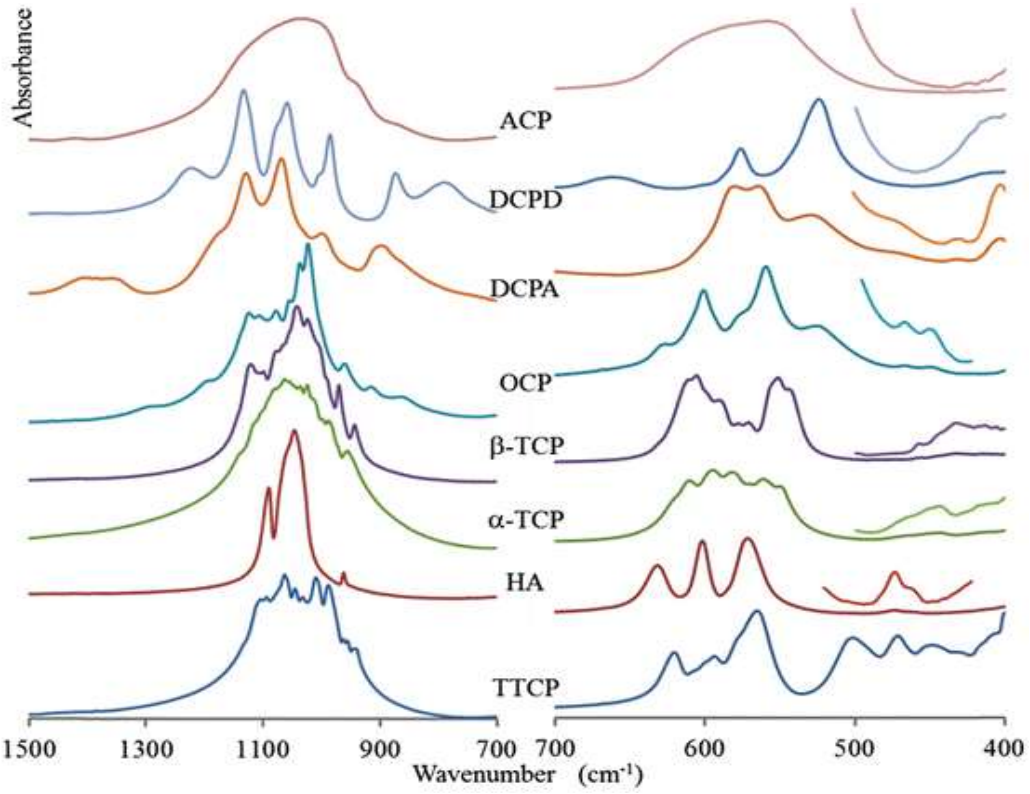

Figure 4.7 FTIR spectra of calcium phosphates in the domains of internal vibrations of phosphate ions FTIR spectra of calcium phosphates in the domains of internal vibrations of phosphate ions (Rey et al., 2014)

TTCP powder is demonstrated with a green line. The FTIR spectrum of TTCP powder shows a band at 1028 cm-1, which is characteristic of P-O stretching in hydroxyapatite (Fig 4.7). However, it does not show a band at 1637 cm-1, which is characteristic of H-O-H bending in hydroxyapatite, respectively. This suggests that TTCP powder does not contain hydroxyapatite.

Setted bulk CPC is demonstrated with blue lines. The FTIR spectrum of setted bulk CPC CC shows bands at, 1639 cm-1, 1057, and 994 cm-1, which are characteristic of hydroxyapatite. This suggests that set bone cement contains hydroxyapatite which is biocompatible and closely mimics the composition of natural bone, making it well-suited for bone repair and regeneration. CPC Scaffold which is demonstrated with a black line, the FTIR spectrum of the scaffold shows bands at 1638 cm-1, and 1055 and 992 cm-1, which are characteristic of hydroxyapatite. This suggests that the CPC scaffold contains hydroxyapatite. The FTIR analysis shows that setted bulk CPC and scaffold contain hydroxyapatite, while TTCP powder does not.

4.1.4 Cell viability (Alamar Blue^{TM}) test of CPC scaffolds

Porous scaffolds with interconnected macropores create a supportive environment for the migration and growth of cells, while mesenchymal stem cells, with their multi-differentiation potential, immune regulation, and self-renewal abilities, hold promise for various regenerative medicine applications, including the repair and regeneration of diverse tissue types.

Cells seeded on various CPCs demonstrated successful osteogenic differentiation, as noted in studies by Vater et al. (2010) (Vater et al., 2010) and He et al. (2013) (F. He, Li, & Ye, 2013). Despite these positive outcomes, BMSCs come with inherent drawbacks, such as the need for an invasive harvesting procedure, limited MSC yield per extraction, and diminished potency in hBMSCs sourced from elderly individuals and those with diseases or disorders. Consequently, there is a pressing need to explore alternative sources of stem cells for applications in tissue engineering. Therefore, the adipose-derived mesenchymal stem cells were selected to evaluate the cell adhesion, proliferation, and differentiation behaviors of the prepared scaffolds.

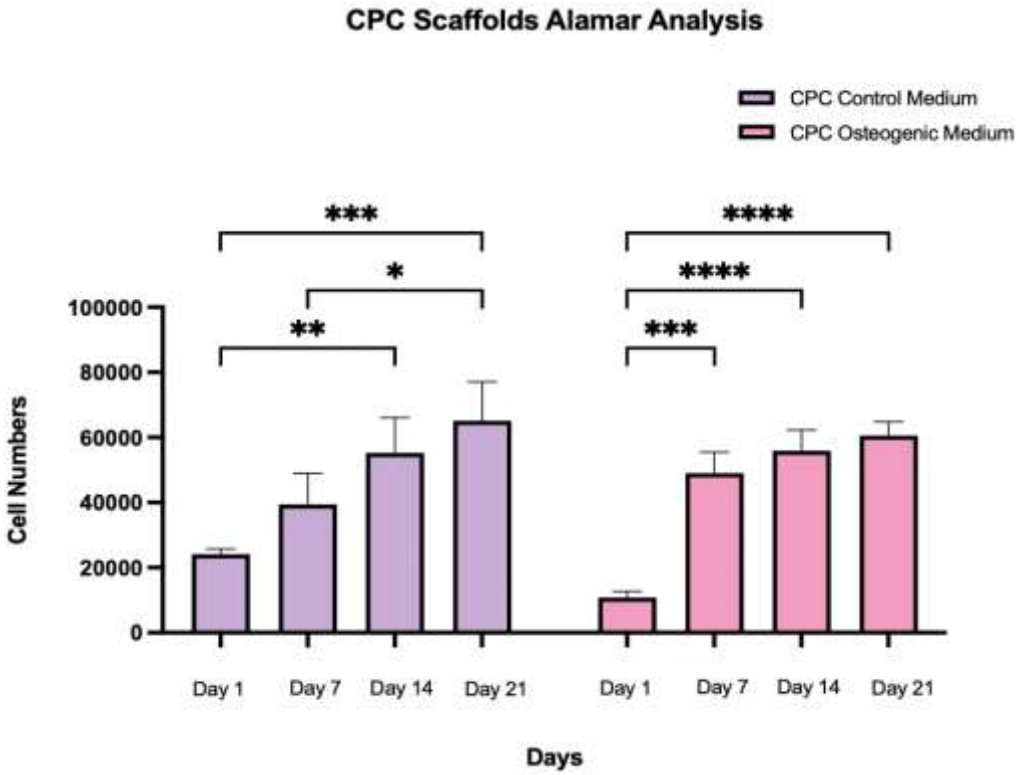

Figure 4.8 Cell proliferation of AD-MSCs cultured on CPC scaffolds of biphasic scaffolds with different mediums

(* p value= 0.0134 ** p value = 0,0025, *** p value = 0,0003, **** p value <0,0001, n=3)

The present study aimed to investigate and compare the viability of adipose-derived mesenchymal stem cells (AD-MSCs) on this novel CPC scaffolds using the Alamar Blue assay. The cells were cultured in osteogenic and control media supplemented with FGF-2 for 1, 7, 14, and 21 days. The impact of the different media on cell viability was evaluated (Fig 4.8). The cell viability measured by the Alamar Blue assay increased over time for AD-MSC cultured in either osteogenic medium or control medium which further supports that the cells survive in the CPC scaffolds.

On day 1, more cell attachment was observed in the control media unlike in the osteogenic media; however, there was a significantly increased proliferation rate on day 7 compared to the control media. The cells could survive and proliferate on these scaffolds, which could be clearly shown in a significant difference in cell numbers from day 1 to day 21. Even though, there was an insignificant increase in cell numbers on days 14 and 21. This

may be a result of a lack of space on the scaffold for cells to grow and start to detach from the surface.

The metabolic activity appeared higher in cells cultured in the control medium compared with cells cultured in the osteogenic medium on day 1, although the difference was not significant. Cell–material interaction may influence the proliferation, differentiation, and mineralization of the cells. Indeed, greater numbers of cells initially grew on the CPC scaffold surfaces both in the presence of osteogenic differentiation media and control media. Cell–material interaction may influence the proliferation, differentiation, and mineralization of the cells. Indeed, greater numbers of cells initially grew on the CPC scaffold surfaces both in the presence of osteogenic differentiation media and control media. Supplementing the culture medium with osteogenic agents can produce stronger and more effective differentiation of AD-MSCs, but not increase their proliferation. As described in existing literature, the reduced metabolic activity observed in cells cultured in osteogenic media could be attributed to a diminished cell population, given that fully differentiated osteoblasts exhibit limited division compared to their less mature cells (Malaval, Liu, Roche, & Aubin, 1999).

The osteogenic differentiation of mesenchymal stem cells is delineated into three stages according to Huang, Nelson, Smith, and Goodman (2007). The initial stage involves an increase in cell numbers, succeeded by an early differentiation phase marked by the transcription and protein expression of ALP (alkaline phosphatase), as noted by Aubin in 2001. Following the initial peak in ALP, its levels subsequently begin to decline, signifying the transition beyond the early differentiation stage in the osteogenic differentiation process (Huang, Nelson, Smith, & Goodman, 2007).

The scaffolds were stable in size and shape during the cell culture period; cell adhesion and proliferation on the scaffolds did not deform or shrink the surfaces. With the extension of culture time, results showed that the number of cells of all scaffolds evidently increased over time. These results demonstrated that the CPC scaffolds all had good cytocompatibility, while the macropores of the CPC scaffolds were conducive to the

ingrowth of AD-MSCs. Furthermore, supplementing the culture medium with osteogenic agents can indeed enhance the differentiation of AD-MSCs into osteoblasts, which is beneficial for bone tissue engineering. However, this enhanced differentiation does not result in increased cell proliferation, and the lower metabolic activity observed in cells cultured in osteogenic media may be attributed to the reduced proliferation of more differentiated osteoblasts, as they typically divide less frequently than less mature cell types. These findings align with existing literature in the field.

In previous studies, osteoblast cells of an MC3T3-E1 cell line were cultured on the CPC of the TTCP–DCPA system (Xu & Simon, 2005), or bone marrow-derived MSCs were used for osteogenic differentiation on the CPC (Schumacher, Lode, Helth, & Gelinsky, 2013) or hDPSCs (Xia et al., 2018). First time, the present study showed that the high-strength TTCP-based CPC scaffold supported AD-MSC attachment and proliferation.

Also, The study demonstrates that the dissolution and resorption rate of calcium phosphate cement (CPC) can be increased without compromising the proliferation and osteogenic differentiation of AD-MSCs making them a potentially superior and cost-effective alternative to the gold-standard human bone marrow-derived mesenchymal stem cells (hBMSCs). Moreover, it has been reported that the inclusion of stem cells accelerates the degradation of Calcium Phosphate Cement (CPC), potentially contributing to a more balanced regulation of the catabolic and anabolic processes involved in bone remodeling. This suggests that the presence of stem cells may play a role in influencing the dynamic equilibrium between the breakdown and formation of bone tissue (J. Wang et al., 2014). The implications for stem-cell-based regenerative medicine are significant. However, the study underscores the need for in vivo animal studies to further investigate the delivery of AD-MSCs via CPC-based scaffolds for osteochondral tissue engineering, considering potential variations between in vitro and in vivo conditions.

4.1.5 SEM analysis of CPC scaffolds

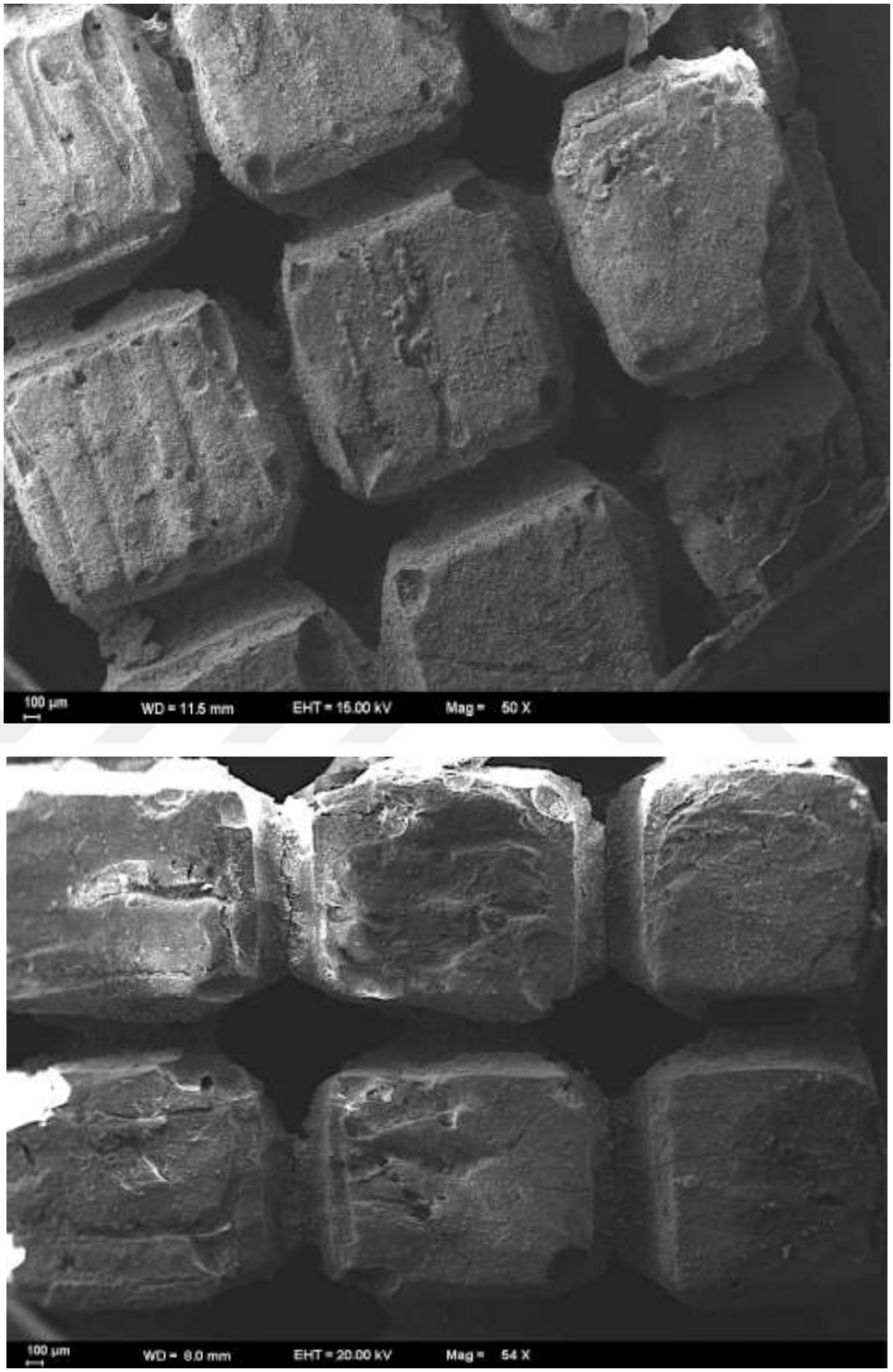

Figure 4.9 SEM Images of CPC Scaffold's surface with cultured in control media at day 21 (100 µm)

The optimal pore size for promoting osteogenic differentiation depends on several factors such as the specific cell type, scaffold material, culture conditions, and mechanical loading. However, in general, it has been observed that pore sizes in the range of 100-300 μm are commonly considered favorable for osteogenic differentiation and bone regeneration. A pore size falling within the specified range facilitates crucial processes such as cell infiltration, nutrient diffusion, and vascularization within the scaffold. This favorable environment supports osteogenic cell attachment, proliferation, and differentiation. Larger pore sizes are suggested to enhance cell infiltration and vascularization to a greater extent, potentially fostering more extensive tissue development. Conversely, smaller pore sizes might impede cell infiltration, resulting in limited bone formation. Therefore, the selection of appropriate pore size is pivotal in influencing the effectiveness of scaffolds for bone tissue engineering applications (Kafi, Aktar, Phanny, & Todo, 2019).

Therefore, while a pore size range of 100-300 μm is often considered favorable for osteogenesis, in this thesis bone part of the scaffold pore size was designed to 300 μm as seen in figure 4.9. These pores provide the nutrients to flow in and waste products of the cells to flow out, besides allowing the cells to communicate with each other. Furthermore, they offer larger surface areas for the cells to proliferate. Empty scaffolds were observed on the day after preparation (Figure 4.10), while the cell-seeded ones were analyzed on days 7, 14, and 21 of incubation in control and differentiation media.

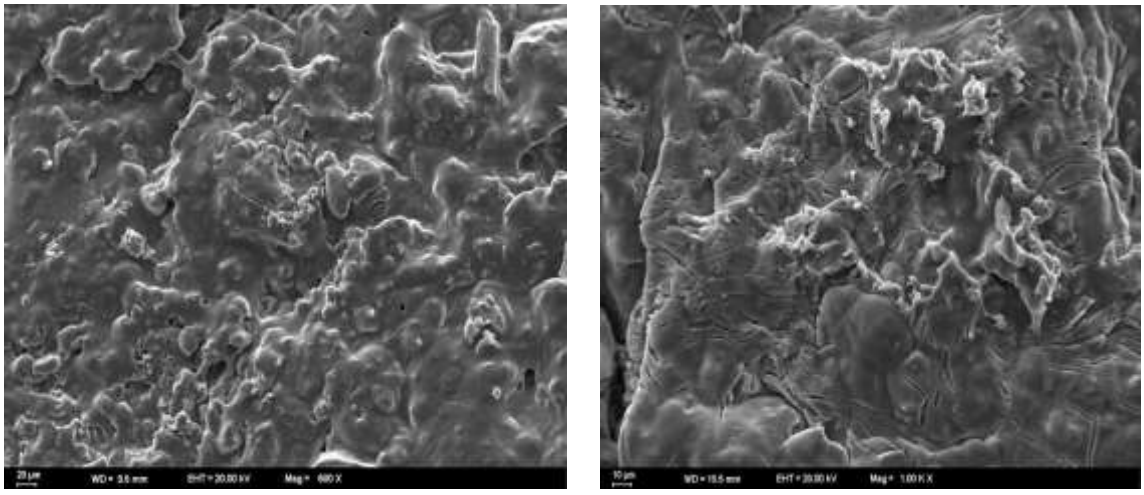

Figure 4.10 Sem Images of CPC scaffold without cells

	Control Medium
Day 7	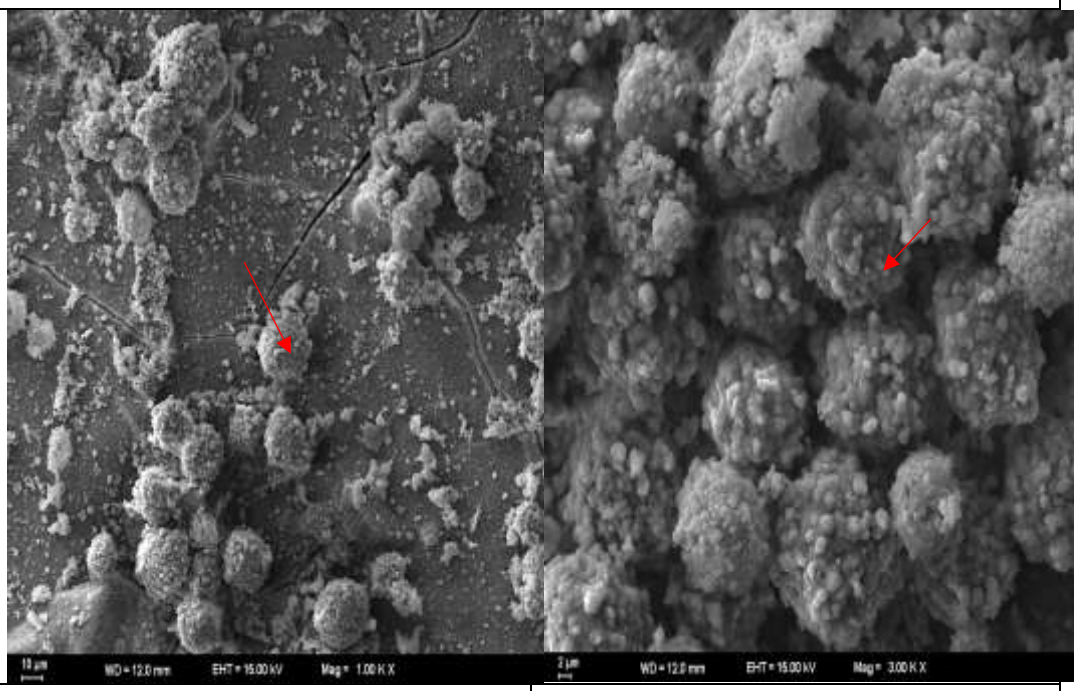
Day 14	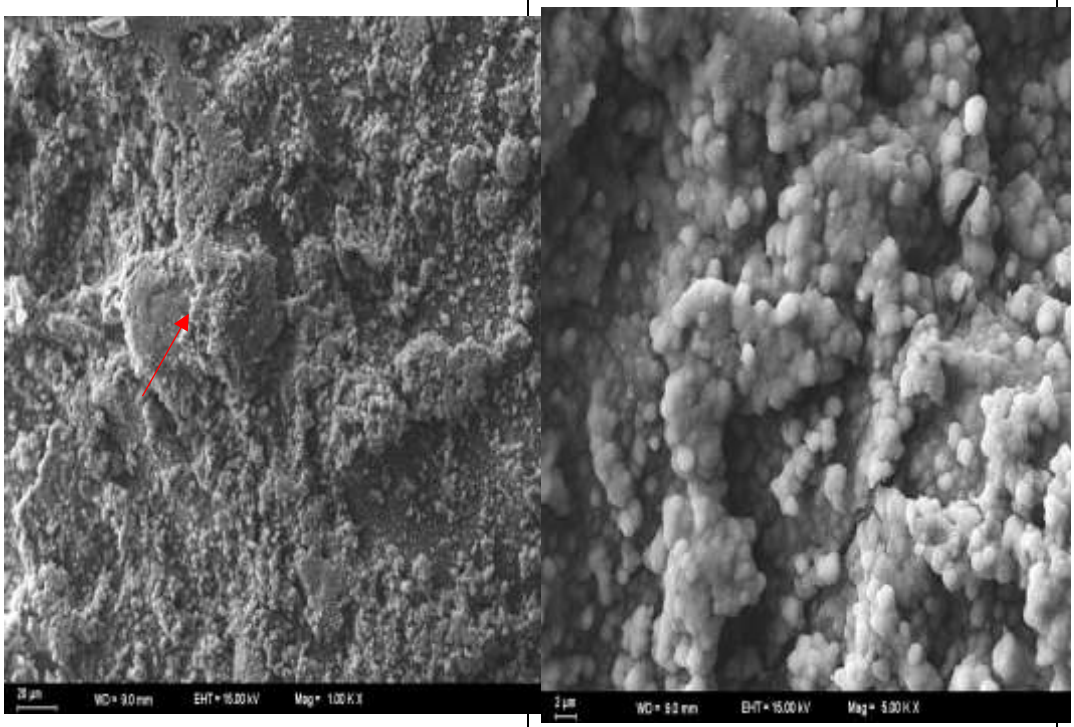

Figure 4.11 SEM images of AD-MSCs cultured on the CPC scaffold surfaces for 7,14 and 21 days in the control medium (red arrows indicate cells,blue arrows indicates cytoplasmic extensions)

	Control Medium	
Day 21	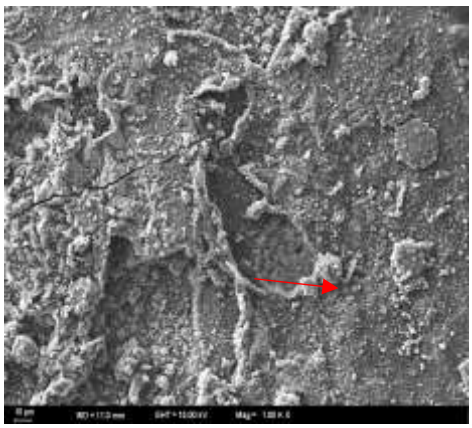	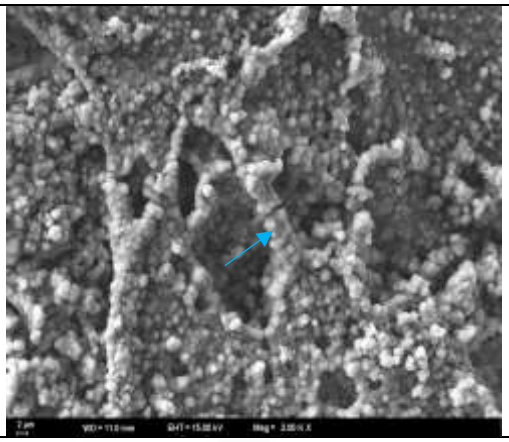

Figure 4.11 SEM images of AD-MSCs cultured on the CPC scaffold surfaces for 7,14 and 21 days in the control medium (red arrows indicate cells,blue arrows indicates cytoplasmic extensions) (continue)

In the control medium, the morphology of cells on all the scaffolds was examined by SEM after 21 days of cell seeding. Fig 4.11 shows that cells (red arrows) remained in the pores of the construct, as shown under different magnifications, and developed short cytoplasmic extensions that anchored them onto the CPC scaffold. SEM images also revealed that the cells were spread all over the scaffold and made contact with each other. Moreover, it was seen that the cells preserved their alignment along the scaffold surface even over time. The observed differences in cell morphology between scaffolds cultured in osteogenic medium and those in control medium suggest that the cellular response is influenced by the specific culture conditions. In osteogenic medium, which contains factors promoting osteogenic differentiation, cells tend to exhibit a more confluent and organized growth pattern on the scaffold surface. This could indicate that the cells are actively undergoing osteogenic differentiation, aligning and forming structures characteristic of bone tissue. On the other hand, in the control medium, which lacks specific osteogenic-inducing factors, the cells may adopt a more random or spread-out morphology. This could suggest a more undifferentiated or general cellular state, with cells not undergoing the specialized processes associated with osteogenesis. The observed variations in cell morphology highlight the importance of the culture environment in influencing cellular behavior and differentiation.

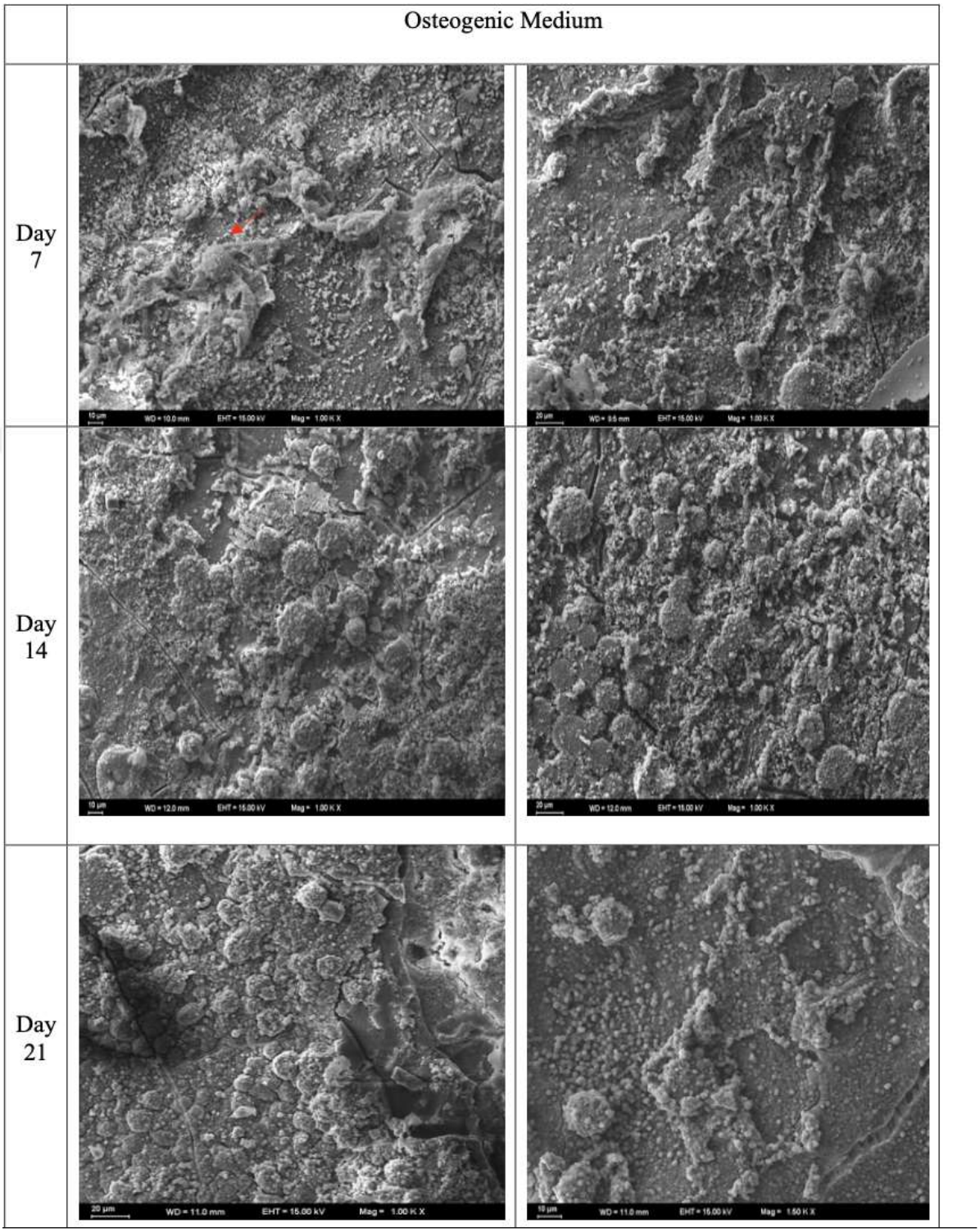

Figure 4.12 SEM images of AD-MSCs cultured on the CPC scaffold surfaces for 7,14 and 21 days in the osteogenic medium

In the osteogenic medium, cell morphology on all scaffolds was assessed via SEM after 21 days of cell seeding (Figure 4.12). Initially, osteoblasts exhibited a round shape after 1 day, but over time, cell proliferation occurred, leading to the formation of multilayers covering the scaffold surface by day 21. The AD-MSCs were initially cultured on a surface and spread across the surfaces of the scaffold during a 21-day culture period. After this duration, the scaffold surface showed almost complete coverage with a confluence of cells in all groups, suggesting a strong compatibility between the cells and the cement samples. The morphology of MSCs seeded on CPC surface observed in this study aligns with findings reported in the existing literature (Liang et al., 2016).

The SEM images illustrate cells attaching to pore walls and creating bridges between these walls, indicating a dynamic and proliferative cellular response within the scaffold environment. In addition, some cells could grow in the pores of the 3D scaffolds. After 21 days of cell culture, cells were spread, and they covered a relatively larger area on the scaffold compared to day 7. It was concluded that this scaffold has the potential to serve as a subchondral bone for osteochondral tissue engineering.

4.1.6 Alizarin Red Staining

Alizarin Red S staining is a common histochemical technique used to detect calcium deposits in mineralized tissues and cultures. AD-MSCs were seeded on CPC scaffolds and cultured in the osteogenic induction medium for 21 days. Osteogenic differentiation of the cells on these scaffolds was evaluated via Alizarin Red staining. The mineralized matrix synthesis was analyzed using Alizarin Red S staining, which identifies calcium deposition. The resulting red color intensity and the high number of dark spots indicate mineral accumulation and hence higher osteogenic differentiation (Jeon, Lee, & Yang, 2018).

After culturing for 7, 14, and 21 days, respectively, the cells were washed with PBS. This was followed by staining for 20 min in 0.5% Alizarin Red S in PBS at room temperature. Low-magnification views of AD-MSCs seeded CPC scaffolds stained with Alizarin Red Stain after culture for 7, 14, and 21 days are shown in Fig 4.12. When there was no osteogenic differentiation medium, nodule formation was not significant in cells cultured on CPC on days 7,14, and 21. In contrast, clearly, calcified tissue formation was observed in the osteogenic medium cultures grown on the CPC scaffold after 21 days. When the CPC scaffold was cultured in an osteogenic medium, the mineralized matrix synthesis was more evident in the cultured control medium. Noticeable differences were observed after the cell was cultured in an osteogenic medium on the CPC scaffold surfaces from day 1 to day 21.

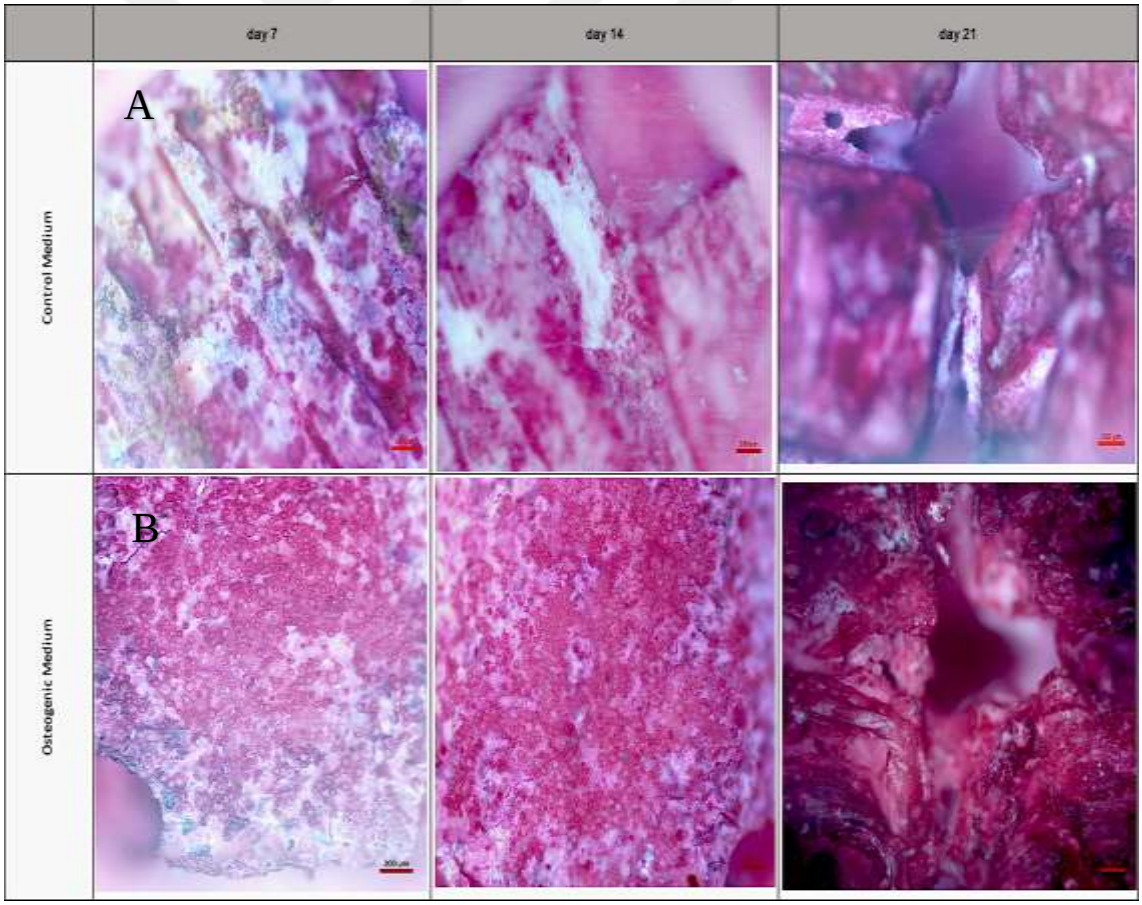

Figure 4.13 Photographs of AD-MSC cells in culture medium, (A) without and (B) with osteogenic differentiation agents, after staining with Alizarin Red S for identification of the calcium deposit in cells on days 7, 14, and 21

The seeding of Adipose-Derived Mesenchymal Stem Cells (AD-MSCs) on Calcium Phosphate Cement (CPC) scaffolds and the subsequent evaluation of osteogenic differentiation in this context have not been previously reported. Insights gained from this investigation could potentially advance our understanding of how AD-MSCs interact with CPC scaffolds and their capability for osteogenic differentiation. When seeded onto CPC scaffolds, these cells exhibited good attachment, proliferation, and osteogenic differentiation. Mesenchymal stem cells do not exhibit extracellular calcium accumulation before differentiation. However, following the differentiation protocol, cells that undergo osteogenic differentiation show significant calcium accumulation, indicating successful differentiation into osteoblasts and bone formation. This calcium accumulation is visualized in a red-orangish color through Alizarin Red staining. Figure 4.13 depicts the staining results of tissue scaffolds cultured for 21 days, revealing a substantial increase in calcium accumulation in the group cultured in osteogenic medium. The Alizarin Red staining confirms the induction of osteogenic differentiation in tissue scaffolds cultured in osteogenic media, supporting the conclusion that the obtained results align with existing literature on osteogenic differentiation (Tao et al., 2021).

The culture media used in the study were enhanced with osteogenic differentiation agents, which typically include substances like dexamethasone, beta-glycerophosphate, or ascorbic acid. These agents are known to promote the differentiation of cells into bone-forming cells (osteoblasts). When the culture media were supplemented with these osteogenic differentiation agents, the CPC scaffolds demonstrated a notable response. Specifically, they formed bone-like nodules with a mineralized extracellular matrix. This observation aligns with previous reports in the field, indicating that the agents were effective in encouraging osteogenic differentiation (Gough, Notingher, & Hench, 2004).

Importantly, the study found that the presence of calcium deposits was more pronounced in CPC scaffolds cultured in an osteogenic medium compared to those cultured in a control medium. This suggests that the osteogenic differentiation agents had a positive effect on the mineralization process within the CPC scaffolds. The addition of osteogenic differentiation agents to the culture media had a significant impact on CPC scaffolds. It promoted the formation of bone-like nodules with a mineralized extracellular matrix, and

the presence of calcium deposits was more prominent when cultured in the osteogenic medium, indicating successful osteogenic differentiation. These results support studies that suggest a crucial role of osteocalcin in the regulation of osteoblast activity that can be extended to MSC as their precursors (Hauschka & Wians, 1989)

ALP (alkaline phosphatase) analysis can indeed provide valuable insights into osteogenic differentiation. The amount of ALP produced by osteogenic cells serves as a quantifiable marker for osteogenic differentiation. This can be particularly useful in assessing the efficacy and progression of osteogenic processes in vitro. In future studies, incorporating ALP analysis alongside established markers like calcium deposition and osteogenic gene expressions promises a more comprehensive understanding of osteogenic differentiation. While calcium deposition and gene expressions offer insights into later stages and molecular aspects, ALP serves as an extracellular enzyme, providing dynamic measurements crucial in the early phases of biomineralization. This integrated approach allows for a nuanced exploration of temporal dynamics, enhancing our ability to monitor osteogenic efficacy and providing a holistic interpretation of the intricate cellular events involved in bone tissue formation.

4.2 3D printing trials of CPC

Extrusion-based 3D printing, also known as 3D plotting, has gained increasing prominence in both biomedical research and clinical applications. 3D bioprinting is a groundbreaking technology that combines the principles of additive manufacturing with biocompatible materials to create three-dimensional biological constructs. It has the potential to revolutionize medicine and healthcare by enabling the creation of functional tissues and organs for transplantation and research purposes. It is particularly valuable for handling pasty materials, including biomaterial inks or bio-inks. One promising application of this technique is in the creation of bioscaffolds for bone formation using CPC. Calcium phosphate cements (CPCs) are biocompatible and bioactive materials used in medical applications, particularly in bone repair and regeneration. They are composed of calcium-phosphate phases that set and harden when mixed with an aqueous solution,

forming a solid structure with properties similar to natural bone. It can fill in voids and defects within bones, providing mechanical support and aiding in the healing process. This ability to act as a structural replacement is crucial for patients who require bone reconstruction due to injuries or diseases (J. Zhang et al., 2014).

In 2014, Lode et al. demonstrated the viability of 3D plotting by successfully building an open-porous scaffold from paste-like CPC. This specific CPC formulation consisted of 60% α-tricalcium phosphate and an oil-based carrier phase (Lode et al., 2014). In the existing literature, most researchers have utilized a pasty form of calcium phosphate cement (CPC), which comprises a precursor powder based on alpha-tricalcium phosphate (α-TCP) and an oil-based carrier liquid (Kilian et al., 2022).

A unique CPC paste, as discussed by Kilian et al. in 2022, stands out for its water-free composition, enabling prolonged storage without viscosity changes. This CPC paste is particularly well-suited for 3D extrusion printing, devoid of time constraints before hardening. What makes it intriguing is that its self-setting reaction is solely triggered upon contact with water, achievable through immersion in aqueous solutions or exposure to a humid environment. This reaction results in the formation of nanocrystalline hydroxyapatite (HAp). The primary challenge addressed in this thesis is the use of water-based CPC, which complicates maintaining its paste-like consistency, posing difficulties in 3D printing bone scaffolds for osteochondral defects.

The versatility of CPC formulations allows for the production of various types of hydroxyapatite (HA). CPCs are categorized into two main groups: apatite and brushite cement. Apatite cement contains hydroxyapatite (HA) and calcium-deficient HA (CDHA) and is created by mixing a powder component containing calcium orthophosphates with an aqueous solution. This process dissolves the initial calcium orthophosphates and precipitates HA or CDHA crystals, providing mechanical rigidity and leading to cement setting. Brushite cement consists of dicalcium phosphate dihydrate (DCPD) and undergoes a similar formation process, with the dissolution and precipitation of DCPD crystals resulting in cement hardening.

Additionally, HA can be formed through an acid-base reaction involving tetra-calcium phosphate (TTCP) and dicalcium phosphate anhydrous (DCPA), offering an alternative CPC formulation pathway. In the context of CPCs, α-tricalcium phosphate (α-TCP) fully hydrolyzes into calcium-deficient hydroxyapatite (CDHA), while β-tricalcium phosphate (β-TCP) remains unreacted and becomes embedded in the CDHA matrix. Increasing the proportion of β-TCP in the CPC formulation extends the setting time and reduces the compressive strength of the final cement. Notably, pastes composed solely of β-TCP and water are used as models for unset CPCs since they are not set (S. V. Dorozhkin, 2013).

Cements containing this specific calcium phosphate type have proven highly suitable for 3D printing due to their ability to maintain a paste-like consistency for extended periods. A key factor in 3D bioprinting is the printing time, with calcium phosphate cement based on tetra calcium phosphate (TTCP) usually having a setting time of 8-10 minutes. However, this duration may fall short of meeting the requirements for effective scaffold creation in the bioprinting process.

In this thesis, the primary objective was to prolong the setting time of TTCP-based calcium phosphate cement, specifically employed for 3D bioprinting applications. To achieve this, several viscous binders were investigated for their potential use in the 3D bioprinting of calcium phosphate cement (CPC). These include aqueous solutions containing sodium hyaluronate, methylcellulose (MC), hydroxypropyl methylcellulose (HPMC), salts of alginic acid, Pluronic F-127, carboxymethyl cellulose (CMC), gelatin, and polyethylene glycol (PEG). These binders are investigated for their potential to enhance the viscosity of the bio-ink and improve the 3D bioprinting process, ensuring better control and precision during scaffold creation and increasing the setting time. Viscous binders showed promising results in mitigating phase separation and improving the scaffold's shape retention during the setting process. However, they also exhibited certain limitations.

In this thesis, the summary and results of the experiments carried out to make CPC 3D printable are given in the table below:

Table 4.4 Several Experiments to make CPC 3D printable in this thesis

Materials	Compositions	Our Results	Protocol reference
CPC Powder + CPC Liquid /Sodium Alginate	• %2 w/w Sodium Alginate / 1 gr CPC Powder / 0.81632 ml CPC Liquid • %3 w/w Sodium Alginate / 1 gr CPC Powder / 0.81632 ml CPC Liquid	A mixture of %2 w/w sodium alginate and cpc cement paste set time expanded to 20 min and mixture of %2 w/w sodium alginate and cpc cement paste set time expanded to 30 min. However water comes out of the tip of the syringe during compression. It was thought that it was due to the alginate not being crosslinked.	(Komath & Varma, 2003)
CPC Powder + CPC Liquid / Gelatin + MC + Citric Acid	• 2.5 w/v % Gelatine • 10 w/v % MC • 8 w/v % SC	Mechanical strength has increased but the set time of the cement has been shortened. It was decided that final mixture is not suitable for 3D printing because of the short set time. 	(Demir Oğuz & Ege, 2018)
CPC Powder + CPC Liquid / PVA+Alginate	6 %wt PVA (Dissolved in distile water) + CPC Powder + Alginate Powder (1:1)	The final mixture had a fluid, printable consistency but the paste could not be set despite being sintered at high temperature.	(Musskaya et al., 2020)

Table 4.4 Several Experiments to make CPC 3D printable in this thesis(continue)

Materials	Compositions	Our Results	Protocol reference
CPC Powder / Glycerol + PVA	0,025 gr PVA powder dissolved in 5 ml glycerol + 0,305 gr CPC powder	Final mixture is plottable but has low mechanical strength and a hemogeneous mixture could not be obtained. 	(Rajzer, Castano, Engel, & Planell, 2010)
CPC Powder / MC / Pluronic F-127	%17 w/w Pluronic F-127 powder (dissolved in dH20) + %4 w/w MC powder + 1.5 gr CPC powder	The final mixture plottable, injectable, can be stored at +4 , for set to obtained paste sintering process (1200°C) however while trying to print in 3D bioplotter, could not maintain the desired structure while trying to print the 2nd layer of scaffold. 	(Paul D L, Praveen, Čepová, & Elangovan, 2023)
CPC Powder/PEG/Gelatin/MC	0,5 gr CPC + 0,1666 gr gelatine + 0,5 ml dH20 + 0,375 gr PEG 400 + 0,015 gr MC	The final mixture plottable, injectable, can be stored at +4 , for paste set sintering process at 1200°C should be done however couldn't optimize printer parameters. 	(Boonlai, Hirun, Suknuntha, & Tantishaiyakul, 2023)

For example, increasing the concentration of Pluronic F-127 elevated the extrusion force required during printing but diminished the strength of the cement. This trade-off emphasized the importance of carefully considering binder concentrations and their impact on both printability and the final properties of the printed structures.

What is more, it was noted that cement formulated with methylcellulose (MC), hydroxypropyl methylcellulose (HPMC), and modified starch exhibited noticeably lower compressive strengths in comparison to cement utilizing water as the liquid phase. This reduction in strength was attributed to an increase in porosity resulting from the entrapment of air bubbles within the calcium phosphate cement (CPC) during the paste production process when these binders were incorporated. The utilization of gelatin solution in precise proportions as the liquid phase has demonstrated a significant impact on the properties of calcium phosphate cement (CPC). This has led to a considerable enhancement in the mechanical strength of the CPC. However, this improvement in strength has been observed to be accompanied by a reduction in the setting time, thereby indicating a trade-off between the strength and the rate at which the cement is set. When alginate powder was dissolved in specific ratios in a polyvinyl alcohol (PVA) solution and used as the liquid phase, it resulted in an extended setting time for the calcium phosphate cement (CPC). However, this extension in the setting time came at the cost of decreased homogeneity within the CPC. This effect was believed to be associated with the particle structure of tetracalcium phosphate (TTCP).

Homogeneity is important for CPC paste because obtaining accurate and meaningful measurements from rheological tests of pastes is challenging due to their inherent complexity and heterogeneity. This complexity can lead to issues like liquid migration, sedimentation, wall slip, cohesion failure, and localized shear, all of which can introduce errors in the measurements, making them less reliable for analysis. Therefore, when examining factors like setting time and injectability, it's important to consider both the permeability and rheological traits of the paste system. This approach not only helps in understanding the impact of these properties on phase separation but also aids in identifying any additional mechanisms that might play a role in phase separation during extrusion. Glycerol was also explored as a potential liquid phase component in calcium

phosphate cement (CPC). While glycerol extended the setting time of CPC, it had the drawback of diminishing its mechanical strength. Furthermore, it was deemed too brittle for suitable use in osteochondral tissue applications. This brittleness can lead to scaffold fractures and subsequent dislocation of smaller fragments. In the final phase of the study, the liquid phase for calcium phosphate cement (CPC) was prepared by blending methylcellulose (MC), Pluronic, and a small quantity of gelatin. The incorporation of gelatin aimed to enhance the mechanical strength of the material, while Pluronic and MC were added to extend the setting time and achieve an appropriate consistency for 3D bioprinting purposes. The experimental results indicated that the composite reached a suitable consistency for 3D bioprinting and cement optimal strength. However, challenges encountered during the optimization of 3D bioprinting parameters such as clogging of the syringe tip after printing the first layer during printing were attributed to difficulties likely arising from the particle structure and size of tetra calcium phosphate (TTCP). Consequently, it was determined that further investigation of comprehensive material properties about this issue is necessary for future research endeavors.

The presence of integrated macro pores in bone substitution materials is crucial for allowing rapid infiltration of blood, bone, and stem cells upon implantation, which is essential for successful integration into the body. However, the size of these pores plays a critical role. Larger pores can enhance cell infiltration but may reduce the scaffold's surface area, potentially decreasing its ability to support bone tissue growth, known as osteoconductivity. Moreover, wider pores and a smaller surface area can compromise the scaffold's stability, an important factor in designing effective bone substitution materials (Q. L. Loh & C. Choong, 2013).

For the sake of conclusion, the primary objective and goal of this research is to focus on transforming calcium phosphate cement (CPC) into a 3D-printable format with optimized porosity. The aim was to enhance the osteogenic differentiation of bone scaffolds by controlling macroporosity levels. Various methods such as particle washing, ice molding, and 3D printing have been proposed to create interconnected macropores in the calcium phosphate cement (CPC) (Saeed Hesaraki, Fathollah Moztarzadeh, & Diako Sharifi, 2007). However, these methods have limitations such as difficult control of pore and

junction morphology, and issues such as structural collapse during 3D printing, which affect the quality and compressive strength of CPC scaffolds. To address these challenges, indirect 3D printing, which combines elements of direct 3D printing and conventional scaffold preparation, offers a promising solution (Chua, Liu, & Chou, 2011). This method consists of three main steps: (a) creation of sacrificial scaffolds; (b) injection into these scaffolds, and (c) removal of sacrificial components.

Indirect 3D printing is a valuable approach to preparing porous CPC scaffolds, as it allows precise control of pore structure and size, scaffold porosity, and reproducibility without affecting CPC hydration. Based on the outcomes of these investigations, the decision was made to employ an indirect 3D printing method as the approach to achieve the desired macroporosity in CPC scaffolds. By employing the indirect 3D printing technique, a scaffold with finely tuned porosity was successfully produced, all while preserving the hydrolysis reaction of calcium phosphate cements (CPCs). To enhance chondrogenesis and osteogenesis in future work, growth factors such as TGF-β1 and BMP-2 are recommended to add in different layers of the scaffolds, which can be further implanted in the knee of large animals for in vivo tests.

4.3 Chondral Part of Biphasic Scaffold

4.3.1 Cell toxicity analysis of alginate/recombinant collagen scaffold

The cytotoxicity properties of Alginate/Recombinant Collagen Scaffold samples were examined by indirect toxicity. At 24, 48, and 72 hours after the addition of extraction fluid, cell layer spreading and the number of dead cells were examined by light microscopy at 10x magnification according to the experimental groups. The cell layer spread observed at 24, 48, and 72 hours is given in Figure 4.14. Changes in cell morphology throughout the culture were examined at 40x magnification and the results are presented in Figure 4.15.

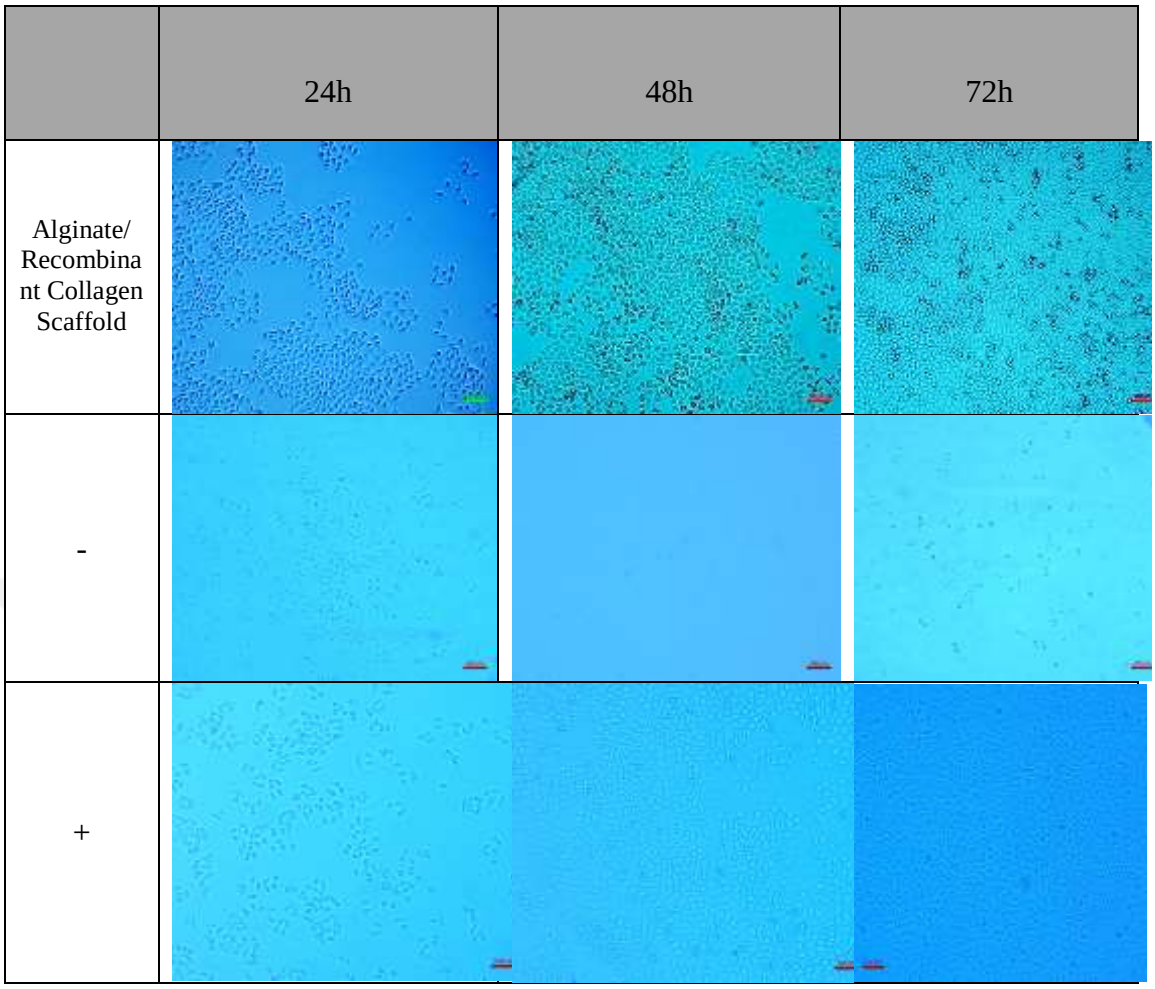

Figure 4.14 Variation of cell layer spreading at 24, 48, and 72 hours according to experimental groups after the addition of extraction fluid. (10x)

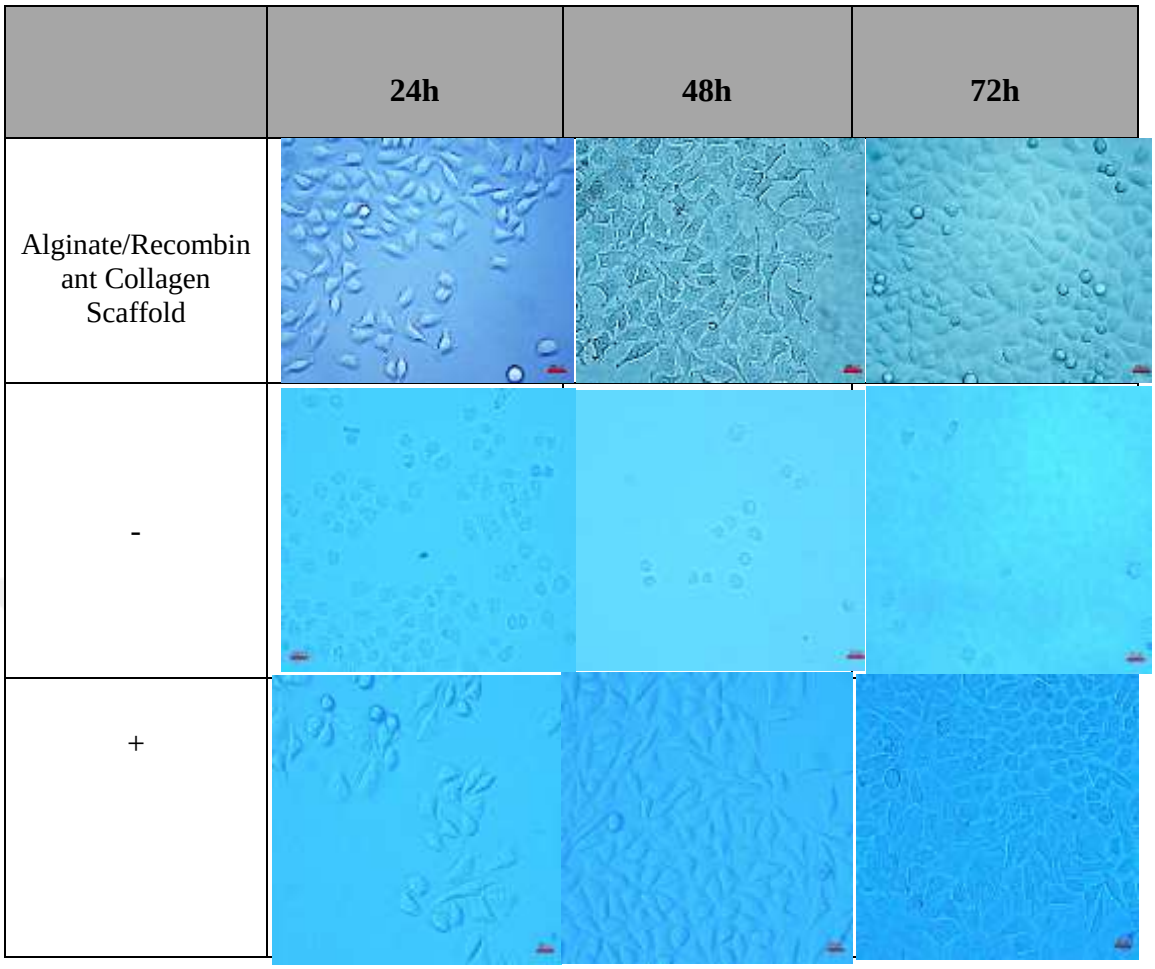

Figure 4.15 Variation of cell layer spreading at 24, 48, and 72 hours according to experimental groups after the addition of extraction fluid. (40x) According to these data, Alginate/Recombinant Collagen scaffold is non-toxic

4.3.2 Cell Viability (Alamar Blue$^{TM)}$ Test of Alginate/Recombinant Collagen Scaffolds

The present study aimed to investigate and compare the viability of adipose-derived mesenchymal stem cells (AD-MSCs) on alginate/recombinant collagen scaffolds using the Alamar Blue assay. The cells were cultured in chondrogenic and control media supplemented with FGF-2 for 1, 7, 14, and 21 days. The impact of the different media on cell viability was evaluated.

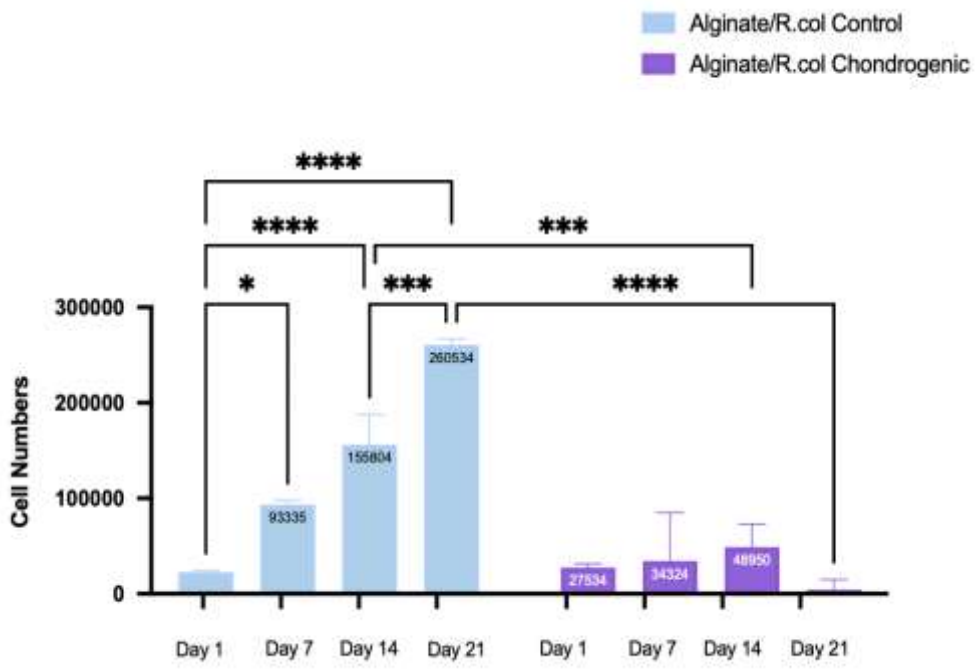

Figure 4.16 The effect of chondrogenic differentiation medium and control medium on cell viability of Alginate/Recombinant Collagen Scaffolds. Cell numbers were determined by measurement of Alamar blue assay

(* p value= 0,0305, *** p-value = 0,0008, **** p value <0,0001)

As can be seen, the cells attached and grew on the surface of both scaffolds over time. On day 1, cell attachment on Alginate/Recombinant Collagen Scaffolds in both the chondrogenic medium and control medium are nearly the same. In the control medium, there was a significant increase in cell numbers from day 1 to day 21($p < 0,0001$) on the contrary, in chondrogenic media the increase in cell counts on day 7 is not significant. Also, in chondrogenic media, there was no significant increase in cell number on days 7 and 14 (Fig 4.16).

In the chondrogenic medium by day 21, a decrease in cell numbers becomes evident, primarily attributed to scaffold degradation. This decline in cell count suggests that rapid scaffold degradation has an adverse impact on cell viability and their ability to migrate into the scaffold in vitro. It is likely that this effect is driven by the pronounced acidification of the local environment, which is a consequence of the chondrogenic media's high pH. A low pH can inhibit chondrogenesis by decreasing the activity of

chondrocyte-specific enzymes while a high pH can also inhibit chondrogenesis by causing hypermineralization of the cartilage matrix.

Chondrogenic differentiation is commonly characterized through a four-stage process. The initial phase, occurring within 0-48 hours, involves the commitment of stem cells or progenitor cells to the chondrogenic lineage. Subsequently, during the 1-10 days of cell proliferation, chondrogenic cells undergo multiplication, contributing to an increased cell population. The third stage, spanning 7-28 days, marks chondrogenic differentiation, where committed cells express specific genes associated with cartilage formation, signifying the initiation of chondrocyte development. Finally, between 10-42 days, the maturation and functionality of chondrocytes become evident as they produce a cartilage-specific extracellular matrix, including collagen and proteoglycans. This four-stage framework provides a comprehensive understanding of the temporal dynamics and molecular events characterizing chondrogenic differentiation in various experimental contexts and cell types (O'Driscoll & Fitzsimmons, 2001). Chondrogenesis is influenced by multiple factors beyond pH. These factors include the presence of growth factors and signaling molecules like TGF-β, mechanical properties of the environment that affect cell response to forces, cell density impacting cell-cell interactions, hypoxic conditions, nutrient availability, inflammatory molecules, and cell-cell interactions with neighboring cells. Together, these factors regulate the differentiation of mesenchymal stem cells into chondrocytes and the production of cartilage matrix components, making them crucial considerations in cartilage tissue engineering and maintenance (Johnstone, 2002).

Researchers are consistently striving to develop scaffolds that can augment mesenchymal stem cell (MSC) chondrogenic differentiation. Proposals suggest that the physical properties of these scaffolds play a crucial role in governing MSC chondrogenic differentiation. This emphasizes the importance of considering and optimizing the mechanical and structural characteristics of scaffolds to create an environment conducive to the desired chondrogenic differentiation of MSCs.

In conclusion, the statistics of the figure demonstrate that the number of cells cultured in the control medium prominently increases from day 1 to day 21 ($p < 0.0001$). AD-MSC

cells could grow and proliferate on Alginate/Recombinant Collagen Scaffolds in control media. This result could be explained by the optimum pH value of the medium. Also, the integrity of Alginate/Recombinant Collagen Scaffolds was more preserved when the control medium was used. Unfortunately, using the chondrogenic media resulted in lower integrity of Alginate/Recombinant Collagen Scaffolds and degraded these scaffolds, which further decreased the cell attachment and proliferation. Cell culture medium also be considered as a parameter in these results.

While existing studies have provided insights into the general effects of scaffold properties on cell behavior, there is a distinct lack of comprehensive research focusing on the specific interactions between AD-MSCs and the scaffold parameters employed in this study. The delayed growth observed suggests that these scaffold-related factors may play a pivotal role in modulating ADMSC behavior, necessitating a more targeted exploration to decipher the intricate relationship between scaffold characteristics and cellular responses. This entails a systematic examination of key scaffold parameters, including pore size, crosslinking methods, and material concentration, to elucidate their individual and collective impact on cell proliferation.

4.3.3 Mechanical testing of alginate/recombinant collagen scaffolds

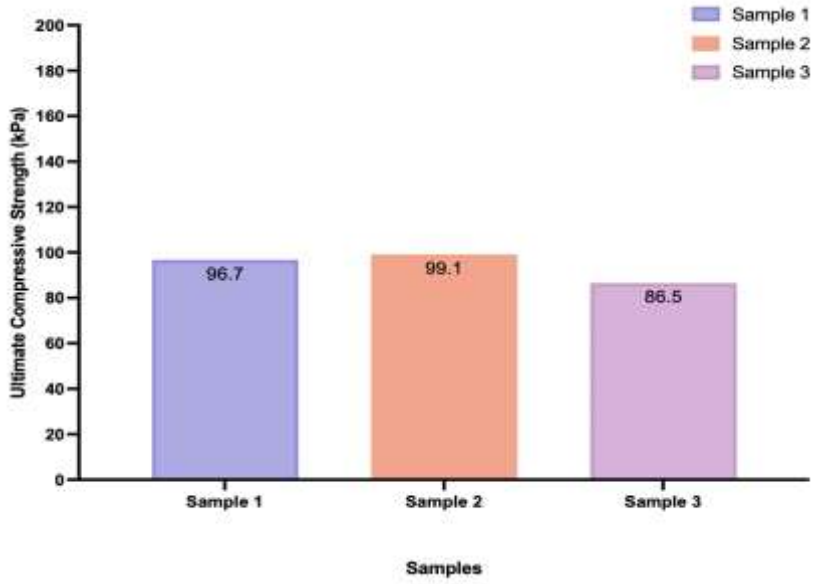

Figure 4.17 Compressive Strength of Alginate/Recombinant Collagen Scaffolds

Table 4.5 Compressive Strength of Alginate/Recombinant Collagen Scaffolds Samples

Samples	Ultimate Compressive Strength (kPa)	Sample Length	Sample Area
ALG-1	96,7	0,0092	81
ALG-2	99,1	0,0092	81
ALG-3	86,5	0,0092	81

The mechanical strength of a scaffold is crucial in tissue engineering, ensuring it can support tissue regeneration and maintain integrity during cell growth. Different tissues have varied mechanical requirements; for example, bone tissue necessitates higher strength compared to softer tissues. In cell culture, scaffold stiffness influences cell behavior, with a minimum stiffness of 100 kPa reported as necessary for functional tissue formation. Adequate stiffness provides mechanical cues that influence cell activities like proliferation and differentiation. It's essential to recognize that specific mechanical requirements vary based on factors such as cell type, scaffold design, and experimental conditions. Thus, careful consideration of the tissue engineering application's needs and consultation with relevant sources is advised for precise guidelines (Engler, Sen, Sweeney, & Discher, 2006).

Biomimetic injectable hydrogels are considered highly promising for cartilage treatment due to their ability to seamlessly integrate with tissues and facilitate cell isolation, thereby avoiding the need for extensive in vitro expansion (Sittinger, Hutmacher, & Risbud, 2004). However, these hydrogels have limitations that significantly impede articular cartilage regeneration. The lower mechanical strength of hydrogels, attributed to their low cell density, makes them unsuitable for long-term load-bearing applications, leading to potential degradation.

A significant challenge in scaffold preparation is achieving a delicate balance between porosity and mechanical strength. Various porosity factors, including volume, size, shape, orientation, and pore connectivity, significantly influence scaffold mechanical properties.

Striking the right porosity level is crucial for promoting cell infiltration, nutrient diffusion, and tissue regeneration, but it must be balanced with the need for mechanical strength to support cell growth and tissue development. Additionally, the choice of scaffold material and its concentration play critical roles in influencing both porosity and mechanical properties. Different materials with unique characteristics impact scaffold strength directly, and concentration variations affect density and arrangement, influencing porosity. Balancing these factors is crucial for determining overall scaffold strength, porosity, and suitability for tissue engineering, making optimal design a complex yet essential aspect for successful outcomes in both structural integrity and biological functionality (Dhandayuthapani, Yoshida, Maekawa, & Kumar, 2011).

4.3.4 SEM analysis of alginate/recombinant collagen scaffolds

SEM images were taken to characterize the structure of the Alginate/Recombinant Collagen Scaffolds. It is known that the surface roughness and porosity of a scaffold are important factors in promoting cell attachment. Adequate porosity also enables the infiltration of cells and the formation of new tissue within the scaffold. The size, distribution, and interconnectivity of pores are important factors in determining how effectively cells can colonize and grow within the scaffold. A moderately rough surface can enhance cell adhesion and spread by providing more surface area for cells to attach to and allowing for better mechanical interlocking between cells and the scaffold. It can also facilitate the formation of focal adhesions, which are critical for cell attachment and signaling (Fig 4.19).

Pore size is a critical factor in tissue engineering applications due to its impact on cell penetration, extracellular matrix production, neovascularization within scaffold structures and the differantiation (Matsiko, Gleeson, & O'Brien, 2015). If pores are too small, these essential processes can be impeded, hindering the overall effectiveness of the scaffold. To facilitate proper cell infiltration and support the development of a functional tissue construct, a minimum pore size of around 100 μm is generally considered necessary in tissue engineering applications. For cartilage regeneration, pores of 50–300 μm are usually considered suitable for stimulating appropriate differentiation and tissue

formation (McBride, Falls, & Knothe Tate, 2008). This threshold ensures that cells can effectively navigate the scaffold, promoting the formation of a well-organized extracellular matrix and fostering the establishment of neovascular networks within the inner regions of the scaffold. In this thesis, scaffolds with a macroporosity of 150 μm were designed to positively affect chondrogenic differentiation and increase cell attachment (Fig. 4.18).

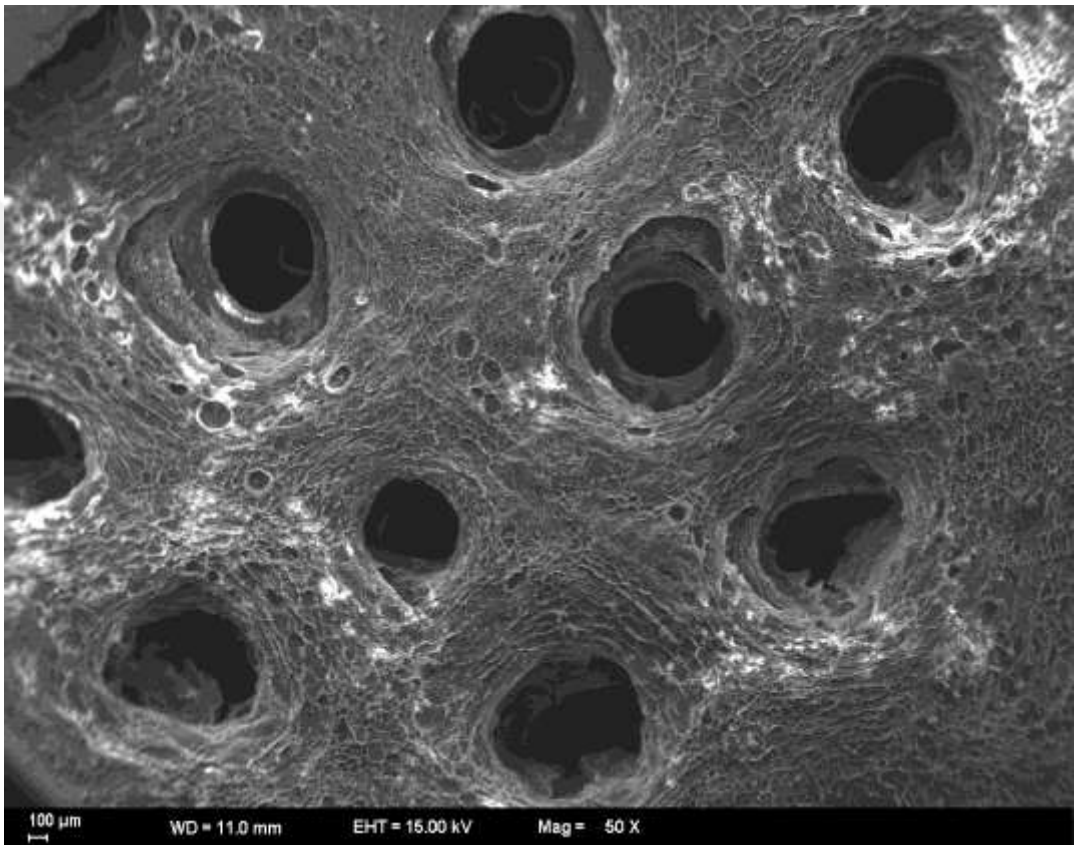

Figure 4.18 Sem Image of Alginate/Recombinant Collagen Scaffolds surface (100 μm)

The shape of pores may exert influence on cellular fate, with studies demonstrating that progenitor cells can be directed towards specific lineages by artificially controlling their shape. For instance, bone marrow-derived mesenchymal stem cells (BMMSCs) exhibiting a more rounded cell shape have been correlated with higher expression of chondrogenic markers (McBride et al., 2008). In this thesis, the chondral scaffolds were designed with a rounded pore shape.

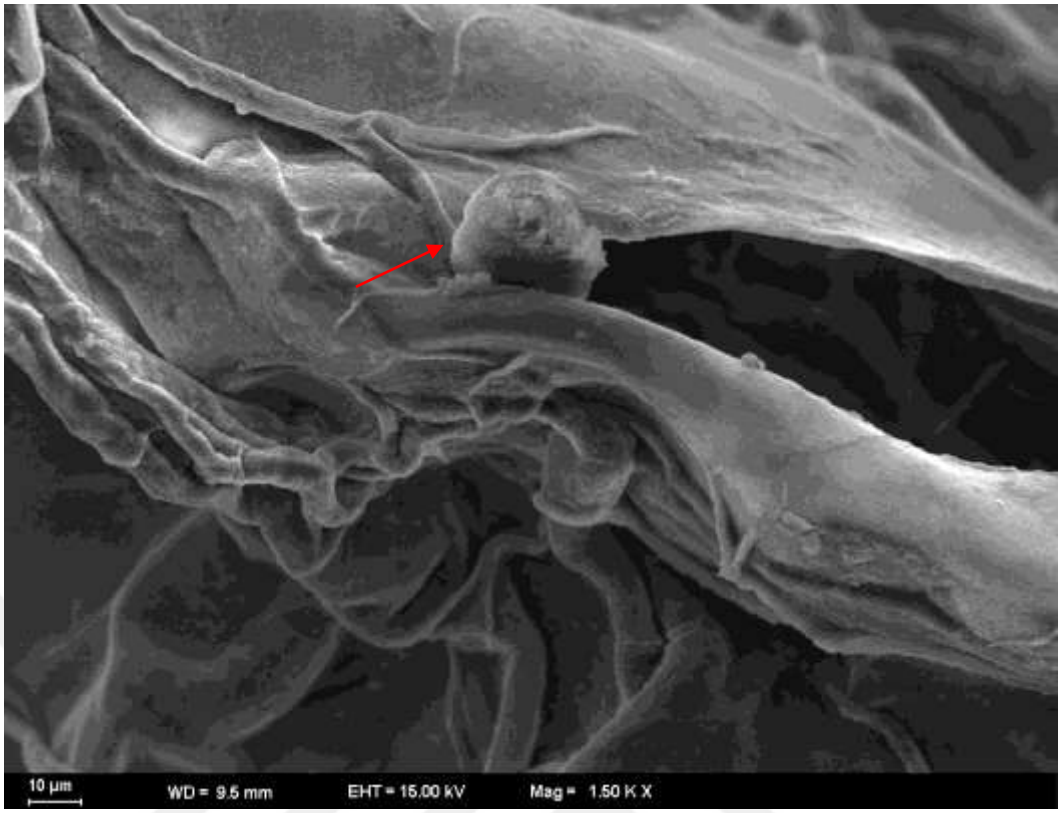

Figure 4.19 Sem Image of AD-MSC cell attached to the scaffolds macropores (10 µm)

The SEM image also shows the cell structure that was attached to the scaffold on days 1 and 21 (Fig 4.11). The images indicate that the scaffold could support AD-MSC proliferation. SEM images of tissue formation on the scaffold were obtained on day 21 to examine the tissue structure as the cell had reached full density on the scaffold surface. Cell attachment and spread on the surface of the optimized Alginate/Recombinant collagen scaffold are obvious in Fig 4.11.

	Control Medium	
Day 7	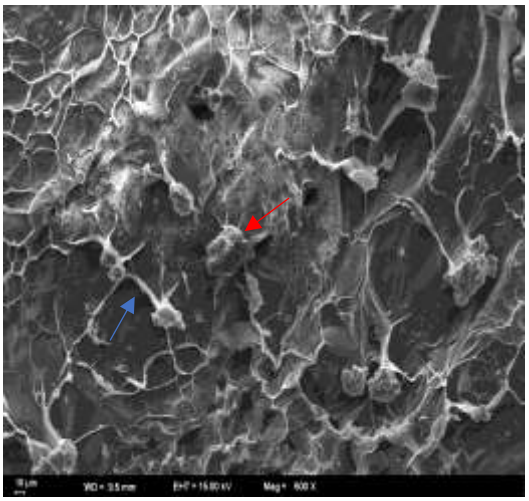	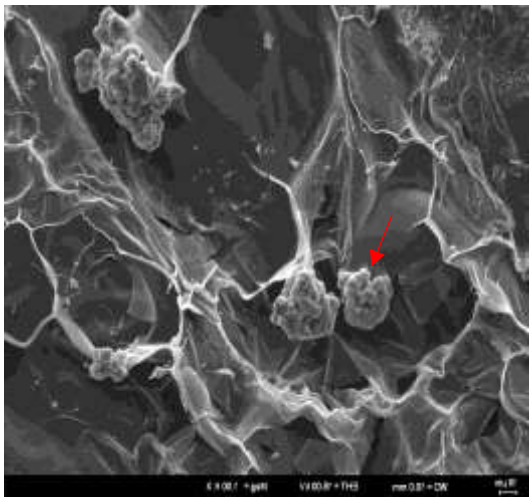
Day 14	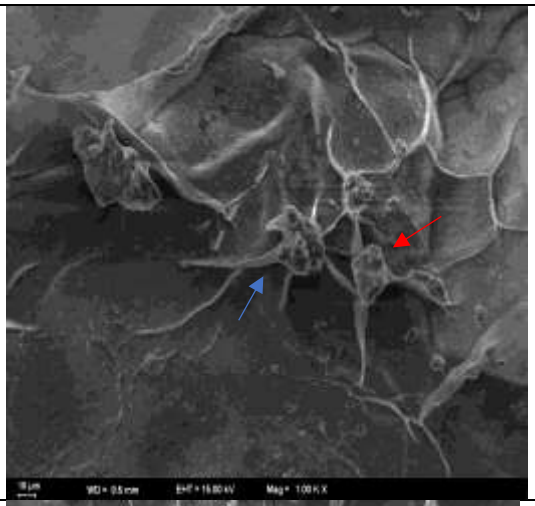	
Day 21	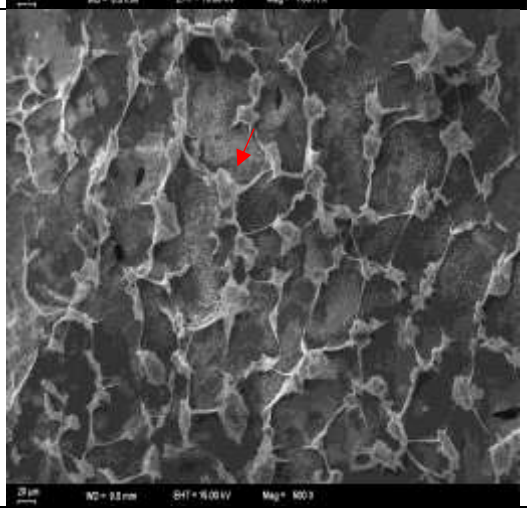	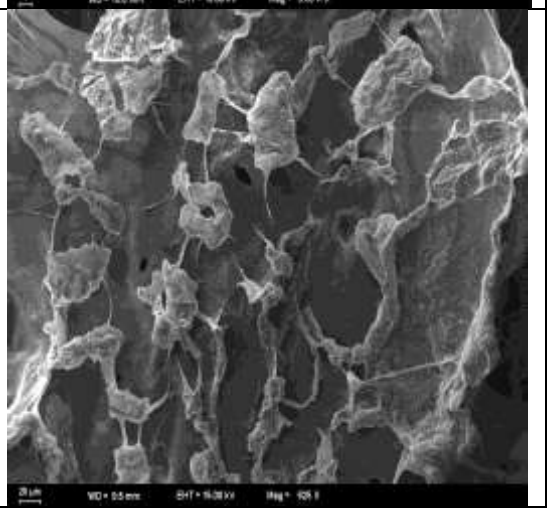

Figure 4.20 Sem Images of AD-MSC cell seeded Alginate/Recombinant Collagen Scaffolds from day 7 to day 21 cultured in control medium. (Red arrows show AD-MSC cells Blue shows cytoplasm extension).

The scaffold surfaces are almost completely covered with cells and clearly indicate the excellent adherence of the cells and layers to the scaffold surface. The SEM showed the microstructure with a cell population adhered and distributed on individual pore walls with partial filling of the scaffold pores. Morphology of AD-MSC cells which seeded Alginate/Recombinant Collagen Scaffolds cultured in a control medium corresponds to the studies conducted by Barlian et al. (Barlian, Judawisastra, Alfarafisa, Wibowo, & Rosadi, 2018).

	Chondrogenic Medium
Day 7	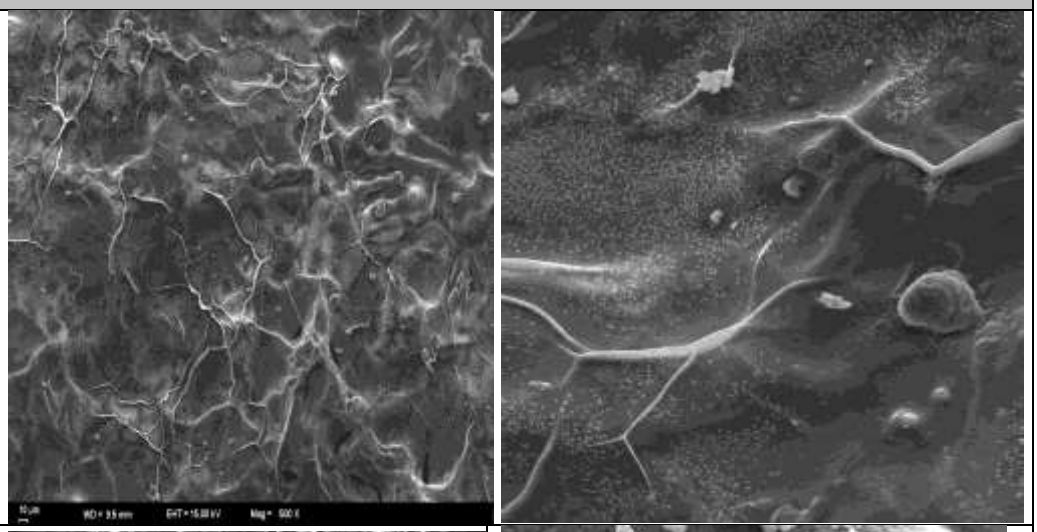
Day 14	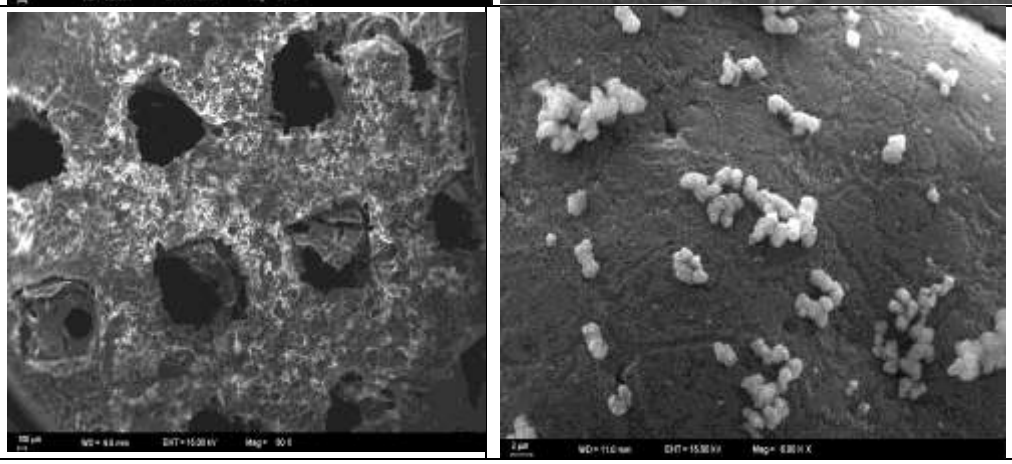

Figure 4.21 SEM Images of AD-MSC cell seeded Alginate/Recombinant Collagen Scaffolds from day 7 to day 21 cultured in chondrogenic mediu

Day 21	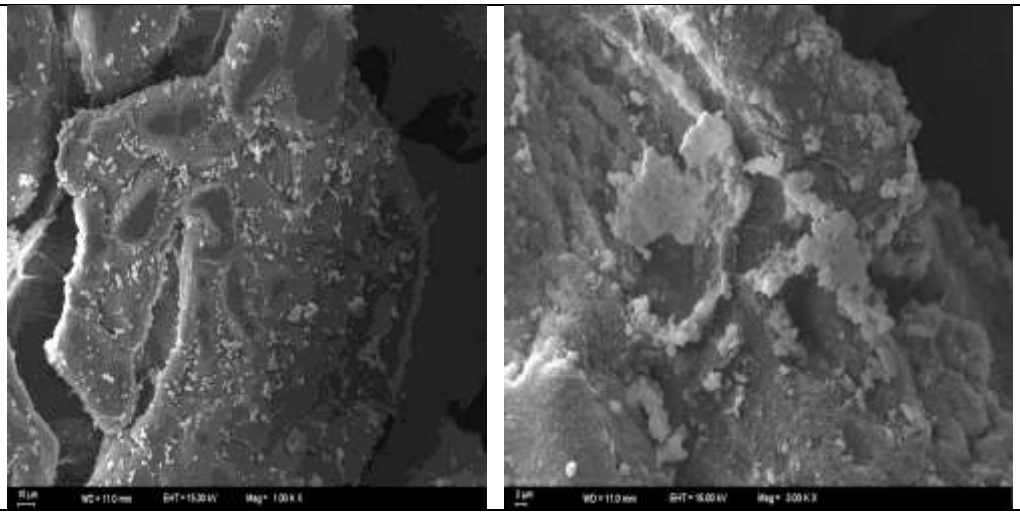

Figure 4.21 SEM Images of AD-MSC cell seeded Alginate/Recombinant Collagen Scaffolds from day 7 to day 21 cultured in chondrogenic mediu (continue)

Chondrogenic cells have traditionally been linked to a more rounded cell shape. Previous research has demonstrated that a random mesh of fibers more closely resembles the extracellular matrix (ECM) of cartilage. In contrast, aligned fibers have been shown to promote fibrous differentiation over cartilaginous differentiation in MSCs. A macroporous structure with interconnected pores was observed on the surface of the scaffolds. It was seen that the cells made contact with each other in both of the groups, which is very important to enhance cell proliferation.

4.3.5 Alcian Blue Staining

Days	Control	Chondrogenic
Day 7	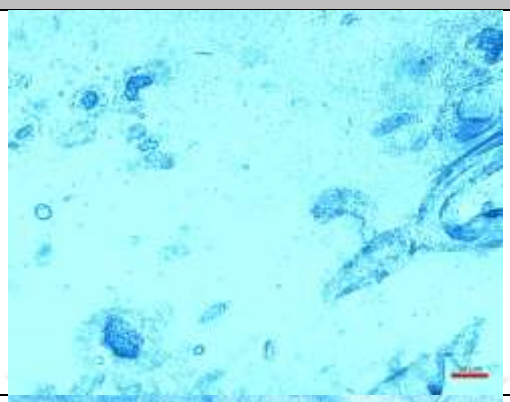	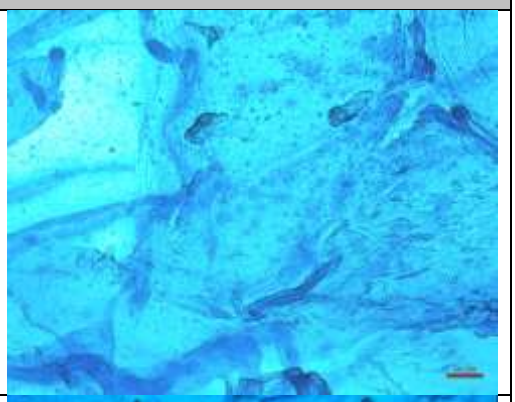
Day 14	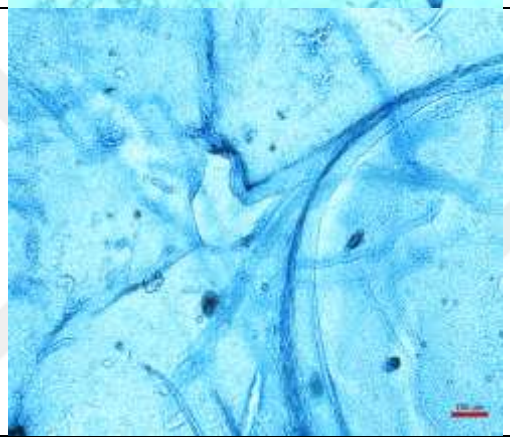	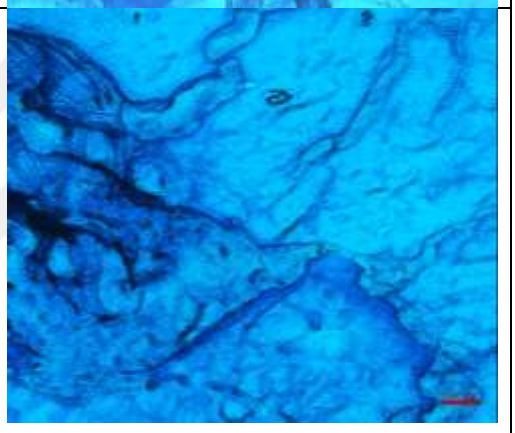
Day 21	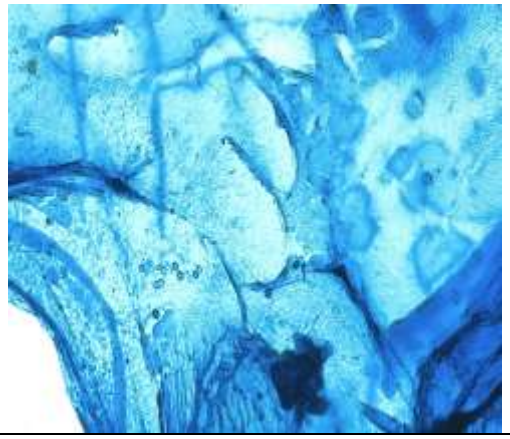	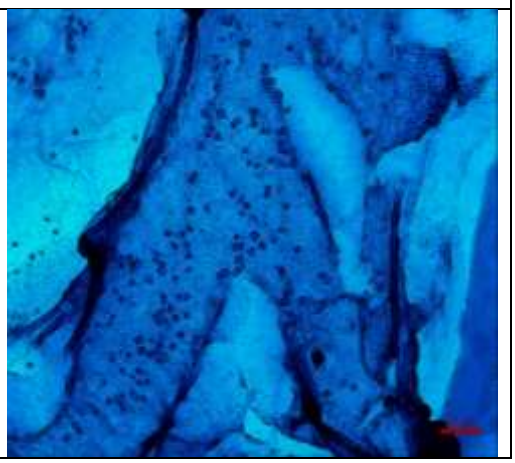

Fig 4.22 Microscope Images of Alcian Blue Staining Alginate/Recombinant Collagen Scaffolds

In Fig 4.22 Alcian blue staining of GAG deposition in AD-MSC seeded scaffolds during chondrogenesis can be seen. The scaffold containing AD-MSCs cultered in a

chondrogenic medium appeared more pigmented, possibly due to greater ECM deposition. As seen in the images, the areas where the cells are concentrated are more darkened.

In cell analysis experiments, a decrease in overall cell numbers is observed, but staining results indicate the presence of cells that have successfully transformed into chondrocytes. This suggests a dynamic process of cellular behavior, where the decrease in total cell count may be attributed to factors such as differentiation or changes in proliferation rates. The focus on chondrocyte-specific markers in the staining underscores the importance of assessing phenotypic changes, emphasizing successful chondrogenic differentiation despite the numerical decrease in cells.

Various scaffolds have been explored for chondrogenic differentiation, each with its own pros and cons. Synthetic polymers, though mechanically suitable, lack biocompatibility and cell adhesion properties, while natural scaffolds face issues like low stability and rapid degradation (Wasyłeczko, Sikorska, & Chwojnowski, 2020). Alginate, a natural polysaccharide, was chosen for its ease of gelation without solvents, simple preparation without pH alterations or heat, and favorable properties such as porosity. In this study, alginate's ability to support cell viability and create an environment conducive to chondrogenic differentiation in adipose-derived mesenchymal stem cells was assessed.

The use of alginate scaffolds in chondrogenic differentiation has been extensively researched. Alginate, a natural polymer from seaweed, can be shaped into three-dimensional structures, providing an ideal environment for directing stem cells into chondrocytes—cells crucial for cartilage tissue formation. A study explored strategies to enhance mesenchymal stem cell (MSC) chondrogenic differentiation, emphasizing factors like optimizing bioactive substances, culture conditions, cell types, coculture, gene editing, scaffolds, and physical stimulation. The review specifically underscored the significant role of scaffolds, particularly alginate, in promoting chondrogenesis (Zha et al., 2021). In a study focused on in vitro chondrogenic differentiation, alginate hydrogel served as a scaffold for human bone marrow-derived mesenchymal stem cells. The research compared cell differentiation on the alginate scaffold with and without

differentiation medium. The findings confirmed the suitability of alginate scaffolds for promoting chondrogenic differentiation, emphasizing their effectiveness in supporting this specific cellular transformation (Herlofsen, Küchler, Melvik, & Brinchmann, 2011).

While various materials have been extensively studied, a notable gap exists in the literature regarding the use of recombinant collagen for this purpose recombinant collagen into this scaffold, which is produced through genetic engineering techniques, offers advantages such as batch-to-batch consistency and potential customization. To date, no comprehensive studies or research endeavors have explored the potential of recombinant collagen in guiding chondrogenic differentiation. This knowledge gap signifies an unexplored dimension within the field of tissue engineering, emphasizing the more need for focused investigations into the efficacy and implications of utilizing recombinant collagen for chondrogenic differentiation.

While the alcian blue staining provides visual evidence of chondrogenic differentiation, further molecular analysis through PCR would provide more accurate and detailed insights into the specific genes associated with chondrogenesis. There is a critical need for further exploration into the molecular aspects of chondrogenic differentiation. To advance our understanding, it is strongly recommended to incorporate Polymerase Chain Reaction (PCR) analysis as a more robust method.

5. CONCLUSION

Three-dimensional porous scaffolds play an important role in tissue engineering as a temporary support to accommodate a sufficient number of cells and to guide new tissue formation. Numerous scaffolds for osteochondral tissue engineering have been developed by using biodegradable polymers, hydroxyapatite, tricalcium phosphate, etc. The natural osteochondral tissue consists of cartilage and supplying bone parts that have distinctly different structures and mechanical properties. The optimal scaffold for osteochondral tissue engineering should also have a stratified structure similar to the natural osteochondral tissue.

This study represents the first effort in culturing AD-MSCs on the high-strength, CPC-Recombinant collagen/Alginate scaffold to study AD-MSC proliferation and osteogenic and chondrogenic differentiation. This research used biphasic scaffolds to mimic bone and cartilage tissues separately. The upper layer of the cartilage scaffold was composed of recombinant collagen, a precise and controllable material with a reduced risk of immunogenicity compared to animal-derived collagens, in conjunction with alginate. For bone engineering, the lower layer consisted of calcium phosphate cement (CPC), a biocompatible, osteoconductive, and bioactive material known for its ability to support both bone and cartilage tissue growth. CPC scaffolds with approximately 300 μm macropores were explored to promote osteogenesis and tissue ingrowth therefore, an indirect 3D printing method was employed to create CPC scaffolds with interconnected macropores. Polycaprolactone (PCL) sacrificial models were initially 3D printed, and CPC pastes were perfused into these models, followed by self-setting. Subsequent removal of the PCL models resulted in macroporous CPC scaffolds with uniform shapes, a 3D interconnected structure, and the required compressive strength for subchondral bone repair. Hence, the CPC Scaffold in this study, with regard to proper pore size, porosity, mechanical strength, material composition, biocompatibility, and osteogenic differentiation capacity demonstrates a promising composite material for the purpose of osteochondral tissue engineering.

For the cartilage component, sodium alginate and recombinant collagen scaffolds were designed and 3D printed. These calcium phosphate cement scaffolds and recombinant

collagen/alginate scaffolds were then separately tested for their osteochondrogenic and chondrogenic differentiation potential in vitro using adipose-derived mesenchymal stem cells (ADMSCs). Various aspects, including mechanical properties, cell viability, proliferation, morphology, and differentiation characteristics, were thoroughly investigated.

Alginate-based scaffolds hold promise in applications related to cartilage and bone substitutes, but optimizing their mechanical, physical, and chondrogenesis properties is crucial for their successful use. The incorporation of recombinant collagen into these scaffolds can enhance their biological response and biodegradability, potentially making them more conducive to tissue replacement. The research results are expected to provide valuable insights into the interactions between cells and biodegradable scaffolds, which is essential for refining the manufacturing process and ensuring the survival of tissue constructs. Additionally, the addition of growth factors can further improve the chondrogenic differentiation of cells within these scaffolds, enhancing their potential for tissue regeneration. Also, it requires an investigation of alternative additives to get an additional amelioration of mechanical properties and stability of alginate/recombinant collagen scaffold, the alginate density can be increased or different polymers can be added or increase the cross-linking degree. In addition, a transitional layer between bone and cartilage layers to mimic calcified cartilage should be integrated to prevent site-specific cell migration and not to allow vascularization of the cartilage part.

Alginate/Recombinant collagen scaffolds and CPC scaffolds had good cytocompatibility, non-toxic to cells and the pore size of about 300 μm for the CPC scaffolds could evidently promote osteogenic differentiation and promise for osteochondral tissue engineering. The findings from our study indicate that both the morphology and chemistry of scaffolds can significantly impact the differentiation of mesenchymal stem cells (MSCs), influencing chondrogenic and osteogenic pathways.The study findings suggest that the combination of biphasic calcium phosphate bone cement and recombinant collagen/alginate scaffolds holds promise for repairing osteochondral defects. This approach provides mechanical support resembling subchondral bone while offering a chondrogenic scaffold for cartilage repair. This work contributes to the ongoing efforts to develop effective biomaterials for tissue engineering applications.

REFERENCES

Abarrategi, A., Gutiérrez, M. C., Moreno-Vicente, C., Hortigüela, M. J., Ramos, V., López-Lacomba, J. L., . . . del Monte, F. (2008). Multiwall carbon nanotube scaffolds for tissue engineering purposes. *Biomaterials, 29*(1), 94-102.

Acebes, C., Roman-Blas, J. A., Delgado-Baeza, E., Palacios, I., & Herrero-Beaumont, G. (2009). Correlation between arthroscopic and histopathological grading systems of articular cartilage lesions in knee osteoarthritis. *Osteoarthritis and cartilage, 17*(2), 205-212. doi:https://doi.org/10.1016/j.joca.2008.06.010

Adamiak, K., & Sionkowska, A. (2020). Current methods of collagen cross-linking: Review. *International Journal of Biological Macromolecules, 161*, 550-560. doi:https://doi.org/10.1016/j.ijbiomac.2020.06.075

Ahmed, T. A., & Hincke, M. T. (2010). Strategies for articular cartilage lesion repair and functional restoration. *Tissue Engineering Part B: Reviews, 16*(3), 305-329.

Akkineni, A. R., Ahlfeld, T., Funk, A., Waske, A., Lode, A., & Gelinsky, M. (2016). Highly concentrated alginate-gellan gum composites for 3D plotting of complex tissue engineering scaffolds. *Polymers, 8*(5), 170.

Alford, J. W., & Cole, B. J. (2005). Cartilage restoration, part 2: techniques, outcomes, and future directions. *The American journal of sports medicine, 33*(3), 443-460.

Apelt, D., Theiss, F., El-Warrak, A., Zlinszky, K., Bettschart-Wolfisberger, R., Bohner, M., . . . von Rechenberg, B. (2004). In vivo behavior of three different injectable hydraulic calcium phosphate cements. *Biomaterials, 25*(7-8), 1439-1451.

Appelman, T. P., Mizrahi, J., & Seliktar, D. (2011). A finite element model of cell-matrix interactions to study the differential effect of scaffold composition on chondrogenic response to mechanical stimulation.

Arden, N., & Nevitt, M. C. (2006). Osteoarthritis: epidemiology. *Best practice & research Clinical rheumatology, 20*(1), 3-25.

Axpe, E., & Oyen, M. L. (2016). Applications of Alginate-Based Bioinks in 3D Bioprinting. *Int J Mol Sci, 17*(12). doi:10.3390/ijms17121976

Bajek, A., Olkowska, J., Gurtowska, N., Kloskowski, T., Walentowicz-Sadlecka, M., Sadlecki, P., . . . Drewa, T. (2014). Human amniotic-fluid-derived stem cells: a unique source for regenerative medicine. *Expert Opinion on Biological Therapy, 14*(6), 831-839.

Baksh, D., Yao, R., & Tuan, R. S. (2007). Comparison of proliferative and multilineage differentiation potential of human mesenchymal stem cells derived from umbilical cord and bone marrow. *Stem Cells, 25*(6), 1384-1392.

Bal, B. S., Rahaman, M. N., Jayabalan, P., Kuroki, K., Cockrell, M. K., Yao, J. Q., & Cook, J. L. (2010). In vivo outcomes of tissue-engineered osteochondral grafts. *Journal of Biomedical Materials Research Part B: Applied Biomaterials: An Official Journal of The Society for Biomaterials, The Japanese Society for Biomaterials, and The Australian Society for Biomaterials and the Korean Society for Biomaterials, 93*(1), 164-174.

Banihashemian, A., Zamanlui Benisi, S., Hosseinzadeh, S., Shojaei, S., & Abbaszadeh, H. (2023). Structural and biological investigation of alginate-nano-hydroxyapatite with chitosan-hyaluronic acid for potential osteochondral regeneration. *International Journal of Polymeric Materials and Polymeric Biomaterials*, 1-15. doi:10.1080/00914037.2023.2215378

Barlian, A., Judawisastra, H., Alfarafisa, N. M., Wibowo, U. A., & Rosadi, I. (2018). Chondrogenic differentiation of adipose-derived mesenchymal stem cells induced by L-ascorbic acid and platelet rich plasma on silk fibroin scaffold. *PeerJ, 6*, e5809. doi:10.7717/peerj.5809

Barry, F. P., & Murphy, J. M. (2004). Mesenchymal stem cells: clinical applications and biological characterization. *The international journal of biochemistry & cell biology, 36*(4), 568-584.

Bartlett, W., Skinner, J. A., Gooding, C. R., Carrington, R. W., Flanagan, A. M., Briggs, T. W., & Bentley, G. (2005). Autologous chondrocyte implantation versus matrix-induced autologous chondrocyte implantation for osteochondral defects of the knee: a prospective, randomised study. *J Bone Joint Surg Br, 87*(5), 640-645. doi:10.1302/0301-620x.87b5.15905

Bassas-Galia, M., Follonier, S., Pusnik, M., & Zinn, M. (2017). 2 - Natural polymers: A source of inspiration. In G. Perale & J. Hilborn (Eds.), *Bioresorbable Polymers for Biomedical Applications* (pp. 31-64): Woodhead Publishing.

Baumann, C. A., Hinckel, B. B., Bozynski, C. C., & Farr, J. (2019). Articular cartilage: Structure and restoration. *Joint preservation of the knee: A clinical casebook*, 3-24.

Bayliss, M. T., & Roughley, P. J. (1985). The properties of proteoglycan prepared from human articular cartilage by using associative caesium chloride gradients of high and low starting densities. *Biochemical Journal, 232*(1), 111-117. doi:10.1042/bj2320111

Bayrak, A., Prüger, P., Stock, U. A., & Seifert, M. (2013). Absence of immune responses with xenogeneic collagen and elastin. *Tissue Engineering Part A, 19*(13-14), 1592-1600.

Berg, L. C., Koch, T., Heerkens, T., Besonov, K., Thomsen, P., & Betts, D. (2009). Chondrogenic potential of mesenchymal stromal cells derived from equine bone marrow and umbilical cord blood. *Veterinary and Comparative Orthopaedics and Traumatology, 22*(05), 363-370.

Bian, W., Li, D., Lian, Q., Li, X., Zhang, W., Wang, K., & Jin, Z. (2012). Fabrication of a bio-inspired beta-Tricalcium phosphate/collagen scaffold based on ceramic stereolithography and gel casting for osteochondral tissue engineering. *Rapid Prototyping Journal, 18*(1), 68-80. doi:10.1108/13552541211193511

Boeuf, S., & Richter, W. (2010). Chondrogenesis of mesenchymal stem cells: role of tissue source and inducing factors. *Stem cell research & therapy, 1*, 1-9.

Bohner, M. (2000). Calcium orthophosphates in medicine: from ceramics to calcium phosphate cements. *Injury, 31 Suppl 4*, 37-47. doi:10.1016/s0020-1383(00)80022-4

Boonlai, W., Hirun, N., Suknuntha, K., & Tantishaiyakul, V. (2023). Development and characterization of pluronic F127 and methylcellulose based hydrogels for 3D bioprinting. *Polymer Bulletin, 80*(4), 4555-4572. doi:10.1007/s00289-022-04271-6

Brown, W. (1986). chow LC. A new Calcium Phosphate, water-setting cement. *Cement Research progress wasterville, ohio: American ceramic society, 352*.

Buckwalter, J., & Mankin, H. (1997). Articular cartilage: part I. *Journal of Bone and joint surgery, 79*(4), 600.

Camarero-Espinosa, S., Rothen-Rutishauser, B., Foster, E. J., & Weder, C. (2016). Articular cartilage: from formation to tissue engineering. *Biomaterials Science, 4*(5), 734-767. doi:10.1039/C6BM00068A

Camarero-Espinosa, S., Rothen-Rutishauser, B., Foster, E. J., & Weder, C. (2016). Articular cartilage: from formation to tissue engineering. *Biomater Sci, 4*(5), 734-767. doi:10.1039/c6bm00068a

Casanova, M. R., Reis, R. L., Martins, A., & Neves, N. M. (2018). The Use of Electrospinning Technique on Osteochondral Tissue Engineering. *Adv Exp Med Biol, 1058*, 247-263. doi:10.1007/978-3-319-76711-6_11

Castro Viñuelas, R., Sanjurjo-Rodríguez, C., Piñeiro-Ramil, M., Hermida Gómez, T., Fuentes Boquete, I. M., De-Toro, J., . . . Díaz-Prado, S. (2018). Induced pluripotent stem cells for cartilage repair: current status and future perspectives. *European Cells and Materials, 36*, 96-109.

Chaala, M., Sebba, F. Z., Fuster, M. G., Moulefera, I., Montalbán, M. G., Carissimi, G., & Víllora, G. (2023). Accelerated simple preparation of curcumin-loaded silk fibroin/hyaluronic acid hydrogels for biomedical applications. *Polymers, 15*(3), 504.

Chan, E. F., Liu, I.-L., Semler, E. J., Aberman, H. M., Simon, T. M., Chen, A. C., . . . Sah, R. L. (2012). Association of 3-dimensional cartilage and bone structure with articular cartilage properties in and adjacent to autologous osteochondral grafts after 6 and 12 months in a goat model. *Cartilage, 3*(3), 255-266.

Chaves, C., Alshomer, F., Palgrave, R. G., & Kalaskar, D. M. (2016). Plasma surface modification of polyhedral oligomeric silsequioxane-poly (carbonate-urea) urethane with allylamine enhances the response and osteogenic differentiation of adipose-derived stem cells. *ACS applied materials & interfaces, 8*(29), 18701-18709.

Chen, D. X., & Chen, D. X. (2019). *Extrusion bioprinting of scaffolds*: Springer.

Chen, L., Liu, J., Guan, M., Zhou, T., Duan, X., & Xiang, Z. (2020). Growth Factor and Its Polymer Scaffold-Based Delivery System for Cartilage Tissue Engineering. *Int J Nanomedicine, 15*, 6097-6111. doi:10.2147/ijn.S249829

Chen, M.-Y., Lie, P.-C., Li, Z.-L., & Wei, X. (2009). Endothelial differentiation of Wharton's jelly–derived mesenchymal stem cells in comparison with bone marrow–derived mesenchymal stem cells. *Experimental hematology, 37*(5), 629-640.

Chen, Y., Xiong, X., Liu, X., Cui, R., Wang, C., Zhao, G., . . . Weng, J. (2020). 3D Bioprinting of shear-thinning hybrid bioinks with excellent bioactivity derived from gellan/alginate and thixotropic magnesium phosphate-based gels. *Journal of Materials Chemistry B, 8*(25), 5500-5514.

Chiesa, I., Ligorio, C., Bonatti, A. F., De Acutis, A., Smith, A. M., Saiani, A., . . . De Maria, C. (2020). Modeling the Three-Dimensional Bioprinting Process of β-Sheet Self-Assembling Peptide Hydrogel Scaffolds. *Front Med Technol, 2*, 571626. doi:10.3389/fmedt.2020.571626

Chimene, D., Lennox, K. K., Kaunas, R. R., & Gaharwar, A. K. (2016). Advanced Bioinks for 3D Printing: A Materials Science Perspective. *Annals of Biomedical Engineering, 44*(6), 2090-2102. doi:10.1007/s10439-016-1638-y

Choe, R., Devoy, E., Jabari, E., Packer, J. D., & Fisher, J. P. (2021). Biomechanical Aspects of Osteochondral Regeneration: Implications and Strategies for Three-Dimensional Bioprinting. *Tissue Engineering Part B: Reviews, 28*(4), 766-788. doi:10.1089/ten.teb.2021.0101

Choe, R., Devoy, E., Kuzemchak, B., Sherry, M., Jabari, E., Packer, J. D., & Fisher, J. P. (2022). Computational investigation of interface printing patterns within 3D printed multilayered scaffolds for osteochondral tissue engineering. *Biofabrication, 14*(2), 025015.

Chow, L. C. (2009). Next generation calcium phosphate-based biomaterials. *Dental materials journal, 28*(1), 1-10.

Chow, L. C., & Takagi, S. (2001). A Natural Bone Cement-A Laboratory Novelty Led to the Development of Revolutionary New Biomaterials. *J Res Natl Inst Stand Technol, 106*(6), 1029-1033. doi:10.6028/jres.106.053

Chua, C., Liu, M., & Chou, S. (2011). *Additive manufacturing-assisted scaffold-based tissue engineering.* Paper presented at the Innovative Developments in Virtual and Physical Prototyping, Proceedings of the 5th International Conference on Advanced Research in Virtual and Rapid Prototyping, Leiria, Portugal.

Chubinskaya, S., Di Matteo, B., Lovato, L., Iacono, F., Robinson, D., & Kon, E. (2019). Agili-C implant promotes the regenerative capacity of articular cartilage defects in an ex vivo model. *Knee surgery, sports traumatology, arthroscopy, 27*(6), 1953-1964. doi:10.1007/s00167-018-5263-1

Chubinskaya, S., Di Matteo, B., Lovato, L., Iacono, F., Robinson, D., & Kon, E. (2019). Agili-C implant promotes the regenerative capacity of articular cartilage defects in an ex vivo model. *Knee Surg Sports Traumatol Arthrosc, 27*(6), 1953-1964. doi:10.1007/s00167-018-5263-1

Compaan, A. M., Christensen, K., & Huang, Y. (2017). Inkjet Bioprinting of 3D Silk Fibroin Cellular Constructs Using Sacrificial Alginate. *ACS Biomater Sci Eng, 3*(8), 1519-1526. doi:10.1021/acsbiomaterials.6b00432

Cooper, A., Bhattarai, N., & Zhang, M. (2011). Fabrication and cellular compatibility of aligned chitosan–PCL fibers for nerve tissue regeneration. *Carbohydrate Polymers, 85*(1), 149-156.

D'Ambrosi, R., Valli, F., De Luca, P., Ursino, N., & Usuelli, F. G. (2019). MaioRegen Osteochondral Substitute for the Treatment of Knee Defects: A Systematic Review of the Literature. *Journal of Clinical Medicine, 8*(6), 783. Retrieved from https://www.mdpi.com/2077-0383/8/6/783

da Silva Meirelles, L., Fontes, A. M., Covas, D. T., & Caplan, A. I. (2009). Mechanisms involved in the therapeutic properties of mesenchymal stem cells. *Cytokine & growth factor reviews, 20*(5-6), 419-427.

Dai, Z., Ronholm, J., Tian, Y., Sethi, B., & Cao, X. (2016). Sterilization techniques for biodegradable scaffolds in tissue engineering applications. *Journal of Tissue Engineering, 7*, 2041731416648810. doi:10.1177/2041731416648810

Darling, E. M., & Athanasiou, K. A. (2005). Rapid phenotypic changes in passaged articular chondrocyte subpopulations. *J Orthop Res, 23*(2), 425-432. doi:10.1016/j.orthres.2004.08.008

Davidson, D., Blanc, A., Filion, D., Wang, H., Plut, P., Pfeffer, G., . . . Henderson, J. E. (2005). Fibroblast growth factor (FGF) 18 signals through FGF receptor 3 to promote chondrogenesis. *Journal of Biological Chemistry, 280*(21), 20509-20515.

de Vries–van Melle, M. L., Narcisi, R., Kops, N., Koevoet, W. J., Bos, P. K., Murphy, J. M., . . . van Osch, G. J. (2014). Chondrogenesis of mesenchymal stem cells in an osteochondral environment is mediated by the subchondral bone. *Tissue Engineering Part A, 20*(1-2), 23-33.

Del Real, R., Ooms, E., Wolke, J., Vallet-Regi, M., & Jansen, J. (2003). In vivo bone response to porous calcium phosphate cement. *Journal of Biomedical Materials Research Part A: An Official Journal of The Society for Biomaterials, The Japanese Society for Biomaterials, and The Australian Society for Biomaterials and the Korean Society for Biomaterials, 65*(1), 30-36.

Demir Oğuz, Ö., & Ege, D. (2018). Rheological and Mechanical Properties of Thermoresponsive Methylcellulose/Calcium Phosphate-Based Injectable Bone Substitutes. *Materials, 11*(4), 604. Retrieved from https://www.mdpi.com/1996-1944/11/4/604

Deng, C., Lin, R., Zhang, M., Qin, C., Yao, Q., Wang, L., . . . Wu, C. (2019). Micro/Nanometer-Structured Scaffolds for Regeneration of Both Cartilage and Subchondral Bone. *Advanced functional materials, 29*(4), 1806068. doi:https://doi.org/10.1002/adfm.201806068

Dhandayuthapani, B., Yoshida, Y., Maekawa, T., & Kumar, D. S. (2011). Polymeric Scaffolds in Tissue Engineering Application: A Review. *International Journal of Polymer Science, 2011*, 290602. doi:10.1155/2011/290602

Dhollander, A. A., Liekens, K., Almqvist, K. F., Verdonk, R., Lambrecht, S., Elewaut, D., . . . Verdonk, P. C. (2012). A pilot study of the use of an osteochondral scaffold plug for cartilage repair in the knee and how to deal with early clinical failures. *Arthroscopy, 28*(2), 225-233. doi:10.1016/j.arthro.2011.07.017

Di Luca, A., Longoni, A., Criscenti, G., Lorenzo-Moldero, I., Klein-Gunnewiek, M., Vancso, J., . . . Moroni, L. (2016). Surface energy and stiffness discrete gradients in additive manufactured scaffolds for osteochondral regeneration. *Biofabrication, 8*(1), 015014.

Diduch, D. R., Jordan, L. C., Mierisch, C. M., & Balian, G. (2000). Marrow stromal cells embedded in alginate for repair of osteochondral defects. *Arthroscopy: The Journal of Arthroscopic & Related Surgery, 16*(6), 571-577.

Dominici, M., Le Blanc, K., Mueller, I., Slaper-Cortenbach, I., Marini, F., Krause, D., . . . Horwitz, E. (2006). Minimal criteria for defining multipotent mesenchymal stromal cells. The International Society for Cellular Therapy position statement. *Cytotherapy, 8*(4), 315-317. doi:10.1080/14653240600855905

Dormer, N. H., Berkland, C. J., & Detamore, M. S. (2010). Emerging techniques in stratified designs and continuous gradients for tissue engineering of interfaces. *Annals of Biomedical Engineering, 38*, 2121-2141.

Dorozhkin, S. V. (2007). Calcium orthophosphates. *Journal of materials science, 42*(4), 1061-1095. doi:10.1007/s10853-006-1467-8

Dorozhkin, S. V. (2013). Self-setting calcium orthophosphate formulations. *J Funct Biomater, 4*(4), 209-311. doi:10.3390/jfb4040209

Dragoo, J. L., & Chang, W. (2017). Arthroscopic harvest of adipose-derived mesenchymal stem cells from the infrapatellar fat pad. *The American journal of sports medicine, 45*(13), 3119-3127.

Duan, P., Pan, Z., Cao, L., Gao, J., Yao, H., Liu, X., . . . Ding, J. (2019). Restoration of osteochondral defects by implanting bilayered poly (lactide-co-glycolide) porous scaffolds in rabbit joints for 12 and 24 weeks. *Journal of Orthopaedic Translation, 19*, 68-80.

Dwivedi, R., Kumar, S., Pandey, R., Mahajan, A., Nandana, D., Katti, D. S., & Mehrotra, D. (2020). Polycaprolactone as biomaterial for bone scaffolds: Review of literature. *Journal of oral biology and craniofacial research, 10*(1), 381-388.

Engler, A. J., Sen, S., Sweeney, H. L., & Discher, D. E. (2006). Matrix elasticity directs stem cell lineage specification. *Cell, 126*(4), 677-689. doi:10.1016/j.cell.2006.06.044

Erickson, A. E., Sun, J., Lan Levengood, S. K., Swanson, S., Chang, F.-C., Tsao, C. T., & Zhang, M. (2019). Chitosan-based composite bilayer scaffold as an in vitro osteochondral defect regeneration model. *Biomedical microdevices, 21*, 1-16.

Evonik achieves a major biotech breakthrough with a new animal-free and fermentation-based collagen platform. Evonik Industries. (2021, March 16). . Retrieved from https://healthcare.evonik.com/en/evonik-achieves-major-biotech-breakthrough-with-a-new-animal-free-and-fermentation-based-collagen-pl-125478.html

Farr, J., & Gomoll, A. H. (2014). *Cartilage restoration: Practical clinical applications*.

Farr, J., & Gomoll, A. H. (2018). *Cartilage restoration: practical clinical applications*: Springer.

Fawns, H. T., & Landells, J. W. (1953). Histochemical studies of rheumatic conditions. I. Observations on the fine structures of the matrix of normal bone and cartilage. *Ann Rheum Dis, 12*(2), 105-113. doi:10.1136/ard.12.2.105

Félix Lanao, R., Hoekstra, J. W. M., Wolke, J. G., Leeuwenburgh, S. C., Plachokova, A. S., Boerman, O. C., . . . Jansen, J. A. (2014). Porous calcium phosphate cement for alveolar bone regeneration. *Journal of tissue engineering and regenerative medicine, 8*(6), 473-482.

Friess, W. (1998). Collagen–biomaterial for drug delivery. *European journal of pharmaceutics and biopharmaceutics, 45*(2), 113-136.

Frisbie, D. D., Kisiday, J. D., Kawcak, C. E., Werpy, N. M., & McIlwraith, C. W. (2009). Evaluation of adipose-derived stromal vascular fraction or bone marrow-derived mesenchymal stem cells for treatment of osteoarthritis. *Journal of Orthopaedic Research, 27*(12), 1675-1680. doi:https://doi.org/10.1002/jor.20933

Fu, J.-N., Wang, X., Yang, M., Chen, Y.-R., Zhang, J.-Y., Deng, R.-H., . . . Yuan, F.-Z. (2022). Scaffold-Based Tissue Engineering Strategies for Osteochondral Repair. *Frontiers in bioengineering and biotechnology, 9*. doi:10.3389/fbioe.2021.812383

Fu, L., Yang, Z., Gao, C., Li, H., Yuan, Z., Wang, F., . . . Guo, Q. (2020). Advances and prospects in biomimetic multilayered scaffolds for articular cartilage regeneration. *Regenerative biomaterials, 7*(6), 527-542.

Fuchs, S., Shariati, K., & Ma, M. (2020). Specialty tough hydrogels and their biomedical applications. *Advanced healthcare materials, 9*(2), 1901396.

Furth, M. E., & Atala, A. (2014). Chapter 6 - Tissue Engineering: Future Perspectives. In R. Lanza, R. Langer, & J. Vacanti (Eds.), *Principles of Tissue Engineering (Fourth Edition)* (pp. 83-123). Boston: Academic Press.

Galarraga, J. H., Kwon, M. Y., & Burdick, J. A. (2019). 3D bioprinting via an in situ crosslinking technique towards engineering cartilage tissue. *Scientific Reports, 9*(1), 19987. doi:10.1038/s41598-019-56117-3

Gao, F., Xu, Z., Liang, Q., Liu, B., Li, H., Wu, Y., . . . Ruan, C. (2018). Direct 3D printing of high strength biohybrid gradient hydrogel scaffolds for efficient repair of osteochondral defect. *Advanced functional materials, 28*(13), 1706644.

Gazit, Z., Pelled, G., Sheyn, D., Kimelman, N., & Gazit, D. (2011). Chapter 17 - Mesenchymal Stem Cells. In A. Atala, R. Lanza, J. A. Thomson, & R. Nerem (Eds.), *Principles of Regenerative Medicine (Second Edition)* (pp. 285-304). San Diego: Academic Press.

Gelse, K., Pöschl, E., & Aigner, T. (2003). Collagens—structure, function, and biosynthesis. *Advanced Drug Delivery Reviews, 55*(12), 1531-1546. doi:https://doi.org/10.1016/j.addr.2003.08.002

Getgood, A., Brooks, R., Fortier, L., & Rushton, N. (2009). Articular cartilage tissue engineering: today's research, tomorrow's practice? *The Journal of Bone & Joint Surgery British Volume, 91*(5), 565-576.

Ghassemi, T., Shahroodi, A., Ebrahimzadeh, M. H., Mousavian, A., Movaffagh, J., & Moradi, A. (2018). Current concepts in scaffolding for bone tissue engineering. *Archives of bone and joint surgery, 6*(2), 90.

Gilbert, J. E. (1998). Current treatment options for the restoration of articular cartilage. *The American journal of knee surgery, 11*(1), 42-46.

Ginebra, M. P., Traykova, T., & Planell, J. A. (2006). Calcium phosphate cements: competitive drug carriers for the musculoskeletal system? *Biomaterials, 27*(10), 2171-2177. doi:10.1016/j.biomaterials.2005.11.023

Goh, W. H., & Hashimoto, M. (2018). Dual Sacrificial Molding: Fabricating 3D Microchannels with Overhang and Helical Features. *Micromachines (Basel), 9*(10). doi:10.3390/mi9100523

Gonzalez-Fernandez, T., Rathan, S., Hobbs, C., Pitacco, P., Freeman, F., Cunniffe, G., . . . O'Brien, F. (2019). Pore-forming bioinks to enable spatio-temporally defined gene delivery in bioprinted tissues. *Journal of Controlled Release, 301*, 13-27.

Gotterbarm, T., Richter, W., Jung, M., Berardi Vilei, S., Mainil-Varlet, P., Yamashita, T., & Breusch, S. J. (2006). An in vivo study of a growth-factor enhanced, cell free, two-layered collagen–tricalcium phosphate in deep osteochondral defects. *Biomaterials, 27*(18), 3387-3395. doi:https://doi.org/10.1016/j.biomaterials.2006.01.041

Gough, J. E., Notingher, I., & Hench, L. L. (2004). Osteoblast attachment and mineralized nodule formation on rough and smooth 45S5 bioactive glass monoliths. *J Biomed Mater Res A, 68*(4), 640-650. doi:10.1002/jbm.a.20075

Goyal, D., Keyhani, S., Lee, E. H., & Hui, J. H. P. (2013). Evidence-based status of microfracture technique: a systematic review of level I and II studies. *Arthroscopy: The Journal of Arthroscopic & Related Surgery, 29*(9), 1579-1588.

Graceffa, V., Vinatier, C., Guicheux, J., Stoddart, M., Alini, M., & Zeugolis, D. I. (2019). Chasing Chimeras–The elusive stable chondrogenic phenotype. *Biomaterials, 192*, 199-225.

Griffin, M., Ibrahim, A., Seifalian, A., Butler, P., Kalaskar, D., & Ferretti, P. (2017). Chemical group-dependent plasma polymerisation preferentially directs adipose stem cell differentiation towards osteogenic or chondrogenic lineages. *Acta Biomaterialia, 50*, 450-461.

Gruber, S. M., Ghosh, P., Mueller, K. W., Whitlock, P. W., & Lin, C.-Y. (2019). Novel process for 3D printing decellularized matrices. *JoVE (Journal of Visualized Experiments)*(143), e58720.

Gudas, R., Gudaitė, A., Mickevičius, T., Masiulis, N., Simonaitytė, R., Čekanauskas, E., & Skurvydas, A. (2013). Comparison of osteochondral autologous transplantation, microfracture, or debridement techniques in articular cartilage lesions associated with anterior cruciate ligament injury: a prospective study with a 3-year follow-up. *Arthroscopy: The Journal of Arthroscopic & Related Surgery, 29*(1), 89-97.

Gugjoo, M. B., Amarpal, Abdelbaset-Ismail, A., Aithal, H. P., Kinjavdekar, P., Pawde, A. M., . . . Sharma, G. T. (2017). Mesenchymal stem cells with IGF-1 and TGF- β1 in laminin gel for osteochondral defects in rabbits. *Biomed Pharmacother, 93*, 1165-1174. doi:10.1016/j.biopha.2017.07.032

Guo, H., Su, J., Wei, J., Kong, H., & Liu, C. (2009). Biocompatibility and osteogenicity of degradable Ca-deficient hydroxyapatite scaffolds from calcium phosphate cement for bone tissue engineering. *Acta Biomaterialia, 5*(1), 268-278.

Guo, X., Wang, C., Duan, C., Descamps, M., Zhao, Q., Dong, L., . . . Song, Y. Q. (2004). Repair of Osteochondral Defects with Autologous Chondrocytes Seeded onto Bioceramic Scaffold in Sheep. *Tissue engineering, 10*(11-12), 1830-1840. doi:10.1089/ten.2004.10.1830

Guo, Y., Liang, K., & Ji, Y. (2019). New degradable composite elastomers of POC/PCL fabricated via in-situ copolymerization blending strategy. *European Polymer Journal, 110*, 337-343.

Gutierrez-Aranda, I., Ramos-Mejia, V., Bueno, C., Munoz-Lopez, M., Real, P. J., Mácia, A., . . . Menendez, P. (2010). Human induced pluripotent stem cells develop teratoma more efficiently and faster than human embryonic stem cells regardless the site of injection. *Stem Cells, 28*(9), 1568-1570. doi:10.1002/stem.471

Han, Y., Jia, B., Lian, M., Sun, B., Wu, Q., Sun, B., . . . Dai, K. (2021). High-precision, gelatin-based, hybrid, bilayer scaffolds using melt electro-writing to repair cartilage injury. *Bioactive Materials, 6*(7), 2173-2186.

Hass, R., Kasper, C., Böhm, S., & Jacobs, R. (2011). Different populations and sources of human mesenchymal stem cells (MSC): a comparison of adult and neonatal tissue-derived MSC. *Cell Communication and Signaling, 9*(1), 1-14.

Hauschka, P. V., & Wians, F. H., Jr. (1989). Osteocalcin-hydroxyapatite interaction in the extracellular organic matrix of bone. *Anat Rec, 224*(2), 180-188. doi:10.1002/ar.1092240208

Hauselmann, H. J., Masuda, K., Hunziker, E. B., Neidhart, M., Mok, S., Michel, B. A., & Thonar, E. (1996). Adult human chondrocytes cultured in alginate form a matrix similar to native human articular cartilage. *American Journal of Physiology-Cell Physiology, 271*(3), C742-C752.

He, A., Liu, L., Luo, X., Liu, Y., Liu, Y., Liu, F., . . . Liu, W. (2017). Repair of osteochondral defects with in vitro engineered cartilage based on autologous bone marrow stromal cells in a swine model. *Scientific Reports, 7*(1), 40489.

He, F., Li, J., & Ye, J. (2013). Improvement of cell response of the poly (lactic-co-glycolic acid)/calcium phosphate cement composite scaffold with unidirectional pore structure by the surface immobilization of collagen via plasma treatment. *Colloids and Surfaces B: Biointerfaces, 103*, 209-216.

He, X., Fu, W., Feng, B., Wang, H., Liu, Z., Yin, M., . . . Zheng, J. (2013). Electrospun collagen/poly (L-lactic acid-co-ε-caprolactone) hybrid nanofibrous membranes combining with sandwich construction model for cartilage tissue engineering. *Journal of nanoscience and nanotechnology, 13*(6), 3818-3825.

Hench, L. L., & Polak, J. M. (2002). Third-generation biomedical materials. *Science, 295*(5557), 1014-1017. doi:10.1126/science.1067404

Herlofsen, S. R., Küchler, A. M., Melvik, J. E., & Brinchmann, J. E. (2011). Chondrogenic differentiation of human bone marrow-derived mesenchymal stem cells in self-gelling alginate discs reveals novel chondrogenic signature gene clusters. *Tissue Eng Part A, 17*(7-8), 1003-1013. doi:10.1089/ten.TEA.2010.0499

Hesaraki, S., Moztarzadeh, F., & Sharifi, D. (2007). Formation of interconnected macropores in apatitic calcium phosphate bone cement with the use of an effervescent additive. *Journal of Biomedical Materials Research Part A, 83A*(1), 80-87. doi:https://doi.org/10.1002/jbm.a.31196

Hesaraki, S., Moztarzadeh, F., & Sharifi, D. (2007). Formation of interconnected macropores in apatitic calcium phosphate bone cement with use of an effervescent additive. *Journal of biomedical materials research. Part A, 83*, 80-87. doi:10.1002/jbm.a.31196

Hu, K., & Olsen, B. R. (2016). Osteoblast-derived VEGF regulates osteoblast differentiation and bone formation during bone repair. *The Journal of clinical investigation, 126*(2), 509-526.

Hu, T., & Lo, A. C. Y. (2021). Collagen-Alginate Composite Hydrogel: Application in Tissue Engineering and Biomedical Sciences. *Polymers (Basel), 13*(11). doi:10.3390/polym13111852

Huang, Z., Nelson, E. R., Smith, R. L., & Goodman, S. B. (2007). The sequential expression profiles of growth factors from osteroprogenitors to osteoblasts in vitro. *Tissue engineering, 13*(9), 2311-2320.

Huckle, J., Dootson, G., Medcalf, N., McTaggart, S., Wright, E., Carter, A., . . . Ratcliffe, A. (2003). Differentiated Chondrocytes for Cartilage Tissue Engineering. In *Tissue Engineering of Cartilage and Bone* (pp. 103-117).

Hunter, D. J., & Bierma-Zeinstra, S. (2019). Osteoarthritis. *The Lancet, 393*(10182), 1745-1759. doi:https://doi.org/10.1016/S0140-6736(19)30417-9

Hunter, D. J., March, L., & Chew, M. (2020). Osteoarthritis in 2020 and beyond: a Lancet Commission. *The Lancet, 396*(10264), 1711-1712. doi:https://doi.org/10.1016/S0140-6736(20)32230-3

Hutmacher, D. W. (2000). Scaffolds in tissue engineering bone and cartilage. *Biomaterials, 21*(24), 2529-2543. doi:https://doi.org/10.1016/S0142-9612(00)00121-6

Hutmacher, D. W. (2000). Scaffolds in tissue engineering bone and cartilage. *Biomaterials, 21*(24), 2529-2543. doi:10.1016/s0142-9612(00)00121-6

Ishikawa, K. (2014). Calcium phosphate cement. *Advances in calcium phosphate biomaterials*, 199-227.

Jeon, J., Lee, M. S., & Yang, H. S. (2018). Differentiated osteoblasts derived decellularized extracellular matrix to promote osteogenic differentiation. *Biomaterials Research, 22*(1), 4. doi:10.1186/s40824-018-0115-0

Johnstone, B. (2002). Mesenchymal stem cells and chondrogenesis. *European Cells and Materials, 4*(SUPPL. 1).

Kafi, M. A., Aktar, M. K., Phanny, Y., & Todo, M. (2019). Adhesion, proliferation and differentiation of human mesenchymal stem cell on chitosan/collagen composite scaffold. *J Mater Sci Mater Med, 30*(12), 131. doi:10.1007/s10856-019-6341-8

Karageorgiou, V., & Kaplan, D. (2005). Porosity of 3D biomaterial scaffolds and osteogenesis. *Biomaterials, 26*(27), 5474-5491. doi:10.1016/j.biomaterials.2005.02.002

Kesireddy, V., & Kasper, F. K. (2016). Approaches for building bioactive elements into synthetic scaffolds for bone tissue engineering. *Journal of Materials Chemistry B, 4*(42), 6773-6786.

Kilian, D., von Witzleben, M., Lanaro, M., Wong, C. S., Vater, C., Lode, A., . . . Gelinsky, M. (2022). 3D Plotting of Calcium Phosphate Cement and Melt Electrowriting of Polycaprolactone Microfibers in One Scaffold: A Hybrid Additive Manufacturing Process. *J Funct Biomater, 13*(2). doi:10.3390/jfb13020075

Kim, H. J., & Im, G. I. (2009). Chondrogenic differentiation of adipose tissue-derived mesenchymal stem cells: Greater doses of growth factor are necessary. *Journal of Orthopaedic Research, 27*(5), 612-619.

Kim, H. T., Teng, M. S., & Dang, A. C. (2008). Chondrocyte apoptosis: implications for osteochondral allograft transplantation. *Clinical orthopaedics and related research, 466*, 1819-1825.

Kim, K., Yeatts, A., Dean, D., & Fisher, J. P. (2010). Stereolithographic bone scaffold design parameters: osteogenic differentiation and signal expression. *Tissue Eng Part B Rev, 16*(5), 523-539. doi:10.1089/ten.TEB.2010.0171

Knight, M., & Evans, G. (2004). Tissue Engineering: Progress and Challenges. *Plastic and Reconstructive Surgery, 114*, 26E-37E. doi:10.1097/01.PRS.0000132678.97041.53

Kolambkar, Y. M., Peister, A., Soker, S., Atala, A., & Guldberg, R. E. (2007). Chondrogenic differentiation of amniotic fluid-derived stem cells. *J Mol Histol, 38*(5), 405-413. doi:10.1007/s10735-007-9118-1

Komath, M., & Varma, H. K. (2003). Development of a fully injectable calcium phosphate cement for orthopedic and dental applications. *Bulletin of Materials science, 26*(4), 415-422. doi:10.1007/BF02711186

Komori, T. (2016). Cell death in chondrocytes, osteoblasts, and osteocytes. *International Journal of Molecular Sciences, 17*(12), 2045.

Komori, T. (2019). Regulation of proliferation, differentiation and functions of osteoblasts by Runx2. *International Journal of Molecular Sciences, 20*(7), 1694.

Kon, E., Delcogliano, M., Filardo, G., Busacca, M., Di Martino, A., & Marcacci, M. (2011). Novel nano-composite multilayered biomaterial for osteochondral regeneration: a pilot clinical trial. *The American journal of sports medicine, 39*(6), 1180-1190.

Kon, E., Delcogliano, M., Filardo, G., Fini, M., Giavaresi, G., Francioli, S., . . . Quarto, R. (2010). Orderly osteochondral regeneration in a sheep model using a novel nano-composite multilayered biomaterial. *Journal of Orthopaedic Research, 28*(1), 116-124.

Kon, E., Delcogliano, M., Filardo, G., Fini, M., Giavaresi, G., Francioli, S., . . . Marcacci, M. (2010). Orderly osteochondral regeneration in a sheep model using a novel nano-composite multilayered biomaterial. *J Orthop Res, 28*(1), 116-124. doi:10.1002/jor.20958

Kon, E., Filardo, G., Delcogliano, M., Fini, M., Salamanna, F., Giavaresi, G., . . . Marcacci, M. (2010). Platelet autologous growth factors decrease the osteochondral regeneration capability of a collagen-hydroxyapatite scaffold in a sheep model. *BMC musculoskeletal disorders, 11*(1), 1-12.

Kosik-Kozioł, A., Heljak, M., & Święszkowski, W. (2019). Mechanical Properties of Hybrid Triphasic Scaffolds for Osteochondral Tissue Engineering. *Materials Letters, 261*, 126893. doi:10.1016/j.matlet.2019.126893

Kosik-Kozioł, A., Heljak, M., & Święszkowski, W. (2020). Mechanical properties of hybrid triphasic scaffolds for osteochondral tissue engineering. *Materials Letters, 261*, 126893.

Krebs, J., Aebli, N., Goss, B. G., Sugiyama, S., Bardyn, T., Boecken, I., . . . Ferguson, S. J. (2007). Cardiovascular changes after pulmonary embolism from injecting calcium phosphate cement. *Journal of Biomedical Materials Research Part B: Applied Biomaterials: An Official Journal of The Society for Biomaterials, The Japanese Society for Biomaterials, and The Australian Society for Biomaterials and the Korean Society for Biomaterials, 82*(2), 526-532.

Langer, R., & Vacanti, J. P. (1993). Tissue Engineering. *Science, 260*(5110), 920-926. doi:doi:10.1126/science.8493529

Larson, B. L., Yu, S. N., Park, H., Estes, B. T., Moutos, F. T., Bloomquist, C. J., . . . Freed, L. E. (2019). Chondrogenic, hypertrophic, and osteochondral differentiation of human mesenchymal stem cells on three-dimensionally woven scaffolds. *Journal of tissue engineering and regenerative medicine, 13*(8), 1453-1465. doi:https://doi.org/10.1002/term.2899

Lee, D. H., Kong, C.-G., Shin, Y.-W., Ahmed, S., Shetty, A. A., Moon, M. S., & Kim, S. J. (2020). Which is better for articular cartilage regeneration, cultured stem cells or concentrated stromal cells? *Annals of Translational Medicine, 8*(13), 836. Retrieved from https://atm.amegroups.org/article/view/39272

Lee, H.-p., Gu, L., Mooney, D. J., Levenston, M. E., & Chaudhuri, O. (2017). Mechanical confinement regulates cartilage matrix formation by chondrocytes. *Nature materials, 16*(12), 1243-1251.

LeGeros, R., & Legeros, J. (2003). Calcium Phosphate Bioceramics: Past, Present and Future. *Key Engineering Materials - KEY ENG MAT, 240–242*, 3-10. doi:10.4028/www.scientific.net/KEM.240-242.3

Lementowski, P. W., & Zelicof, S. B. (2008). Obesity and osteoarthritis. *American Journal of Orthopedics-Belle Mead-, 37*(3), 148.

Leone, G., Torricelli, P., Chiumiento, A., Facchini, A., & Barbucci, R. (2008). Amidic alginate hydrogel for nucleus pulposus replacement. *Journal of Biomedical Materials Research Part A, 84*(2), 391-401.

Li, C., Gao, L., Chen, F., & Liu, C. (2015). Fabrication of mesoporous calcium silicate/calcium phosphate cement scaffolds with high mechanical strength by freeform fabrication system with micro-droplet jetting. *Journal of materials science, 50*, 7182-7191.

Li, C.-y., Wu, X.-y., Tong, J.-b., Yang, X.-x., Zhao, J.-l., Zheng, Q.-f., . . . Ma, Z.-j. (2015). Comparative analysis of human mesenchymal stem cells from bone marrow and adipose tissue under xeno-free conditions for cell therapy. *Stem cell research & therapy, 6*(1), 1-13.

Li, F., Bronson, S., & Niyibizi, C. (2010). Derivation of murine induced pluripotent stem cells (iPS) and assessment of their differentiation toward osteogenic lineage. *Journal of cellular biochemistry, 109*(4), 643-652.

Li, G., Yin, J., Gao, J., Cheng, T. S., Pavlos, N. J., Zhang, C., & Zheng, M. H. (2013). Subchondral bone in osteoarthritis: insight into risk factors and microstructural changes. *Arthritis Research & Therapy, 15*(6), 223. doi:10.1186/ar4405

Li, J. J., Kim, K., Roohani-Esfahani, S.-I., Guo, J., Kaplan, D. L., & Zreiqat, H. (2015). A biphasic scaffold based on silk and bioactive ceramic with stratified properties for osteochondral tissue regeneration. *Journal of Materials Chemistry B, 3*(26), 5361-5376. doi:10.1039/C5TB00353A

Li, K., Wang, D., Zhang, F., Wang, X., Chen, H., Yu, A., . . . Dong, C. (2021). Tip-Viscid Electrohydrodynamic Jet 3D Printing of Composite Osteochondral Scaffold. *Nanomaterials (Basel), 11*(10). doi:10.3390/nano11102694

Li, K., Wang, D., Zhang, F., Wang, X., Chen, H., Yu, A., . . . Dong, C. (2021). Tip-Viscid Electrohydrodynamic Jet 3D Printing of Composite Osteochondral Scaffold. *Nanomaterials, 11*(10), 2694.

Li, S., Liu, Y. Y., Liu, L. J., & Hu, Q. X. (2016). A Versatile Method for Fabricating Tissue Engineering Scaffolds with a Three-Dimensional Channel for Prevasculature Networks. *ACS Appl Mater Interfaces, 8*(38), 25096-25103. doi:10.1021/acsami.6b07725

Li, X., Ding, J., Wang, J., Zhuang, X., & Chen, X. (2015). Biomimetic biphasic scaffolds for osteochondral defect repair. *Regenerative biomaterials, 2*(3), 221-228.

Li, X., Liu, B., Pei, B., Chen, J., Zhou, D., Peng, J., . . . Xu, T. (2020). Inkjet Bioprinting of Biomaterials. *Chem Rev, 120*(19), 10793-10833. doi:10.1021/acs.chemrev.0c00008

Liang, W., Li, L., Cui, X., Tang, Z., Wei, X., Pan, H., & Li, B. (2016). Enhanced Proliferation and Differentiation Effects of a CGRP- and Sr-Enriched Calcium Phosphate Cement on Bone Mesenchymal Stem Cells. *Journal of Applied Biomaterials & Functional Materials, 14*. doi:10.5301/jabfm.5000295

Lin, D., Cai, B., Wang, L., Cai, L., Wang, Z., Xie, J., . . . Shen, S. G. (2020). A viscoelastic PEGylated poly (glycerol sebacate)-based bilayer scaffold for cartilage regeneration in full-thickness osteochondral defect. *Biomaterials, 253*, 120095.

Liu, C., Xia, Z., & Czernuszka, J. T. (2007). Design and Development of Three-Dimensional Scaffolds for Tissue Engineering. *Chemical Engineering Research and Design, 85*(7), 1051-1064. doi:https://doi.org/10.1205/cherd06196

Liu, H., Nakagawa, K., Kato, D.-i., Chaudhary, D., & Tadé, M. O. (2011). Enzyme encapsulation in freeze-dried bionanocomposites prepared from chitosan and xanthan gum blend. *Materials Chemistry and Physics, 129*(1), 488-494. doi:https://doi.org/10.1016/j.matchemphys.2011.04.043

Liu, L., Kuffová, L., Griffith, M., Dang, Z., Muckersie, E., Liu, Y., . . . Forrester, J. V. (2007). Immunological responses in mice to full-thickness corneal grafts engineered from porcine collagen. *Biomaterials, 28*(26), 3807-3814.

Liu, S., & Shin, Y. C. (2019). Additive manufacturing of Ti6Al4V alloy: A review. *Materials & Design, 164*, 107552.

Liu, S., Wu, J., Liu, X., Chen, D., Bowlin, G. L., Cao, L., . . . Fan, C. (2015). Osteochondral regeneration using an oriented nanofiber yarn-collagen type I/hyaluronate hybrid/TCP biphasic scaffold. *J Biomed Mater Res A, 103*(2), 581-592. doi:10.1002/jbm.a.35206

Liu, Y., Shu, X. Z., & Prestwich, G. D. (2006). Osteochondral defect repair with autologous bone marrow–derived mesenchymal stem cells in an injectable, in situ, cross-linked synthetic extracellular matrix. *Tissue engineering, 12*(12), 3405-3416.

Lode, A., Meissner, K., Luo, Y., Sonntag, F., Glorius, S., Nies, B., . . . Gelinsky, M. (2014). Fabrication of porous scaffolds by three-dimensional plotting of a pasty calcium phosphate bone cement under mild conditions. *Journal of tissue engineering and regenerative medicine, 8*. doi:10.1002/term.1563

Loeser, R. F. (2010). Age-related changes in the musculoskeletal system and the development of osteoarthritis. *Clinics in geriatric medicine, 26*(3), 371-386.

Loh, Q. L., & Choong, C. (2013). Three-dimensional scaffolds for tissue engineering applications: role of porosity and pore size.

Loh, Q. L., & Choong, C. (2013). Three-dimensional scaffolds for tissue engineering applications: role of porosity and pore size. *Tissue Eng Part B Rev, 19*(6), 485-502. doi:10.1089/ten.TEB.2012.0437

Luo, Y., Tan, J., Zhou, Y., Guo, Y., Liao, X., He, L., . . . Liu, Y. (2023). From crosslinking strategies to biomedical applications of hyaluronic acid-based hydrogels: A review. *International Journal of Biological Macromolecules*, 123308.

Lv, Y. M., & Yu, Q. S. (2015). Repair of articular osteochondral defects of the knee joint using a composite lamellar scaffold. *Bone Joint Res, 4*(4), 56-64. doi:10.1302/2046-3758.44.2000310

Lynn, A., Yannas, I., & Bonfield, W. (2004). Antigenicity and immunogenicity of collagen. *Journal of Biomedical Materials Research Part B: Applied Biomaterials: An Official Journal of The Society for Biomaterials, The Japanese Society for Biomaterials, and The Australian Society for Biomaterials and the Korean Society for Biomaterials, 71*(2), 343-354.

Lyons, T. J., McClure, S. F., Stoddart, R. W., & McClure, J. (2006). The normal human chondro-osseous junctional region: evidence for contact of uncalcified cartilage with subchondral bone and marrow spaces. *BMC musculoskeletal disorders, 7*(1), 1-8.

Ma, K., Titan, A. L., Stafford, M., hua Zheng, C., & Levenston, M. E. (2012). Variations in chondrogenesis of human bone marrow-derived mesenchymal stem cells in fibrin/alginate blended hydrogels. *Acta Biomaterialia, 8*(10), 3754-3764.

Ma, K., Titan, A. L., Stafford, M., Zheng, C., & Levenston, M. E. (2012). Variations in chondrogenesis of human bone marrow-derived mesenchymal stem cells in fibrin/alginate blended hydrogels. *Acta Biomater, 8*(10), 3754-3764. doi:10.1016/j.actbio.2012.06.028

Maazouz, Y., Montufar, E., Guillem-Marti, J., Fleps, I., Öhman, C., Persson, C., & Ginebra, M. (2014). Robocasting of biomimetic hydroxyapatite scaffolds using self-setting inks. *Journal of Materials Chemistry B, 2*(33), 5378-5386.

Madry, H., van Dijk, C. N., & Mueller-Gerbl, M. (2010). The basic science of the subchondral bone. *Knee surgery, sports traumatology, arthroscopy, 18*, 419-433.

Mahapatra, C., Kim, J.-J., Lee, J.-H., Jin, G.-Z., Knowles, J. C., & Kim, H.-W. (2019). Differential chondro-and osteo-stimulation in three-dimensional porous scaffolds with different topological surfaces provides a design strategy for biphasic osteochondral engineering. *Journal of Tissue Engineering, 10*, 2041731419826433.

Maia, F. R., Carvalho, M. R., Oliveira, J. M., & Reis, R. L. (2018). Tissue Engineering Strategies for Osteochondral Repair. *Adv Exp Med Biol, 1059*, 353-371. doi:10.1007/978-3-319-76735-2_16

Malafaya, P. B., & Reis, R. L. (2009). Bilayered chitosan-based scaffolds for osteochondral tissue engineering: Influence of hydroxyapatite on in vitro cytotoxicity and dynamic bioactivity studies in a specific double-chamber bioreactor. *Acta Biomaterialia, 5*(2), 644-660. doi:https://doi.org/10.1016/j.actbio.2008.09.017

Malaval, L., Liu, F., Roche, P., & Aubin, J. E. (1999). Kinetics of osteoprogenitor proliferation and osteoblast differentiation in vitro. *J Cell Biochem, 74*(4), 616-627.

Mancini, I. A. D., Schmidt, S., Brommer, H., Pouran, B., Schäfer, S., Tessmar, J., . . . van Weeren, P. R. (2020). A composite hydrogel-3D printed thermoplast osteochondral anchor as example for a zonal approach to cartilage repair: in vivo performance in a long-term equine model. *Biofabrication, 12*(3), 035028. doi:10.1088/1758-5090/ab94ce

Mano, J. F., & Reis, R. L. (2007). Osteochondral defects: present situation and tissue engineering approaches. *J Tissue Eng Regen Med, 1*(4), 261-273. doi:10.1002/term.37

Marques, C. F., Perera, F. H., Marote, A., Ferreira, S., Vieira, S. I., Olhero, S., . . . Ferreira, J. M. (2017). Biphasic calcium phosphate scaffolds fabricated by direct write assembly: Mechanical, anti-microbial and osteoblastic properties. *Journal of the European Ceramic Society, 37*(1), 359-368.

Matsiko, A., Gleeson, J. P., & O'Brien, F. J. (2015). Scaffold mean pore size influences mesenchymal stem cell chondrogenic differentiation and matrix deposition. *Tissue Eng Part A, 21*(3-4), 486-497. doi:10.1089/ten.TEA.2013.0545

McBride, S. H., Falls, T., & Knothe Tate, M. L. (2008). Modulation of stem cell shape and fate B: mechanical modulation of cell shape and gene expression. *Tissue Engineering Part A, 14*(9), 1573-1580.

Mei, L., Shen, B., Ling, P., Liu, S., Xue, J., Liu, F., . . . Liu, X. (2017). Culture-expanded allogenic adipose tissue-derived stem cells attenuate cartilage degeneration in an experimental rat osteoarthritis model. *PLoS One, 12*(4), e0176107.

Michail, E. K., Hicham, D., & Athanasios, M. (2019). The Use of Alginate Hydrogels for the Culture of Mesenchymal Stem Cells (MSCs): In Vitro and In Vivo Paradigms. In P. Leonel (Ed.), *Alginates* (pp. Ch. 4). Rijeka: IntechOpen.

Miralles, G., Baudoin, R., Dumas, D., Baptiste, D., Hubert, P., Stoltz, J., . . . Payan, E. (2001). Sodium alginate sponges with or without sodium hyaluronate: in vitro engineering of cartilage. *Journal of Biomedical Materials Research: An Official Journal of The Society for Biomaterials, The Japanese Society for Biomaterials, and The Australian Society for Biomaterials and the Korean Society for Biomaterials, 57*(2), 268-278.

Mohan, N., Dormer, N. H., Caldwell, K. L., Key, V. H., Berkland, C. J., & Detamore, M. S. (2011). Continuous gradients of material composition and growth factors for effective regeneration of the osteochondral interface. *Tissue Eng Part A, 17*(21-22), 2845-2855. doi:10.1089/ten.tea.2011.0135

Moroni, L., Boland, T., Burdick, J. A., De Maria, C., Derby, B., Forgacs, G., . . . Vozzi, G. (2018). Biofabrication: A Guide to Technology and Terminology. *Trends Biotechnol, 36*(4), 384-402. doi:10.1016/j.tibtech.2017.10.015

Mu, X., Shi, X.-L., Zhou, J., Chen, H., Yang, T., Wang, Y., . . . Chen, Z.-G. (2023). Self-hygroscopic and smart color-changing hydrogels as coolers for improving energy conversion efficiency of electronics. *Nano Energy, 108*, 108177.

Murata, D., Fujimoto, R., & Nakayama, K. (2020). Osteochondral regeneration using adipose tissue-derived mesenchymal stem cells. *International Journal of Molecular Sciences, 21*(10), 3589.

Murphy, W. L., Dennis, R. G., Kileny, J., & Mooney, D. J. (2002). Salt fusion: an approach to improve pore interconnectivity within tissue engineering scaffolds. *Tissue engineering, 8 1*, 43-52.

Musskaya, O., Krut'ko, V., Kulak, A., Filatov, S., Batyrev, E., & Safronova, T. (2020). Calcium Phosphate Compositions with Polyvinyl Alcohol for 3D Printing. *Inorganic Materials: Applied Research, 11*, 192-197. doi:10.1134/S2075113320010268

Nakao, N., Nakayama, T., Yahata, T., Muguruma, Y., Saito, S., Miyata, Y., . . . Naoe, T. (2010). Adipose tissue-derived mesenchymal stem cells facilitate hematopoiesis in vitro and in vivo: advantages over bone marrow-derived mesenchymal stem cells. *Am J Pathol, 177*(2), 547-554. doi:10.2353/ajpath.2010.091042

Natarajan, A. B. M., Sivadas, V. P. D., & Nair, P. D. P. D. (2021). 3D-printed biphasic scaffolds for the simultaneous regeneration of osteochondral tissues. *Biomedical Materials, 16*(5), 054102.

Natesan, S., Baer, D. G., Walters, T. J., Babu, M., & Christy, R. J. (2010). Adipose-derived stem cell delivery into collagen gels using chitosan microspheres. *Tissue Engineering Part A, 16*(4), 1369-1384.

Neogi, T., Nevitt, M., Niu, J., Sharma, L., Roemer, F., Guermazi, A., . . . Felson, D. (2010). Subchondral bone attrition may be a reflection of compartment-specific mechanical load: the MOST Study. *Annals of the Rheumatic Diseases, 69*(5), 841-844.

Ng, W. L., Lee, J. M., Zhou, M., Chen, Y.-W., Lee, K.-X. A., Yeong, W. Y., & Shen, Y.-F. (2020). Vat polymerization-based bioprinting—process, materials, applications and regulatory challenges. *Biofabrication, 12*(2), 022001.

Niemeyer, P., Pestka, J. M., Kreuz, P. C., Erggelet, C., Schmal, H., Suedkamp, N. P., & Steinwachs, M. (2008). Characteristic complications after autologous chondrocyte implantation for cartilage defects of the knee joint. *The American journal of sports medicine, 36*(11), 2091-2099.

Nuernberger, S., Cyran, N., Albrecht, C., Redl, H., Vécsei, V., & Marlovits, S. (2011). The influence of scaffold architecture on chondrocyte distribution and behavior in matrix-associated chondrocyte transplantation grafts. *Biomaterials, 32*(4), 1032-1040. doi:10.1016/j.biomaterials.2010.08.100

O'brien, F. J. (2011). Biomaterials & scaffolds for tissue engineering. *Materials today, 14*(3), 88-95.

O'Driscoll, S. W., & Fitzsimmons, J. S. (2001). The role of periosteum in cartilage repair. *Clin Orthop Relat Res*(391 Suppl), S190-207. doi:10.1097/00003086-200110001-00019

Ochi, M., Uchio, Y., Tobita, M., & Kuriwaka, M. (2001). Current concepts in tissue engineering technique for repair of cartilage defect. *Artificial organs, 25*(3), 172-179.

Ogueri, K. S., Jafari, T., Escobar Ivirico, J. L., & Laurencin, C. T. (2019). POLYMERIC BIOMATERIALS FOR SCAFFOLD-BASED BONE REGENERATIVE ENGINEERING. *Regen Eng Transl Med, 5*(2), 128-154. doi:10.1007/s40883-018-0072-0

Ohira, T., & Ishikawa, K. (1986). Hydroxyapatite deposition in articular cartilage by intra-articular injections of methylprednisolone. A histological, ultrastructural, and x-ray-microprobe analysis in rabbits. *J Bone Joint Surg Am, 68*(4), 509-520.

Oliver-Ferrándiz, M., Milián, L., Sancho-Tello, M., Martín de Llano, J. J., Gisbert Roca, F., Martínez-Ramos, C., . . . Mata, M. (2021). Alginate-Agarose Hydrogels Improve the In Vitro Differentiation of Human Dental Pulp Stem Cells in Chondrocytes. A Histological Study. *Biomedicines, 9*(7). doi:10.3390/biomedicines9070834

Omarov, S., Nauryz, N., Talamona, D., & Perveen, A. (2023). Surface Modification Techniques for Metallic Biomedical Alloys: A Concise Review. *Metals, 13*(1), 82. Retrieved from https://www.mdpi.com/2075-4701/13/1/82

Orava, H., Huang, L., Ojanen, S. P., Mäkelä, J. T. A., Finnilä, M. A. J., Saarakkala, S., . . . Tanska, P. (2022). Changes in subchondral bone structure and mechanical properties do not substantially affect cartilage mechanical responses – A finite element study. *Journal of the Mechanical Behavior of Biomedical Materials, 128*, 105129. doi:https://doi.org/10.1016/j.jmbbm.2022.105129

Orimo, H. (2010). The mechanism of mineralization and the role of alkaline phosphatase in health and disease. *J Nippon Med Sch, 77*(1), 4-12. doi:10.1272/jnms.77.4

Ouyang, L., Armstrong, J. P. K., Lin, Y., Wojciechowski, J. P., Lee-Reeves, C., Hachim, D., . . . Stevens, M. M. (2020). Expanding and optimizing 3D bioprinting capabilities using complementary network bioinks. *Sci Adv, 6*(38). doi:10.1126/sciadv.abc5529

Ozbolat, I. T., & Hospodiuk, M. (2016). Current advances and future perspectives in extrusion-based bioprinting. *Biomaterials, 76*, 321-343.

Pan, J., Zhou, X., Li, W., Novotny, J. E., Doty, S. B., & Wang, L. (2009). In situ measurement of transport between subchondral bone and articular cartilage. *Journal of Orthopaedic Research, 27*(10), 1347-1352.

Park, J. Y., Choi, J.-C., Shim, J.-H., Lee, J.-S., Park, H., Kim, S. W., . . . Cho, D.-W. (2014). A comparative study on collagen type I and hyaluronic acid dependent cell behavior for osteochondral tissue bioprinting. *Biofabrication, 6*(3), 035004.

Park, Y., Sugimoto, M., Watrin, A., Chiquet, M., & Hunziker, E. B. (2005). BMP-2 induces the expression of chondrocyte-specific genes in bovine synovium-derived progenitor cells cultured in three-dimensional alginate hydrogel. *Osteoarthritis and cartilage, 13*(6), 527-536.

Pashuck, E. T., & Stevens, M. M. (2012). Designing regenerative biomaterial therapies for the clinic. *Science translational medicine, 4*(160), 160sr164-160sr164.

Patel, A., Zaky, S. H., Schoedel, K., Li, H., Sant, V., Beniash, E., . . . Sant, S. (2020). Design and evaluation of collagen-inspired mineral-hydrogel nanocomposites for bone regeneration. *Acta Biomaterialia, 112*, 262-273.

Paul D L, B., Praveen, A. S., Čepová, L., & Elangovan, M. (2023). Rheological Behavior and Printability Study of Tri-Calcium Phosphate Ceramic Inks for Direct Ink Writing Method. *Polymers, 15*(6), 1433. Retrieved from https://www.mdpi.com/2073-4360/15/6/1433

Placone, J. K., & Engler, A. J. (2018). Recent Advances in Extrusion-Based 3D Printing for Biomedical Applications. *Advanced healthcare materials, 7*(8), 1701161. doi:https://doi.org/10.1002/adhm.201701161

Placone, J. K., & Engler, A. J. (2018). Recent advances in extrusion-based 3D printing for biomedical applications. *Advanced healthcare materials, 7*(8), 1701161.

Puetzer, J. L., Petitte, J. N., & Loboa, E. G. (2010). Comparative review of growth factors for induction of three-dimensional in vitro chondrogenesis in human mesenchymal stem cells isolated from bone marrow and adipose tissue. *Tissue Engineering Part B: Reviews, 16*(4), 435-444.

Qian, G., Wu, T., & Ye, J. (2023). Hierarchically porous calcium phosphate scaffold with degradable PLGA microsphere network. *Materials Chemistry and Physics, 301*, 127633. doi:https://doi.org/10.1016/j.matchemphys.2023.127633

Radhakrishnan, J., Manigandan, A., Chinnaswamy, P., Subramanian, A., & Sethuraman, S. (2018). Gradient nano-engineered in situ forming composite hydrogel for osteochondral regeneration. *Biomaterials, 162*, 82-98. doi:10.1016/j.biomaterials.2018.01.056

Rahaman, M. N., Day, D. E., Bal, B. S., Fu, Q., Jung, S. B., Bonewald, L. F., & Tomsia, A. P. (2011). Bioactive glass in tissue engineering. *Acta Biomaterialia, 7*(6), 2355-2373.

Rajzer, I., Castano, O., Engel, E., & Planell, J. A. (2010). Injectable and fast resorbable calcium phosphate cement for body-setting bone grafts. *Journal of materials science. Materials in medicine, 21*, 2049-2056. doi:10.1007/s10856-010-4078-5

Rao, H., Harini, B., Shadamarshan, P., Kalimuthu, B., & Selvamurugan, N. (2017). Natural and Synthetic Polymers/Bioceramics/Bioactive Compounds-mediated Cell Signaling in Bone Tissue Engineering. *International Journal of Biological Macromolecules, 110*. doi:10.1016/j.ijbiomac.2017.09.029

Reddy, M. S. B., Ponnamma, D., Choudhary, R., & Sadasivuni, K. K. (2021). A comparative review of natural and synthetic biopolymer composite scaffolds. *Polymers*, *13*(7), 1105.

Redman, S., Oldfield, S., & Archer, C. (2005). Current strategies for articular cartilage repair. *Eur Cell Mater, 9*(23-32), 23-32.

Ren, X., Zhao, M., Lash, B., Martino, M. M., & Julier, Z. (2020). Growth factor engineering strategies for regenerative medicine applications. *Frontiers in bioengineering and biotechnology, 7*, 469.

Revell, C. M., & Athanasiou, K. A. (2009). Success rates and immunologic responses of autogenic, allogenic, and xenogenic treatments to repair articular cartilage defects. *Tissue Engineering Part B: Reviews*, *15*(1), 1-15.

Rey, C., Marsan, O., Combes, C., Drouet, C., Grossin, D., & Sarda, S. (2014). Characterization of Calcium Phosphates Using Vibrational Spectroscopies. In (Vol. 2, pp. 229-266).

Roseti, L., Parisi, V., Petretta, M., Cavallo, C., Desando, G., Bartolotti, I., & Grigolo, B. (2017). Scaffolds for Bone Tissue Engineering: State of the art and new perspectives. *Mater Sci Eng C Mater Biol Appl, 78*, 1246-1262. doi:10.1016/j.msec.2017.05.017

Rozila, I., Azari, P., Munirah, S. b., Safwani, W. K. Z. W., Pingguan-Murphy, B., & Chua, K. H. (2021). Polycaprolactone-Based Scaffolds Facilitates Osteogenic Differentiation of Human Adipose-Derived Stem Cells in a Co-Culture System. *Polymers, 13*(4), 597. Retrieved from https://www.mdpi.com/2073-4360/13/4/597

Salamanca, E., Tsai, C.-Y., Pan, Y.-H., Lin, Y.-T., Huang, H.-M., Teng, N.-C., . . . Chang, W.-J. (2016). In vitro and in vivo study of a novel porcine collagen membrane for guided bone regeneration. *Materials, 9*(11), 949.

Sánchez-Téllez, D. A., Téllez-Jurado, L., & Rodríguez-Lorenzo, L. M. (2017). Hydrogels for cartilage regeneration, from polysaccharides to hybrids. *Polymers, 9*(12), 671.

Sasaki, A., Mizuno, M., Ozeki, N., Katano, H., Otabe, K., Tsuji, K., . . . Sekiya, I. (2018). Canine mesenchymal stem cells from synovium have a higher chondrogenic potential than those from infrapatellar fat pad, adipose tissue, and bone marrow. *PLoS One, 13*(8), e0202922.

Schumacher, M., Lode, A., Helth, A., & Gelinsky, M. (2013). A novel strontium(II)-modified calcium phosphate bone cement stimulates human-bone-marrow-derived mesenchymal stem cell proliferation and osteogenic differentiation in vitro. *Acta Biomaterialia, 9*(12), 9547-9557. doi:https://doi.org/10.1016/j.actbio.2013.07.027

Scott, D., Smith, C., Lohmander, S., & Chard, J. (2003). Osteoarthritis. *Clin Evid*(10), 1402-1430.

Seo, S.-J., Mahapatra, C., Singh, R. K., Knowles, J. C., & Kim, H.-W. (2014). Strategies for osteochondral repair: Focus on scaffolds. *Journal of Tissue Engineering, 5*, 2041731414541850. doi:10.1177/2041731414541850

Shafiee, A., & Atala, A. (2017). Tissue engineering: toward a new era of medicine. *Annual review of medicine, 68*, 29-40.

Shafiee, A., Soleimani, M., Chamheidari, G. A., Seyedjafari, E., Dodel, M., Atashi, A., & Gheisari, Y. (2011). Electrospun nanofiber-based regeneration of cartilage enhanced by mesenchymal stem cells. *Journal of Biomedical Materials Research Part A, 99*(3), 467-478.

Shao, G., Hanaor, D. A., Shen, X., & Gurlo, A. (2020). Freeze casting: from low-dimensional building blocks to aligned porous structures—a review of novel materials, methods, and applications. *Advanced Materials, 32*(17), 1907176.

Shi, R., Bi, J., Zhang, Z., Zhu, A., Chen, D., Zhou, X., . . . Tian, W. (2008). The effect of citric acid on the structural properties and cytotoxicity of the polyvinyl alcohol/starch films when molding at high temperature. *Carbohydrate Polymers, 74*(4), 763-770.

Shim, J.-H., Lee, J.-S., Kim, J. Y., & Cho, D.-W. (2012). Bioprinting of a mechanically enhanced three-dimensional dual cell-laden construct for osteochondral tissue engineering using a multi-head tissue/organ building system. *Journal of Micromechanics and Microengineering, 22*(8), 085014.

Shoulders, M. D., & Raines, R. T. (2009). Collagen structure and stability. *Annual review of biochemistry, 78*, 929-958.

Shyam, R., & Palaniappan, A. (2023). Effect of sterilization techniques on biomaterial inks' properties and 3D bioprinting parameters. *Bioprinting, 33*, e00294. doi:https://doi.org/10.1016/j.bprint.2023.e00294

Simkin, P. A. (2012). Consider the tidemark. *J Rheumatol, 39*(5), 890-892. doi:10.3899/jrheum.110942

Sin, D., Miao, X., Liu, G., Wei, F. S., Chadwick, G., Yan, C., & Friis, T. E. (2010). *Polyurethane (PU) scaffolds prepared by solvent casting/particulate leaching (SCPL) combined with centrifugation*.

Sing, S. L., Wang, S., Agarwala, S., Wiria, F. E., Ha, T. M. H., & Yeong, W. Y. (2017). Fabrication of titanium based biphasic scaffold using selective laser melting and collagen immersion. *International Journal of Bioprinting, 3*(1).

Sittinger, M., Hutmacher, D. W., & Risbud, M. V. (2004). Current strategies for cell delivery in cartilage and bone regeneration. *Current Opinion in Biotechnology, 15*(5), 411-418. doi:https://doi.org/10.1016/j.copbio.2004.08.010

Sohier, J., Vlugt, T. J., Cabrol, N., Van Blitterswijk, C., de Groot, K., & Bezemer, J. M. (2006). Dual release of proteins from porous polymeric scaffolds. *J Control Release, 111*(1-2), 95-106. doi:10.1016/j.jconrel.2005.11.016

Song, L., Baksh, D., & Tuan, R. (2004). Mesenchymal stem cell-based cartilage tissue engineering: cells, scaffold and biology. *Cytotherapy, 6*(6), 596-601.

Sophia Fox, A. J., Bedi, A., & Rodeo, S. A. (2009). The basic science of articular cartilage: structure, composition, and function. *Sports Health, 1*(6), 461-468. doi:10.1177/1941738109350438

St-Pierre, J.-P., Gan, L., Wang, J., Pilliar, R. M., Grynpas, M. D., & Kandel, R. A. (2012). The incorporation of a zone of calcified cartilage improves the interfacial shear strength between in vitro-formed cartilage and the underlying substrate. *Acta Biomaterialia, 8*(4), 1603-1615. doi:https://doi.org/10.1016/j.actbio.2011.12.022

Steck, E., Bertram, H., Abel, R., Chen, B., Winter, A., & Richter, W. (2005). Induction of intervertebral disc–like cells from adult mesenchymal stem cells. *Stem Cells, 23*(3), 403-411.

Stewart, H. L., & Kawcak, C. E. (2018). The Importance of Subchondral Bone in the Pathophysiology of Osteoarthritis. *Front Vet Sci, 5*, 178. doi:10.3389/fvets.2018.00178

Sun, A. R., Udduttula, A., Li, J., Liu, Y., Ren, P.-G., & Zhang, P. (2021). Cartilage tissue engineering for obesity-induced osteoarthritis: Physiology, challenges, and future prospects. *Journal of Orthopaedic Translation, 26*, 3-15.

Sun, Y., Deng, W., Yao, G., Chen, W., Tang, X., Feng, X., . . . Sun, L. (2018). Citrullinated fibrinogen impairs immunomodulatory function of bone marrow mesenchymal stem cells by triggering toll-like receptor. *Clinical Immunology, 193*, 38-45.

Suo, H., Chen, Y., Liu, J., Wang, L., & Xu, M. (2021). 3D printing of biphasic osteochondral scaffold with sintered hydroxyapatite and polycaprolactone. *Journal of materials science, 56*(29), 16623-16633. doi:10.1007/s10853-021-06229-x

Takechi, M., Miyamoto, Y., Ishikawa, K., Toh, T., Yuasa, T., Nagayama, M., & Suzuki, K. (1998). Initial histological evaluation of anti-washout type fast-setting calcium phosphate cement following subcutaneous implantation. *Biomaterials, 19*(22), 2057-2063.

Tallheden, T., Bengtsson, C., Brantsing, C., Sjögren-Jansson, E., Carlsson, L., Peterson, L., . . . Lindahl, A. (2005). Proliferation and differentiation potential of chondrocytes from osteoarthritic patients. *Arthritis Research & Therapy, 7*(3), R560. doi:10.1186/ar1709

Tallheden, T., Karlsson, C., Brunner, A., Van Der Lee, J., Hagg, R., Tommasini, R., & Lindahl, A. (2004). Gene expression during redifferentiation of human articular chondrocytes. *Osteoarthritis and cartilage, 12*(7), 525-535.

Tampieri, A., Sandri, M., Landi, E., Pressato, D., Francioli, S., Quarto, R., & Martin, I. (2008). Design of graded biomimetic osteochondral composite scaffolds. *Biomaterials, 29*(26), 3539-3546.

Tanzer, M. L. (1973). Cross-linking of collagen. *Science, 180*(4086), 561-566. doi:10.1126/science.180.4086.561

Tao, Z. S., Zhou, W. S., Zhang, R. T., Li, Y., Xu, H. G., Wei, S., . . . Yang, M. (2021). Co-modification of calcium phosphate cement to achieve rapid bone regeneration in osteoporotic femoral condyle defect with lithium and aspirin. *Am J Transl Res, 13*(3), 952-966.

Temenoff, J. S., & Mikos, A. G. (2000). Tissue engineering for regeneration of articular cartilage. *Biomaterials, 21*(5), 431-440.

Teoh, S. H., Goh, B. T., & Lim, J. (2019). Three-Dimensional Printed Polycaprolactone Scaffolds for Bone Regeneration Success and Future Perspective. *Tissue Eng Part A, 25*(13-14), 931-935. doi:10.1089/ten.TEA.2019.0102

Toh, W. S., Foldager, C. B., Pei, M., & Hui, J. H. P. (2014). Advances in mesenchymal stem cell-based strategies for cartilage repair and regeneration. *Stem Cell Reviews and Reports, 10*, 686-696.

Tsuji, W., Rubin, J. P., & Marra, K. G. (2014). Adipose-derived stem cells: Implications in tissue regeneration. *World J Stem Cells, 6*(3), 312-321. doi:10.4252/wjsc.v6.i3.312

Tsumaki, N., Okada, M., & Yamashita, A. (2015). iPS cell technologies and cartilage regeneration. *Bone, 70*, 48-54. doi:https://doi.org/10.1016/j.bone.2014.07.011

Turnbull, G., Clarke, J., Picard, F., Riches, P., Jia, L., Han, F., . . . Shu, W. (2018). 3D bioactive composite scaffolds for bone tissue engineering. *Bioactive Materials, 3*(3), 278-314.

Tzianabos, A. O. (2000). Polysaccharide immunomodulators as therapeutic agents: structural aspects and biologic function. *Clin Microbiol Rev, 13*(4), 523-533. doi:10.1128/cmr.13.4.523

Ueyama, Y., Ishikawa, K., Mano, T., Koyama, T., Nagatsuka, H., Matsumura, T., & Suzuki, K. (2001). Initial tissue response to anti-washout apatite cement in the rat palatal region: Comparison with conventional apatite cement. *Journal of Biomedical Materials Research: An Official Journal of The Society for Biomaterials, The Japanese Society for Biomaterials, and The Australian Society for Biomaterials and the Korean Society for Biomaterials, 55*(4), 652-660.

van der Harst, M. R., Brama, P. A., van de Lest, C. H., Kiers, G. H., DeGroot, J., & van Weeren, P. R. (2004). An integral biochemical analysis of the main constituents of articular cartilage, subchondral and trabecular bone. *Osteoarthritis Cartilage, 12*(9), 752-761. doi:10.1016/j.joca.2004.05.004

Van Lieshout, E. M., Van Kralingen, G. H., El-Massoudi, Y., Weinans, H., & Patka, P. (2011). Microstructure and biomechanical characteristics of bone substitutes for trauma and orthopaedic surgery. *BMC musculoskeletal disorders, 12*(1), 1-14.

Vashishth, D., Gibson, G., Kimura, J., Schaffler, M. B., & Fyhrie, D. P. (2002). Determination of bone volume by osteocyte population. *Anat Rec, 267*(4), 292-295. doi:10.1002/ar.10114

Vater, C., Lode, A., Bernhardt, A., Reinstorf, A., Heinemann, C., & Gelinsky, M. (2010). Influence of different modifications of a calcium phosphate bone cement on adhesion, proliferation, and osteogenic differentiation of human bone marrow stromal cells. *Journal of Biomedical Materials Research Part A: An Official Journal of The Society for Biomaterials, The Japanese Society for Biomaterials, and The Australian Society for Biomaterials and the Korean Society for Biomaterials, 92*(4), 1452-1460.

Ventura, R. (2021). An Overview of Laser-assisted Bioprinting (LAB) in Tissue Engineering Applications. *Medical Lasers, 10*, 76-81. doi:10.25289/ML.2021.10.2.76

Verhaegen, J., Clockaerts, S., Van Osch, G. J. V. M., Somville, J., Verdonk, P., & Mertens, P. (2015). TruFit Plug for Repair of Osteochondral Defects—Where Is the Evidence? Systematic Review of Literature. *Cartilage, 6*(1), 12-19. doi:10.1177/1947603514548890

Vezenkova, A., & Locs, J. (2022). Sudoku of porous, injectable calcium phosphate cements – Path to osteoinductivity. *Bioactive Materials, 17*, 109-124. doi:https://doi.org/10.1016/j.bioactmat.2022.01.001

Vinardell, T., Thorpe, S. D., Buckley, C. T., & Kelly, D. J. (2009). Chondrogenesis and Integration of Mesenchymal Stem Cells Within an In Vitro Cartilage Defect Repair Model. *Annals of Biomedical Engineering, 37*(12), 2556-2565. doi:10.1007/s10439-009-9791-1

Walker, W. T., Kawcak, C. E., & Hill, A. E. (2013). Medial femoral condyle morphometrics and subchondral bone density patterns in Thoroughbred racehorses. *American Journal of Veterinary Research, 74*(5), 691-699.

Wang, A. Y., Leong, S., Liang, Y.-C., Huang, R. C. C., Chen, C. S., & Yu, S. M. (2008). Immobilization of Growth Factors on Collagen Scaffolds Mediated by Polyanionic Collagen Mimetic Peptides and Its Effect on Endothelial Cell Morphogenesis. *Biomacromolecules, 9*(10), 2929-2936. doi:10.1021/bm800727z

Wang, J., Qiao, P., Dong, L., Li, F., Xu, T., & Xie, Q. (2014). Microencapsulated rBMMSCs/calcium phosphate cement for bone formation in vivo. *Bio-Medical Materials and Engineering, 24*(1), 835-843.

Wasyłeczko, M., Sikorska, W., & Chwojnowski, A. (2020). Review of Synthetic and Hybrid Scaffolds in Cartilage Tissue Engineering. *Membranes (Basel), 10*(11). doi:10.3390/membranes10110348

WE, B. (1983). A new calcium phosphate setting cement. *J Dent Res, 62*, 672.

Wei, W., & Dai, H. (2021a). Articular cartilage and osteochondral tissue engineering techniques: Recent advances and challenges. *Bioactive Materials, 6*(12), 4830-4855. doi:https://doi.org/10.1016/j.bioactmat.2021.05.011

Wei, W., & Dai, H. (2021b). Articular cartilage and osteochondral tissue engineering techniques: Recent advances and challenges. *Bioactive Materials, 6*, 4830-4855. doi:10.1016/j.bioactmat.2021.05.011

Wei, X., Liu, B., Liu, G., Yang, F., Cao, F., Dou, X., . . . Zhao, D. (2019). Mesenchymal stem cell-loaded porous tantalum integrated with biomimetic 3D collagen-based scaffold to repair large osteochondral defects in goats. *Stem Cell Res Ther, 10*(1), 72. doi:10.1186/s13287-019-1176-2

Wen, Y., Xun, S., Haoye, M., Baichuan, S., Peng, C., Xuejian, L., . . . Shibi, L. (2017). 3D printed porous ceramic scaffolds for bone tissue engineering: a review. *Biomater Sci, 5*(9), 1690-1698. doi:10.1039/c7bm00315c

Woodruff, M. A., & Hutmacher, D. W. (2010). The return of a forgotten polymer—Polycaprolactone in the 21st century. *Progress in polymer science, 35*(10), 1217-1256.

Worster, A. A., Nixon, A. J., Brower-Toland, B. D., & Williams, J. (2000). Effect of transforming growth factor β1 on chondrogenic differentiation of cultured equine mesenchymal stem cells. *American Journal of Veterinary Research, 61*(9), 1003-1010. doi:10.2460/ajvr.2000.61.1003

Wu, J., Li, X., Yan, Y., Hu, Y., Zhang, Y., & Tang, Y. (2013). Protein adsorption onto nanozeolite: effect of micropore openings. *Journal of colloid and interface science, 406*, 130-138.

Xia, Y., Chen, H., Zhang, F., Bao, C., Weir, M. D., Reynolds, M. A., . . . Xu, H. H. (2018). Gold nanoparticles in injectable calcium phosphate cement enhance osteogenic differentiation of human dental pulp stem cells. *Nanomedicine: Nanotechnology, Biology and Medicine, 14*(1), 35-45.

Xiao, D., Zhang, J., Zhang, C., Barbieri, D., Yuan, H., Moroni, L., & Feng, G. (2020). The role of calcium phosphate surface structure in osteogenesis and the mechanisms involved. *Acta Biomaterialia, 106*, 22-33. doi:https://doi.org/10.1016/j.actbio.2019.12.034

Xiao, Y., Mareddy, S., & Crawford, R. (2010). Clonal Characterization of Bone Marrow Derived Stem Cells and Their Application for Bone Regeneration. *International Journal of Oral Science, 2*(3), 127-135. doi:10.4248/IJOS10045

Xigeng, M. (2008). Bilayered scaffolds for osteochondral tissue engineering. *Tissue Eng: Part B, 14*, 4.

Xu, H. H., & Simon, C. G., Jr. (2005). Fast setting calcium phosphate-chitosan scaffold: mechanical properties and biocompatibility. *Biomaterials, 26*(12), 1337-1348. doi:10.1016/j.biomaterials.2004.04.043

Xu, H. H., Wang, P., Wang, L., Bao, C., Chen, Q., Weir, M. D., . . . Reynolds, M. A. (2017). Calcium phosphate cements for bone engineering and their biological properties. *Bone Res, 5*, 17056. doi:10.1038/boneres.2017.56

Xue, D., Zheng, Q., Zong, C., Li, Q., Li, H., Qian, S., . . . Pan, Z. (2010). Osteochondral repair using porous poly(lactide-co-glycolide)/nano-hydroxyapatite hybrid scaffolds with undifferentiated mesenchymal stem cells in a rat model. *Journal of Biomedical Materials Research Part A, 94A*(1), 259-270. doi:https://doi.org/10.1002/jbm.a.32691

Yan, L. P., Wang, Y. J., Ren, L., Wu, G., Caridade, S. G., Fan, J. B., . . . Oliveira, J. T. (2010). Genipin-cross-linked collagen/chitosan biomimetic scaffolds for articular cartilage tissue engineering applications. *Journal of Biomedical Materials Research Part A, 95*(2), 465-475.

Yang, J., Zhang, Y. S., Yue, K., & Khademhosseini, A. (2017). Cell-laden hydrogels for osteochondral and cartilage tissue engineering. *Acta Biomaterialia, 57*, 1-25. doi:https://doi.org/10.1016/j.actbio.2017.01.036

Yang, P. J., & Temenoff, J. S. (2009). Engineering orthopedic tissue interfaces. *Tissue Eng Part B Rev, 15*(2), 127-141. doi:10.1089/ten.teb.2008.0371

Yang, T., Tamaddon, M., Jiang, L., Wang, J., Liu, Z., Liu, Z., . . . Xue, Q. (2021). Bilayered scaffold with 3D printed stiff subchondral bony compartment to provide constant

mechanical support for long-term cartilage regeneration. *J Orthop Translat, 30*, 112-121. doi:10.1016/j.jot.2021.09.001

Yang, X., Chen, L., Xu, X., Li, C., Huang, C., & Deng, C.-X. (2001). TGF-β/Smad3 Signals Repress Chondrocyte Hypertrophic Differentiation and Are Required for Maintaining Articular Cartilage. *Journal of Cell Biology, 153*(1), 35-46. doi:10.1083/jcb.153.1.35

Yang, Y., Yang, G., Song, Y., Xu, Y., Zhao, S., & Zhang, W. (2020). 3D bioprinted integrated osteochondral scaffold-mediated repair of articular cartilage defects in the rabbit knee. *Journal of Medical and Biological Engineering, 40*, 71-81.

Yao, D., Smith, A., Nagarajan, P., Vasquez, A., Dang, L., & Chaudhry, G. R. (2006). Fabrication of polycaprolactone scaffolds using a sacrificial compression-molding process. *J Biomed Mater Res B Appl Biomater, 77*(2), 287-295. doi:10.1002/jbm.b.30419

You, F., Chen, X., Cooper, D., Chang, T., & Eames, B. F. (2018). Homogeneous hydroxyapatite/alginate composite hydrogel promotes calcified cartilage matrix deposition with potential for three-dimensional bioprinting. *Biofabrication, 11*(1), 015015.

Yousefi, A. (2019). A review of calcium phosphate cements and acrylic bone cements as injectable materials for bone repair and implant fixation. *Journal of Applied Biomaterials & Functional Materials, 17*, 228080001987259. doi:10.1177/2280800019872594

Yousefi, A. M., Hoque, M. E., Prasad, R. G., & Uth, N. (2015). Current strategies in multiphasic scaffold design for osteochondral tissue engineering: a review. *Journal of Biomedical Materials Research Part A, 103*(7), 2460-2481.

Zha, K., Sun, Z., Yang, Y., Chen, M., Gao, C., Fu, L., . . . Liu, S. (2021). Recent Developed Strategies for Enhancing Chondrogenic Differentiation of MSC: Impact on MSC-Based Therapy for Cartilage Regeneration. *Stem Cells Int, 2021*, 8830834. doi:10.1155/2021/8830834

Zhang, B., Huang, J., & Narayan, R. (2020). Gradient scaffolds for osteochondral tissue engineering and regeneration. *Journal of Materials Chemistry B, 8*. doi:10.1039/D0TB00688B

Zhang, B., Huang, J., & Narayan, R. J. (2020). Gradient scaffolds for osteochondral tissue engineering and regeneration. *Journal of Materials Chemistry B, 8*(36), 8149-8170. doi:10.1039/D0TB00688B

Zhang, J., Liu, W., Schnitzler, V., Tancret, F., & Bouler, J. M. (2014). Calcium phosphate cements for bone substitution: chemistry, handling and mechanical properties. *Acta Biomater, 10*(3), 1035-1049. doi:10.1016/j.actbio.2013.11.001

Zhang, Y., Wang, F., Tan, H., Chen, G., Guo, L., & Yang, L. (2012). Analysis of the Mineral Composition of the Human Calcified Cartilage Zone. *International Journal of Medical Sciences, 9*(5), 353-360. doi:10.7150/ijms.4276

Zhao, X., Shah, D., Gandhi, K., Wei, W., Dwibedi, N., Webster, L., & Sambamoorthi, U. (2019). Clinical, humanistic, and economic burden of osteoarthritis among noninstitutionalized adults in the United States. *Osteoarthritis and cartilage, 27*(11), 1618-1626.

Zheng, Y.-L., Sun, Y.-P., Zhang, H., Liu, W.-J., Jiang, R., Li, W.-Y., . . . Zhang, Z.-G. (2015). Mesenchymal stem cells obtained from synovial fluid mesenchymal stem cell-derived induced pluripotent stem cells on a matrigel coating exhibited enhanced proliferation and differentiation potential. *PLoS One, 10*(12), e0144226.

Zhong, C., Liu, M., Pan, X., & Zhu, H. (2022). Tumorigenicity risk of iPSCs in vivo: nip it in the bud. *Precis Clin Med, 5*(1), pbac004. doi:10.1093/pcmedi/pbac004

Zhu, Y., Liu, T., Song, K., Fan, X., Ma, X., & Cui, Z. (2008). Adipose-derived stem cell: a better stem cell than BMSC. *Cell Biochem Funct, 26*(6), 664-675. doi:10.1002/cbf.1488

Żylińska, B., Stodolak-Zych, E., Sobczyńska-Rak, A., Szponder, T., Silmanowicz, P., Łańcut, M., . . . Polkowska, I. (2017). Osteochondral Repair Using Porous Three-dimensional Nanocomposite Scaffolds in a Rabbit Model. *In Vivo, 31*(5), 895-903. doi:10.21873/invivo.11144

APPENDICES

APPENDIX 1

Adipose derived- MSC Alamar Calibration Curve

